

City Research Online

City St George's, University of London

Citation: Comineli, O. G. (1998). The influence of cooling rate and microalloying additions of Ti and Nb on the hot ductility of HSLA steels. (Unpublished Doctoral thesis, City, University of London)

This is the accepted version of the paper.

This version of the publication may differ from the final published version. To cite this item please consult the publisher's version.

Permanent repository link: https://openaccess.city.ac.uk/id/eprint/30762/

Copyright and Reuse: Copyright and Moral Rights remain with the author(s) and/or copyright holders. Copies of full items can be used for personal research or study, educational, or not-for-profit purposes without prior permission or charge, unless otherwise indicated, provided that the authors, title and full bibliographic details are credited, a hyperlink and/or URL is given for the original metadata page and the content is not changed in any way. For full details of reuse please refer to City Research Online policy.

City Research Online: http://openaccess.city.ac.uk/ publications@citystgeorges.ac.uk

The influence of cooling rate and microalloying additions of Ti and Nb on the hot ductility of HSLA steels

by

Osvaldo Guilherme Comineli

A dissertation submitted to

City University

in fulfilment of the requirement for the degree of

Doctor of Philosophy

Department of Mechanical Engineering and Aeronautics

City University

London

September, 1998

To my family: my parents Guilherme and Maria; Cosi, my brother; Tatinha and Solange, my sisters and Eliane, my wife.

List of Content ..... page

List of figures vi

List of tables x

Grants of discretion xi

Abstract xii

List of symbols xiii

Chapter 1 - INTRODUCTION 1

Chapter 2 - LITERATURE SURVEY 5

THE IMPORTANCE OF THE CONTINUOUS CASTING TECHNIQUE 5

PROCESS VARIABLES 8

OSCILLATION MARKS 8

MULTIPLE POINT BENDING 10

CASTING SPEED 11

THERMAL STRESSES 11

THE HOT DUCTILITY OF STEELS 12

THE HOT DUCTILITY TESTS 12

THE HOT DUCTILITY CURVE 14

HIGH DUCTILITY, LOW TEMPERATURE REGION(HDL): 27

HIGH DUCTILITY, HIGH TEMPERATURE REGION(HDH) 28

RELEVANCE OF HOT DUCTILITY TEST TO THE PROBLEM OF TRANSVERSE CRACKING 33

THE Ar_3 AND Ae_3 TEMPERATURES 44

METHODS TO OBTAIN THE Ae_3 AND Ar_3 45

INFLUENCE OF MICROSTRUCTURE ON TRANSVERSE CRACKING 47

GRAIN SIZE 47

PRECIPITATES 48

INFLUENCE OF THE STRAIN RATE 54

INFLUENCE OF COMPOSITION ON HOT DUCTILITY 57

KINETICS OF DISSOLUTION AND FORMATION OF PRECIPITATES; 103

THE IMPORTANCE OF PRECIPITATES ON HOT DUCTILITY; 103

INFLUENCE OF GRAIN SIZE ON HOT DUCTILITY AND TRANSVERSE CRACK; 117

Chapter 3 - EXPERIMENTAL TECHNIQUES 122

THE CASTING AND TENSILE TESTING 122

INDUCTION UNIT AND SPECIMEN DESIGN 122

REDUCTION OF AREA MEASUREMENTS - THE SHADOW GRAPH MACHINE 125

PREPARATION FOR OPTICAL MICROSCOPY AND CARBON REPLICA EXTRACTION 126

SCANNING ELECTRON MICROSCOPY 127

TRANSMISSION ELECTRON MICROSCOPY (PRECIPITATE MEASUREMENTS) 127

RELIABILITY OF RESULTS DATA 128

Chapter 4 - THE EFFECT OF Ti ON THE HOT DUCTILITY OF C-Mn-Al-Ti STEELS AND ITS RELEVANCE TO THE PROBLEM OF TRANSVERSE CRACKING IN CONVENTIONAL AND THIN SLAB CASTING 137

BACKGROUND 137

INTRODUCTION 138

EXPERIMENTAL 141

RESULTS 146
INFLUENCE OF COOLING RATE 146
FRACTURE ANALYSIS 155
DISCUSSION 191
THE HOT DUCTILITY OF AS CAST C-Mn-Al-Ti STEELS 191
REGRESSION ANALYSIS 204
CONTROL OF DIMPLE SIZE 208
COMMERCIAL IMPLICATIONS 209
CONCLUSIONS 210

Chapter 5 INFLUENCE OF Ti AND N ON THE HOT DUCTILITY C-Mn-Al-Nb STEELS 213

INTRODUCTION AND SUMMARY 213
EXPERIMENTAL 214
RESULTS 216
Ti CONTAINING Nb STEELS 219
METALLOGRAPHIC EXAMINATIONS 224
TRANSMISSION ELECTRON MICROSCOPY 232
DISCUSSION 246
INFLUENCE OF COMPOSITION ON HOT DUCTILITY OF C-Mn-Nb-Al-Ti STEELS. 252
INFLUENCE OF [Ti]X[N] PRODUCT 257
REGRESSION ANALYSIS DATA 258
COMMERCIAL IMPLICATIONS 263
CONCLUSIONS 272

Chapter 6 -SUGGESTIONS FOR FUTURE WORK AND ACKNOWLEDGEMENTS 275

FUTURE WORKS 275

ACKNOWLEDGEMENTS 277

Chapter 7 - REFERENCES AND SCIENTIFIC PRODUCTION 280

REFERENCES 280

SCIENTIFIC PRODUCTION CONCERNED TO THE WORK 295

Chapter 8 - Appendix 296

List of figures

Figure 2–1: Schematic diagram of a typical continuous casting machine 6

Figure 2–2 Transverse cracking severe transverse edge cracking 7

Figure 2–3 Schematic diagram of ductility curve 15

Figure 2–4- Schematic and actual thin ferrite film 19

Figure 2–5 The dependence of the hot ductility on the proportion of the ferrite phase 19

Figure 2–6 (w and r cracks) 21

Figure 2–7- Precipitate free zone around the grain boundary 22

Figure 2–8 Intergranular microvoid coalescence 23

Figure 2–9 - Schematic models showing formation of wedge cracks by grain boundary sliding 25

Figure 2–10 - Mechanism for void formation at grain boundary ledge 25

Figure 2–11 - Schematic diagram of hot ductility curves illustrating the ductility levels 30

Figure 2–12 - Typical high temperature ductile rupture failure 31

Figure 2–13a Top curve: Percentage distressed casts as a function of Nb content 36

Figure 2-13b Percentage distressed casts as a function of soluble Al content 37

Figure 2–14 The effect of sulphur content on the hot ductility of reheated C-Mn-Nb-Al steels 38

Figure 2–15 Influence of temperature oscillations on the hot ductility 41

Figure 2–16 Hot ductility curves 43
Figure 2–17 Variation of reduction of area with strain rate for HSLA 49
Figure 2–18 Hot ductility curves for as cast C-Mn-Nb-Al steel 50
Figure 2–19 Typical slab precipitation 51
Figure 2–20 Dependence of ductility on strain rate 55
Figure 2–21 Influence of temperature and Mn 60
Figure 2–22 Hot ductility curves for as cast C-Mn-Nb-Al steels 62
Figure 2–23 Hot ductility curves for series of plain C-Mn steels 68
Figure 2–24 Relationship of shape and position of hot ductility curves 69
Figure 2–25 Schematic illustration showing austenite structure in solidified 71
Figure 2–26 Schematic diagrams for hot ductility curves for C-Mn-Al steels with different grain sizes 72
Figure 2–27 Hot ductility curves for C-Mn-Al steels with various levels of soluble Al and N 75
Figure 2–28 Influence of N on the hot ductility of Nb containing steels 78
Figure 2–29 Influence of N on hot ductility curves of C-Mn-Nb-Al 79
Figure 2–30 Calculated volume fractions of NbC precipitating as a function of test temperatures 80
Figure 2–31 Hot ductility curves for a series of steels having different levels of V and N 82
Figure 2–32 The effect of product of total V and N contents on width of the trough. 83
Figure 2–33 Influence of small Ti additions on the hot ductility of reheated Nb containing steels 87
Figure 2–34 Influence of a 0.04%Ti addition to a C-Mn-Nb-Al steel 88
Figure 2–35 Influence of Ti on the hot ductility of as cast steels 91
Figure 2–36 Influence of Ti on the hot ductility 92
Figure 2–37 Influence of particle size and interparticle spacing 94
Figure 2–38 Effect of reducing cooling rate during casting to 25K/min 95
Figure 2–39 Influence of the Nb level in as cast C-Mn-Nb-Al steel 100
Figure 2–40 Microstructures and corresponding precipitates size distributions in C-Mn-V-Al steel 107
Figure 2–41 Microstructures and corresponding precipitates size distributions in C-Mn-V-Al steel 108
Figure 2–42 Influence of soluble Al and N on hot ductility of C-Mn-steels 111

Figure 2–43 Influence of small additions of Ti (0.02-0.03%) on hot ductility behaviour 115

Figure 2–44 Hot ductility curves for 0.19%C steel at various grain sizes 119

Figure 2–45 Influence of D_0 (initial undeformed grain size after heat treatment) on minimum RA value.... 121

Figure 3–1 Schematic drawing of the test. 123

Figure 3–2 Schematic drawing of induction test specimen. 123

Figure 3–3 Temperature gradient along the central axe of the induction coil 129

Figure 4–1 Hot Ductility curves for Al containing steels tested at 25 and 100/200K/min 147

Figure 4–2 Hot ductility curves for steels with different Ti:N ratios cooled at 25K/min. 149

Figure 4–3 Hot ductility curves for steels with different Ti:N ratio cooled at 100-200 K/min 150

Figure 4–4 Effect of Ti on the ductility of as-cast, low Al steels, steels 12 and 7B cooled at 100K/min..... 152

Figure 4–5 Effect of Ti on ductility of as-cast high Al steels 153

Figure 4–6 Typical deformation induced ferrite film 154

Figure 4–7 SEM of the fracture surfaces for low Al steel tested at 800°C 159

Figure 4–8 Comparison of the dimple sizes found in the high Al steel 161

Figure 4–9 SEM of the fracture surfaces of low Al containing steel with Ti:N ratio of 1.6:1 164

Figure 4–10 SEM of the fracture surfaces for steel with a Ti:N ratio of 3.0:1. 165

Figure 4–11 Low Ti (Ti:N ratio of 1.6:1) steel tested at 950°C 167

Figure 4–12 Same as before but tested at 800°C 168

Figure 4–13 SEM of the fracture surfaces for high Al steel with Ti:N ratio of 2.8:1 169

Figure 4–14 SEM of the fracture surfaces for the high Al steel with ratio of Ti:N ratio of 2.8:1 172

Figure 4–15 SEM of the fracture surfaces for High Al steel with Ti:N ratio of 2.8:1. 173

Figure 4–16 High Ti:N (6.2:1) steel tested at 800°C 175

Figure 4–17 showing the intergranular fracture at both cooling rates for high Ti:N steel 176

Figure 4–18 Coarse precipitates in Ti free, very low Al containing steels tested at 800°C 178

Figure 4–19 Similar size distribution of precipitates found in the Ti free high Al containing steel 180

Figure 4–20 Edax analysis of precipitate showing presence of Al and Ti 181

Figure 4–21 Precipitates in the steel with the low Ti:N ratio of 1.6:1 at 950°C and cooled at 100K/min..... 182

Figure 4–22 TEM of the carbon replicas for the steel with Ti:N ratio 183

Figure 4–23 Precipitates in the steel with a Ti:N of 1.6:1 tested at 1000°C 184

Figure 4–24 TEM of the carbon replicas for steel having Ti:N ratio of 2.8:1. 185

Figure 4–25 TEM of the carbon replica for high Al steel having Ti:N ratio of 2.8 186

Figure 4–26 Steel with the Ti:N ratio of 6.2:1 showing marked coarsening of precipitates 188

Figure 4–27 Steel 5B, high Ti:N ratio 6.2:1 steel, fractured at 950°C cooled at 25K/min 189

Figure 4–28 Influence of particle size on the Reduction of Area values. 195

Figure 4–29 Average particle size against Ti:N ratio for steels tested at 950°C 202

Figure 4–30 Average particle size against Ti:N ratio for steels tested at 1000°C 203

Figure 4–31 Relationship between the observed Reduction of Area and that calculated. 207

Figure 5–1 Hot ductility curves for C-Mn-Al-Ti-Nb steels tested at 25 and 100K/min 217

Figure 5–2 Hot ductility curves of Nb-Ti steels tested at slower cooling rate of 25K/min 220

Figure 5–3 Hot ductility curves for Nb-Ti steels tested at faster cooling rates of 100/200K/min. 223

Figure 5–4 Thin film of ferrite surrounding coarse austenite grain 224

Figure 5–5 SEM of the intergranular fracture surfaces for the Nb containing steel 227

Figure 5–6 Fracture surfaces of the Nb containing low N steel 229

Figure 5–7 Similar fracture surfaces found in steel 4B 231

Figure 5–8 Finer precipitation of Nb(CN) found in higher Al vacuum melted C-Mn-Nb-Al 233

Figure 5–9 Fine Nb,Ti(CN) found in the low Ti:N ratio steel, tested at 950°C 234

Figure 5–10 Fine Nb,Ti(CN) precipitation found in the high Ti:N ratio steel 235

Figure 5–11 Reduction of area curves for Ti and Nb-Ti steels at similar Ti:N ratio close to stoichiometric. 236

Figure 5–12 Effect of the cooling rate on the Nb containing steel 237

Figure 5–13 Hot ductility curves for steels with similar Ti and N levels 238

Figure 5–14 Coarse Ti rich precipitates present in the Nb containing steel 240

Figure 5–15 Nb containing steel, steel 1B, with high Ti:N ratio (8.0:1) tested at 1050°C 242

Figure 5–16 Nb containing steels, steels 3B and 4B with Ti:N ratios less than stoichiometric 244

Figure 5–17 Edax examination of particles taken from carbon replica for C-Mn-Al-Ti-Nb 245

Figure 5–18 Influence of particle size on the Reduction of Area in the temperature range 950-1000°C..... 247

Figure 5–19 Influence of Ti:N ratio on particle size for samples tested at 950°C. 248

Figure 5–20 Influence of Ti:N ratio on particle size for samples tested at 1000°C. 249

Figure 5–21 Influence of product of [Ti]x[N] on the R of A for a cooling rate of 25K/min. 250

Figure 5–22 Influence of the product of [Ti]x[N] on the R of A for the faster cooling rates. 251

Figure 5–23 Comparison betweem R of A measured and calutated 260

Figure 5–24 Reduction of area calculated against measured 262

Figure 5–25 Reduction of area for steels with and without Nb having high Ti:N ratios 266

Figure 5–26 Reduction of area for steels with Ti:N ratio below the stoichiometric cooled at 100K/min. 267

Figure 5–27 Hot ductility of a selection of steels examined at a cooling rate of 200K/min 268

List of tables

Table 2-1 Solubility product for Al and N in which the presence of AlN has first been detected 112

Table 3-1 Changes in composition after melting wt per cent. 130

Table 3-2 Precipitates size and number counted for temperatures of 950 and 1000°C. 132

Table 3-3 Austenite grain size and ferrite film measurements for samples 134

Table 3-4 Ar_3 and Ae_3 temperatures of the steels analysed 136

Table 4-1 Chemical composition of the steels analysed 143

Table 4-2 R of A, dimple size and particle size for fast and slow cooling rates 156

Table 5-1 Chemical composition of the steels analysed 216

Table 5-2 Measurement of particle size and dimple size. 226

Table 5-3 Variables used in the regression equation. 261

Declaration

I grant powers of discretion to the University Librarian to allow this thesis to be copied in whole or in part without further reference to me. This permission covers only single copies made for study purposes, subject to normal conditions of acknowledgement.

Abstract

The influence of cooling rate and microalloying additions of Ti and Nb on the hot ductility of HSLA steels

A series of C-Mn-Al and C-Mn-Al-Nb steels having nominal composition 0.1%C, 1.4% Mn, 0.3% Si and 0.006%N with Ti additions from 0 to 0.04% have had their hot ductility determined over the temperature range 1100°C to 700°C. Tensile specimens were cast in situ and cooled at cooling rates of 25 and 100K/min to the test temperature and strained to failure using a strain rate of $3x10^{-3}s^{-1}$.

For the C-Mn-Al steels, Ti additions were generally found to impair ductility due to the formation of fine TiN precipitates. Increasing the cooling rate resulted in general, in finer AlN precipitation finer MnS inclusion distributions and finer TiN particles.

A regression equation was obtained which showed that the best ductility was obtained when the cooling rate was slow, the particle size coarse and the N and Al levels low, to limit the volume fraction of the detrimental TiN and AlN precipitation.

Coarse particle distributions could be achieved by having a high Ti:N ratio.

On the basis of the present results it seems unlikely that Ti additions will benefit ductility significantly particularly at the faster cooling rate.

For Ti containing C-Mn-Nb-Al steel, it was found that ductility in the Ti containing Nb steels improved with decrease in cooling rate, increase in the size of the Ti containing precipitates and decrease in the volume fraction of precipitates. Again an excellent regression equation was obtained linking the R of A value to these variables.

Coarser particles could be obtained by increasing the Ti:N ratio above the stoichiometric ratio for TiN and by testing at higher temperatures. However, ductility was generally poor for these Ti containing steels being equally poor as to whether Nb was present or absent. For steels with ~ 0.005%N ductility was very poor at the stoichiometric Ti:N ratio of 3.4:1. Ductility was better at the higher Ti:N ratios but only one of the Ti containing Nb steels gave better ductility than Ti free Nb containing steels and then only at temperatures <900°C. This steel had the lowest Ti addition, (0.01%) thus limiting the volume fraction of fine Ti containing particles and gave good ductility even though the steels composition was at the stoichiometric for TiN. However, ductility was nevertheless much worse for this steel in the higher temperature range. The commercial implications of these results are discussed. It can be concluded that Ti cannot be benefit to continuous casting of Al steels. Addition may only be give some benefit to some Nb steels in conventional continuous casting where the straightening temperatures is relatively low (850°C) but not so for thin slab casting conditions where straightening temperatures are much higher.

List of symbols:

α ferrite phase

γ austenite phase

δ delta phase

D_0 or D grain size

D_i D_f initial or final diameter

L liquid phase

[]x[] product of solubility

p or p_s particle size

n_i number of precipitates considered in the "i" range of size

s_i size precipitates in the "i" range

CR cooling rate

ε strain

ε_t total strain

ε_g strain due to grain boundary sliding

HDH high ductility, high temperature region of the hot ductility diagram

HDL High ductility, low temperature region of the hot ductility diagram

HSLA high strength low alloy steels

HAZ heat affected zone in welding

Ar_3 temperature which the ferrite formation starts on cooling out of equilibrium

Ae_3 temperature which ferrite starts on cooling on equilibrium

w wedge crack

r rounded crack

PFZ precipitates free zone

σ stress

D depth of void

H height of void

L length of void

CP cooling pattern

Ac_3 temperature at which austenite starts forming on heating, out of equilibrium

RA R of A Reduction of Area

$\dot{\varepsilon}$ strain rate

t thickness of the slab

V casting velocity

R bending radius

L gauge length

SEM scanning electronic microscope

TEM transmission electronic microscope

Edax energy dispersive X ray analysis

Chapter 1 - INTRODUCTION

The mastering of metal processing has been synonymous with power for all the nations since the iron age. Steel, however did not become a high tonnage available material until the Industrial Revolution in the late 1800's. Nowadays, metals continue to have an enormous importance in the wealth and prosperity of nations either to make weapons or ships, railways or medical devices. Steels have their pre eminence in the World due to their versatility in processing and properties, their ease of weldability, workability, and ability to the change properties by simple heat-treatments and small changes in composition. Steel can be also readily recycled a crucial consideration in modern times where environmental concerns are so important. These particular characteristics and its abundant supply make steel almost irreplaceable. However, the pressure for environmental protection added to the strong competition between the metals themselves and the advent of plastics in engineering and the modern new technology of composites and ceramics materials, are pushing the steel producers to develop better and cheaper steels.

Despite the big improvements in steel technology that have taken place in the last decades, a lot of work still needs to be done to improve the efficiency of the process and guarantee the prominent position of steels in the future. The consequences of this improvement will be labour, processing and energy savings as well as better and cheaper materials.

By the end of the second World War, the maximum strength for a structural steel was 300 MPa. At that time a typical composition for a steel was .2/.4%C, .04%S, .04%P, .5/1% Mn small levels of Si and no Al and 0.006%N.

Microalloyed steels were developed around 1960 to improve the mechanical properties by adding small amounts of elements like Al, Ti, Nb and V which produce precipitates that act as grain refiners and pin the grain boundaries. This results in a material with better mechanical properties in terms of strength and impact behaviour. Control rolling and accelerated cooling have since been introduced in the last 20 years which can further refine the grain size. Today the maximum strength is around 450 MPa in normalised steels and up to 520 MPa in controlled rolled microalloyed steels.

Unfortunately, the presence of these precipitates during continuous casting impairs the hot ductility of the steels when the strand is straightened, producing surface and edge cracks. The slabs then need to be scarfed and often have to be rolled wide and the edges trimmed to remove the cracks thus increasing the scrap losses.

An understanding of the formation of these precipitates, their size and distribution is essential for the understanding of the hot ductility behaviour of the steel during the straightening operation. The precipitation is affected by many variables such as strain, cooling rate, temperature and the actual microalloying addition.

Although considerable head way has been made into resolving the problem, continued laboratory research is required for the following reasons:[Mintz et al, 1991]

Transverse cracking can often arise when new continuous casters are introduced into production;

Information is required for new steels programmed through the continuous casting route;

Scarfing is needed at times for the most difficult grades of steel. Cracks are also formed at the edges of the strand and it is not uncommon to roll wide and trim off the edges, adding considerably to scrap losses;

With the advent of direct rolling particularly for thin slab casting it is essential to obtain a defect clean surface for the economic production of steel;

The new technology of thin slab casting is being developed and it is necessary to know the behaviour of the steels under the new conditions of faster cooling rates and higher strain rates.

Hence there is a strong incentive to gain an understanding into the formation of these defects in order to prevent their occurrence. To achieve this aim, a simple tensile hot ductility test has generally been used by research centres and universities. The test is devised to reproduce the straightening operation as closely as possible. Thus the tensile sample is heated to 1330°C to dissolve the microalloying precipitates and cooled to the test temperature at the same cooling rate close to the surface as that undergone by the continuous cast strand. The tensile tests are carried out at slow strain rate, $3x10^{-3}s^{-1}$ to simulate that pertaining to the straightening operation. However, most of the tests to date have been carried out using reheated hot rolled samples. This simulation of the process is very useful for predicting the cracking behaviour of the steels having Nb and V as

microalloying additions; additions which are taken back into solution at 1330°C. However, this simple heat-treatment cannot be used for steels with Ti or S, [Turkdogan et al, 1955]. For these steels, melting the sample "in situ" is necessary as heating to 1330°C does not take all of the precipitates back into solution.

The present work is concerned which the effect of the cooling rate and composition. The influence of Ti, Nb, Al and N on the hot ductility of plain C-Mn-Al vacuum cast steels has been examined. Conditions have been chosen to be as close as possible to the industrial, i.e. similar average strain rate and the tensile samples cast "in situ" and cooled direct to the test temperature. Although these testing conditions are closer to the industrial process, the oxidation and often columnar structure that is present are not taken account of in the present analysis.

Chapter 2 - LITERATURE SURVEY

THE IMPORTANCE OF THE CONTINUOUS CASTING TECHNIQUE

The continuous casting of steel was introduced commercially around 1960. This process has improved the production of steel and reduced the costs of the final product. Compared to the ingot route, continuous casting has introduced an enormous saving in handling, mechanical work and energy consumption for casting, reheating and hot rolling of steel. In these days, the use of the continuous casting process by the steel industry is becoming necessary for survival due to the high competition among the steel companies themselves and also the competition from new materials (plastics, ceramics, composites, light alloys of titanium, aluminium and magnesium). The conventional continuous casting process that is used for thick slab casting, is now also being adapted to thin slab casting, a technology that is already being employed by some steel producers. This process allows a large reduction in cost and price of steel for the producers. However, the problems inherent are still very high and the technology for thin slab casting is mainly being used for producing only the simpler plain C-Mn steels used in the strip industry.

This process is shown schematically in Fig. 2-1.

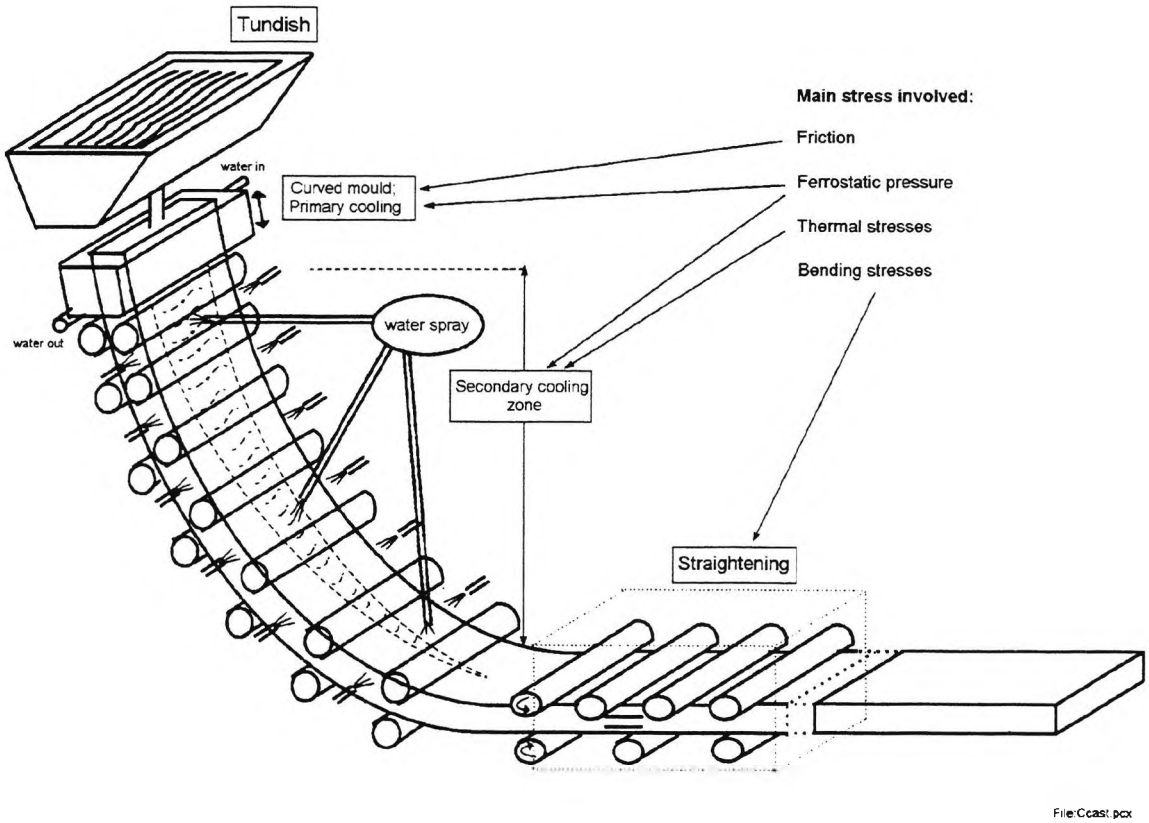


Figure 2–1: Schematic diagram of a typical continuous casting machine

The molten steel is poured from a ladle into a oscillating water cooled copper mould. It is believed that cracks may form high up in the mould in certain grades of steel. After leaving the mould, the strand is cooled by water sprays while it is straightened. This operation puts the top surface and the edges into tension and is carried out in the temperature range from 1000°C down to 700°C, which coincides with the low ductility range when the steels are laboratory tested in a tensile test. As a consequence of the temperature and deformation, the cracks can grow and penetrate 5-8 mm below the slab surface. These cracks are very easy to see by scarfing, as shown in Fig. 2-2 (a) and (b).

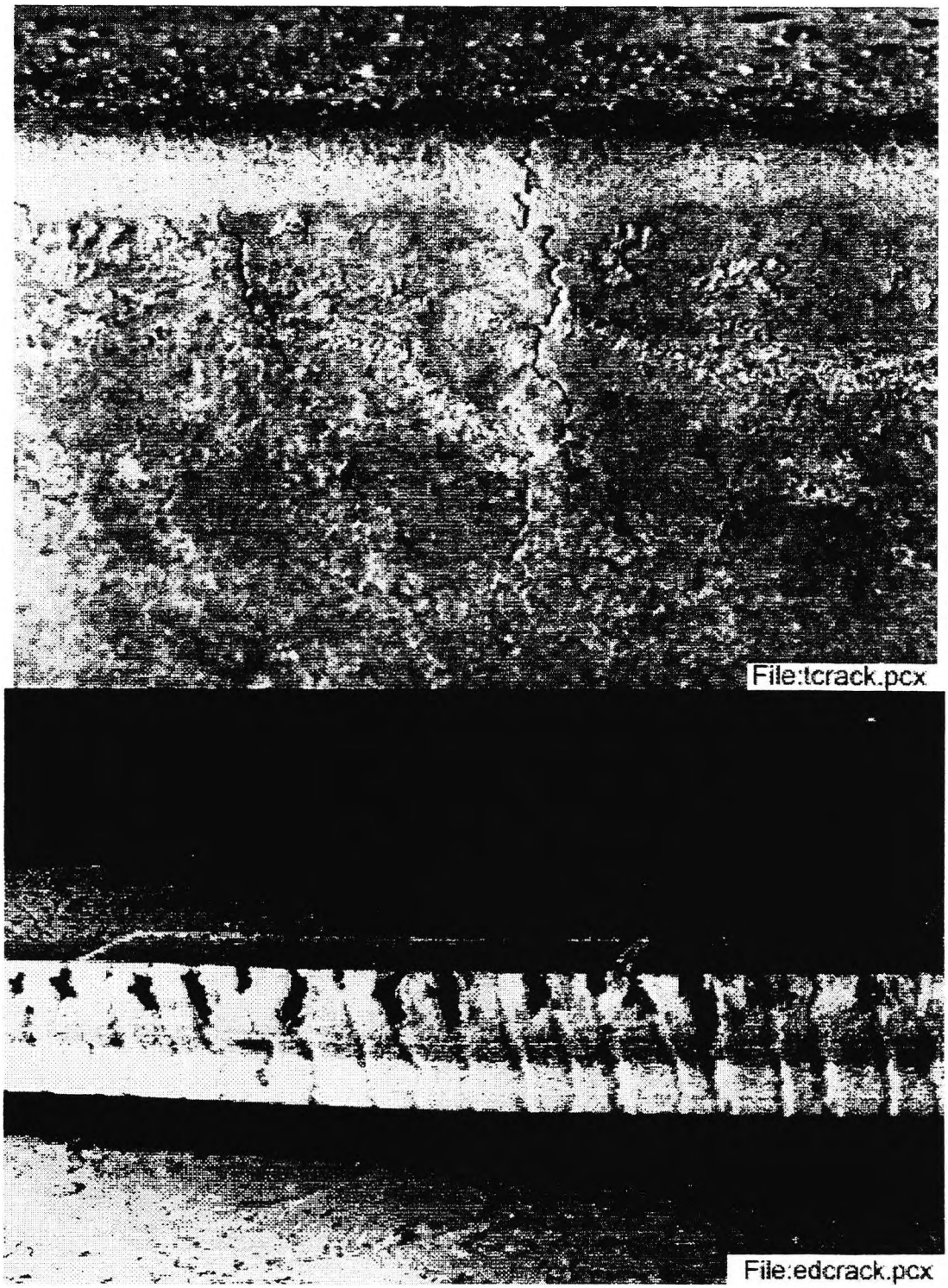


Figure 2–2 ***(a) cold machine scarfed slab showing transverse cracking and (b) slab that has been partially rolled showing severe transverse edge cracking [R. E. Mercer and N.A. McPherson, 1979].***

Cracks always occur on the top surface of the slab which is submitted to the natural strain on its way from vertical to horizontal.

In broad terms, transverse cracking will occur if the tensile strains and stresses experienced during continuous casting exceed the fracture strength of the solidifying, or solidified, strand. The degree of straining and stressing undergone by the strand is dictated by factors peculiar to the continuous casting process like radius of curvature and geometry of the moulding machine. These have been discussed by [Lankford, 1972] and are not covered in any detail in this review. However, there are several variables of the continuous casting process that affect the susceptibility of cracking of the strand, and these are discussed below.

Oscillation marks

To prevent sticking to the mould wall during continuous casting an up and down oscillating vibration in the range of 60 to 120 Hz is given to the water cooled copper mould. This motion is responsible for the ripples that appear on the surfaces of slabs and billets [Turkdogan, 1987]. The depth and pitch of these oscillation marks normally fall in the ranges 0.1-1 mm and 5-10 mm, respectively [Okazaki et al, 1982]. Increasing the frequency of oscillation and reducing the stroke have been found to reduce the depths of these

ripples, with a corresponding marked improvement in surface quality and a reduction in the frequency of transverse cracks[Mercer et al, 1979]; [Hammer et al, 1984] and [Harada et al, 1990]. These ripples act as notches and it is possible that the stress concentrations associated with them may favour crack propagation. [Mintz and Arrowsmith, 1979p24]; [Maehara et al., 1987p103] Maehara et al have used the hot ductility test to examine the influence of notch geometry on the hot ductility of HSLA and stainless steels. They found that increasing the depth of the notch generally reduced the elongation in the temperature range 800-1100°C. The notch radius was found to be unimportant, as sharp notches were rounded in the early stages of deformation.

It has however, been suggested that the micro-structural changes at the base of the ripples may in themselves be responsible for transverse cracking since.

(i) there are regions of high interdendritic segregation of elements such as P [Hammer et al., 1984] and [Harada et al, 1990] and;

(ii) there is a loss of efficiency in the heat extraction caused by the larger gap between the strand and the water cooled mould in this region favouring both a coarser grain structure and a thinner shell[Takeuchi et al, 1985] and Maehara et al, 1985].

Both (i) and (ii) are obviously detrimental do the hot ductility and therefore increase the susceptibility of the strand to transverse cracking.

Multiple point bending

Together with the evolution of thin slab casting, there has been a trend with conventional continuous casting in recent years away from single to multiple point bending to suppress surface and internal cracking by dispersing the applied stress. Maehara et al[Maehara et al, 1987p499] have examined, using the tensile testing, the consequences of increasing the number of straightening points on both the stress and ductility for C-Mn-Al and C-Mn-Nb-Al steels. Small consecutive strains (0.3 or 1%) were applied at a low strain rate of $4x10^{-4}s^{-1}$. After each incremental strain, the sample was held for 3 min before restraining. They found that stress relaxation did not fully occur, even at 1300°C, and concluded that, at lower temperatures (850-750°C), stress relaxation is largely suppressed between bending points. This is particularly marked for Nb-containing steels because of dynamic precipitation. They also noted that, although these precipitates can grow during the relaxation time between bending points, more strain induced precipitation Nb(C,N) occurs at each successive deformation, rendering the coarsening ineffective.

Increasing the number of bending points increases the effective gauge length over which the constant total strain is applied. This lowers the average strain rate, allowing more precipitation to occur, causing the hot ductility to deteriorate. Thus, no benefit to ductility was noted at the lower temperature, suggesting that surface cracking would not be reduced. Indeed, in the Nb-containing steels, the frequency of transverse cracking may even increase. However, at higher temperatures, stress relaxation does occur and multiple point bending may be effective in reducing internal cracking. The depth to which cracks can

propagate below the surface is likely to be very much reduced because of the lower applied surface strain in the region of limited ductility.

Casting speed

Maximum casting speeds are determined by ensuring that the steel shell emerging from the mould is thick enough to withstand the ferrostatic pressure of the liquid core, preventing breakouts. Casting speeds are also designed so that the output is compatible with the steelmaking facilities supporting the caster. Thus, the range of casting speeds applicable to a particular caster is limited, most running between 0.6 and 1.3m/min[Mills et al, 1977]. However, a small increase in casting speed can significantly raise the surface temperature along the whole length of the strand. This may confer benefits by reducing the amount of precipitation, thereby reducing transverse cracking if the straightening procedure is executed in the higher temperatures region of the trough.

Thermal stresses

The control of the microstructure by varying the cooling rate, particularly in the secondary zone immediately below the mould, has frequently been considered as a method of reducing the crack susceptibility. Reducing the cooling rate leads to the coarsening of precipitates, and this has been found to give good ductility. In addition to this, a reduction in the cooling rate has the important dividend of reducing the thermal stresses in the strand.

Indeed, removal of the thermal stresses is generally regarded as a prime requirement for minimising the likelihood of cracking, as is achieved by more even cooling across the slab width and in the direction of casting[Ushijima et al, 1984] However, increasing the cooling rate has also been reported to give improvements in ductility, possibly by refining the grain size [Offerman et al, 1981] and [Schmidt et al, 1974].

The hot ductility tests

The closest simulation of the straightening operation in the continuous casting should be the hot bending test. However it is rarely used due to the difficulty of analysing the results.[Lankford, 1972] and [Blake, 1987]. Recent work by Crowther, Green and Mitchell [Crowther et al, 1998]have used this to show V steels are less susceptible to cracking than Nb containing steels but generally the expense of this testing route makes it unpopular. Trying to solve this, an alternative test has been developed in a which a flange sample is used. The measure of the hot ductility is represented by hoop strain corresponding to the first appearance of a crack. [Fu et al, 1988]. Torsion testing has also been used but the anhomogeneous strain and the difficulties in interpreting the fracture appearance make it unsuitable [Cepeda et al, 1989]. Of all the laboratory tests, the simple hot tensile test has proved to be the best in the simulation of the continuous casting process. This is because it is easy to carry out and can be easily adapted to the conventional tensile machines

available in almost all materials laboratories. Also the simple parameters involved are familiar and easy to interpret.

In the test, conditions are chosen to simulate, as closely as possible, the conditions pertaining to the straightening operation during continuous casting. The test temperature is also chosen between 700°C to 1100°C in order to match the straightening operation temperature and the hot ductility trough.

The samples are heated, in an inert atmosphere, to a temperature above the solution temperature (~1350°C) of precipitates, both to dissolve the microalloying particles and grain refining additions and to produce the coarse grain size typical of the continuous casting structure. Casting "in situ" can also be performed, making the conditions closer to the real situation, considering the segregation, grain size and dissolution of precipitates like TiN and MnS. This is possible by using a quartz tube in the melting region to keep the shape of the tensile sample after cooling. The rate of cooling and the strain rate during continuous casting are 60K/min and between $3x10^{-3}$ and $3x10^{-4}s^{-1}$ respectively. These parameters nevertheless, are considerably increased to 200K/min and the strain rate by a factor of 5 for the thin slab casting technology. These variables are also very important in controlling the hot ductility of steels and as such are the subject of many studies[Mintz et al, 1991].

Some investigators [Wilcox et al, 1984], [Wilcox et al, 1987] and [Wilcox et al, 1980] have used total elongation to fracture as a measure of the hot ductility. This is useful to provide information about the role of dynamic recrystallisation in influencing the ductility. However, the majority of the researches have used the reduction of area (RA) to measure the ductility

of the steels. Although the RA at the onset of the fracture is probably a better measurement, the total reduction of area has been generally used because it is the easier measurement. The RA measurement has the advantage that it is independent of the fracture geometry of the sample.

If this test is carried out then the hot ductility curve shown in Fig. 2-3 is obtained. Ductility is good at high and low temperatures but at the temperature range 800-900°C, the temperature at which the straightening operation is carried out ductility is often poor.

The hot ductility curve

The reduction of area against temperature curve

Typical hot ductility curves for C-Mn-Al and C-Mn-Nb-Al steels have been shown schematically in Fig. 2-3, and it is important to be able to recognise the various regions on the curves and how these regions relate to the problem of transverse cracking.

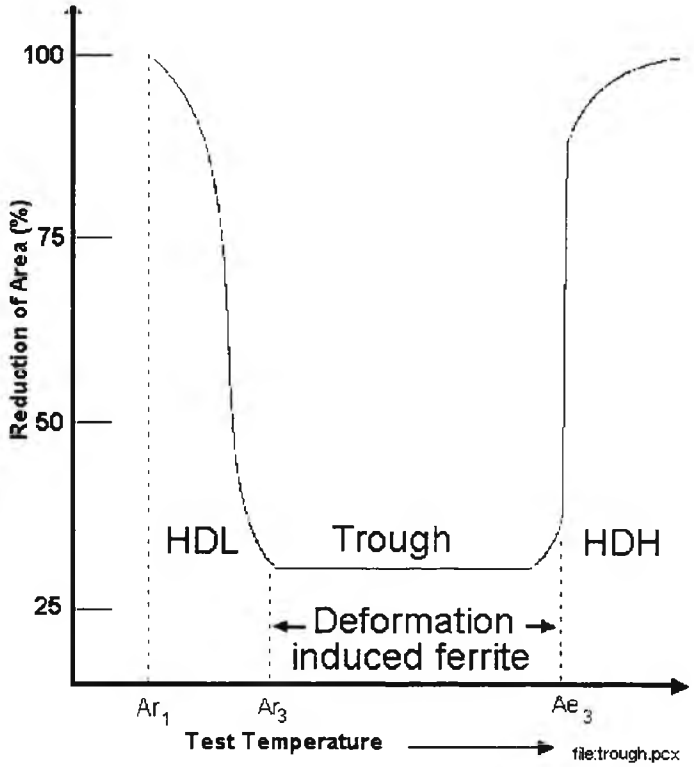


Figure 2-3 ***Schematic diagram of ductility curve defining the three characteristics regions of hot ductility***

(i) an embrittlement region in the trough;

(ii) a high ductility, low temperature (HDL) region;

(iii) a high temperature, high ductility (HDH) region.

Below the mechanisms and characteristics of the fracture appearance are given in detail for each region.

The Trough

The poor ductility in the trough is always related to intergranular failure at the γ grain boundaries[Mintz et al, 1991]. This is the most important region because here the steels can have very poor ductility. Understanding what is happening in this region is essential if solutions are to be found for improving the hot ductility of a steel. The fracture is invariably associated with intergranular fracture, the fracture facets being either covered with dimples (microvoids) or they are smooth, suggesting two distinct mechanisms. Cracks are formed along these boundaries and can be caused by two mechanisms grain boundary sliding in the austenite and/or transformation controlled intergranular failure. The former is very much encouraged by having particles at the boundaries and can be enhanced further, as in Nb containing steels, by the presence of a fine matrix precipitation which is often accompanied by precipitate free zones; all of which concentrate the strain onto the boundary. The mechanism appears to be grain boundary sliding in the single phase austenite followed by wedge cracking.

Transformation controlled intergranular failure is due to the formation of thin films of ferrite surrounding the γ grain boundaries. Since ferrite is softer than γ, all the strain concentrates in these thin films, encouraging voiding around the MnS inclusions situated at the boundaries and these voids gradually link up to give failure. The deformation is caused by the precipitates and inclusions in the grain boundary which leads to intergranular failure via microvoid coalescence. These mechanisms are discussed below.

Embrittlement by transformation controlled intergranular coalescence failure caused by strain concentration and microvoid coalescence at grain boundaries

There are two microstructural features that can be present at austenite grain boundaries and lead to strain concentrations at these locations: thin ferrite films and precipitate free zones.

Ferrite films

At the low temperature side of the trough, intergranular failure can occur when the austenite starts to transform to ferrite. A thin film (~5-20 μm thick) forms around the austenitic grain. In this condition of temperature and thickness, the ferrite film is softer than the austenite and, as a consequence, the strain concentrates in this film. The voids originate at the inclusions, generally MnS inclusions, formed at the prior austenite grain boundaries. This thin film of ferrite can form either on natural cooling with no deformation or on deformation. In all laboratory tests, the ferrite film is deformation induced as shown by all the research work in the last 10 years [Crowther and Mintz, 1986p671]; [Maki et al, 1985]; [Rizio et al, 1988]; [Cardoso et al, 1989]. Also, there is some evidence that the small strain in continuous casting is enough to produce the same effect [Essadiqui et al, 1988].

This strain induced ferrite film can start to form in the range between Ar_3 to Ae_3 temperatures, Fig. 2-4 and can at times span this whole temperature range.[Crowther and Mintz, 1986p671] and [Cardoso et al, 1989].

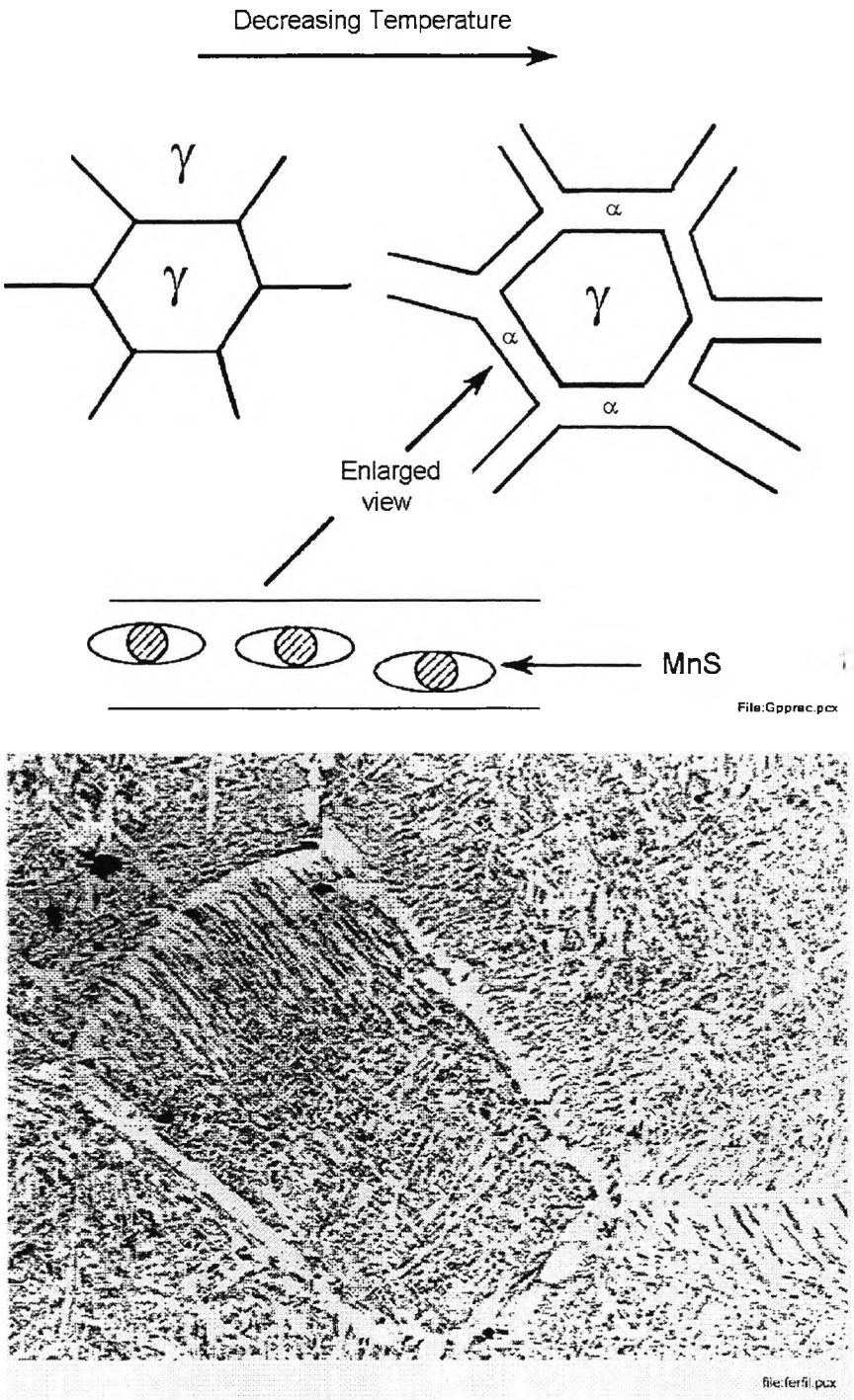


Figure 2–4- ***Schematic and actual thin ferrite film surrounding an austenitic grain[Cardoso et al, 1986].***

Often its thickness does not change very much until the Ar_3 (undeformed)is reached. Further reduction in the test temperature will rapidly thicken the ferrite film as the ferrite then forms normally before the test in large quantities and the ductility recovers fully when ~50% of ferrite is present before the start of the test. Fig. 2-5.

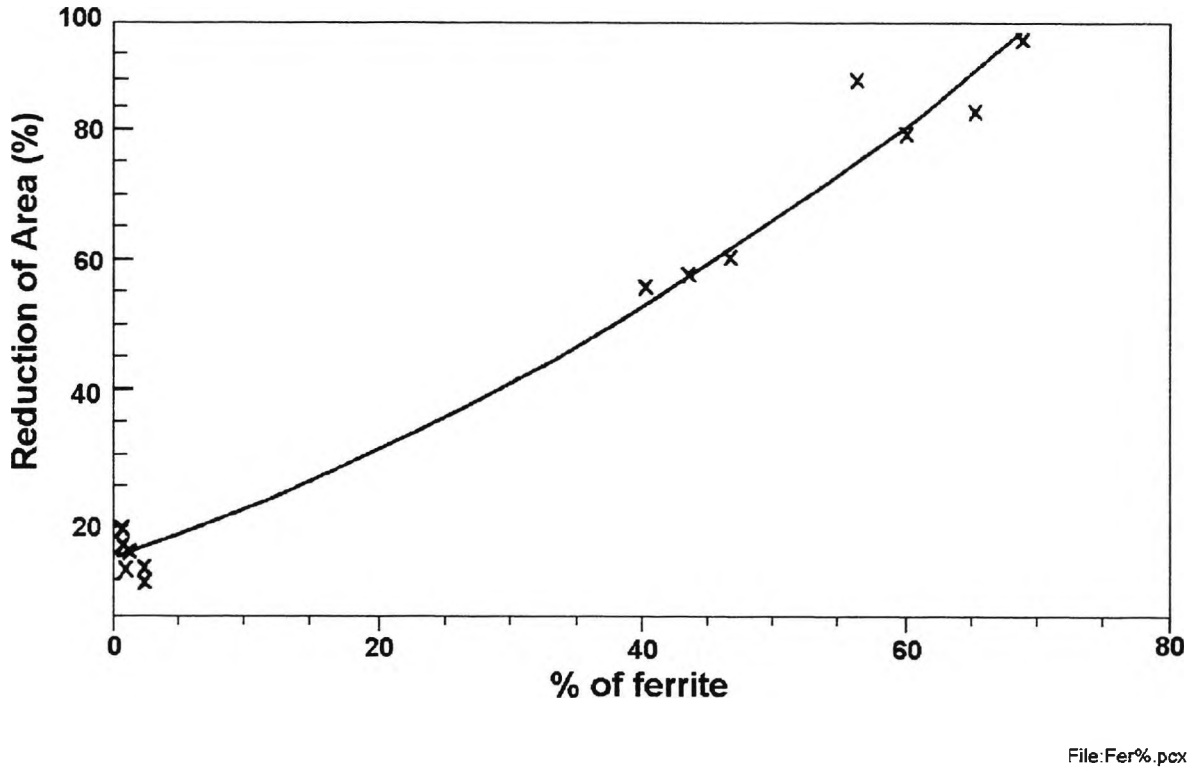


Figure 2–5 ***The dependence of the hot ductility on the proportion of the ferrite phase[Cardoso and Mintz, 1995]***

Various theories have been proposed to explain the accelerating effect of the deformation on the nucleation rate of the ferrite: (a) deformation causes local grain boundary migration leading to bulges at the austenite boundaries, which act as nuclei [Sandenberg et al, 1982]; (b)subgrains are formed near the boundaries which raise the stored energy locally [Amin et

al, 1982], (c) the increased dislocation density in deformed austenite increases the strain energy favouring the nucleation of ferrite [Umemoto et al, 1985].

Although deformation induced ferrite can be formed readily during straining in a hot tensile test there is as yet no positive confirmation of its presence in coarse grained steels at the low strains (~2%) applied during straightening. Nevertheless, there is limited evidence that this may occur from the work of Essadiqi et al[Essadiqi et al, 1988] who have shown that strain induced ferrite can be produced in a fine grained (~25μm) low C, Mo steel, deformed to a true strain of 0.016 at a low strain rate of $7.4x10^{-4}s^{-1}$. This strain and strain rate are similar to those undergone during straightening. More recent work [Mintz and Shaker, 1993] has also shown that deformation induced ferrite can be produced with as little strain as 2% in a compression test at a strain rate of $10^{-3}s^{-1}$ in C-Mn-Al steels.

It should be mentioned that wedge shaped cracks are often present at the interface between the prior austenite grain boundaries and the ferrite thin films Fig. 2-6[Crowther and Mintz, 1986p671].

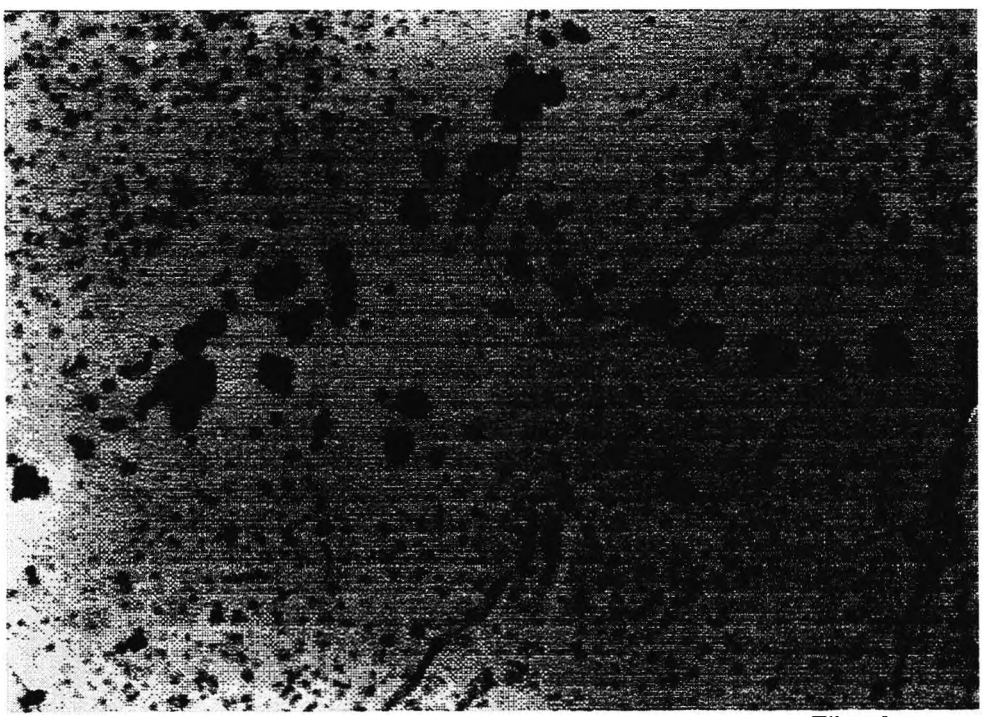


Figure 2-6 ***(w and r cracks)***

These are presumably formed by shear displacement of the austenite grains along the softer ferrite bands, rather than by conventional grain boundary sliding.

Precipitate free zones (PFZ's)

In Nb-containing steels that have been solution treated before cooling to the test temperature, precipitation takes place during deformation in the austenite. The grain boundary precipitation which usually occurs causes diffusion of solute from the neighbourhood so it is frequently accompanied by the formation of relatively weak precipitate free zones (PFZ) on either side of the boundaries (500nm wide), Fig. 2-7[Mintz and Wilcox, 1986].



File:pfz.pcx

Figure 2–7- ***Precipitate free zone around the grain boundary in a Nb-containing steel fractured at 950°C; grain boundary contains fine precipitates of NbCN and coarse MnS inclusions[Mintz and Wilcox, 1986]***

Some fine precipitation inside the matrix can also take place, leading to significant matrix strengthening. The situation is then similar to the soft films of deformation induced ferrite and microvoid coalescence fractures are frequently observed. In this case, however, void formation takes place at the microalloying precipitates (Nb(C,N), and AlN when Nb and Al are present together). This fracture process is shown schematically in Fig. 2-8[Maehara et al, 1984].

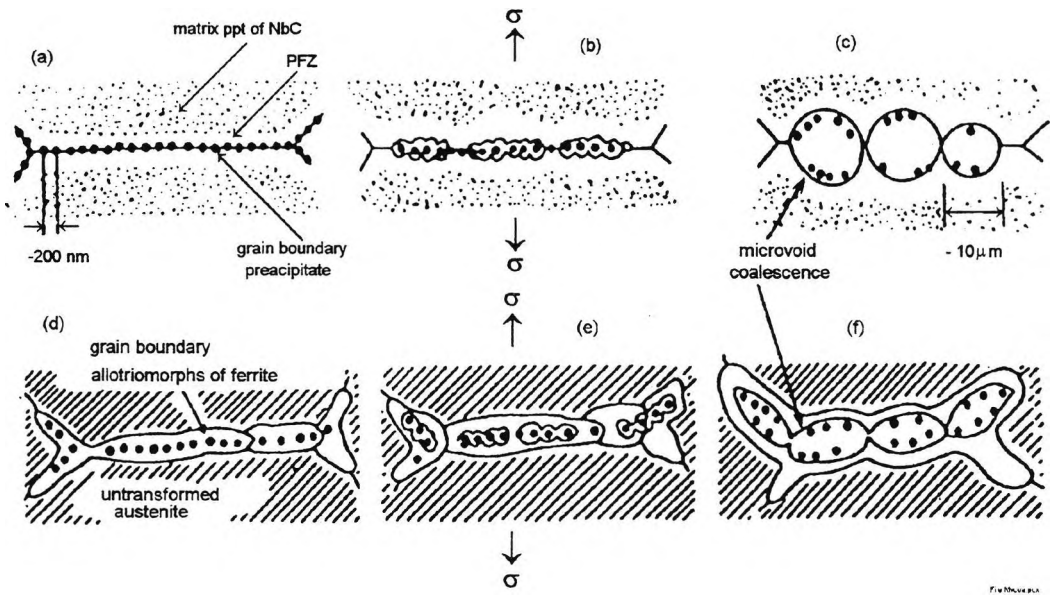


Figure 2–8 ***Schematic illustrations showing intergranular microvoid coalescence of Nb-bearing steels by deformation in a-c low temperature austenite region and d-f duplex phase region[after Maehara et al, 1984].***

It should be added that, because the deformation is taking place in the single phase austenite region, the fracture is not transgranular and grain boundary sliding is also likely to be instrumental in the embrittling process, most probably contributing to crack enlargement.

Grain boundary sliding

Grain boundary sliding followed by cracking is seen in austenite rather than ferrite, because the former shows only limited dynamic recovery. This gives rise to high flow stresses and work hardening rates, preventing the accommodation, by lattice deformation, of the stresses built up at triple points or grain boundary particles, leading to intergranular failure by the nucleation of grain boundary cracks. This rupture mechanism is usually associated with creep, the latter occurring at strain rates typically below $10^{-4}s^{-1}$. However, fractures characteristic of failure initiated by grain boundary sliding are frequently found at the strain rate generally used in hot tensile testing ($10^{-3}s^{-1}$). Furthermore, Ouchi et al [Ouchi et al, 1982] have observed grain boundary sliding at strain rates as high as $10^{-1}s^{-1}$ in a 0.054%Nb containing steel strained in tension at 900°C. Much can be learned therefore about the factors that influence intergranular crack nucleation and growth at high temperatures from a study of the creep literature [Evans, 1984].

Traditionally, intergranular creep defects have been classified as either "grain edge" or *r* type (*r* for rounded), or "grain corner" or *w* type (*w* for wedge) cavities. Both types of cracks are observed in samples tensile tested at strain rates in the range 10^{-3}-$10^{-4}s^{-1}$, and both require grain boundary sliding for their nucleation. The models proposed for the formation of *w* and *r* type cracks are illustrated in Figs. 2-9 and 2-10[Chang et al, 1956] and [Gifkins, 1956] respectively.

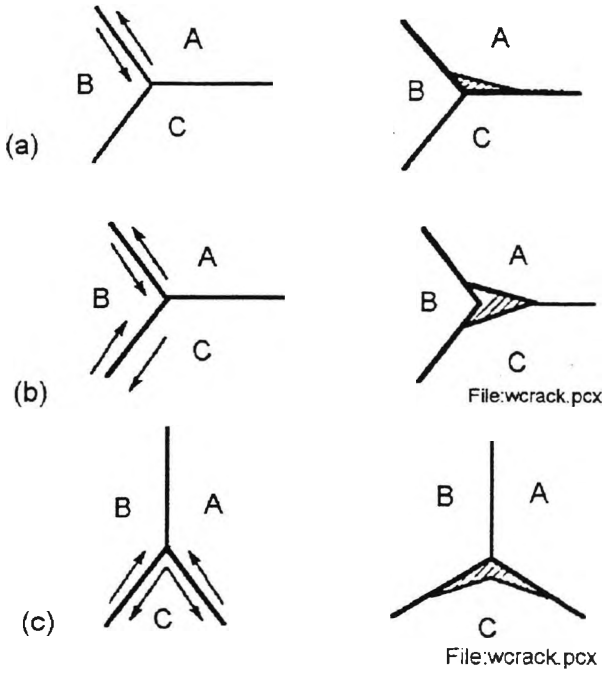


Figure 2–9 - ***Schematic models showing formation of wedge cracks by grain boundary sliding; arrows indicate sliding boundary and sense of translation[Chang et al, 1956]***

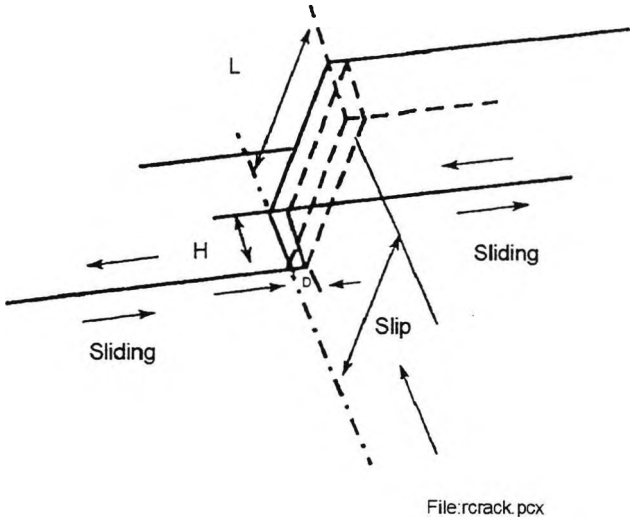


Figure 2–10 - ***Mechanism for void formation at grain boundary ledge: D is depth, H height, and L length of cavity formed by sliding in grain boundary containing jog or ledge(here supposed to have been formed by crystal slip) [Gifkins, 1956]***

In the case of *r* type cracks, the ledges produced by the impingement of slip bands against the grain boundaries lead to the formation of cavities as grain boundary sliding proceeds.

The above models indicate that intergranular failure can take place without the presence of particles at the boundaries. Nevertheless, [Grant et al, 1965] and [Servi et al, 1951] have demonstrated experimentally that cavity or crack formation by grain boundary sliding in creeping alloys progresses most easily in the presence of grain boundary particles. In steels, there are invariably sulphides, oxides, nitrides, and/or carbides at the boundaries which will act as stress concentrators and favour cavitation and crack formation. If the stress concentration at such grain boundary particles is produced by grain boundary sliding alone, the dislocation pile-up distance corresponds to the interparticle spacing, so that large applied stresses are required for particle fracture or particle-matrix decohesion. However, for the case of intergranular slip band impingement against a grain boundary particle, much smaller applied stresses are required for particle fracture, as the slip distances are much greater. It should be noted that the critical stresses required for the nucleation of *r* type cavities are much lower than those required for *w* cavity nucleation, and so the former is favoured in low stress, high temperature creep tests, or low strain rate, hot workability tests.

Many mechanisms have been proposed to describe the growth of *r* type cavities, and they can be classified as either cavity growth by deformation mechanisms or cavity growth by vacancy diffusion mechanisms. The subject is complex and is dealt with in detail by [Evans, 1984].

Finally, it is worth noting that, because of the large part played by grain boundary sliding in intergranular failure in the austenite region, the ductility may actually decrease with increasing temperature[White et al, 1968].

High Ductility, Low Temperature Region(HDL)

On decreasing the test temperature below the Ar_3 temperature, the "driving force" for ferrite formation is greatly increased, leading to large amounts of ferrite. As a consequence, ductility at the low temperature end always improves, because eventually sufficient ferrite is present via normal transformation, prior to deformation, to prevent strain concentration from occurring and the ductility of ferrite is excellent.

A common feature of the embrittlement mechanisms is preferential deformation at the region of grain boundaries and their PFZ neighbourhood. To avoid embrittlement it is therefore essential to reduce the strain concentration in those regions. This is a typical situation for the case of the high ductility, low temperature (HDL) region, where a relatively high volume fraction of ferrite can reduce the stress concentration and the embrittlement. In these new conditions, the strain is no longer concentrated in a thin ferrite film at the austenite grain boundaries. Furthermore, the strength differential between austenite and ferrite decreases with decreasing temperature, thus increasing the plastic strain in the austenite and, more importantly, decreasing the strain in the ferrite [Wray, 1981]. The concentration of strain at the grain boundaries is thus very small, and ductilities are rapidly improved. Also, ferrite has a high stacking fault energy, and therefore dynamic recovery

readily takes place, this being a recovering of the original crystalline structure process and often operates at all strains, [Keene et al, 1968] Ductility is generally very good when high percentages of ferrite are present in the microstructure, just below the Ar_3, i.e., in the vicinity of 700°C [Crowther and Mintz, 1986p671], [Maki et al, 1985], [Rizio et al, 1988], [Cardoso et al, 1989] and [Ouchi et al, 1982] as has already been shown before in Fig. 2-5. At this temperature, recovery in the ferrite takes place with ease, the subgrain size is large, and the flow stress is low. Thus, the ferrite grains flow readily at triple points to relieve stress concentrations, therefore discouraging the initiation of *w* type cracks. In addition, metals that are susceptible to dynamic recovery may form "scalloped" grain boundaries, which reduce grain boundary sliding and hence impede the nucleation of intergranular cracks [McQueen et al, 1975].

In these metals, ductility increases with increasing temperature because the stress relieving processes are more sensitive to temperature than those promoting crack nucleation [Gittins, 1977].

High Ductility, High Temperature Region(HDH)

On raising the temperature, the high ductility, high temperature (HDH) region is encountered.

At the high temperature end of the trough, ductility dramatically improves when dynamic recrystallisation occurs, Fig. 2-11[Mintz, 1996]. Any cracks that are formed at the grain boundaries become isolated as the grain boundary moves away from the cracks and new

grains are formed and in consequence crack growth is halted. However, dynamic recrystallisation is not possible during conventional continuous casting since the strain involved in straightening (2%) is too small and the grain size is too coarse. (Although strains may be greater in thin slab casting when predeformation is used and the grain size will be finer, it is still unlikely that conditions will be favourable for dynamic recrystallisation).

The use of the high temperature end of the trough in predicting what happens on straightening during continuous casting must therefore be treated with great caution. Raising the temperature at the straightener can improve ductility by coarsening precipitates or reducing the amount of precipitates formed in the boundary regions, but the improvement in ductility is often small and not sufficient to entirely eliminate the problem of transverse cracking. The form of the hot ductility curve in this case, when dynamic recrystallisation is absent, is shown schematically in Fig. 2-11 (dashed curve) and this is the curve that is relevant to the problem of transverse cracking[Mintz, 1996].

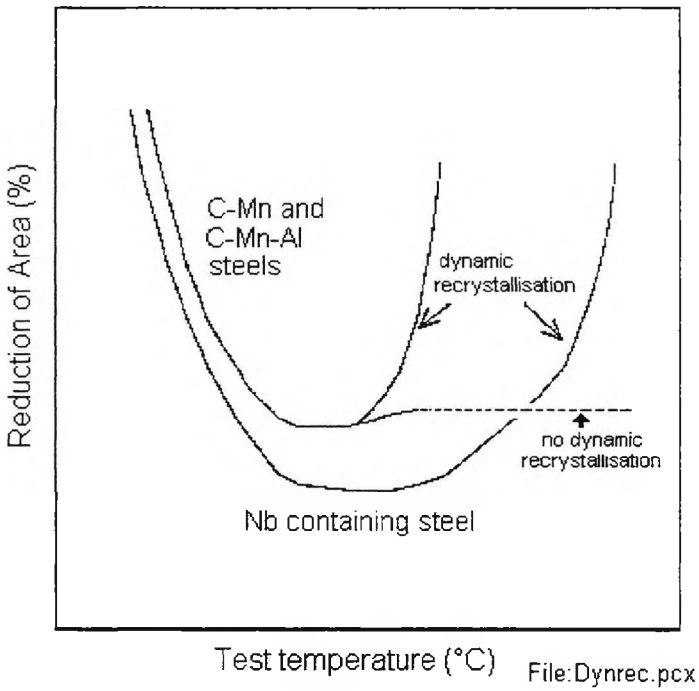


Figure 2-11 - ***Schematic diagram of hot ductility curves illustrating the ductility levels that can be achieved without dynamic recrystallisation at the high temperature end of the trough[Mintz, 1996].***

Continuing with the concept of a reduction in the strain concentration at grain boundaries, one obvious reason for this improvement in ductility is the eventual absence of the thin ferrite film. This, of course, is only effective in the austenite plus ferrite phase region, and does not affect the embrittlement in the single phase austenite region, which occurs either by grain boundary sliding or through strain concentration in the PFZ.

However, higher temperatures also lead to less precipitation in the matrix and at the grain boundaries, which offsets the latter embrittling mechanisms. Finally, increased temperatures lead to lower stresses via increased dynamic recovery, which reduce the stress concentrations at the crack nucleation sites.

However although absent in the continuous casting process, there is a further mechanism of ductility increase which applies to the HDH region, but is not based on the concept of reducing the grain boundary strain concentration but requires the occurrence of grain boundary migration. Moving grain boundaries can isolate cracks which have already been initiated from the prior grain boundaries, and high ductilities result because the growth and coalescence of these cracks is not readily achieved away from grain boundaries. This is evident from the large voids, characteristic of the fracture surfaces generated by testing in the HDH region, which apparently are not associated with second phase particles, Fig. 2-12 [Wray, 1975]; [Crowther and Mintz, 1986p1099].

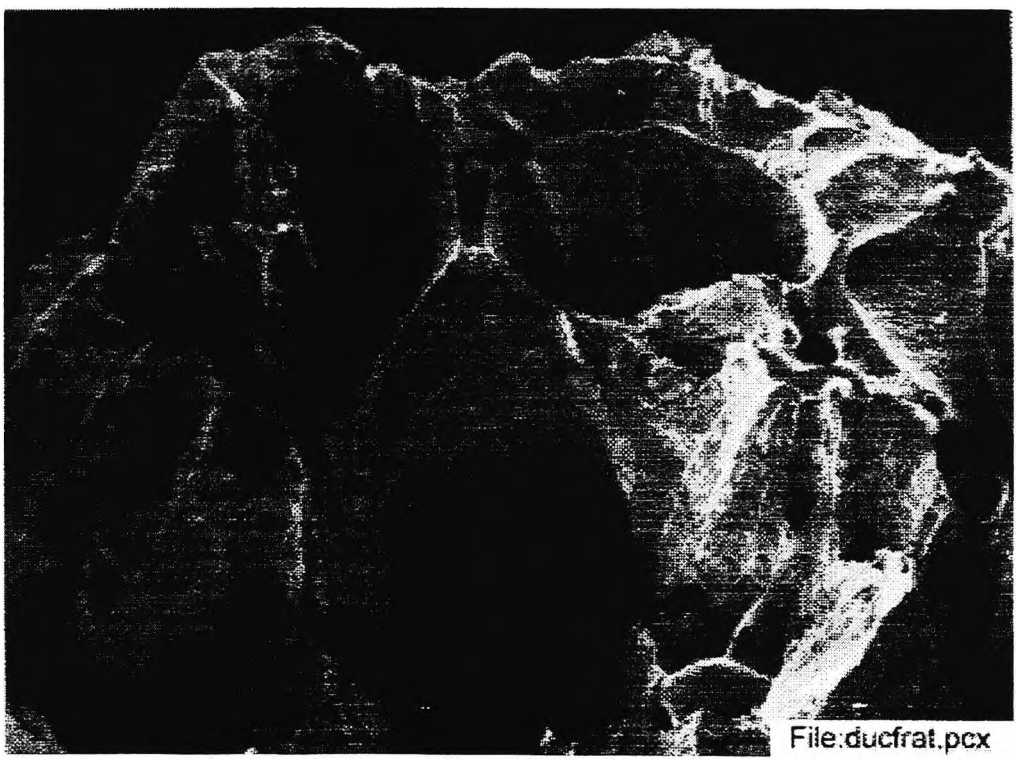


Figure 2–12 ***Typical high temperature ductile rupture failure [Crowther and Mintz, 1986p1099]***

These intergranular cracks are formed at early stages of the deformation, and they become isolated within the grains as a result of grain boundary migration. The original cracks are then distorted into elongated voids, until final failure occurs by necking between these voids.

Although grain boundary migration can isolate cracks from grain boundaries, the cracks can also exert a grain boundary drag force and "capture" moving grain boundaries. Crack growth will then resume along the captured boundary by the combined effects of vacancy diffusion and the applied tensile stress, until the boundary breaks away once more. If the capture frequency and/or the crack drag force are high, intergranular failure may ultimately occur, even if the prior grain boundaries have moved away from the initiated cracks at an earlier stage in the deformation. Thus, in order to offset embrittlement adequately, the driving force for grain boundary migration must be substantially higher than the drag force exerted by the cracks that are present.

One way to achieve a high driving force for grain boundary migration is by dynamic recrystallisation which takes place at existing boundaries at low strain rates [Luton et al, 1969]. Poorly developed sub-boundaries pin sections of the original boundaries, which bulge out and migrate relatively rapidly because of the strain energy difference across a given boundary. This is clearly a potent mechanism of bringing about grain boundary movement. It is not surprising therefore that the HDH region has often been observed to coincide with the onset of dynamic recrystallisation in many studies [Wilcox et al, 1984]; [Bernard et al, 1978] and [Crowther, Mohamed and Mintz, 1987p366]. Unfortunately, this

phenomenon needs quite a high strain and therefore does not occur in the actual continuous casting process.

As far as continuous casting is concerned the four most important variables that control ductility are the strain rate, grain size, precipitation and inclusion content (their size, volume fraction and distribution being important). Increasing the strain rate and refining the grain size (and this has to be below 200μm to have any significant effect[Mintz et al, 1991]) both give rise to improved ductility but unfortunately, it is not generally possible to alter either of these sufficiently in conventional continuous casting to make any significant difference to ductility. These various variables will be dealt with in more detail later on in the survey.

RELEVANCE OF HOT DUCTILITY TEST TO THE PROBLEM OF TRANSVERSE CRACKING.

Limitation of the results from the laboratory hot ductility tests in assessing the probability of transverse cracking occurring

It is important to emphasise[Mintz and Cominelli, 1997] that the laboratory hot ductility test is by no means a close simulation of the straightening operation in continuous casting and there are limitations of the hot ductility tensile test when related to the problem of transverse cracking. The simple test has however been found very useful in assessing a steels susceptibility to cracking but nevertheless, great care has to be

taken in interpreting the results so that they can be used to improve commercial practice[Mintz and Abushosha, 1992 and Mintz and Arrowsmith, 1979p24]

There is for example a large difference between the strains applied during testing and those associated with straightening. Lankford [Lankford, 1972] shows that the strain during the straightening operation are around 1-2% whereas in laboratory tests the strains are much higher in the range of 5-100%.

Another serious defect in the test procedure is that the microstructure differs considerably from the one present in the continuous casting strand. In particular, the grain size of the latter is likely to be 2-5 times larger than the former. Moreover, columnar grains can be present at the surface of the continuously cast slab, and these are rarely observed in tensile samples, even when they are cast *in situ*. The size and morphology of the precipitates and inclusions is also expected to bear little resemblance to those observed at the surface of the strand.

With regard to the embrittlement mechanisms, it is not known with certainty whether the thin films of deformation induced ferrite can form during the straightening operation. There is some evidence for this from low strain compressive tests but more work is required to positively confirm these findings[Mintz and Shaker, 1993]. Furthermore, a similar problem is encountered in the high temperature, high ductility (HDH) region of the hot ductility curve, Fig. 2-3. As the straightening operation involves such low strains and the grain size of the continuously cast slab is coarse ($\geq$500 μm), only dynamic recovery is possible during continuous casting. However, this is not the case for tensile testing, where the strains can be high and dynamic recrystallisation is frequently observed at the high temperature end of

the trough. Hence hot ductility data obtained from the HDH region do not apply directly to the straightening operation and should be treated with caution [Mintz et al, 1991].

Often a value of R of A required to avoid cracking is quoted. However, this value is dependent on the exact test conditions. For the conditions used by Mintz, solution treating at ~1350°C and testing at a strain rate of $3x10^{-3}s^{-1}$, an R of A value of 40% would be required to ensure freedom from cracking[Mintz, 1996].

At best, this simple test gives a semi-quantitative assessment of a steels likelihood to give rise to transverse cracking. At worst, it can lead to quite erroneous predictions. Thus, it readily shows the deleterious effect of Nb and Nb and Al in combination, on hot ductility, which is in accord with these elements' known ability to give rise to severe transverse cracking, Figs. 2-13a and b respectively[Ouchi et al, 1982]. However, using this simple method of testing to examine the influence of S, would lead to the false conclusion that the S level has no effect on transverse cracking, Fig. 2-14a [Mintz, Wilcox and Crowther, 1986; Mintz Abushosha and Cominelli, 1997]. When the tensiles are cast and cooled directly to the test temperature then S can be seen to cause the ductility to deteriorate.

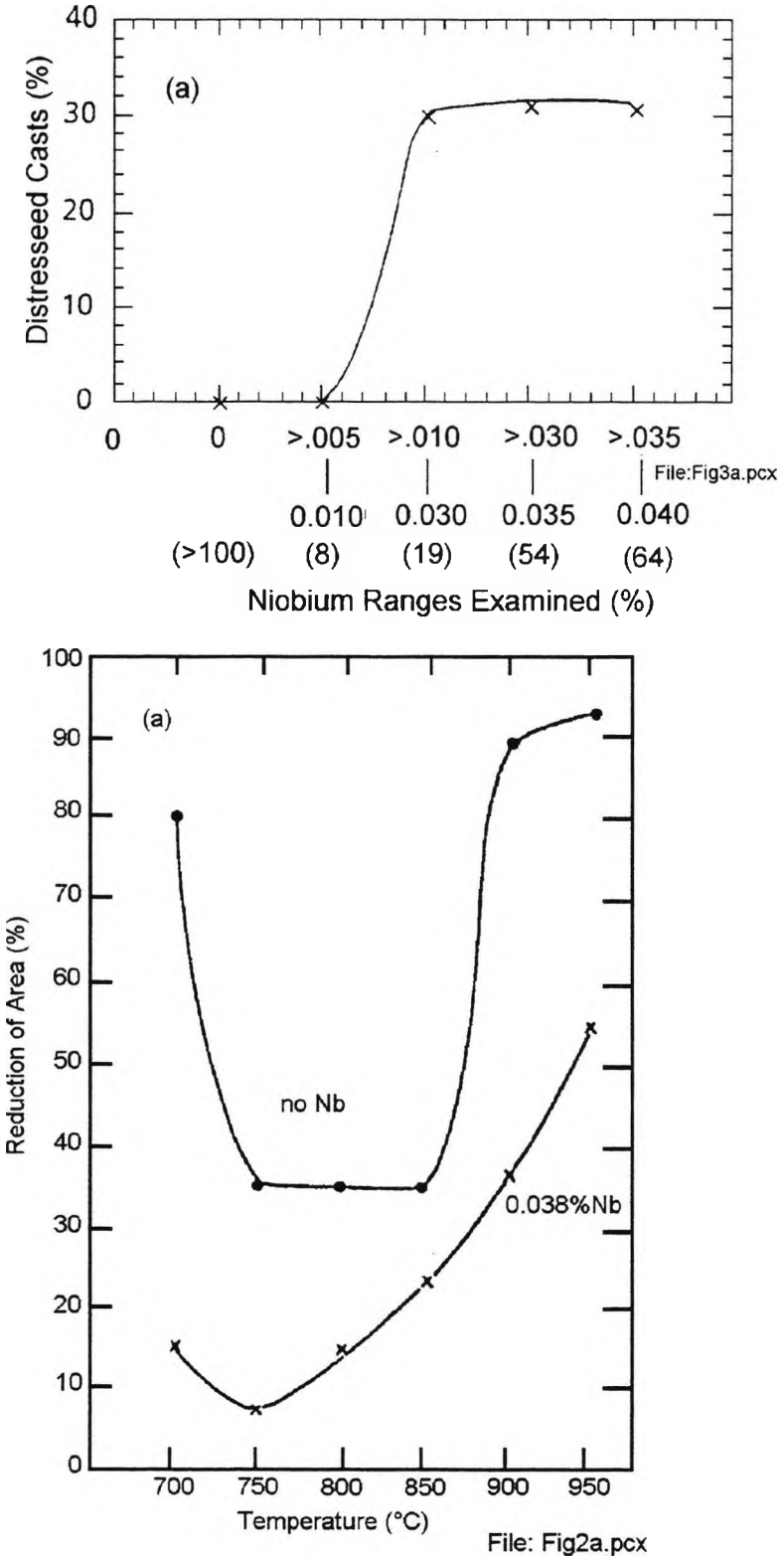
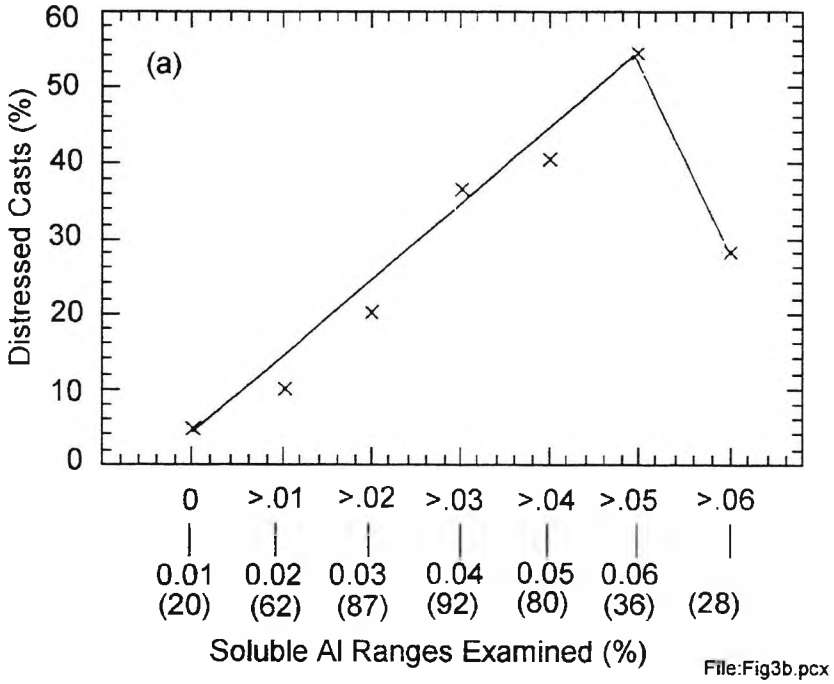


Figure 2–13a ***Top curve: Percentage distressed casts as a function of Nb content: numbers brackets refer to total number of casts in each compositional interval. Bottom curve: Influence of Nb on the hot ductility of steels[Mintz and Arrowsmith, 1979].***



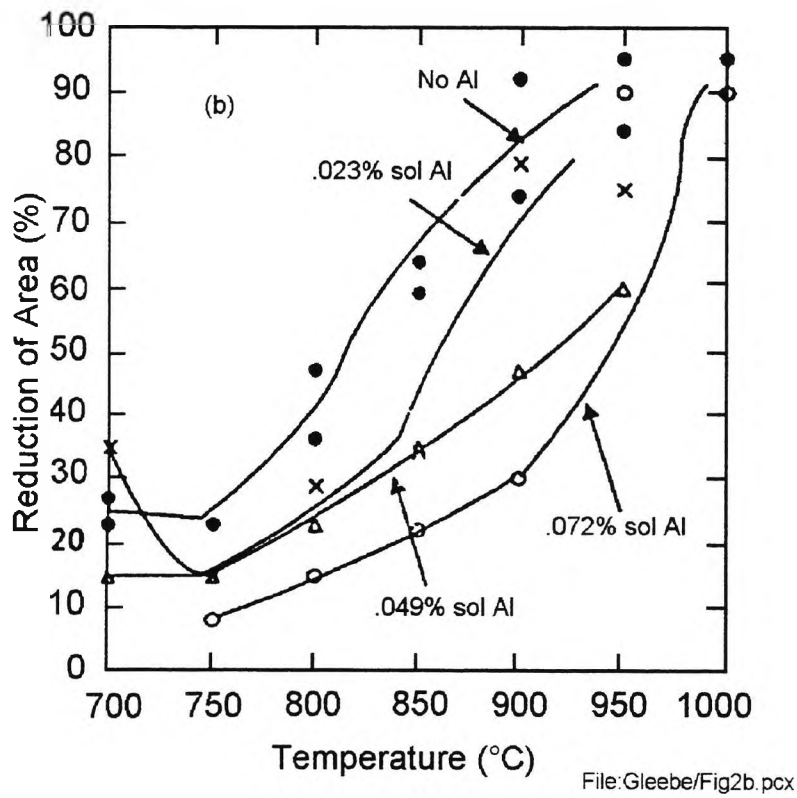


Figure 2.13b -Top curve: Percentage distressed casts as a function of soluble Al content: numbers brackets refer to total number of casts in each compositional interval. Bottom curve: Influence of soluble Al on the hot ductility of Nb containing steels, (0.03%Nb). [Mintz and Arrowsmith, 1979].

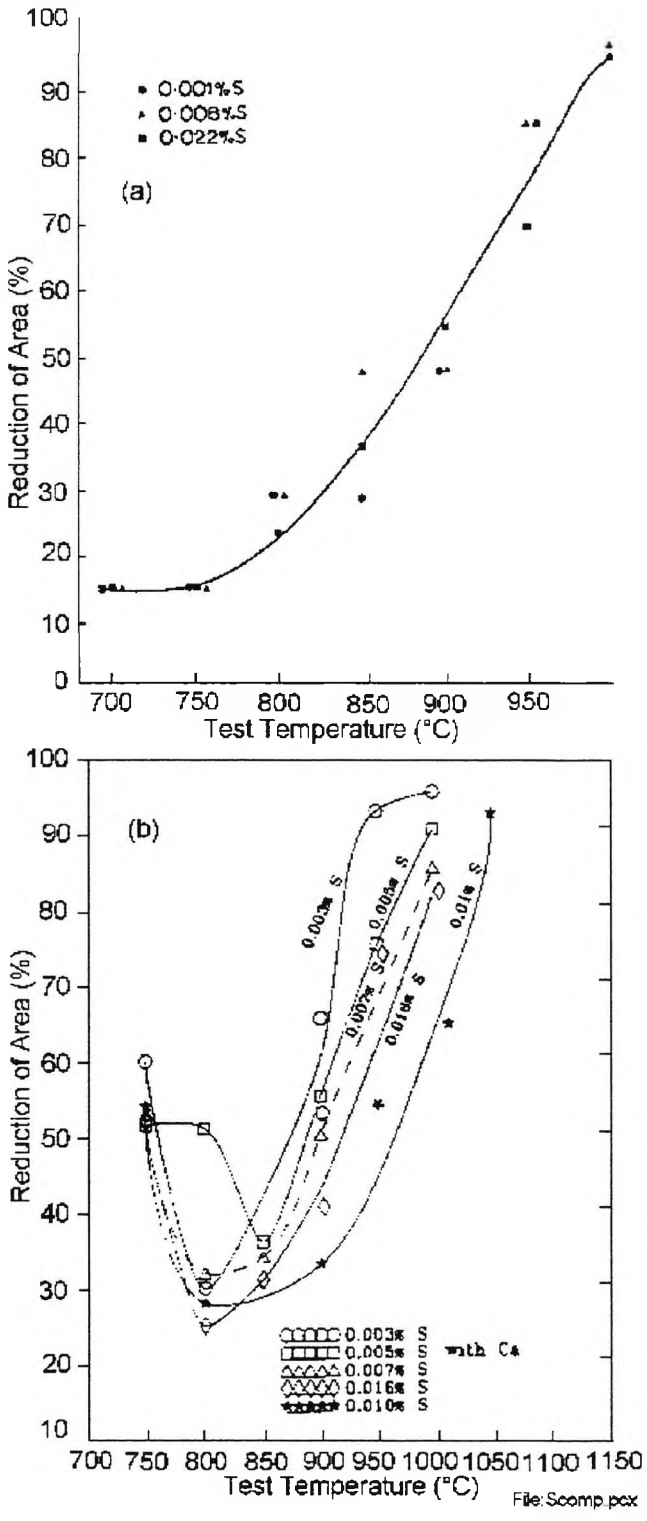


Figure 2-14 ***(a) The effect of sulphur content on the hot ductility of reheated C-Mn-Nb-Al steels [Mintz, Wilcox and Crowther, 1986] and (b) The influence of sulphur on hot ductility of as cast C-Mn-Nb-Al steels[Abushosha et al, 1991p613] Data taken from Abushosha et al, 1991 and Ouchi et al, 1982].***

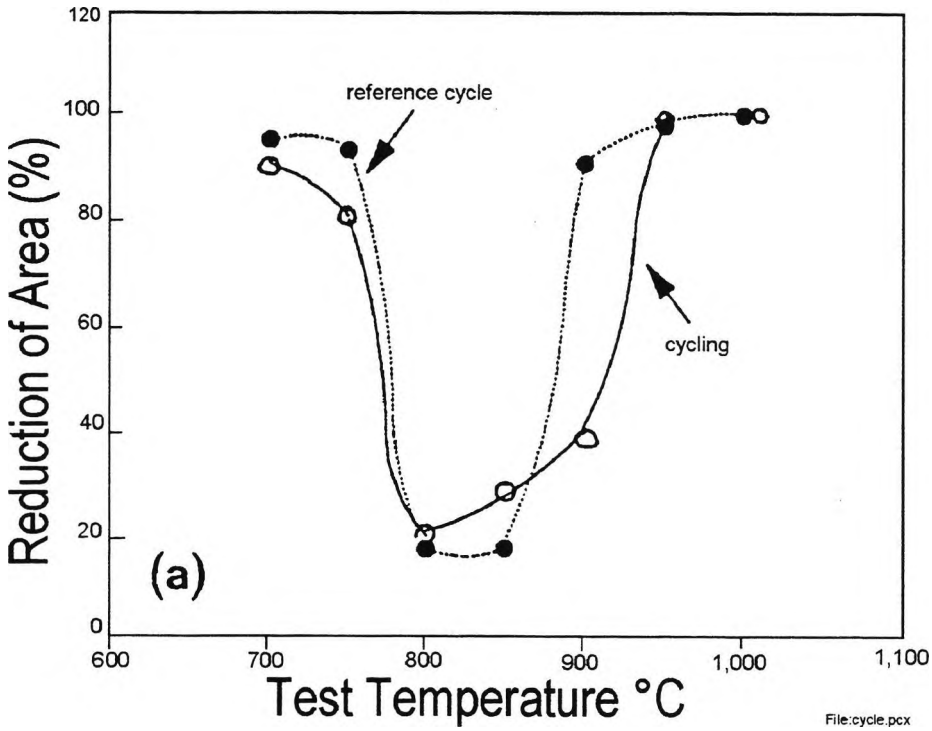
The simple test has indeed a number of drawbacks, some of which can be removed by more sophisticated testing. Thus, casting the tensile samples in situ and cooling directly to the test temperature, allows S to segregate to the interdendritic boundaries and precipitate out more normally, so that its true adverse influence can be determined, Fig. 2-14b[Abushosha et al, 1991p613].

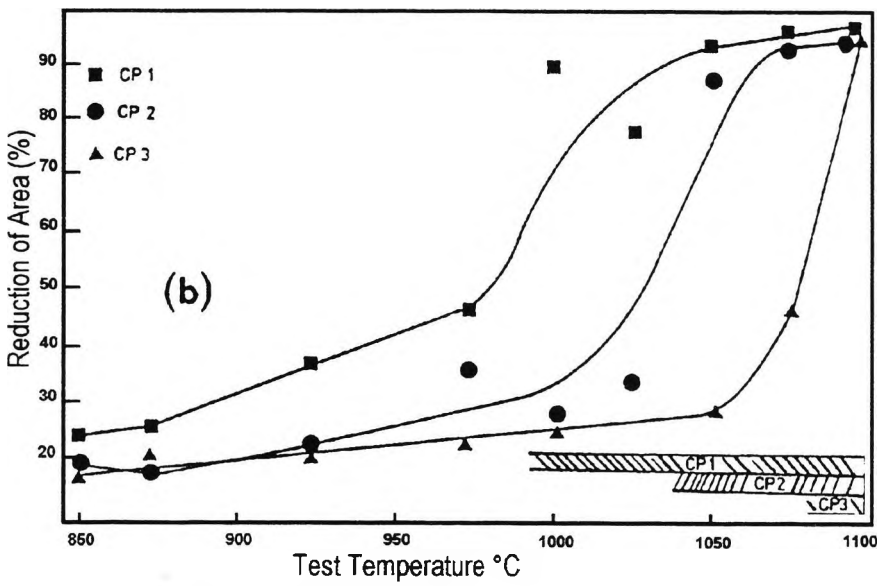
Generally, for the micro-alloying additions Nb and V and Al[Mintz and Abushosha, 1992], "solution treatment" (i.e. heating the steel to ~1350°C), prior to testing, has been found adequate to assess a steel's likelihood to exhibit transverse cracking. However, for Ti and S, the tensiles must be tested directly after casting to ensure resolution of the TiN particles and MnS inclusions[Mintz and Abushosha, 1992]. When these precautions are taken, precipitate size and distribution in the tensile samples follows closely that found near the surface of the continuously cast slabs.

Even casting tensile samples is not ideal, as small castings neither produce the segregation patterns experienced near the surface of conventionally cast strand, nor the columnar grain structure that is often present and may be directly responsible for the ease of crack propagation during straightening. In this respect, the equiaxed grain structure found in the tensile samples may correlate more with the grain structure present in thin slab castings.

Furthermore, the strand undergoes thermal oscillations during cooling: the surface temperature first decreases as the sprays impinge on the strand and this is followed by a temperature rise as the strand moves through the guide rolls. The surface temperatures of the strand then cycles - the temperature rises a little as the strand

enters the rolls and then falls as the sprays impinge on the surface. These temperature oscillations have been shown to have a pronounced influence on the precipitation processes, encouraging precipitation to occur[Cardoso, Yue and Mintz, 1995], [Mintz and Stewart, 1987] and [Coleman et al, 1985] and generally both deepening and widening the trough as can be seen in Figs. 2-15a and 2-15b for "solution treated" C-Mn-Al[Cardoso, Yue and Mintz, 1995] and C-Mn-Nb-Al steels[Mintz and Stewart, 1987] respectively and Fig. 2-16 for as cast[Mintz, Abushosha and Cardoso, 1995]. This deterioration in ductility can be seen to be particularly marked in the Nb containing steel.





Hatched line: Regions in which dynamic recrystallization takes place for cooling patterns (CP), 1, 2 and 3

Hot ductility curves for the various cooling patterns examined.

File: 10b_100.pcx

Figure 2–15: ***Influence of temperature oscillations on the hot ductility of (a) C-Mn-Al steel, (0.026%Al, 0.004%N), Cycling consisted of one temperature oscillation of amplitude ±100K[Cardoso Yue and Mintz, 1995].b) C-Mn-Nb-Al steel, CP1 refers to normal cooling to the test temperature at 60K/min, CP2 and CP3 incorporated a number of temperature oscillations of amplitude ±50 and ±100K respectively[Mintz and Stewart, 1987].***

Whereas temperature cycling has a significant influence on C-Mn-Al steels, widening and deepening the trough, this is not so for Ti treated C-Mn-Al (0.024%Ti and 0.0069%N) steels where the Ti is able to remove the N as TiN and thus prevent any precipitation from occurring during cycling, as can be seen in Figs. 2-16a and b, for as cast C-Mn-Al and C-Mn-Al-Ti steels respectively[Mintz, Abushosha and Cardoso, 1995]. Thus, the hot ductility behaviour, under conditions which are closer to commercial practice, can be very different to that given by the simple hot ductility test. Although the more complex temperature cycling may still generally rank the steels in the same order, this may not always be the case.

Conditions at the surface of the strand are also very different to those to which the surface of the tensile sample is exposed. Tensiles are normally very well protected from oxidation often being both Ni plated and tested in an argon atmosphere. The strand is exposed to the atmosphere and the water sprays will enhance oxidation which may well cause a deterioration in ductility. Copper containing steels are subject to hot shortness. This is caused by the preferential oxidisation of Fe rather than Cu and the build up of low melting point Cu films. The use of an inert atmosphere as used in the tensile tests may mask this phenomenon [Mintz, Abushosha and Cominelli, 1997]. Oxidation itself even without the presence of Cu causes ductility to deteriorate and this is difficult to copy in the laboratory test.

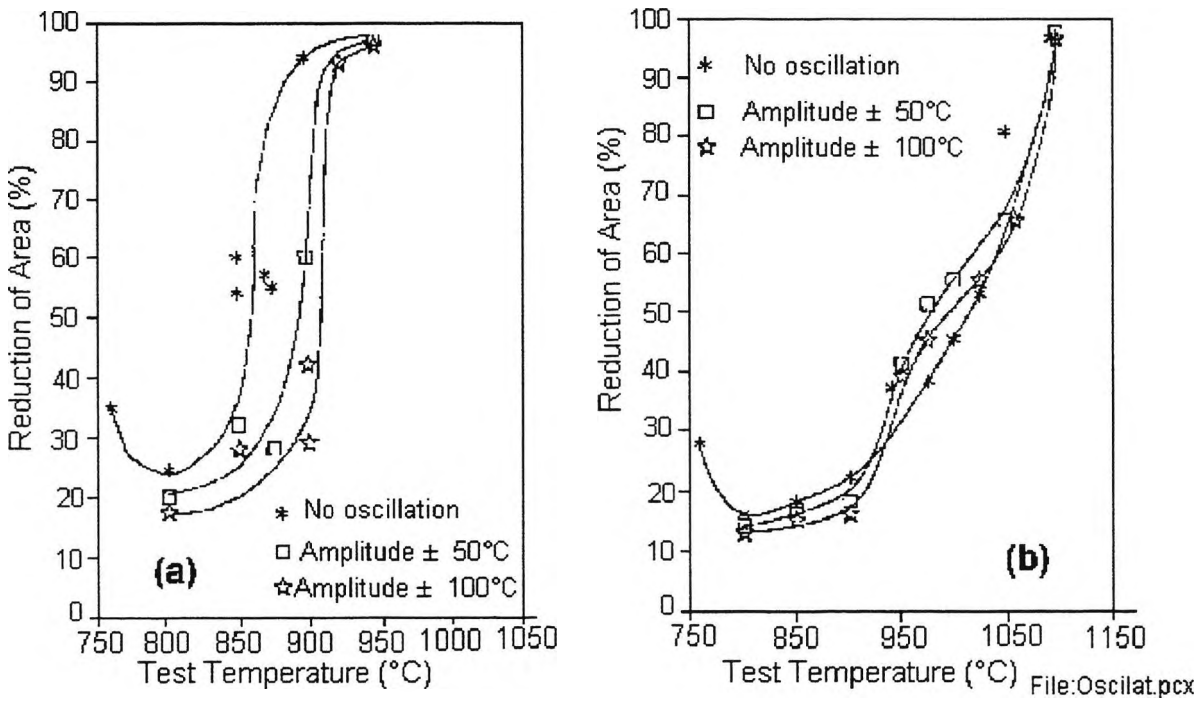


Figure 2–16: ***Hot ductility curves for (a) as cast C-Mn-Al and (b) as cast C-Mn-Al steel with a Ti addition. Steels were tested with and without temperature oscillations[Mintz, Abushosha and Cardoso, 1995].***

Finally, steels having C levels close to the peritectic, as in the present review, have been shown to be particularly susceptible to transverse cracking[Ueda et al, 1981 and Schelenberger et al, 1990]. This probably arises because the δ to γ phase transformation is accompanied by a contraction thus reducing the heat loss from the mould wall[Wolf et al, 1981 and Maehara et al, 1985]. An uneven shell, which is thin in parts, is formed which can be easily broken. Clearly, the simple hot tensile test can give little information on this phenomenon. Furthermore oxidation itself has been found to deteriorate ductility even without the presence of Cu.

The austenite + ferrite phase transformation temperatures, are strictly linked to the composition and rate of cooling of steels. Almost all the compositional elements affect these transformation temperatures as they can increase or decrease the austenitic and ferritic fields. Increasing the rate of cooling causes a delay in the ferrite precipitation and decreases these temperatures.

The transformation temperature is a fundamental variable for hot ductility studies. When cooling a steel, the ferrite phase starts precipitating when the temperature reaches the Ar_3(undeformed). The thin ferrite films formed at this temperature around the austenite grains weaken the steel and encourage rupture when strained in tension. As the temperature goes just below the Ar_3 these rapidly thicken up so that the hot ductility improves, ferrite having excellent ductility.

The recovery in ductility at the low temperature end always corresponds to a large amount of ferrite but it can be produced either by deformation or, as noted above, without strain. The thin films of ferrite will always concentrate the strain into a small volume fraction giving low ductility fracture even though ferrite has excellent ductility. Often one finds particularly with the higher Mn steels that the trough extends from the Ae_3 to Ar_3. Although some growth of the film occurs, it is small and failures are intergranular and ductility remains poor. Below the Ar_3 in these steels ferrite can form in large quantities before straining prior to the test. However, ductility is often seen to

improve rapidly just below the Ae_3 and then a large amount of deformation induced ferrite is able to form.

This type of behaviour is favoured by high strain rates, fine grain size and inclusions (particularly elongated [Mintz and Cominelli, 1997]. In all these instances the ferrite film is believed to work harden sufficiently to cause the strain to be transferred to the γ and deformation induced ferrite forms both at the grain boundaries and within the matrix. More recently this type of behaviour has been found to be linked also to composition,[Cowley et al, 1998] the higher the Ae_3 or Ar_3 temperature the easier it is for both transformation induced and deformation induced ferrite to form. What controls the width of the trough and whether a thin film will remain stable over a wide temperature range is not entirely clear at the present time.

However, because of the strong relationship between the transformation and the width of the trough, there is a considerable variation in the values of RA when the Ar_3 and Ae_3 are changed.

Methods to obtain the Ae_3 and Ar_3

Ae_3: The Andrew's equation

A practical method to determine the equilibrium transformation temperature, Ae_3 temperature, has been developed and given below.

Ae_3=910-25Mn-11Cr-20Cu+60Si+60Mo+40W+100V+700P+3-(+250Al+120As+400Ti)

Ae_3 Temperature in degree Celsius. Number 3 refers to sulphur that is assumed to give a constant rise.

The accuracy is more effective for steels with Mn above 1% and some correction factors must be added to the formula depending on the steels composition.

Andrew also suggests a formula to calculate the transformation temperature on heating the Ac_3. However because Ac_3 and Ar_3 temperatures are particularly affected by the cooling/heating rate, this formula is being omitted. More accurate determinations of the Ae_3 are now possible using thermodynamic calculation[Sundman et al, 1985].

Ar_3: dilatometry test

The out of equilibrium transformation temperature, Ar_3 is determined by a dilatometry test. This test is based in the discontinuity phenomenon present in the continuous cooling curve of metals. On the occurrence of a phase transformation, the temperature fall shows a delay due to the energy production caused by the lower energy phase rearrangement. This temperature is variable according to the cooling rate. Because the start of transformation is very slow the temperatures should be quoted corresponding to a given amount of ferrite (1 or 5%).

Grain size

Considerable amount of hot ductility research has been carried out on solution treated material and the grain size in these tests (~200μm) is always much finer than the as cast range of grain sizes pertinent to continuous casting (0.5-5mm). The present work in which samples are melted "in situ" should give a grain size closer to that found on continuous casting. Work by [Schmidt et al, 1974] have observed the correlation between transverse cracks and coarse austenite grain size and that the problem could be reduced by avoiding formation of a coarse austenite grain structure by increasing the cooling rate in the secondary cooling zones. This grain refinement can also be produced by cycling through the austenite and ferrite-austenite phase transformation temperature, i.e., the Ar_3. Another option is pre-deformation before straightening to refine the grain size. This solution seems very advisable for an ideal microstructure but is not likely to be feasible because appreciable strains are required to recrystallise the coarse as cast grain size. However in thin slab casting pre-deformation is used while the casting is in the "pasty" state. At this high temperature although this will help to break up the as-cast structure, there is little evidence that it is refining the grain size.

Since cracks are at the slab surface and propagate inwards, the role of grain size may have little to do with intrinsic ductility, as measured by RA values, but more with the ease of propagating cracks to a critical depth due to the coarse grain orientation. In this respect, the

presence of columnar grains at the surfaces is likely to encourage the growth of transverse cracks. Composition control may therefore also have an important influence in controlling the grain size, as columnar grains appear to be associated with certain level of C and Al[Maehara et al, 1985] and [Vodopivec et al, 1988].

Precipitates

The other two variables which have a major influence on the hot ductility are precipitation and inclusions and the finer the precipitation the worse is the ductility. Grain boundary precipitation is particularly deleterious and again the finer, the lower are the reduction in area values[Mintz et al, 1991]. Precipitation which is strain induced, is always finer and hence more detrimental to ductility than precipitation that is present before strain[Crowther, Mohamed and Mintz, 1987p1929]. In the case of Nb and V containing steels, a large part of the precipitation comes out during the straightening operation and so is very detrimental to ductility[Mintz et al, 1991].

With thin slab casting, the strain rate is increased by a order of 5 compared to conventional continuous casting and there is also the possibility a small grain refinement. This increase in strain rate will lead to improved hot ductility Fig. 2-17[Maehara, 1988], but the refinement in grain size is unlikely to be sufficient to have any significant influence on ductility.

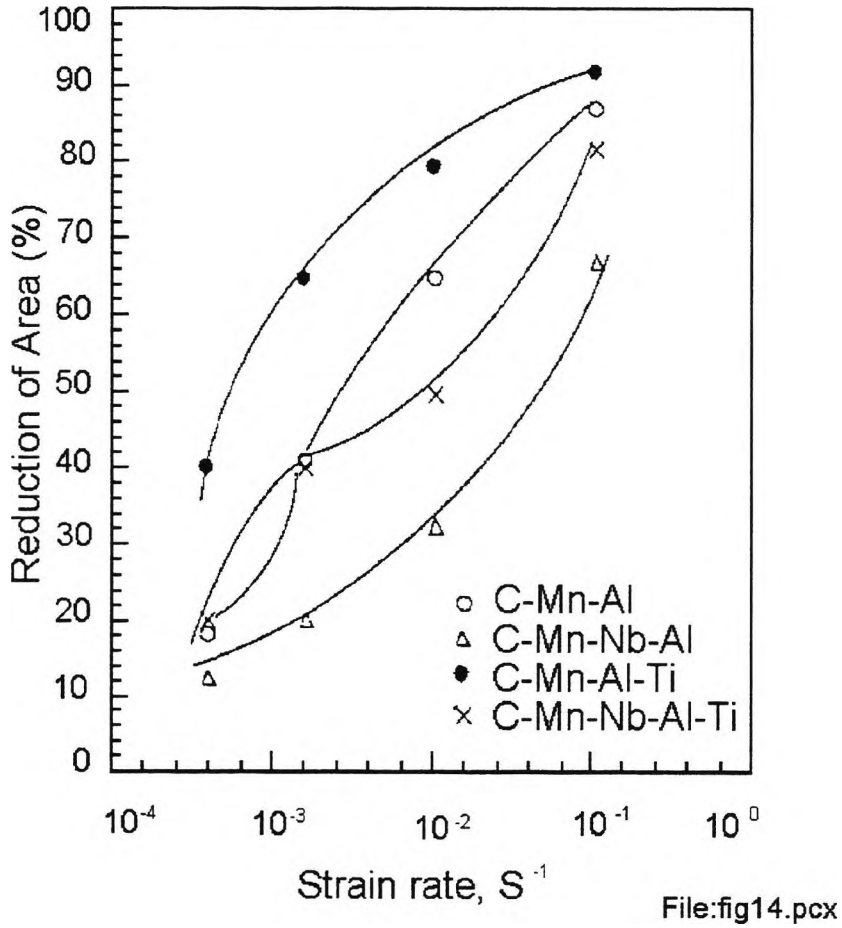


Figure 2–17: ***Variation of reduction of area with strain rate for HSLA steels [Maehara, 1988].***

Industrial experience has shown that the occurrence of transverse cracking is reduced when the temperature at the straightener is raised. Laboratory studies suggests that this effect can be linked to the reduction in the extent of nitride and carbonitride precipitation, the higher temperature giving thermodynamic conditions to discourage precipitation as well as better conditions for diffusion processes and so producing a coarser precipitation. Higher temperatures at the straightener can be achieved by reducing the amount of secondary cooling, or increasing the casting speed.

The faster cooling rate close to the surface of the thin slab strand (~200K/min), causes precipitation to be refined leading to reduced ductility, Fig. 2-18[Mintz, 1994], and this to a large extent, offsets the improvement in ductility from the increased strain rate. Because of this, the hot ductility data information already obtained from conventional thick slab casting is still likely to be relevant to the thin slab casting operation. (Note the effect shown in Fig. 2-18 of increasing the cooling rate in reducing ductility, also applies to simple C-Mn-Al steels[Mintz, 1994].

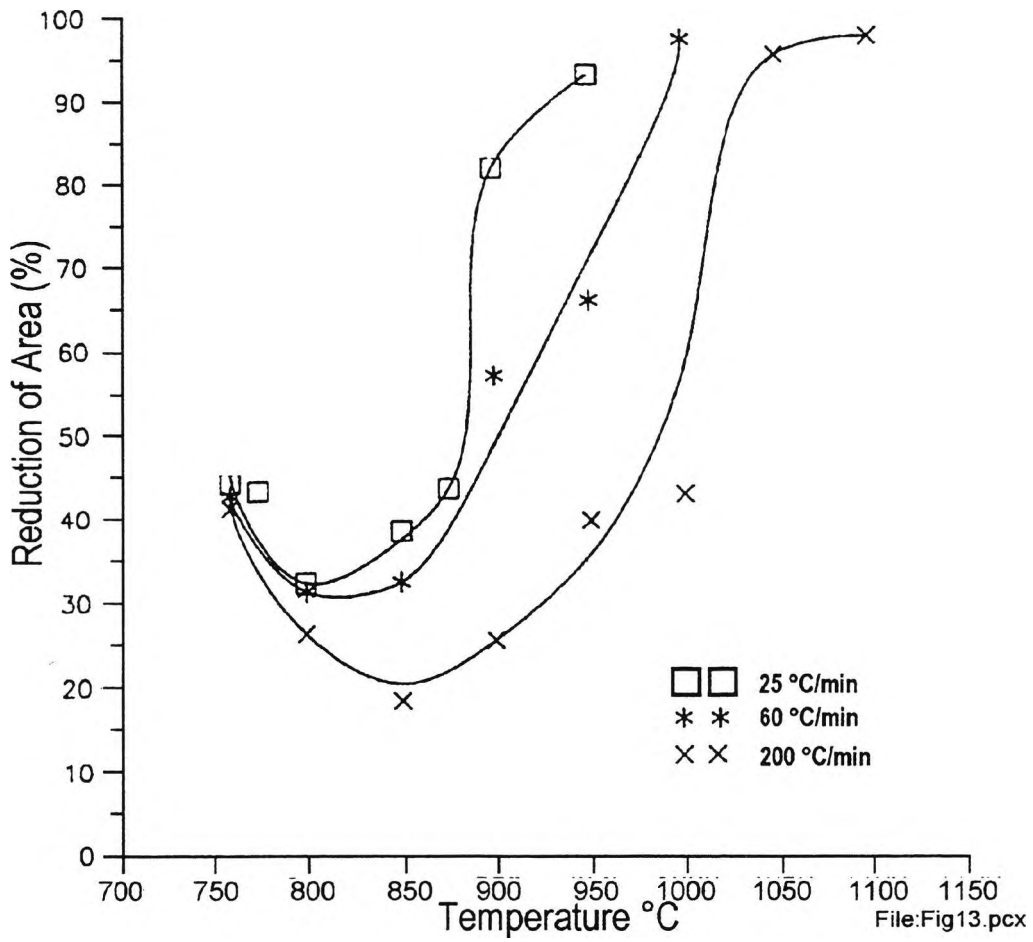


Figure 2–18: ***Hot ductility curves for as cast C-Mn-Nb-Al steel, given different cooling rates to the test temperature[Mintz, 1994].***

In addition to reducing precipitation, comparisons between acceptable slabs and those with appreciable transverse cracking have invariably shown that coarse precipitate distributions are associated with the former, Fig. 2-19.

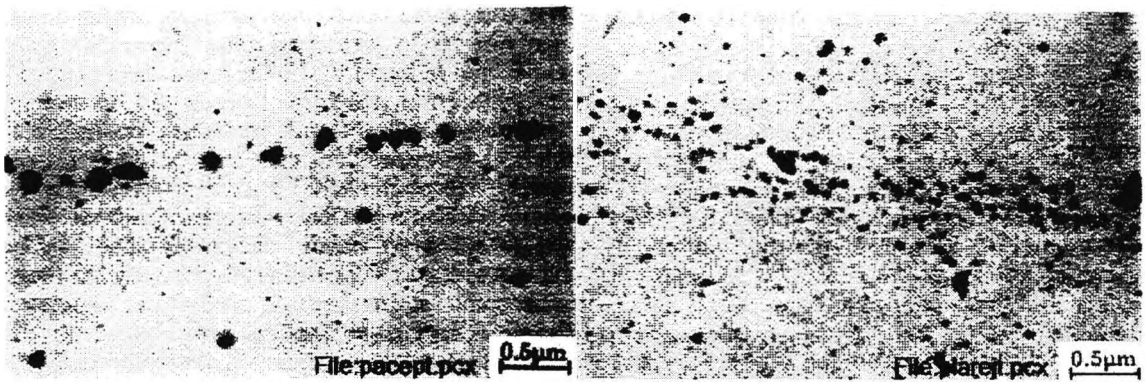


Figure 2–19:***Typical slab precipitation: left no plate rejects; right heavy plate rejects [Mintz and Arrowsmith, 1979p24]***

Because of the obvious benefits many research workers have examined methods of coarsening the precipitates, with the aim of applying these findings to the improvement of continuous casting.

One important laboratory finding is that decreasing the cooling rate from the solution temperature to the test temperature, improves ductility in Nb-containing steels by encouraging the formation of coarse, statically precipitated Nb(C,N), so reducing the amount of fine strain induced Nb(C,N)[Maehara et al, 1987p222]. Similarly, isothermal holding at 1100°C favours the static precipitation of Nb(C,N)[Maehara et al, 1987p222], and the detrimental dynamic precipitation is reduced. High temperatures can also encourage atomic diffusion for coarsening precipitates. Unfortunately, these treatments require long

times and are not practical. Nevertheless, confirming the laboratory findings, reducing the cooling rate on the strand has been shown to improve the quality of slab and reduce transverse cracking[Coleman et al, 1985; Hannerz, 1985], probably through a coarsening of the Nb(C,N) precipitates, and a reduction in the thermal stresses in the strand. However in some cases, increasing the cooling rate has led to improvements by reducing grain size[Shmidt et al, 1974]. It is clear that each case is important in its own way, and a close control of the cooling programme is necessary to achieve predictable results.

Another possible and important coarsening technique concerns predeformation at relatively high temperatures, i.e. ~1050°C, in order to accelerate precipitation and growth. Provided the cooling rate to the test temperature is reduced, 30K/min being recommended,[Maehara et al, 1987p222] growth of the precipitates takes place, leading to good hot ductility. The predeformation strain rates have to be high ($\geq 10^{-2}s^{-1}$), to avoid dynamic recovery, and prestrains of 5-10% are required to provide a large number of dislocations sites for strain induced precipitation. This seems to be a very effective method of improving hot ductility being also less time consuming than the previous methods, but, as mentioned previously, predeformation before straightening introduces great practical difficulties.

Titanium precipitates

Laboratory experience shows that addition of Ti will not grain refine the as cast structure whereas in Ti containing steels heated to 1330°C and cooled to the test temperature substantial grain refinement occurs. Not surprisingly in the latter case ductility is always good. Despite this, some research findings have been reported[Maehara et al, 1990] and [Turkdogan, 1987] that even in coarse grained as-cast Ti containing steels a reduction in transverse cracking occurs for steels which <0.0045%N and Ti is in the range 0.015-0.020%. The same behaviour has been found also for the case of the lower C steels (<0.08%C) and it has been claimed that no scarfing is necessary for Ti-treated Nb-containing steels of this C level[Williams, 1984]. Turkdogan [Turkdogan, 1987] has suggested that Ti improves the hot ductility by reacting with N and providing nucleation at high temperatures for TiN which can subsequently be used by the Nb and V to precipitate on, thus coarsening them and making them less effective in reducing the ductility. Being a very reactive metal, Ti acts during the later stages of solidification, when most of the N would be expected to precipitate in a relatively coarse form as TiN in the interdendritic region. These "coarse" particles would then be expected to form the nucleation sites for the near equilibrium precipitation of NbC at high temperatures.

Dropping the temperature to around 1200°C (assuming the intense segregation of Nb to the interdendritic boundaries), most of the Nb is expected to be precipitated as NbC. As a consequence of that, none of the detrimental low temperature, strain induced Nb(C,N) fine precipitation can occur. Turkdogan [Turkdogan, 1987] has suggested a high Ti:N ratio, to

ensure coarsening of the particles, and it is advisable that the volume fraction, i. e. the [Ti]x[N] product, of TiN particles be kept to a minimum. Again, [Turkdogan, 1987] points out that in normal steels there are so many alumina inclusions that will act as nucleation sites for the high temperature precipitation of nitrides and carbonitrides and there will be little benefit in having coarse TiN particles present. In view of this, the major benefit of adding Ti could be for Ca-treated steels, where the lower calcium aluminate inclusions may not be suitable nucleation sites. However, there are no commercial data available to substantiate these claims.

INFLUENCE OF THE STRAIN RATE

The strain rate is a very important variable affecting the hot ductility behaviour. With respect to the strain rates in the range applicable to straightening operations (~10^{-3}-10^{-4} s^{-1}), increasing the strain rate invariably improves the hot ductility, as shown before in Fig. 2-17 and Fig. 2-20 for the strain rate range 10^{-1}-10^{-4} s^{-1} and temperature range 700-1000°C.[Mintz and Arrowsmith, 1979p24]; [Ouchi, et 1982]; [Crowther, Mohamed and Mintz, 1987p366]; [Maehara et al 1987p103]; [Maehara et al, 1987p222]; [Suzuki et al, 1982]; [Mintz and Mohamed, 1988p895]; [Suzuki et al, 1984p169]; [Gittins et al, 1981]; [Maehara et al, 1988] and [Sakay et all, 1988]

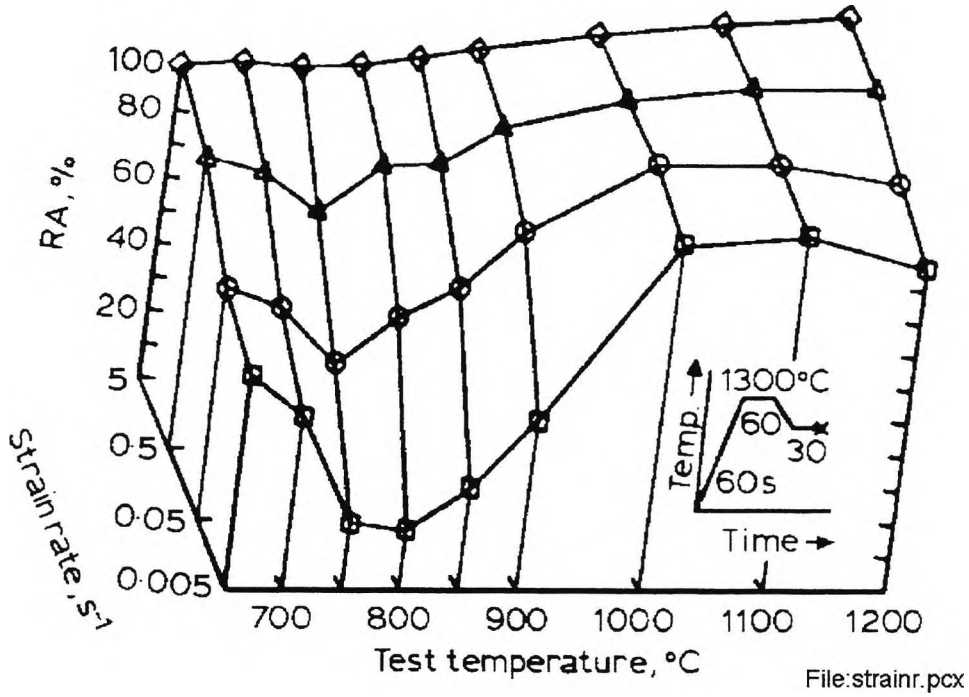


Figure 2-20: ***- Dependence of ductility on strain rate and test temperature of a Nb-bearing steel [Suzuki et al, 1984p169]***

Usually the strain rate can have a very marked effect, and an increase by an order of magnitude often increases the RA values by ~20%, changing the fracture appearance from intergranular to ductile. The trough is also often narrowed by shifting its upper temperature boundary to lower temperatures, Fig. 2-20.

The reasons for the improvement in hot ductility due to higher strain rates seem to be as follows:

1. There is insufficient time for strain induced precipitation.

2. The amount of grain boundary sliding is reduced, i.e. $\varepsilon_g/\varepsilon_t$ where ε_g is the strain due to grain boundary sliding and ε_t the total strain to fracture.[Ouchi et al, 1982]

3. There is insufficient time for the formation and diffusion controlled growth of voids next to the precipitates and inclusions present at the grain boundaries.[Mintz and Yue, 1990]

4. It has also been suggested that increasing the strain rate prevents the formation of deformation induced ferrite perhaps again due to the short time available for transformation.[Maki et al, 1985]

It should noted that in some special situations at a higher strain rate range (10^{-1} to $10^{-2}s^{-1}$) a decrease in strain rate (e.g. form 10^{-1} to 10^{-2} s^{-1}) can actually improve the hot ductility This happens when unstable fine precipitates such as FeMn sulphides are present. In this case, the inclusions probably coarsen, so that they are no longer able to pin the austenite grain boundaries.[Yasumoto et al, 1985]

Even Nb-containing steels at the 1.4% Mn level can display improved hot ductilities at very low strain rates(10^{-4}-10^{-6} s^{-1}). In this case, the reason is explained by the long time available for coarsening of the Nb(C,N) precipitates.[Sakay et al, 1988]

In continuous casting during straightening operations, the strain rates are generally in the range 10^{-3}-$10^{-4}s^{-1}$, and are given by the following relation.[Lankford, 1972]

$$\varepsilon^{\circ} = \frac{tV}{2RL}$$

Where t is the slab thickness, V is the casting velocity, R the bending radius and L the gauge length necessary to develop the full bending strain (which has been shown by [Lankford, 1972] to have a number of definitions). Hence, increase in t and V, and decrease in R and L, tend to increase ε°, and theoretically should give rise to better hot ductilities.

However, an increase in t or a decrease in R would also have a deleterious effect because of the increase in the strain on the top surface ($\varepsilon=t/2R$). The possible range of casting speeds in thick slab casting is limited as V normally lies between 0.6 and 1.3m/min, as has been noted in the section "Casting speed" above. Hence, this change in casting speed increases the strain rate by a factor of only 2. This is a very small change and is therefore unlikely to have a strong direct influence in improving the ductility. (Changes in casting speed can nevertheless modify the temperature distribution and thus have an indirect effect on transverse cracking). Practical difficulties lead to restrictions to changes in R and L. The improvement in hot ductility from increasing strain rate seems to be more technically applicable and effective for the thin slab casting process. In this slab casting V normally lies in the range 5-8 m/min and in consequence the strain rate can be a factor or 5 greater than in conventional casting and this would be expected to give some significant benefit to the ductility.

INFLUENCE OF COMPOSITION ON HOT DUCTILITY

Small changes in composition can have a very marked influence on hot ductility. This is also one of the easiest variables to adjust and much effort has been concentrated in this area. Brief reference will be made to the influence of S, Al and C on hot ductility and more details can be found in the previous reviews on the subject [Thomas et al, 1986] and [Mintz et al, 1991]. However, the effects of Ti, Nb and N all elements very relevant to the present work will be dealt with in detail.

Sulphur and sulphides

Except for special easy cutting steels, S is an unwanted impurity in steels. Nevertheless, S in steels is inevitable because it is always present in fuel and coal. It is important to highlight that as far as hot ductility is concerned it is only the austenite boundary regions which are embrittled by S precipitates. In contrast to their damaging effects at room temperature, sulphides precipitated within the austenite grain have little influence on the hot ductility which is mainly a boundary phenomenon. Sulphur impairs hot ductility by weakening the grain boundary regions due to a variety of possible reasons: (a) atomic S segregation to the austenite grain boundary [Osinkolu et al, 1985]; (b) the formation of low melting point Fe-S compounds; [Kiessling, 1966] and, like any other precipitate,(c) the effect of Mn sulphides on the formation of cavities [Coleman et al, 1985], which then link up to produce the characteristic low ductility intergranular failure. Although the segregation of atomic S may play a part in influencing the hot ductility of HSLA steels, there is much evidence to indicate that it is the sulphides that have the dominating influence. For HSLA steels increasing the cooling rate which would be expected to suppress S segregation actually causes the ductility to deteriorate. This behaviour is found even in simple C-Mn steels.

Sulphides

It is very important when determining the influence of S on transverse cracking from the hot ductility test to cast the sample "in situ" otherwise erroneous results will be obtained. Heating samples cannot redissolve all the sulphides present in the steel. For steels solution treated at 1330°C, it is the amount of S which can reprecipitate as sulphides in a fine form at the boundaries that is effective in reducing the ductility. The amount of S which redissolves depends on the Mn content, as is apparent from Fig. 2-21[Turkdogan et al, 1955].

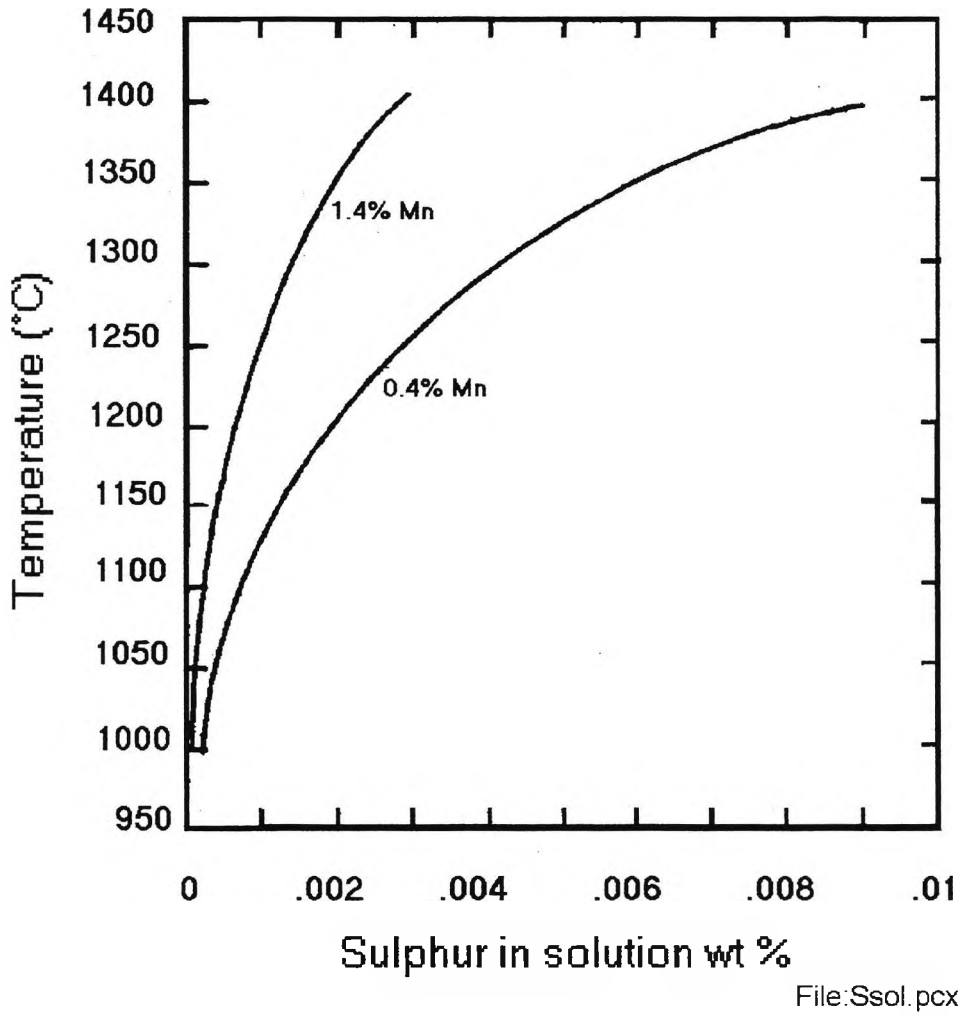


Figure 2-21: ***Influence of temperature and Mn content on the solubility of S in austenite. Data from [Turkdogan et al, 1955]***

Thus, from figure 2-21, for steels with 1.4% Mn, solution treated at 1330°C provided there is >0.0015 S, the hot ductility behaviour will be independent of the S level[Mintz and Wilcox, 1986].

When the test is carried out on as cast steel, it is the total S level which controls ductility. Hence the test sample needs to be cast "*in situ*" if the data is to be relevant to the

transverse cracking problem. To detect any influence of sulphide inclusions on the hot ductility of HSLA steels that have been solution treated before testing, or heated directly to the test temperature, the strain rates have to be low (~$3x10^{-4}s^{-1}$) as the microalloying additions may mask their influence[Crowther and Mintz, 1986pIII-83]. However, undissolved elongated sulphides remaining after solution treatment have been reported to encourage ferrite precipitation so increasing the Ar_3 temperature, thereby giving better hot ductility at the HDL side of the trough [Mintz and Cominelli, 1997]. However, in the as cast condition, increasing the S level in steel has been shown to seriously impair hot ductility, both deepening, widening and extending the ductility trough to higher temperatures at strain rates as high as $3x10^{-3}s^{-1}$[Mintz and Mohamed, 1988p895] and [Zhang Hongtao, 1988]. Moreover, reducing the S level from 0.016 to 0.002% in as cast C-1.4Mn-0.03Nb-Al steel had an effect equivalent to removing the Nb [Abushosha and Vipond, 1991p1101]. Finally, Ca treating as cast HSLA steels has also been reported to be beneficial to hot ductility, Fig. 2-22[Mintz, and Mohamed, 1989]. Being an efficient desulphurizing agent, Ca by acts reducing the total amount of S in the steel, which in turn reduces the volume fraction of sulphides precipitated at the interdendritic and austenite grain boundaries.

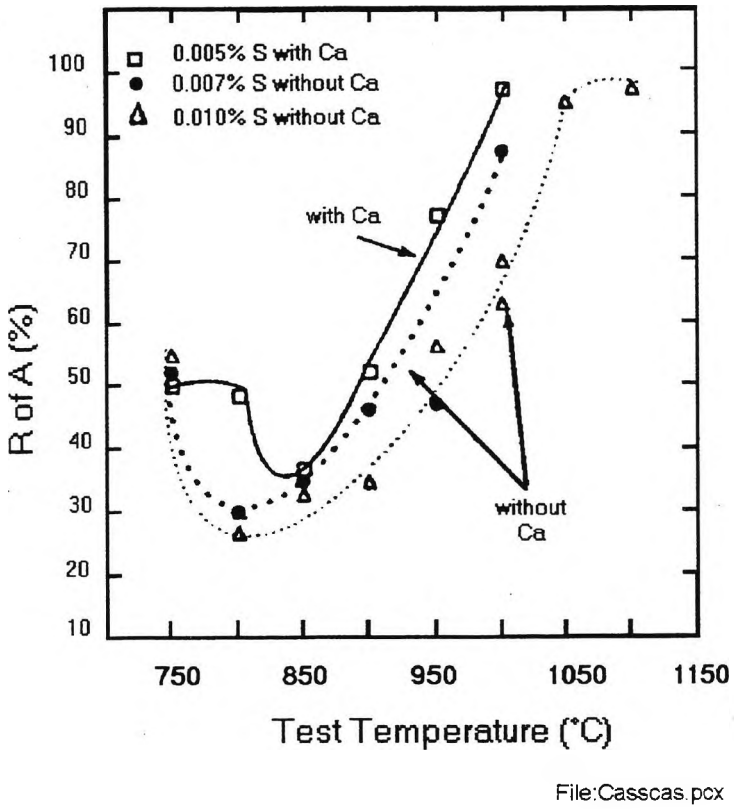


Figure 2–22: ***Hot ductility curves for as cast C-Mn-Nb-Al steels with and without Ca [Mintz and Mohamed, 1989p682]***

From the early survey by [Lankford, 1972] to the recent work by [Hubert et al, 1997] the importance of the Mn/S ratio on the hot ductility of the as cast state is clearly shown. Indeed, high Mn/S ratios are very efficient in preventing the formation of the low melting point compound, FeS, which forms liquid films at the austenitic grain boundaries. Theoretically, a Mn/S ratio of 1.7 is required for this purpose, but because of the marked tendency of S to segregate, much higher values are needed in practice. However, considering the very high Mn/S ratios pertaining to HSLA steels, FeS is not a problem in these materials.

Nevertheless, many different research studies have shown that even when the Mn/S ratio is increased to 60/1, the hot ductility still continues to improve.[Lankford, 1972] and [Weinberg, 1979]. However these investigations refer to plain C-Mn steels, in the absence of microalloying elements. There is no surprise in this case when the Mn/S ratio is increased by lowering the S level since intergranular failure has been shown to be due to the void formation at sulphide inclusions situated at the austenite grain boundaries. One method of raising the Mn/S ratio above 2 or 3 and preventing FeS formation is to lower the S level which also reduces the volume fraction of sulphide inclusions - all beneficial to the hot ductility. Similarly, the effect of lowering the S content in reducing the depth and narrowing the hot ductility trough in as cast low Mn steels [Suzuki et al, 1982] is readily understood. Lankford [Lankford, 1972] has also suggested that, in addition to reducing the volume fraction of MnS that precipitates at the boundaries, the driving force for precipitation increases with Mn concentration, encouraging precipitation within the matrix rather than, more detrimentally, at the austenitic boundaries.

The particle size of sulphides precipitated at the austenite grain boundaries, plays a very important role in hot ductility. The particles are most detrimental the finer their distribution, presumably because the shorter the interparticle distance, the easier it is for cracks to link up. Additionally, [Yasumoto et al, 1985] working with low Mn steels, reported formation at the boundaries of very fine sulphides (100nm) these being FeMnS precipitates, leading to the formation of the weak PFZs and encouraging intergranular failure. When there is a problem of fine sulphides it is advisable to have a prior heat treatment to coarsen them by lowering the cooling rate or strain rate as these sulphides can then grow, leading to

improvements in the hot ductility[Suzuki et al, 1982] and [Yasumoto et al, 1985].Nevertheless, reducing the cooling rate is not always beneficial and it is worth noting that the formation of FeMnS is favoured in both low (0.6%) and even in as high as 1.4% Mn steels when the cooling rate is slow enough to allow the intense segregation of S to the interdendritic boundaries[Mintz and Wilcox, 1986].

Although increasing the volume fraction of sulphides will enable intergranular ductile failure to occur more readily when deformation induced ferrite is present, the sulphides also influence intergranular failure when failure is by grain boundary sliding in the austenite [Mintz and Mohamed, 1989p682]. Generally, very fine particles (<50nm) are required to prevent the austenite grain boundaries from migrating, so allowing time for the cracks that may have formed to join up by grain boundary sliding[Crowther and Mintz, 1986p1099 and Funnel et al, 1978]. The MnS inclusions are often much coarser than the AlN or Nb(C,N) precipitates in the HSLA steels. Their role in influencing ductility may therefore be different to that shown by the finer precipitation. One possibility of explaining the role of inclusions and precipitate is that the fine microalloy carbide and nitride precipitates pin the boundaries. This allows strain concentrations to develop at the comparatively larger MnS inclusions which produce cavitation at the boundaries thus aiding the process of intergranular failure.

Finally, it is worth noting that the presence of elongated MnS inclusions in steels heated directly to the test temperature, shows different behaviour according to the direction of the test, in the same way as when tested at room temperature, the hot ductility being worst in the through thickness directions and best along the rolling direction [Mintz and Mohamed,

1988]. The isotropic behaviour can be restored with calcium additions that modifies the inclusion shape to that of a sphere [Crowther and Mintz, 1986pIII-83]. Elongated sulphides can also encourage ferrite nucleation leading to the hot ductility recovering well above the Ar_3[Mintz and Cominelli, 1997].

Sulphur segregation at austenite grain boundaries

Many authors have suggested in several papers that sulphur segregation to austenite grain boundaries is a possible cause of poor hot ductility [Osinkolu et al, 1985];[Weinberg, 1979]; [Yasumoto et al, 1985] and [Tacikowski et al, 1986].

Sulphur, segregated to grain boundaries has been demonstrated [Messmer et al, 1982] to exert an attractive force on the electrons associated with the bonding of Fe atoms, reducing the strength of the boundaries. Studies in low Mn, ultra high purity steels, heated directly to the test temperature, have found that AlN reduced the hot ductility only indirectly by, pinning the boundaries, so that S was able to segregate to them and embrittle the material [Yasumoto et al, 1985] and [Tacikowiski et al, 1986]. Therefore, reducing the S levels to very low levels (<0.001%), has been found to give excellent hot ductility, even when high volume fractions of AlN were present, either at the austenite boundaries or within the matrix.

Several intergranular fractures of commercial C-Mn-Al and C-Mn-Nb-Al steels, heated directly to the test temperature or cooled after partial solution treatment have been examined by Auger technique [Nachtrab et al, 1986] and have shown S segregation to the boundaries. However, correlation with hot ductility behaviour could not be established. The

impairment in ductility was related to the microalloying precipitation, with possibly some correlation with the segregation of As, Cu and Sn to the boundaries. However it should be noted that, the occurrence of this kind of segregation occurred only during deformation. Recent experiments carried out on HSLA steels suggests the S impairment in hot ductility is due to MnS precipitated at the grain boundaries[Abushosha et al, 1998p227] Nevertheless, it is likely that a similar exercise carried out on plain C-Mn steels with varying S levels would help resolve the question of the relative importance of S segregation as opposed to sulphide precipitation in influencing the hot ductility. Many recent studies on varying the cooling rate after casting have however, tended to rule out S segregation as being important in HSLA steels. Increasing the cooling rate although suppressing S segregation never gives rise to better ductility but to worse. The worse ductility has been shown to be due to finer sulphides being produced at the grain boundaries.

Reduction in S levels is certainly one of the best methods of reducing transverse cracking. Fortunately, commercial S levels in HSLA steels have been progressively reduced over the years, not because of the benefits to hot ductility but because of the benefits that this confers on the fracture toughness.

Aluminium

The impairment caused in hot ductility by aluminium is related to the fine AlN nitrides that are precipitated in the austenite grain boundaries. The AlN precipitation is controlled by the [Al]x[N] product. This controls the volume fraction of precipitates. Another possible explanation to account for increase in transverse cracking related to

increasing Al levels can be deduced from some Auger work by [Edwards, et al, 1982]. This work suggests that Al encourages ferrite formation by segregating to the austenite boundaries during casting in such large amounts that ferrite can form at the boundaries at temperatures much higher than those encountered in typical hot tensile tests on solution treated steel. Also, [Vodopivec, et al, 1988] reported that cracking may be caused by the presence of a coarse dendritic structure, which is favoured by increasing the level of Al in solution to at least 0.04%. The fact that this explanation differs widely from that based on the precipitation of AlN again indicates the need to develop hot tensile tests which simulate the continuous casting operation even more closely than only casting "in situ".

Carbon

Carbon is not surprisingly, one of the elements that has received much attention in recent years due to its importance for steels. It affects the ductility trough since carbon has a very important influence on the austenite to ferrite transformation i. e., the Ae_3 and Ar_3 temperatures. On cooling from high temperatures (1350°C), the mechanism proposed for intergranular failure has been outlined in the section "Embrittlement by strain concentration and microvoid coalescence at grain boundaries" above. As raising the C level lowers the transformation temperatures the hot ductility curve is also displaced to lower temperatures. Such behaviour has indeed been observed by many investigators in both plain C-Mn and C-Mn-Al steels, Fig. 2-23[Crowther and Mintz, 1986p671]; [Hannerz, 1985]; [Suzuki et al, 1984p169].

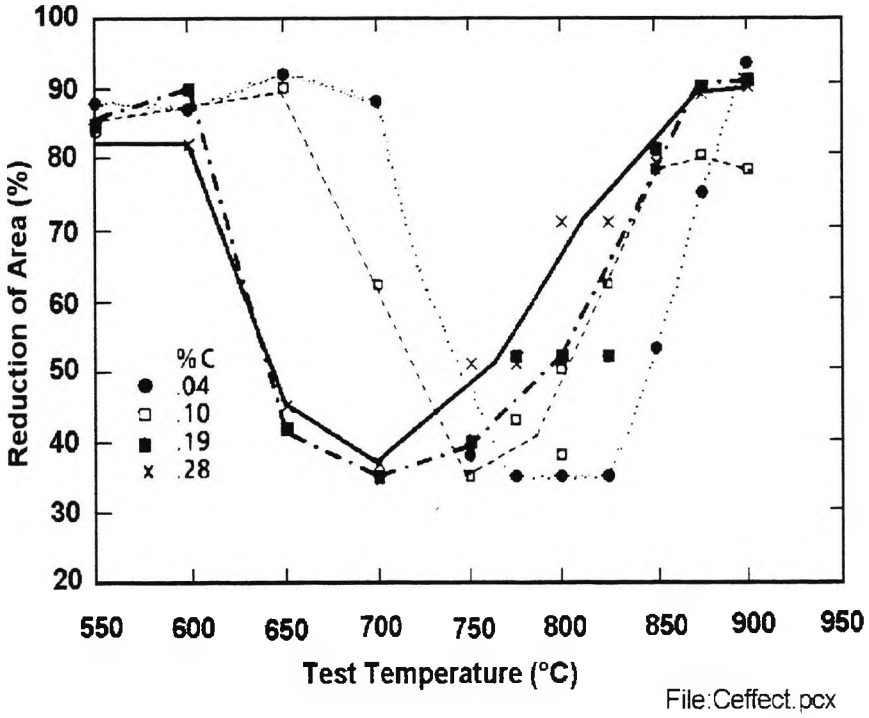


Figure 2–23: ***- Hot ductility curves for series of plain C-Mn steels (C contents in wt-%) having same grain size (300 μm) [Crowther and Mintz, 1986p671].***

The principal effect of carbon is moving the curves down to lower temperatures as the C level is increased. However, [Suzuki et al, 1984p169] have noted that the trough is also deepened. For C-Mn-Nb-Al steels with Nb≤0.03%, it is generally agreed that C has little influence on the position of the trough, [Maehara et al, 1984]; [Ouchi et al, 1982]; [Mintz and Mohamed, 1989] except at C levels ≤0.05%, when both the depth and width of the trough are reduced [Mintz and Mohamed, 1989]. This is because of the overriding influence of Nb(C,N) precipitation in the austenite on ductility. In fact, the ductility deteriorates as the volume fraction of Nb(C,N) precipitation increases (Fig. 2-24).

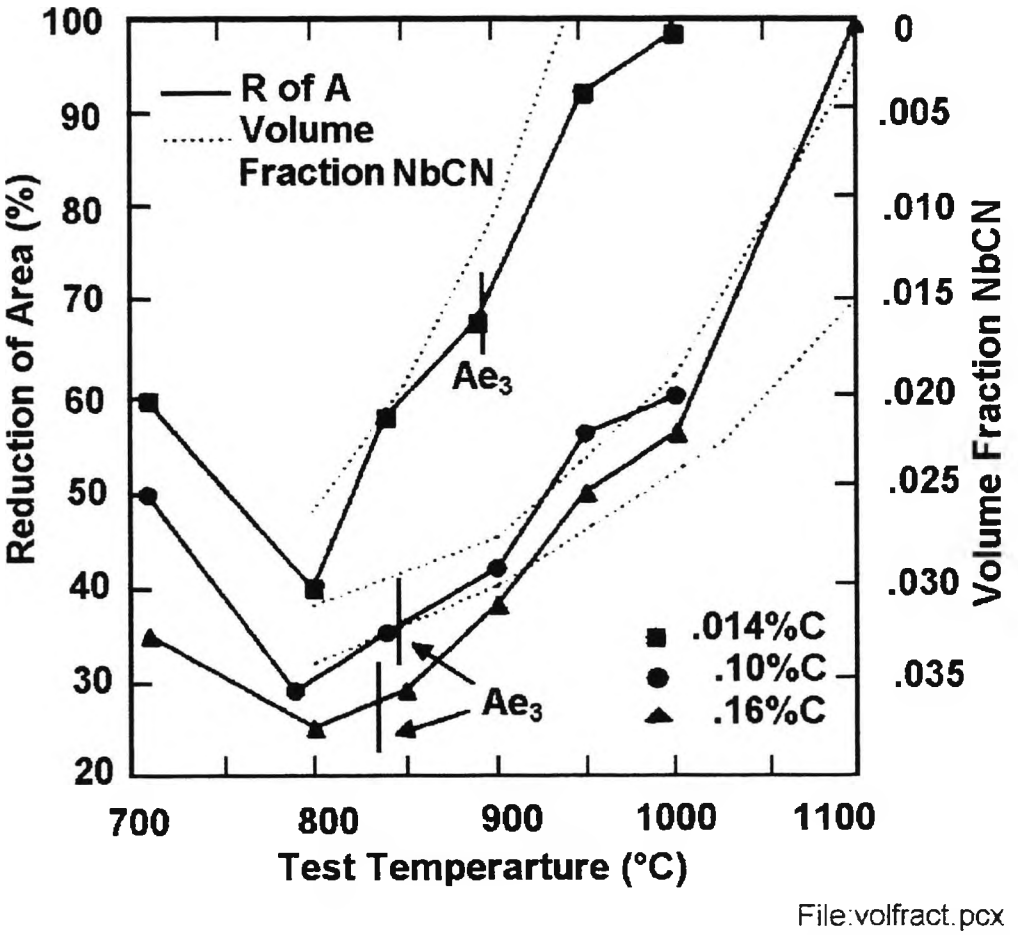


Figure 2-24: ***- Relationship of shape and position of hot ductility curves to volume fraction of NbC precipitated, assuming equilibrium solubility, in steels with 0.025%Nb, but with varying C contents: steels were solution treated, cooled to test temperature, and tested at strain rate of $3x10^{-3}s^{-1}$ [Mintz and Mohamed, 1989].***

Carbonitrides precipitation is also strain induced and occurs relatively rapidly during testing, [Mintz and Mohamed, 1989] so that the volume fractions can reach the equilibrium levels during the long times associated with low strain rate tests. The amount of Nb(C,N) precipitated at a given temperature depends on the Nb, C and, to a lesser extent, the N level. One typical example is for a steel with 0.03%Nb, when the C levels exceeds 0.05%C

there is little further increase in the volume fraction precipitated and hence ductility in the trough region is relatively insensitive to the C level.

Published commercial results concerning the effect on transverse cracking are often sparse and uncertain due to the masking effects of other elements present together such as Al and Nb. Nevertheless, statistical analysis reported of commercial data[Hannerz, 1985] showed that increasing the C level in fine grained C-Mn-Nb-Al steels led to a small reduction in the incidence of transverse cracking. More specifically, it has been found that there is an increased level of transverse cracking in the carbon range of 0.08-0.17%. [Ueda et al, 1981] and [Schelenberger et al, 1990]. Again, commercial data on longitudinal cracking, which has the same origins as those of transverse cracking, has indicated more clearly, a marked increase in cracking occurring when C is in the range 0.1-0.15% [Gray et al, 1979]; [Irving et al, 1977] and [Saeki et al, 1982]. The explanation for this is related to the peritectic reaction itself. The cause is reported to be due to the uneven thickness developed in the solidified shell in steels with carbon in this range during the delta ferrite to austenite transformation. The contraction accompanying that reaction, produces a gap between the shell and the mould, resulting in the reduction of heat extraction from the mould [Wolf et al, 1981], Fig. 2-25

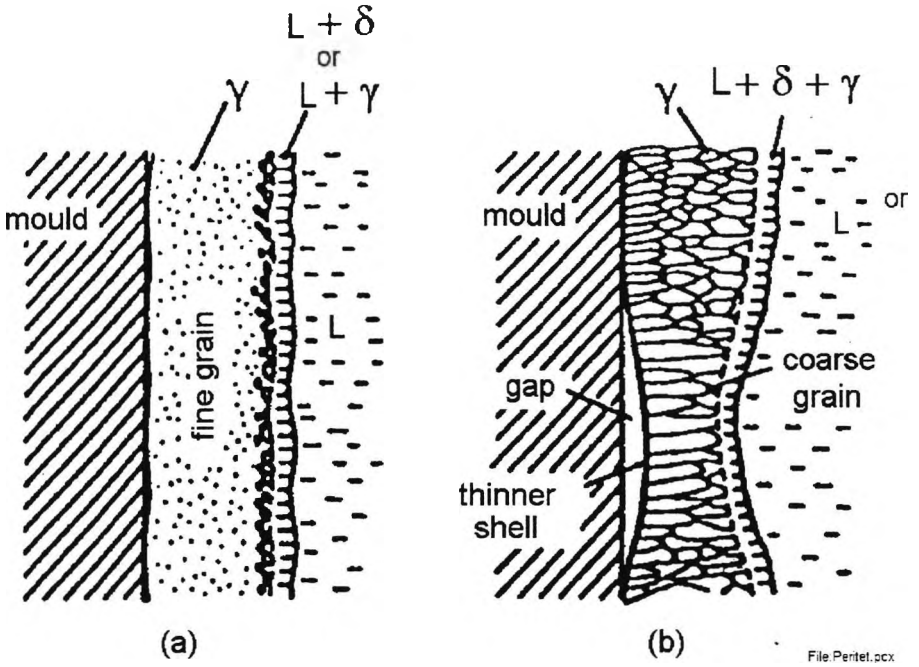


Figure 2–25: ***- Schematic illustration showing austenite structure in solidified shell [Maehara et al, 1985]***

The hotter and thinner areas of the solidified skin of the strand are then more easy to break. This shrinkage that can occur in this C range, is reported to be an important cause of cracking, as transverse cracks have at times been located high up in the mould, [Mercer et al, 1979].

Also some other work, [Harada et al, 1990] has pointed out that the incidence of cracking is largely affected by the C range close to the peritectic composition. However, this works suggests that the problem is due to the intense microsegregation of P to regions below the roots of the oscillation marks, a phenomenon that embrittles the austenite grain boundaries. The microsegregation occurs during the solidification and is related to oscillation marks, i. e. to the manner in which the partially solidified shell is deformed and then entraps liquid

high in segregants between the dendrites. The research shows also that such intense P segregation is absent when the C content is low.

There is a possibility that the conflicting results on the influence of C on transverse cracking is due to difference in the straightening temperature that is used as illustrated schematically in Fig. 2-26.

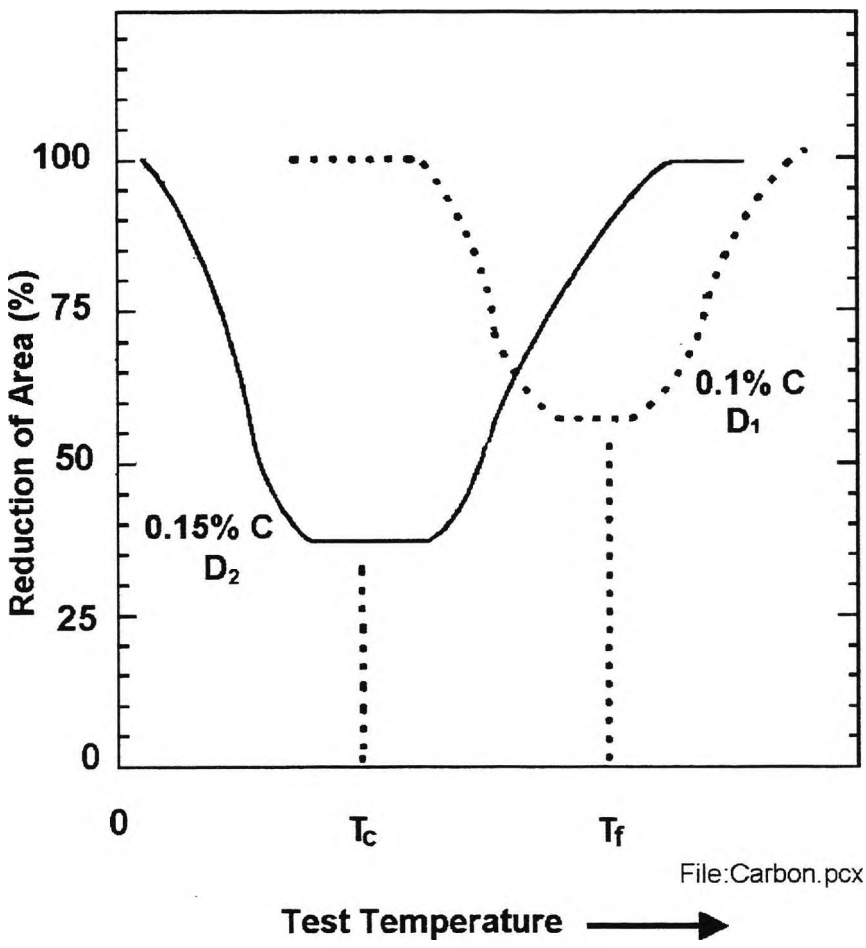


Figure 2-26: ***- Schematic diagrams for hot ductility curves for C-Mn-Al steels with different grain sizes, D_2 and D_1 (D_2>D_1), and two levels of C content 0.1 and 0.15%C. If straightening temperature is T_c then the lower C steel would have the better hot ductility; if straightening temperature is T_f, the coarser grained higher C steel would have the better hot ductility.***

Although a coarser grain size is a consequence of raising the C level to the peritectic in C-Mn-Al steels, it can also shift the trough to lower temperatures due to lowering of the transformation temperatures. The ductility will therefore be strongly dependent on the temperature as can be seen from Fig. 2-26. It is clear that more detailed studies are necessary, particularly for as-cast C-Mn-Nb-Al steels, where raising the C level will not alter the position of the trough. The coarsening of the grain size in the peritectic range may adversely influence the depth of the trough although the degree of coarsening is such as to not likely to have any marked influence.

It might be concluded that in most structural steels, increasing the C level either reduces, or has no influence the incidence of transverse cracking if the straightening operation is carried out at higher temperature. This is a result of decreasing the Ae_3 temperature, as noted in Fig. 26. However, Maehara et al, [Maehara et al, 1985] have argued that the as cast microstructures are sensitive to the C content. They have criticised tests where samples are solution treated and cooled to the test temperature as being unable to assess the influence of C on transverse cracking. They cast a series of ingots with C levels in the range 0.05-0.3% and found the very coarse austenite grain sizes were developed in the 0.1-0.15% C range. This was explained as consequence of the peritectic reaction in steels which results in the formation of coarse columnar grains. The growth of such austenite grains can be impeded by the presence of second phase particles, either to the left (the delta phase) or right (the liquid phase) of the peritectic. It was then concluded that these coarse grains would lead to poor ductility in the peritectic C range, thus favouring transverse cracks.

Interstitial: Nitrogen

In the present study the roles of Titanium and Nitrogen on hot ductility have been examined. The influence of these two elements on hot ductility is therefore reviewed in detail. The following has been abstracted from an unpublished review from Professor Mintz but forms the basis for the present study and is therefore quoted extensively.

Influence of N on transverse cracking and hot ductility

Hannerz's statistical analysis of work's data [Hannerz, 1985] has shown that N is very potent in encouraging transverse cracking in continuously cast steel. Hannerz has also shown that nitrogen itself has little influence on the hot ductility of high Mn steels (1.4%Mn). It is only when N is present with Al that ductility is impaired. It is therefore the influence N has on precipitation processes that dictates the ductility and in consequence the various grain refining and microalloying systems will now be reviewed.

C-Mn-Al steels

There have been a number of investigations into the influence of Al and N on hot ductility[Hannerz, 1985; Chamont et al, 1988; Mintz and Wilcox, 1980; Cardoso and Abushosha, 1994; Suzuki et al, 1984p175 and Bernard, 1980]. Generally, the simple hot tensile procedure is used in which the tensiles are solution treated at 1330°C and cooled to test temperatures in the range 1000 to 700°C and tested at a strain rate of ~$10^{-3}s^{-1}$. It is found that increasing either the Al or N levels leads to a deterioration in

ductility causing both a widening and deepening of the trough, as can be seen from the work of [Chamont et al, 1988] in Fig. 2-27.

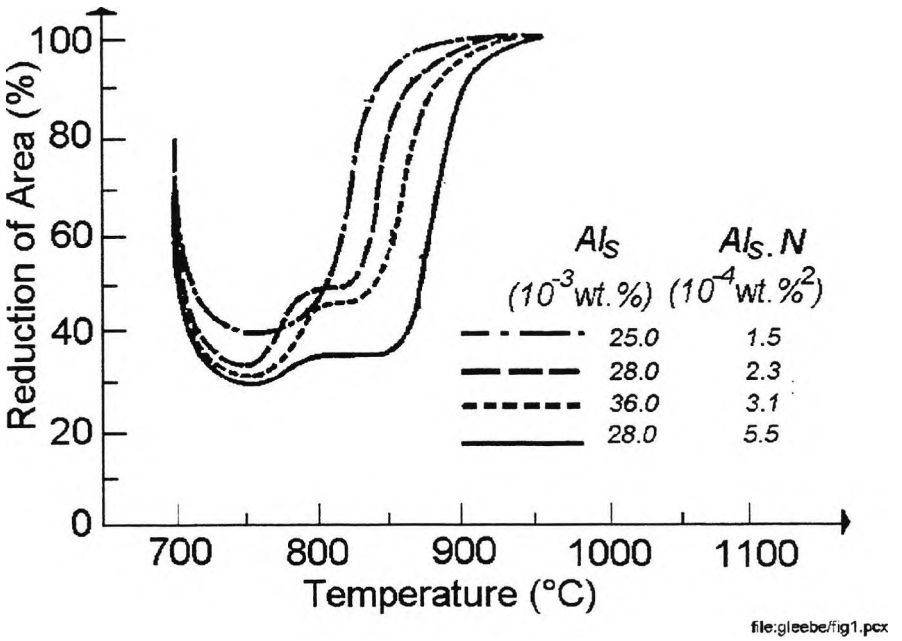


Figure 2–27:: ***Hot ductility curves for C-Mn-Al steels with various levels of soluble Al and N.***

Cardoso [Cardoso and Abushosha, 1994] have recently examined the influence of Al and N in detail. Their work showed that it was the product of the [sol.Al]x[N] which is important in controlling ductility and it does not matter for the same product whether it is the N or Al that is high. Because AlN precipitates from the γ very sluggishly, it is often difficult to find any influence of Al and N on the hot ductility at low levels (0.02/0.04%Al, 0.005%N), as no AlN precipitates out either before or during the test[Ouchi et al, 1982 and Crowther, Mohamed and Mintz, 1987p1929]. For high Mn steels (1.4%Mn), the product of the [sol.Al]x[N] had to approach quite high values of $2x10^{-4}$ (e.g. 0.02%Al and 0.01%N) for precipitation to occur. However, when temperature oscillations are

introduced, AlN precipitation occurs even in low Al/N steels, when the product is as low as $1x10^{-4}$ (e.g. 0.02%Al and 0.005%N)[Cardoso and Abushosha, 1994].

It is likely with temperature oscillations that a large proportion of the N is precipitated out as AlN, so that it is probably the volume fraction of AlN precipitated which mainly controls ductility. It should also be noted, that AlN precipitation in lower Mn steels is likely to be easier, since Mn increases the solubility of carbonitrides in the austenite[Michel et al, 1981].

Coarsening of the AlN precipitation might be expected to improve ductility. Coarser precipitation is likely to be favoured by a) slower cooling rates to the test temperature, b) strain, c) a high value of [Al]x[N] as this will encourage precipitation to occur at higher temperatures, and d) a higher level of dissolved Al as the growth rate of the AlN precipitate will be dependent on the dissolved Al in the Υ, Al being the slower diffusing element in the precipitate. However, such coarsening appears difficult to achieve in the time available during the test or during straightening.

Clearly, for C-Mn-Al steels it is recommended that the Al and N levels are kept low to avoid transverse cracking and where this principal has been followed there have been no problems with cracking[Mintz et al, 1991].

C-Mn-Nb-Al steels

The influence of N on transverse cracking of these steels has been found to be marked[Hannerz, 1985]. The hot ductility behaviour also mirrors the transverse cracking behaviour, in that higher N levels give rise to worse ductility[Ouchi et al, 1982 and Mintz and Arrowsmith, 1979p99]. However, changes in ductility are generally smaller than might have been expected from the transverse cracking behaviour. Fracture examination of tensile samples and from continuously cast slabs, indicate little evidence for AlN precipitation, except at very high Al levels, and then it is coarse[Mintz and Arrowsmith, 1979p24]. The temperature for the maximum rate of precipitation is in the region of 950°C for NbCN and 815°C for AlN so that NbCN would be expected to precipitate out before AlN on cooling, but as mentioned AlN has great difficulty in nucleating on cooling through the ϒ range[Weiss et al, 1979] and [Leslie et al, 1954]. Nevertheless, increasing the Al[Mintz and Arrowsmith, 1979p24]; [Ouchi et al, 1982]; [Bernard et al, 1978] and [Wilcox et al, 1984] or N level[Ouchi et al, 1982] and [Mintz and Arrowsmith, 1979p99] in these Nb containing steels does cause the ductility to deteriorate, Fig. 2-28. There is some evidence to suggest[Mintz and Arrowsmith, 1979p24] that the inferior ductility obtained on adding Al is due to the Al producing a finer precipitation of Nb(CN), rather than precipitation of AlN. It is possible that the Al slows down the movement of the N atoms so that precipitation of Nb(CN) occurs at lower temperatures, and hence is finer. However, precipitation of AlN on increasing the Al or N level cannot be ruled out, since AlN is not always easy to detect.

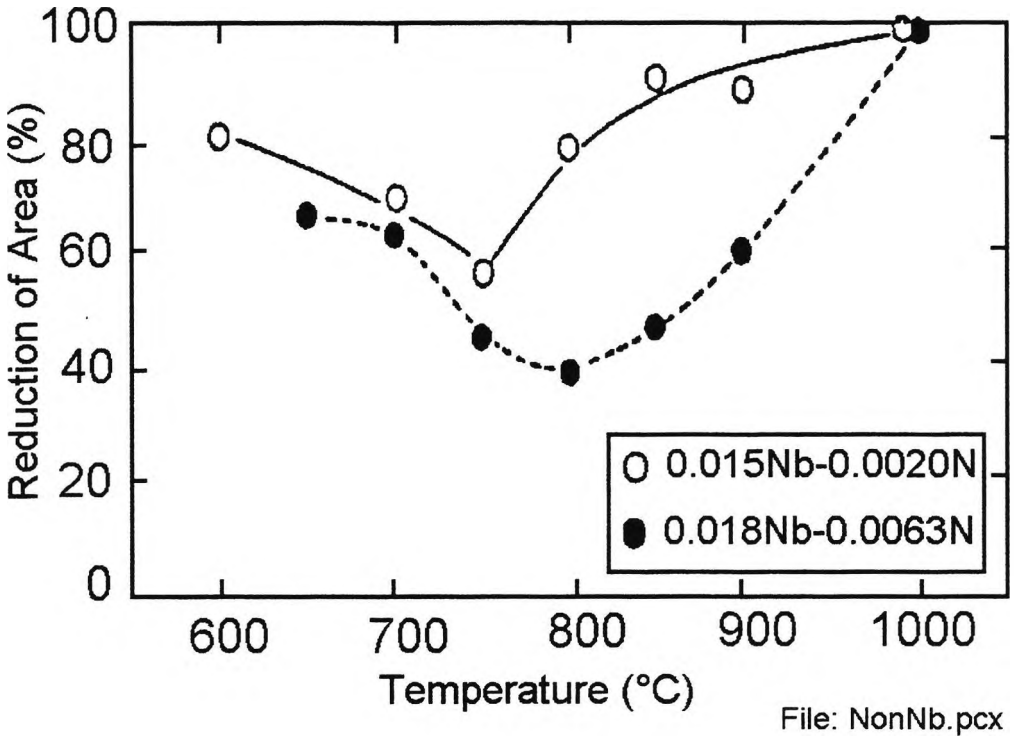


Figure 2–28: ***- Influence of N on the hot ductility of Nb containing steels[Ouchi et al, 1982].***

[Ouchi et al, 1982] have suggested that the effect of N on Nb containing steels may be dependent as to whether the N level is above or below 0.005%, Fig. 2-28. At low N levels (0.002%N), $NbC_{0.85}$ was formed whereas at higher N levels (0.006%), this changed to $NbC_{0.6}$ $N_{0.25}$. It was suggested that Nb(CN) is able to precipitate more readily than NbC in the lower temperature region of γ. Certainly, with microalloyed steels, on cooling down through the austenite field, it is the nitrides which will precipitate first before the carbides. Thus raising the N content might be expected to encourage precipitation in the austenite if the composition of the precipitate approaches closer to a nitride.

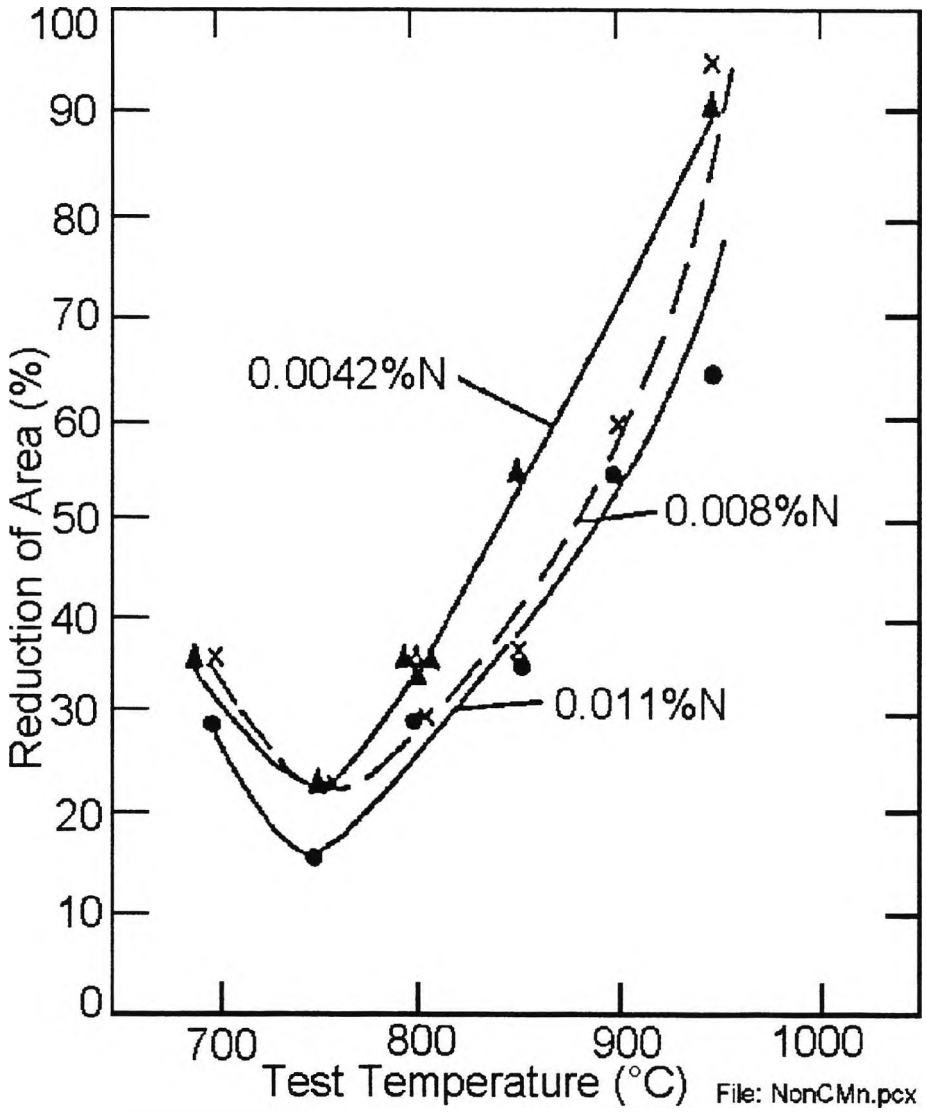


Figure 2–29: ***- Influence of N on hot ductility curves of C-Mn-Nb-Al steels (sol.Al 0.032-0.042%, Nb 0.034%)[Mintz and Arrowsmith, 1979p99].***

Work by [Mintz and Arrowsmith, 1979p99] has however, shown that the deterioration is progressive throughout the range 0.004 to 0.011%N and changes in ductility are relatively small, Fig. 2-29. This is probably because an increase in the nitrogen level will have only a small influence on the volume fraction of Nb(CN) that is precipitated out. Compared to the other microalloying additions, Nb(CN) precipitates out very

rapidly during deformation and often all or a very large part of the Nb is precipitated out in the time of the test at these low strain rates (i.e. equilibrium conditions are achieved), Fig. 2-30[Abushosha and Vipond, 1991p1101] and also Fig. 2-24[Mintz and Mohamed, 1989p2575] for solution treated steels. Again, because the N level would not be expected to have much influence on the volume fraction of Nb(CN) that is precipitated, the detrimental influence of N on transverse cracking is most likely related to the enhancement of AlN precipitation, which occurs during the temperature oscillations to which the strand is subject.

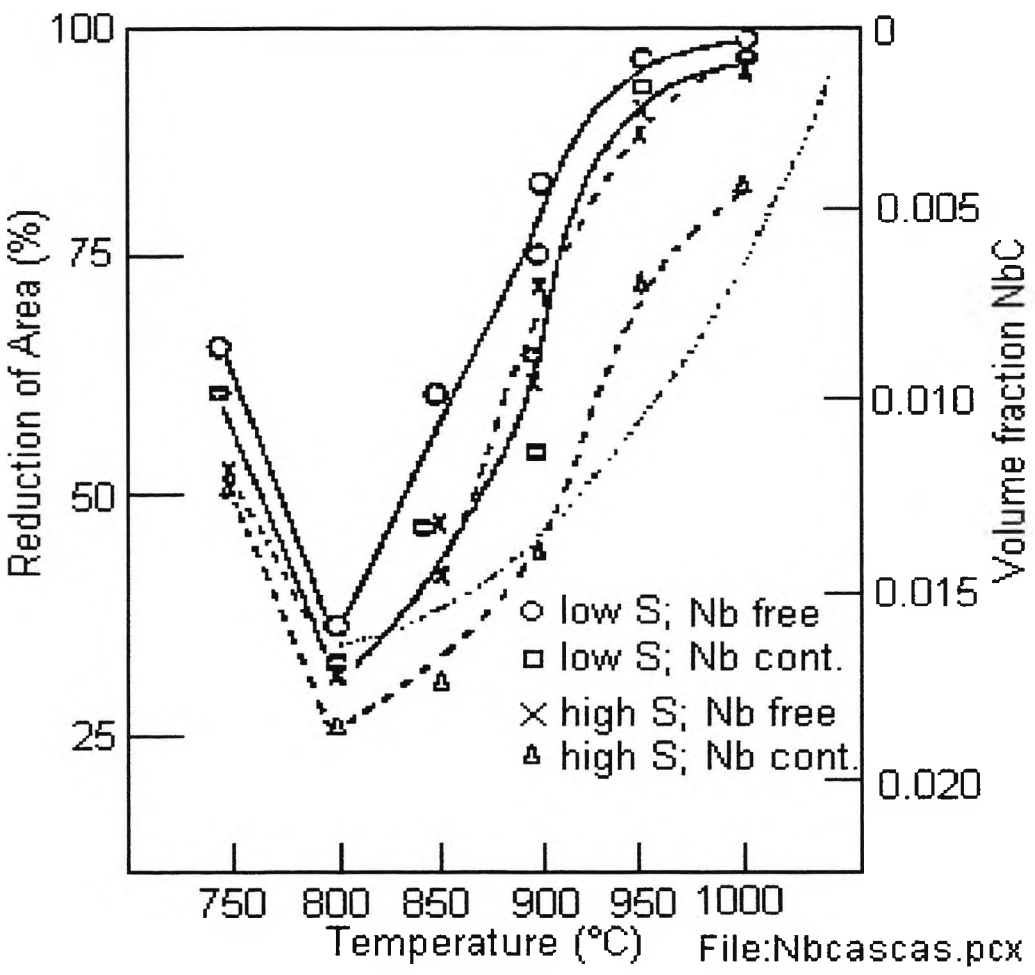


Figure 2–30: ***- Calculated volume fractions of NbC precipitating as a function of test temperatures with accompanying hot ductility curves (as cast)[Abushosha and Vipond, 1991p1101]. (As cast calculation assumes 50% of NbC is in the eutectic.***

Clearly, whatever is the exact mechanism of embrittlement, it is important to keep the N as well as the Al levels as low as possible. Raising the Nb level at constant N level, as would be expected, also causes the hot ductility to deteriorate [Ouchi et al, 1982; Mintz et al, 1991 and Mintz and Arrowsmith, 1979p99] *as well as encouraging transverse cracking[Mintz and Abushosha, 1992 and Ouchi et al, 1982].*

C-Mn-V-Al steels

Until recently there has been very little information on the hot ductility of V containing steels. It is known that high V, high N steels are susceptible to transverse cracking[Coleman et al, 1985]. Hannerz's [Hannerz et al, 1985] statistical analysis of works data gave only a small detrimental effect of V on transverse cracking but only a few V containing steels were included in the analysis.

Hannerz's hot ductility work[Hannerz et al, 1985] suggested that with a high N steel (0.016%N), the V content had to be in excess of 0.07% to produce a significant deterioration in ductility.

More recent work by Mintz and Abushosha[Mintz and Abushosha 1993] has looked at steels with varying amounts of V and N and compared their ductility with a more conventional 0.03%Nb, 0.005%N steel. Samples as before, were solution treated and strained at a strain rate of $3x10^{-3}s^{-1}$ to failure. The curves are shown in Fig. 2-31, and indicate that raising the V or N level causes the ductility to deteriorate. The effect of increasing the product of the total V and total N, $[V_t]x[N_t]$ in reducing the width and depth of the trough, are shown in Figs. 2-32a and 2-32b respectively. Also included in

these figures is the base line for the conventional Nb containing steel so that comparisons can readily be made. It is apparent from these curves that the ductility decreases with increase in V and N levels but provided the product $[V_t]x[N_t]$ is $< 1.2x10^{-3}$, e.g. 0.1%V and 0.012%N, V-N steels will show a reduced tendency to cracking compared with a conventional Nb containing steel.

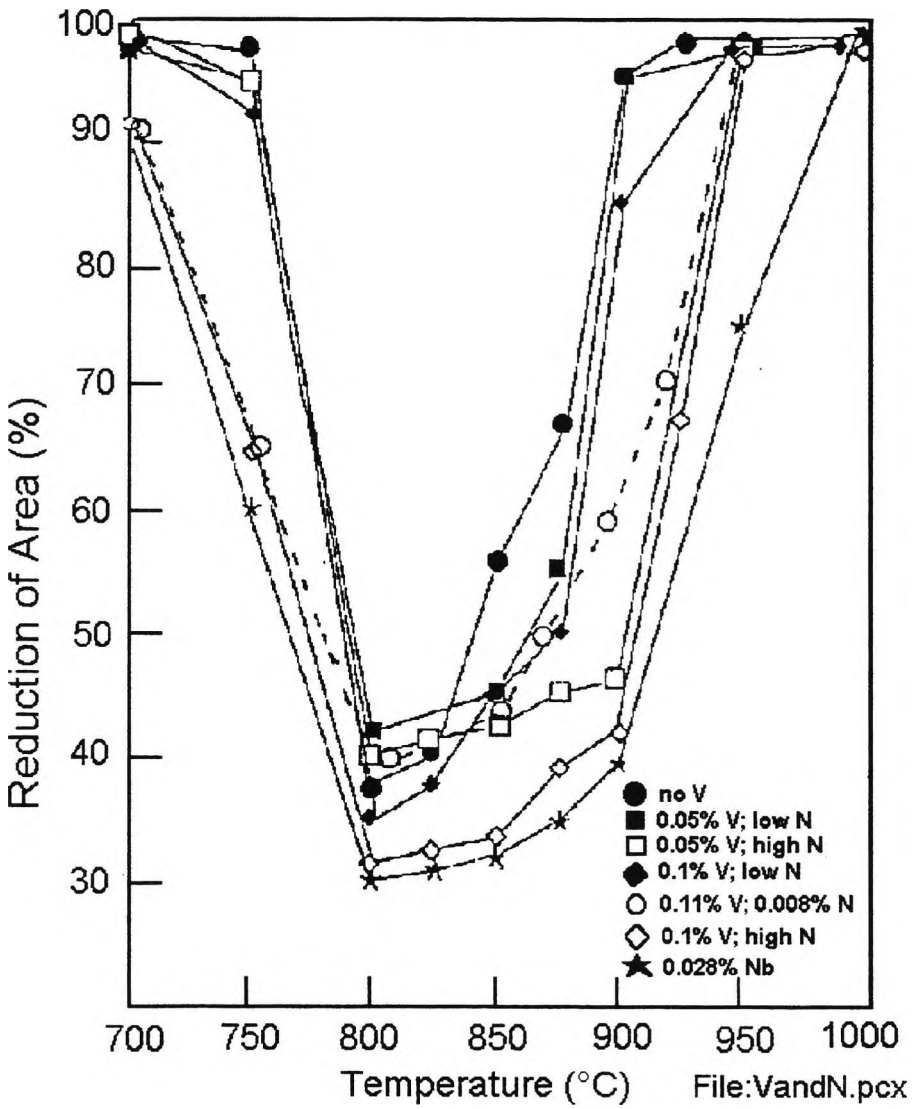
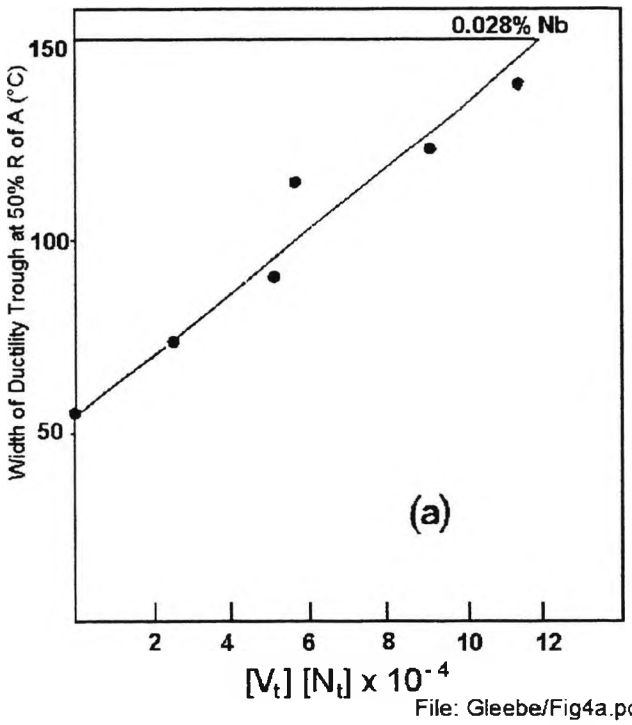
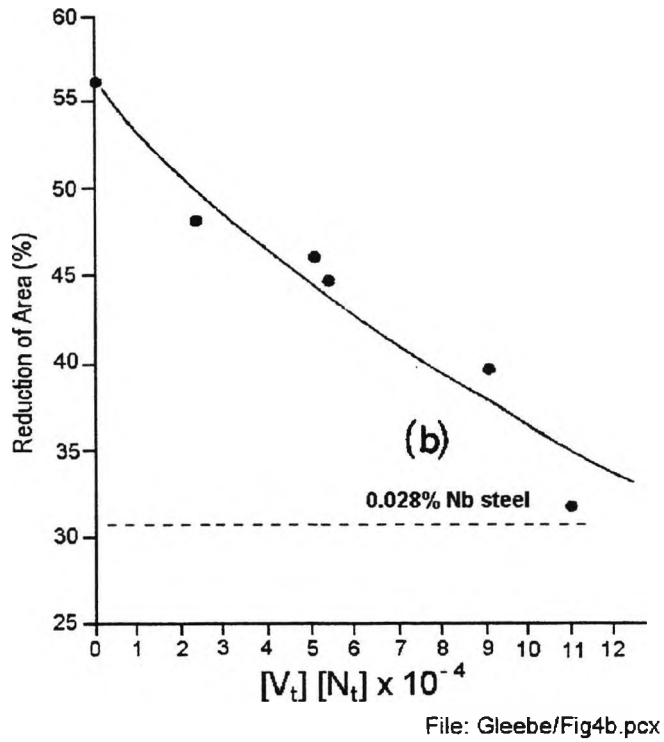


Figure 2-31: ***- Hot ductility curves for a series of steels having different levels of V and N (also included is a curve for a Nb containing steel for comparison). Steels were solution treated at 1330°C[Mintz and Abushosha, 1993].***



File: Gleebe/Fig4a.pcx



File: Gleebe/Fig4b.pcx

Figure 2–32: ***- (a)The effect of product of total V and N contents on width of the trough. (b) The influence of product of total V and N contents on reduction of area values; steels were tested at 850°C in the trough[Mintz and Abushosha, 1993].***

It should be noted, that again, no AlN precipitation was observed in any of these steels, all the nitrogen being combined with the vanadium. Wilson and Gladman[Wilson et al, 1988] have also noted that VN can form in preference to AlN, despite the greater thermodynamic stability of the latter.

Raising the V or N levels was shown to increase the amount of VN precipitation. Although increasing the product generally led to an increase in the volume fraction of VN precipitated this was not always the case, as it can be shown that under equilibrium conditions N is more effective in inducing precipitation than V.

Precipitates were coarser in the V containing steels than in the Nb steel probably as a result of the higher solubility of V in the austenite compared to Nb. Thus V is probably less detrimental to ductility than Nb because it precipitates in a coarser form and a greater volume fraction of precipitate is required to cause the ductility to deteriorate. Recent work by Crowther and Morrison [Crowther et al, 1994] has also shown that the cracking tendency of Nb steels is much greater than V containing steels.

Summarising, it is apparent that nitrogen in V containing steels is detrimental to ductility and should be kept as low as possible. Although V containing steels may show a reduced tendency to exhibit transverse cracks compared to Nb containing steels, the effect of N per se may be more serious in the V containing steels as the detrimental precipitate here is entirely nitrogen based, i.e VN, whereas for Nb it is generally a mixed carbonitride, Nb(CN) with carbon being the major constituent.

Influence of N on Ti containing steels

Commercial Experience

Commercial data on the influence of Ti additions on the problem of transverse cracking, indicates that small Ti additions have a beneficial effect[Coleman et al, 1985]; [Turkdogan, 1987]; [Hater et al, 1973]; [Patrick et al, 1994]; [Private com, 1994]; [Williams, 1984] and [Turkdogan, 1987] reports that when steels have <0.0045%N and Ti is in the range 0.015 to 0.02% transverse cracking is considerably reduced. Hoesch[Hater et al, 1973] have also established that Ti additions in the range 0.02 to 0.04% are beneficial in preventing transverse cracks from forming. Coleman and Wilcox[Coleman et al, 1985] reporting on British Steel experience, similarly state that Ti additions reduce transverse cracking and the recommended range has recently been quoted as 0.015 to 0.04%Ti[Patrick et al, 1994]. More recent experience at the Scunthorpe works of British Steel[Private com, 1994], indicates a reduced scarfing requirement when Ti additions in the range 0.015 to 0.02% are made to Nb grade 50 steels having C in the range 0.1 to 0.17% (i.e. within the peritectic range), and nitrogen contents typically of 0.005%. *Lower Ti additions (0.01%) showed no benefits.*

Unfortunately, the optimum Ti addition for HAZ toughness improvement is around 0.01% and above this level toughness is observed to deteriorate. This is believed to be due to coarse (several microns) TiN particles forming; these particles being favoured by slow cooling[Linaza et al, 1995].

It has also been claimed that for Ti treated Nb containing low C steels (<0.08%C), no scarfing is required but these steels are outside the peritectic range and would be expected not to give problems[Williams, 1994].

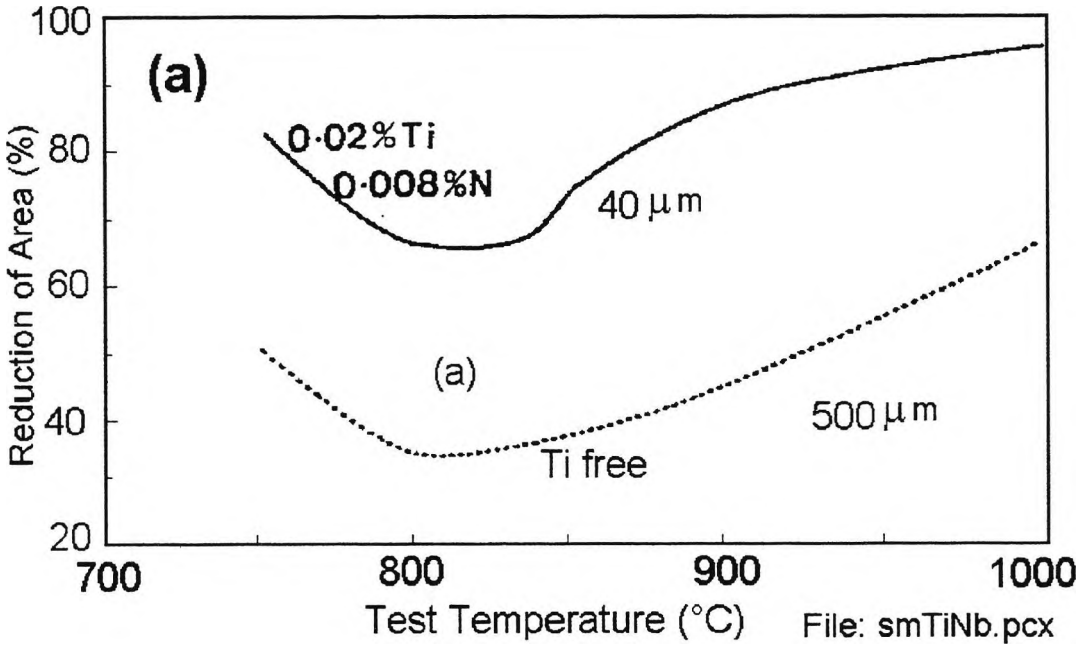
Finally, Russian work[Razunov et al, 1986] on general surface quality (includes all surface defects) of hot rolled skelps from continuously cast billets has found small Ti additions to be beneficial. It is also of interest to note, with regards to any problems with higher residual levels, that their analysis of work's data showed residual Ni to be actually detrimental to surface quality (as was Cu to a lesser extent) while Cr and P were the best elements to have present. They recommended keeping P levels close to the maximum allowable, 0.02%, and raising the Cr level to 0.3%.

Hot ductility data

a) Reheated tensile tests

A review of most of the papers[Mintz and Crowther, 1994] on hot ductility in which Ti has been added to steels suggests that it is the miracle cure for transverse cracking, ductility always improving dramatically[Ouchi et al, 1982]; [Hannerz et al, 1985]; [Anelli et al, 1993]; [Mintz and Wilcox, 1980]; [Mintz and Crowther, 1994]; [Valders et al, 1990]; [Fu et al, 1988] and [Funnel et al, 1978].

Curves from two such examinations are shown in Fig. 2-33.



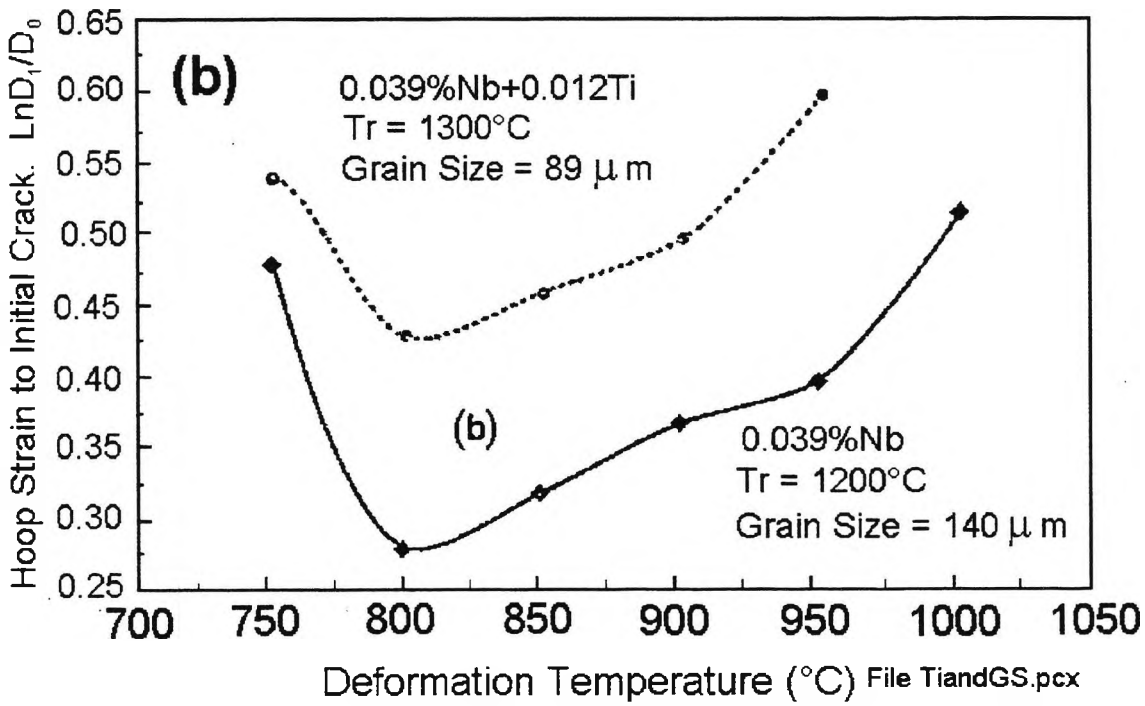


Figure 2–33: ***- Influence of small Ti additions on the hot ductility of reheated Nb containing steels, (a)[Abushosha and Vipond, 1991p613],(b) [Mintz and Mohamed, 1989p2575]. Grain sizes of the steels after solution treatment are indicated on the curves.***

However, all these investigations have been carried out on steels which have been reheated so that the TiN particles have not completely redissolved and are therefore able to grain refine when transformation to γ takes place, (the grain sizes are indicated on the curves)[Mintz and Crowther, 1994]. The large improvements noted in ductility in these examinations are therefore, due to grain refinement, not differences in composition. In the sole investigation in which grain size was not refined on reheating to 1350°C, only a small improvement in ductility was noted, Fig. 2-34[Mintz and Arrowsmith, 1979p99].

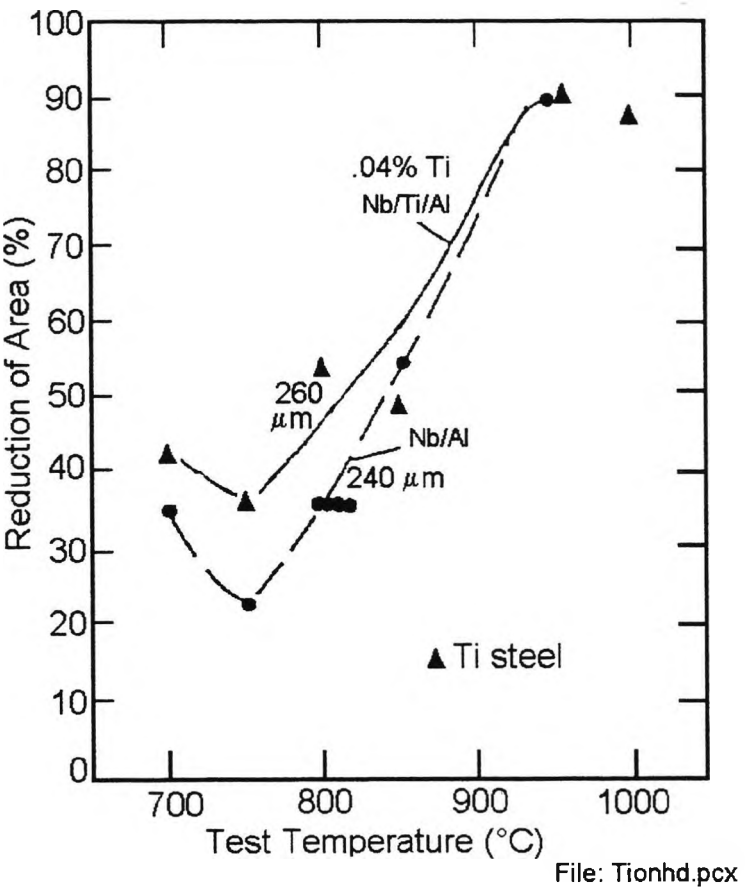


Figure 2–34: ***Influence of a 0.04%Ti addition to a C-Mn-Nb-Al steel containing 0.004%N. The steels had similar grain sizes after solution treatment (grain size marked on curves), and in consequence only a small improvement was noted[Mintz and Arrowsmith, 1979p99].***

The steel in this investigation had a very high Ti:N ratio of 9:1 as well as a high product of [Ti]x[N], $1.72x10^{-4}$, and it is likely that only very coarse TiN particles were formed which would not be able to refine the grain size on subsequent heating. The small improvement in ductility noted is probably due to the Ti removing N as TiN, preventing the detrimental precipitation of AlN.

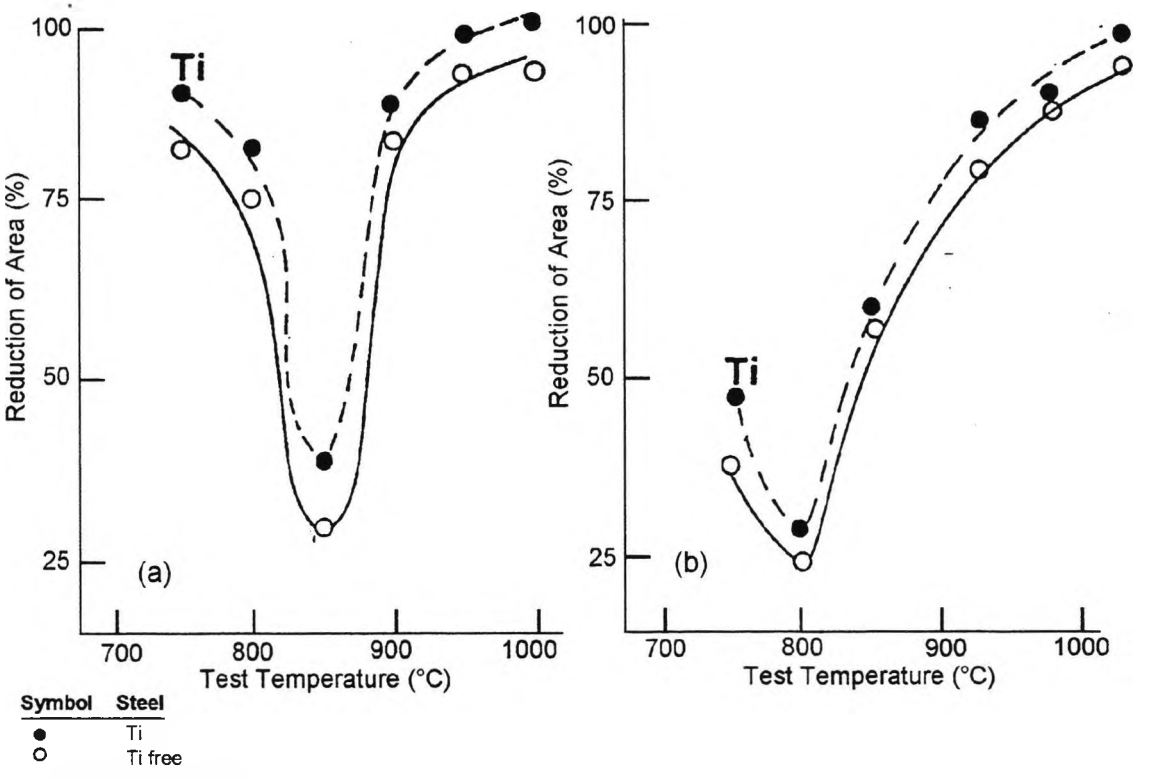
b) As cast tensile tests

To examine the influence of Ti additions on ductility it is essential to cast the tensiles and cool directly to the test temperature. When solidification occurs and the as cast structure is formed, there is then little opportunity for Ti precipitation to cause grain refinement. The results from two such investigations on as cast tensiles are shown in Figs. 2-35 and 2-36[Abushosha and Vipond, 1991p613 and Mintz, Abushosha and Cardoso, 1995]. In both cases, no grain refinement occurred in the Ti containing steels and as a consequence, the large improvements in ductility previously noted for steel reheated to ~1350°C, Fig. 2-33 were absent. In the earlier examination[Abushosha and Vipond, 1991p613], Fig. 2-35, a rather small improvement in ductility similar to that shown in Fig. 2-34, was observed, whereas in the more recent examination[Mintz, Abushosha and Cardoso, 1995], Fig. 2-36, a significant deterioration in ductility was apparent. The small improvement noted was again believed to be due to the Ti removing the nitrogen and preventing the finer more detrimental AlN from forming.

Thus, for as cast conditions, the benefit to ductility on adding Ti seems to be either small or very detrimental.

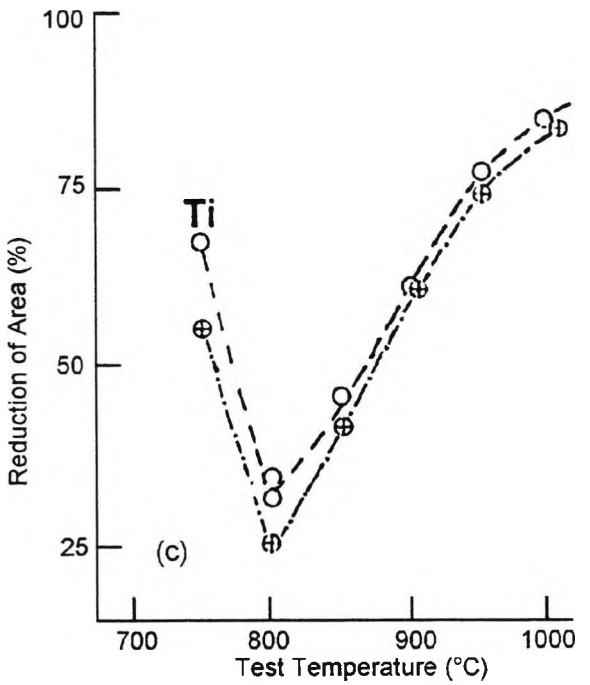
It should, however, be born in mind that for Ti containing steels, as well as it being essential to cast the tensiles, it may also be necessary to introduce temperature oscillations in order to show up the true potential of a Ti addition. It would be expected, for example, in the case of the Ti containing steel in Fig. 2-35, which shows only a small improvement in ductility over the Ti free steel, that this improvement would be magnified if temperature oscillations had been introduced.

Clearly, it is very important to be able to precisely define the conditions which give rise to the small improvements shown in Fig. 2-35, and those which cause the marked deterioration in Fig. 2-36.



(a) 0.005%C; (b) 0.15%C

Hot ductility curves for as cast C-Mn-Al steels of different C content and with and without Ti addition: cooling rate to test temperature 60°C/min.



File:Tiadd.pcx

Figure 2–35: ***Influence of Ti on the hot ductility of as cast; (a)0.05%C, C-Mn-Al steel (b) 0.15%C, C-Mn-Al steel (c) 0.1%C, C-Mn-Nb-Al steel. Ti levels were ~0.019% and N was 0.009%[Abushosha and Vipond 1991p613]. Cooling rates were 60 to 100K/min***

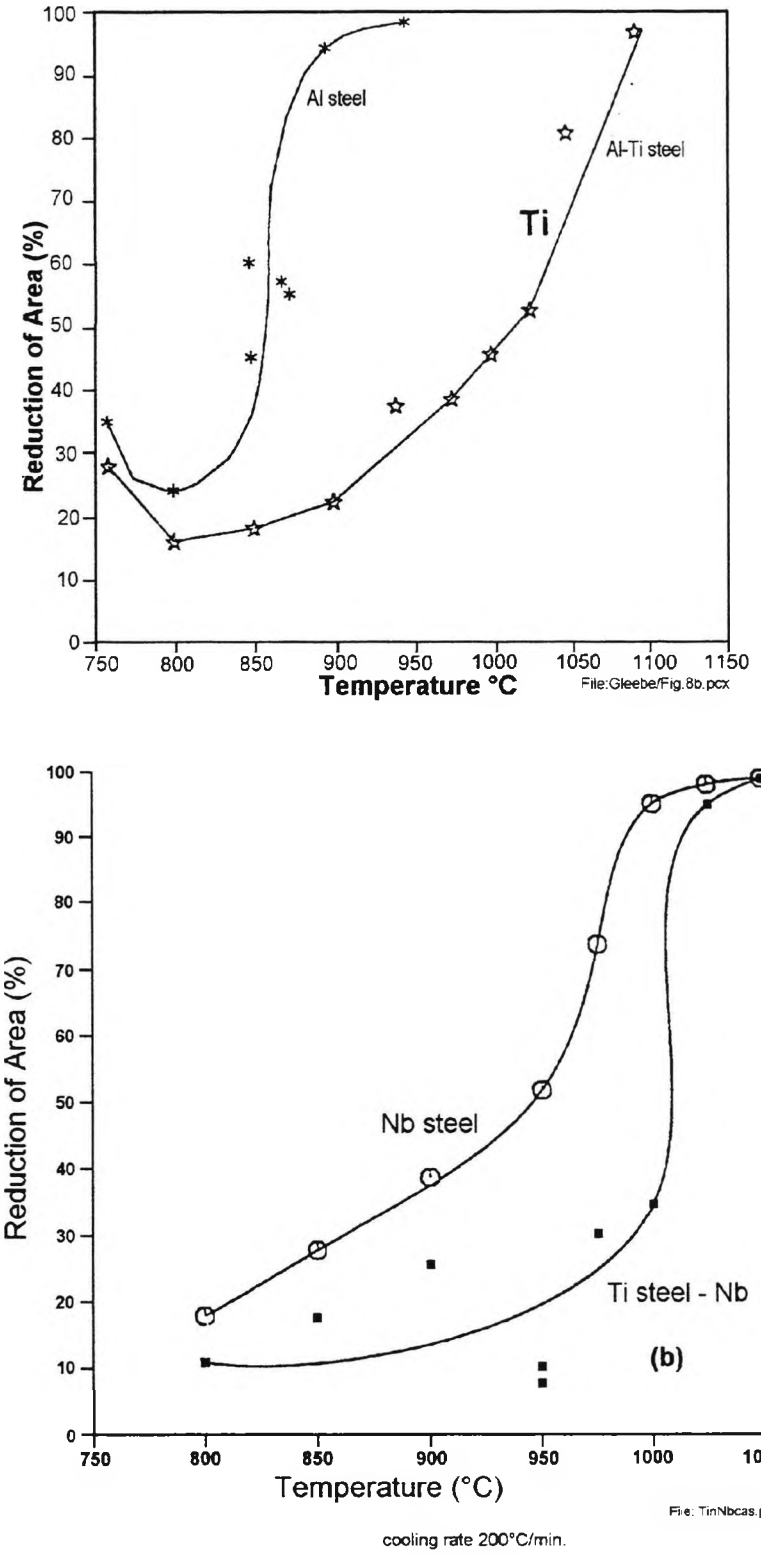


Figure 2–36: ***Influence of Ti on the hot ductility of: (a) as cast C-Mn-Al (b) as cast C-Mn-Nb-Al steels. Ti and N levels were 0.20% and 0.006% respectively[Abushosha, 1997].***

Examination of their compositions suggests that it is the Ti:N ratio and levels of Ti and N present in the steel, which are important. The Ti steels used in the latest investigation, Fig. 2-36, had compositions very close to the stoichiometric composition for TiN, 3.4:1, whereas in the first examination, Fig. 2-35 on a higher N steel (~0.009%N), the Ti:N ratio was 2. Replica examination of the Ti steel with the stoichiometric composition, has shown the presence of fine TiN particles at the boundaries <10nm [Abushosha, 1997]. In contrast, in the earlier examination[Abushosha et, al, 1991], coarser particles were found. In the C-Mn-Al steel, the cuboidal TiN particles were in excess of 50nm, while in the Nb containing steel, dendritic particles of NbTi(CN) richer in niobium were obtained of similar size[Abushosha and Vipond, 1991p613]. (It should be noted that TiN and Nb(CN) are mutually soluble so that mixed carbonitrides are formed in as cast material, often rich in Nb rather than Ti. It has been calculated that the segregation coefficient of niobium is very high between 8 and 25, while that of Ti is between 3 and 6[Chen et al, 1987]. Generally, particles start to reduce ductility when they are less than 50nm in size and are likely to give rise to serious transverse cracking problems when they are in the region of ~10nm, Fig. 2-37[Mintz et al, 1991]. Thus compositional control may be very important if Ti is to be a beneficial addition to ductility.

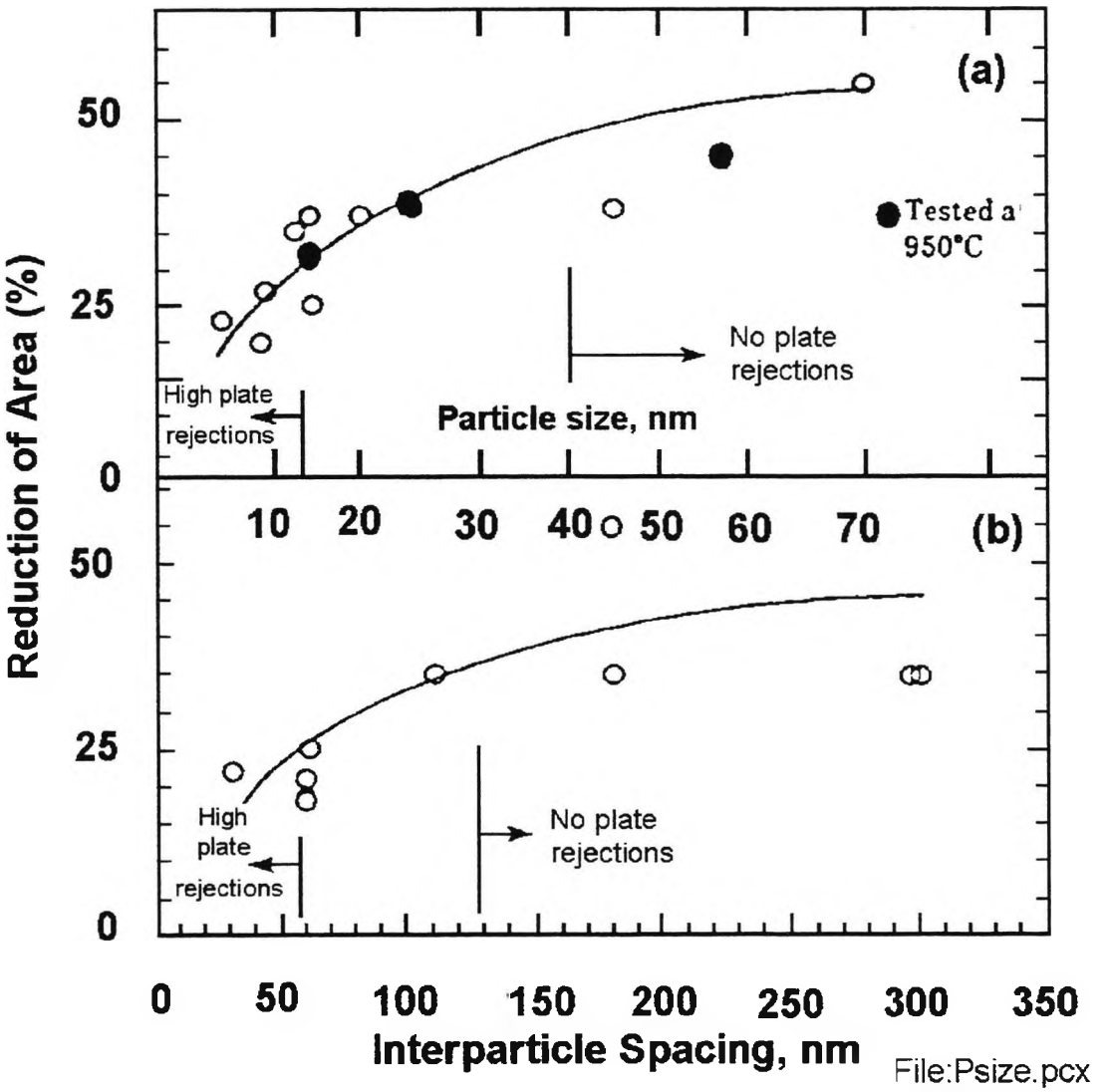


Figure 2-37: ***- Influence of a particle size and b interparticle spacing on hot ductility of Nb-containing steels, solution treated at 1330°C, cooled to test temperature of 850°C, and fractured at a strain rate of $3x10^{-3}s^{-1}$[Mintz et al, 1991]. [data extracted from Mintz and Arrowsmith, 1979p24; Crowther Mohamed and Mintz, 1987p1992; Mintz and Stewart, 1987; Mintz and Mohamed, 1989p2545 and Mintz and Arrowsmith, 1979p99]***

Influence of cooling rate

The greatest improvement in ductility that has been found so far on adding Ti to as cast steel, is when slow cooling to the test temperature has been used[Abushosha and Vipond, 1991p613]. Whereas cooling a Nb containing steel at 100K/min to the test temperature only gave a small improvement in ductility when Ti was present,

reducing the cooling rate to 25K/min resulted in a substantial benefit, Fig. 2-38. This slower cooling rate allowed the NbC to precipitate out at high temperatures on the coarse TiN precipitates. Precipitation was generally coarser and there was less of the fine NbC present.

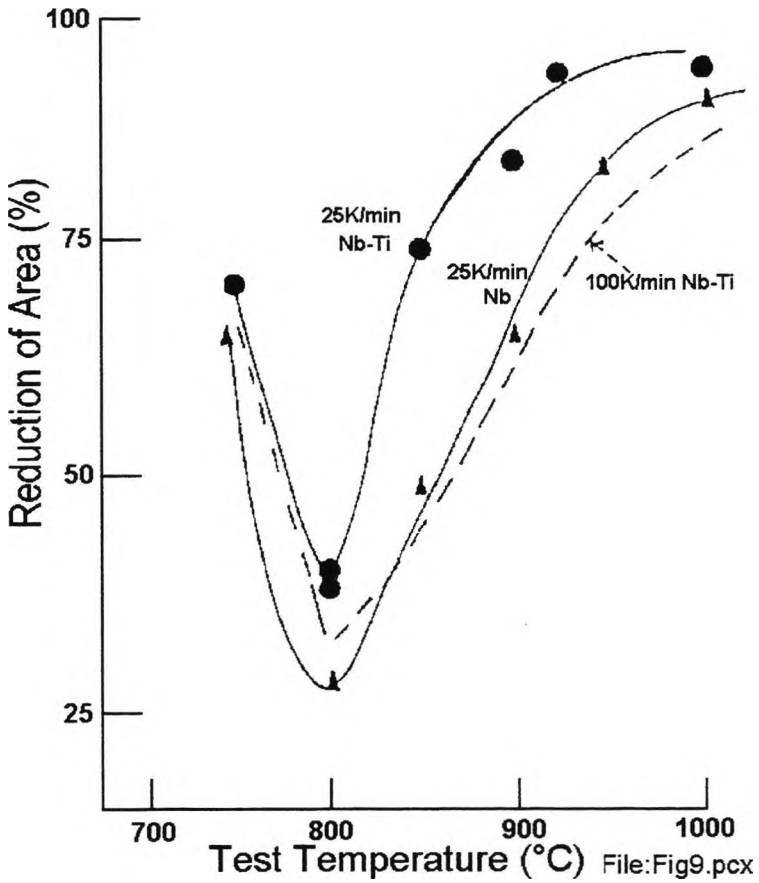


Figure 2–38: ***- Effect of reducing cooling rate during casting to 25K/min on an as cast C-Mn-Nb-Al steel with and without a Ti addition (curve for the same Nb-Ti steel cooled at 100K/min, broken line is shown for comparison). Levels of Ti and N were 0.02% and 0.009% respectively[Abushosha and Vipond, 1991p613].***

Turkdogan[Turkdogan, 1987] has suggested that during the later stages of solidification, most of the N would be expected to precipitate in a relatively coarse form as TiN in the interdendritic regions. These coarse particles would then form the nucleation sites for NbC and or VN, to precipitate out on at high temperatures.

Turkdogan [Turkdogan, 1987] suggests that by the time the temperature has dropped to 1200°C, (assuming the intense segregation of Nb to the interdendritic boundaries) most of the Nb will have precipitated as NbC so that none of the detrimental fine strain induced NbCN precipitation can occur at lower temperatures in the range of the straightening operation and as a result of this transverse cracking is reduced. This process would be favoured by slow cooling.

It is not clear whether precipitation of coarse TiN particles at high temperatures is enough to ensure precipitation of NbC at higher temperatures, or whether slower cooling rates are also necessary.

Clarification of this is of course very important for thin slab casting, in which the faster cooling rate of 200K/min applies, since benefits from Ti additions may arise only from nitrogen removal and hence be small.

The importance of the Ti:N ratio in controlling ductility

Experimental evidence has largely validated Turkdogan's model[Abushosha and Vipond, 1991p613 and Chen et al, 1987], but not all the TiN precipitates out during solidification as coarse particles and much finer Ti rich nitride particles also form during cooling when solid, as for example, the 10nm TiN particles in the steel with the stoichiometric composition in Fig. 2-36a. Roberts[Roberts, 1984] has also found 8nm size particles of TiN in a continuously cast slab having a high N, (0.008%N) and low Ti content (0.011%Ti) and these fine particles would be expected to give rise to poor ductility being within the same size range as the detrimental Nb(CN) precipitation, Fig. 2-37.

Ideally, for Ti additions to give good ductility, one needs to remove nitrogen in a form which is sufficiently coarse not to influence ductility and in the case of Nb and V containing steels to be able to precipitate some of these microalloying additions at high temperature. Removal of nitrogen presents no problems, but having the TiN in the right form does and this requires tight compositional control. *Unfortunately, data to define the required levels of Ti, N, and Al is often lacking.*

Coarse TiN particles can be achieved by ensuring that they are formed at high temperatures and that the Ti in solution is high so that they can coarsen readily during cooling after solidification and act as nucleation sites for Nb precipitation.

One way of producing coarse particles would be by increasing the product of [Ti]x[N], so encouraging precipitation at high temperatures. Ti being a powerful nitride former will virtually remove all the N from solution and for a given N content, raising the Ti level will increase the volume fraction of precipitation. When the stoichiometric composition for TiN is reached, i.e. Ti:N ratio is 3.4:1, the maximum volume fraction of precipitate can form. Furthermore, the Ti rich nitride particles then precipitate at lower temperatures so that they are fine (<10nm). These fine particles will then be additional to the NbC precipitation, reducing ductility even more. Such a composition, although good for grain refinement in the final product, is likely to be the worst possible for ductility. Thus, the poor ductility shown in Fig. 2-36, for a steel with the stoichiometric composition can be readily explained.

Raising the Ti further, above the stoichiometric level, will result in excess Ti in solution which will encourage growth of the particles as well as ensure that they come out at higher temperatures. Wilson and Gladman [Wilson et al, 1988] have

recommended >0.06%Ti to ensure there are no problems with hot ductility, but such high amounts of Ti produce coarse particles prior to solidification and the impact behaviour of plate steel suffers.

To reduce the amount of Ti required, low N levels have been preferred which reduce the volume fraction of precipitates and allow the excess Ti in solution to coarsen the particles, thus ensuring good ductility. Subramanian et al[Subramanian, et al 1985], examined a Nb containing continuously cast slab with a very high Ti:N ratio of 9:1 in which the N level was very low at 0.0025%. Here precipitation was found to consist mainly of coarse dendritic TiN particles formed at high temperatures and mixed carbides of Nb and Ti particles formed at much lower temperatures, the temperature of transition to mixed carbides being about 1065°C. This coarse precipitation would be expected to give good ductility.

Alternatively, raising the N level by increasing the product of the [Ti]x[N] will encourage precipitation at higher temperatures, but now there will be little tendency for growth. However, not all the nitrogen will be removed from solution. Nevertheless, such a steel with a lower Ti:N ratio of 2, has indeed given a small improvement in ductility over a Ti free Nb containing steel, presumably because much of the nitrogen has been removed as coarse particles, Fig. 2-35, and this benefit is likely to be enhanced when temperature cycling is introduced.

However, very low Ti:N ratios, 1.5, as in the steel examined by Roberts [Roberts, 1984] are likely to be detrimental to ductility as the Ti rich particles form at low temperatures as fine particles and there is a large excess of nitrogen which is not combined with the Ti.

Importance of Nb and Al in influencing the size of the TiN particles

Both Nb and Al have been found to influence the size of the TiN particles.

Subramanian et al[Subramanian et al, 1985] have shown that the effect of increasing the Nb content in a steel with .008%N and .01%Ti would be to increase the temperature for the start of the precipitation of niobium carbonitride, Fig. 2-39. It is not clear how this will influence ductility as the coarser particle size would be accompanied by a greater volume fraction of precipitate.

Subramanian et al[Subramanian et al, 1985] have examined precipitation in a continuously cast slab having a very high Nb level (0.06%) with a high N low Ti level, (0.008%N and .011%Ti, Ti:N ratio of 1.38:1). The precipitate size of the Ti containing particles was found to vary from 1900 to 80nm for dendritic particles to 30-50nm for cuboidal. Although the latter precipitates would be expected to reduce ductility, they are generally coarser than found in Ti free Nb containing steels and as such might be expected to have better ductility and be less prone to cracking.

In contrast, Roberts[Roberts, 1984] found in a continuously cast slab of a V containing Nb *free* steel, having similar Ti and N contents, very fine TiN particles (8nm) indicating that they had precipitated out at low temperature in accord with the predicted behaviour noted in Fig. 2-39.

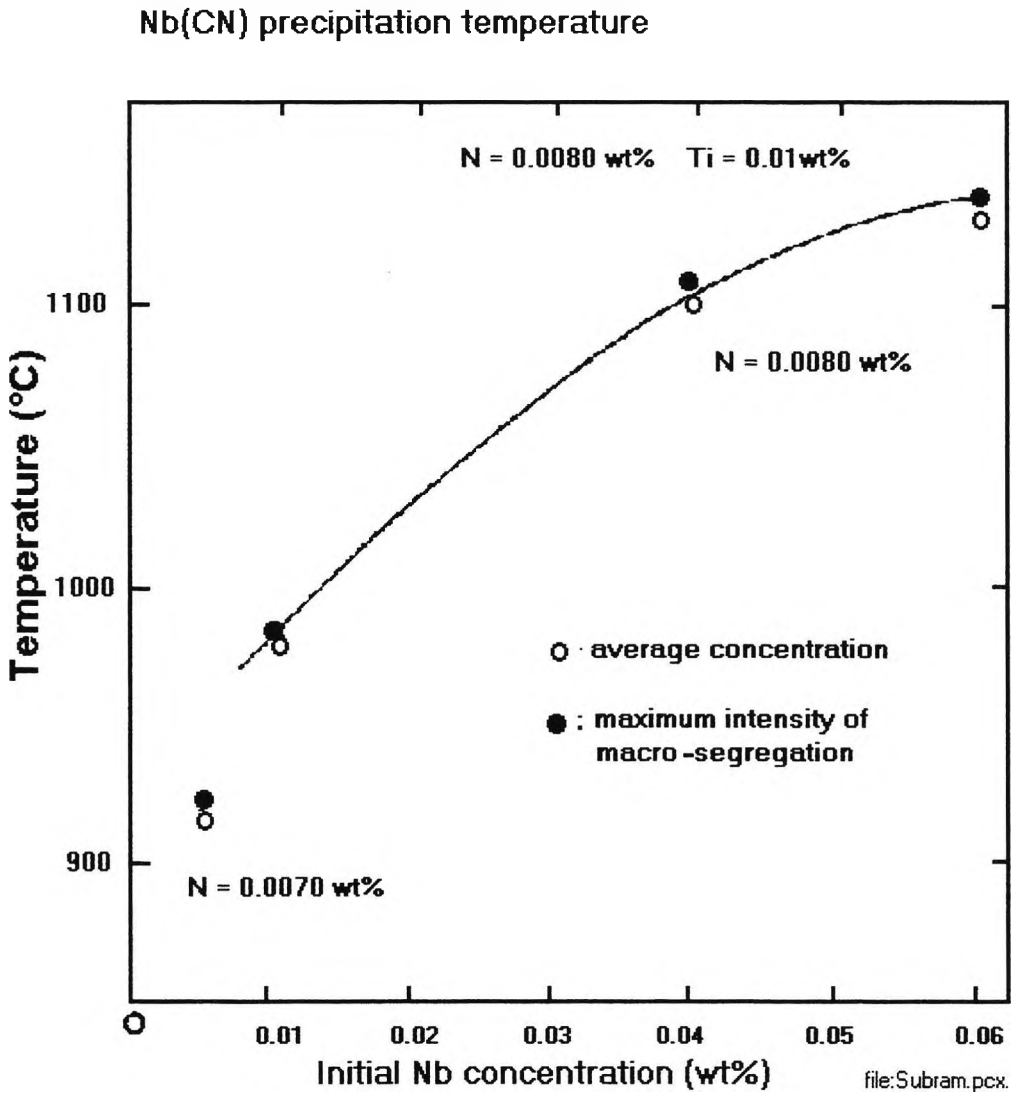


Figure 2-39: ***- Influence of the Nb level in as cast C-Mn-Nb-Al steel on the temperature at which Nb(CN) precipitation starts. Steel contained 0.01%Ti and 0.008%N[Subramanian, 1985].***

Similar behaviour applies to the presence of Al which has been shown by Kirkwood to result in coarser TiN particles[Loberg et al, 1084 and Kirkwood, 1987]. This could be an additional reason for the ductility being better in the steels with the Ti:N ratios of 2, as these steel had higher soluble Al levels (0.03-0.04% compared to 0.02% sol.Al for the steels with the stoichiometric compositions). Loberg et al[Loberg et al, 1984] have suggested that Al associates with the N and, although not producing a

precipitate, this effectively increases the amount of Ti in solution encouraging growth. A similar explanation could apply to the effect of Nb.

Clearly there is a need to examine both the C-Mn-Nb-Al-Ti and C-Mn-Al-Ti systems in more detail.

Recommended levels for the Ti:N ratio in high N steels

For strip steel where impact behaviour is not important a high Ti:N ratio can be accommodated. For plate steel the Ti:N ratio chosen ideally has to give both freedom from transverse cracking as well as good properties in the plate.

The two are difficult to achieve because the high degree of grain refinement required in the plate, which relies on fine particles, is exactly what gives rise to the transverse cracking problem. Ideally, one requires to have either no precipitation or coarse precipitation during casting and then the opportunity to refine the grain size during subsequent processing by allowing fine precipitation to take place. In thin slab casting in which direct rolling follows, this becomes even more difficult to achieve as there is little opportunity to take the coarse precipitates back into solution. The faster cooling rates relating to the process will also tend to suppress precipitation so that more of the very detrimental fine strain induced precipitation will occur on straightening. It has been shown that slow cooling at 25K/min leads to a significant improvement in ductility when Ti is added, but faster cooling rates only give rise to a small improvement.

It is interesting to note that the present industrial practice for conventional continuous casting seems to favour two ranges for the Ti:N ratios; either close to stoichiometry, between 2 to 4, although Turkdogan [Turkdogan, 1987] has stated

that the favoured ratio is 4, or ratios well in excess of this 7 to 10[Patrick et al, 1994].

Nevertheless, the hot ductility work clearly indicates that the stoichiometric composition can lead to extremely poor ductility for a Ti containing steel and that any improvement for steels having Ti:N ratios in the range 2 to 4 may be small.

It should be noted, however, that this apparently poor ductility could be a result of the hot ductility work not as yet including temperature oscillations. It is possible for example that although a Ti containing steel at the stoichiometric composition, does give worse ductility than a Ti free Nb containing steel, Fig. 2-36b, this behaviour is reversed when temperature oscillations are introduced. Benefits from Ti additions may therefore be much better than indicated by the simple hot ductility test without temperature oscillations. This is clearly an area requiring further study.

High Ti:N ratios in high N steels (7:1) may possibly not only remove nitrogen, but also encourage precipitation of NbC at high temperature, giving a substantial improvement in ductility and this needs to be examined.

A Ti:N ratio in a high N steel of 4:1, i.e. 0.04%Ti, 0.01%N should give improvements in ductility, as there will be a small excess of Ti in solution, to coarsen the precipitates at high temperatures and all the nitrogen will be removed from solution. Certainly, for C-Mn-Al steels in which the higher nitrogen levels are giving problems, this offers itself as a likely solution.

It may be that lower Ti additions in the range 0.02 to 0.025%Ti to steels with .01%N will also be satisfactory as indicated in the hot ductility curve in Fig. 2-35. Very low Ti additions in a high N steel are however, likely to give poor ductility producing fine

TiN particles, as indicated by the work of Roberts[Roberts, 1984], and a large amount of free nitrogen.

Summarising, Ti has been shown to be a good addition to add to steels to reduce transverse cracking. This improvement in ductility may in part be due to, nitrogen removal preventing the detrimental precipitation of AlN from occurring and on occasions, due to the higher temperature precipitation of Ti rich particles providing nucleation sites for NbC precipitation, thus reducing the amount of Nb available for precipitation in the very fine detrimental form during the straightening operation. The precise Ti:N ratio required particularly for thin slab casting is not clear. Further work is required to clarify these compositional limits.

KINETICS OF DISSOLUTION AND FORMATION OF PRECIPITATES;

The importance of precipitates on hot ductility

The role of precipitates in promoting embrittlement is clearly defined [Thomas et al, 1986]; [Maehara et al, 1990] and [Turkdogan, 1987]. In the case of grain boundary sliding in the austenite, fine precipitation pins the boundaries, allowing the cracks to join up[Mintz and Arrowsmith, 1979p24]. In addition, both precipitates and inclusions cause void formation extending the crack length [Maehara et al, 1984]. Microvoid coalescence failures are also encouraged by an increase in the precipitate or inclusion density at the boundaries, these being preferential sites for void formation.

A survey conducted by Guillet [Guillet, 1989] has shown that there is a large body of evidence which indicates that low RA values in common microalloyed steels are associated with fine precipitation. It is also generally accepted that it is the precipitation at the austenite boundaries that has the greatest influence[Crowther, Mohamed and Mintz, 1987p1929]. This was already seen more clearly in Fig. 2-37, where the influence of the Nb(C,N) precipitates at the austenite grain boundaries (particle size and interparticle spacing) on the hot ductility of C-Mn-Nb-Al steels is shown, for the rare instance where all the other variables have been kept reasonably constant.

Also included in figure 2-37 are the results from a commercial examination into the precipitate distributions at the austenite grain boundaries taken close to the surface of continuously cast slabs[Mercer et al, 1979]. Casts without cracks had along the boundary mean particle size and interparticle spacing of $\geq$40 and $\geq$140nm, respectively. Rejected slabs had mean particle sizes and interparticle spacing of $\leq$14 and $\leq$60 nm, respectively. These values also indicate that transverse cracks can be avoided when the RA values $\geq$40%.

From the preceding discussion, it is clear that the effect of precipitates on hot ductility depends strongly on their size distribution and location. These characteristics are, in turn, controlled by composition and the thermomechanical details of the test. Thus considerable research effort has been channelled into examining the influence of thermal history and deformation on participate size distribution, with the aim of reducing the incidence of transverse cracking. The findings are summarised below.

It is well known that the precipitation of AlN, Nb(C,N), and V(C,N) is accelerated by deformation compared with the rates measured for undeformed structures at the same

temperature[le Bon, et al, 1975]; [Abken at al, 1981]; [Weiss et al, 1980] and [Vodopivek, 1973]. This acceleration results from the introduction of favourable nucleation sites, such as dislocation networks and vacancy clusters, by the deformation process. The observation of NbC precipitated on dislocations [Ohmori et al, 1984] following high temperature testing in austenitic stainless steel supports this view.

Precipitate size distributions are also influenced by whether the precipitates are formed statically before testing, statically after testing, or dynamically during deformation. Slow cooling or heating to the test temperature, as in normalising and holding, favours static precipitation; such particles are generally coarser than their strain induced or dynamically precipitated counterparts. Dynamic precipitation does not occur at very high testing strain rates, since deformation ceases before the incubation time for dynamic precipitation has been reached. However, static precipitation can occur subsequently in the deformed structure at rates much faster than that of static precipitation in undeformed metal, and close to those associated with dynamic precipitation[Weiss et al, 1980].

Both Nb(C,N) and VN can precipitate rapidly during testing at strain rates $<10^{-1}s^{-1}$ [Abken et al, 1981]; [Weiss et al, 1979], and hence can have a very important influence on hot ductility and transverse cracking. For steels which are solution treated and cooled to the test temperature, Nb is more effective in extending the ductility trough to higher temperatures (i. e. reducing the ductility) than V[Mintz and Arrowsmith, 1980p99]. This is probably because, for typical microalloy compositions, the nose temperature for Nb(C,N) precipitation is at 950°C [le Bon et al, 1975] and [Weiss, et al 1979], whereas it is about 885°C for VN[Abken et al, 1981]. Similarly, Al steels are more ductile (have narrower troughs) than Nb-containing steels, the nose temperature for AlN being as low as

815°C[Leslie et al, 1954]. In addition, the formation of AlN is particularly sluggish. In fact, it has been shown that, unless the solubility product is very high, cooling from the solution temperature at an average cooling rate of 60K/min to simulate continuous casting conditions will not cause the precipitation of AlN during testing, either statically or dynamically [Crowther, Mohamed and Mintz, 1987p1929]. Nevertheless, the temperature cycling that occurs during the cooling of continuously cast strands can accentuate AlN production [Cardoso et al, 1989]; [Mintz, Stewart and Crowther, 1987]; [Coleman et al, 1985] and [Nozaki et al, 1978]. This can be very detrimental to the ductility, particularly as AlN precipitates mainly at the austenite boundaries [Crowther, Mohamed and Mintz, 1987p1929]; [Coleman, et al 1985] and [Nozaki, et al 1978]. Note that V precipitates randomly throughout the matrix, whereas Nb(C,N) is found both at the boundaries and within the matrix[Crowther and Mintz, 1986p1099].

Investigations into the influence of static and dynamic precipitation have led to the conclusion that, for V and Al-containing steels, the precipitates present before deformation are more detrimental than those formed during testing[Wilcox et al, 1987] and [Crowther, Mohamed and Mintz, 1987p1929]. In this case, the static precipitates are more effective than the dynamic ones in reducing the hot ductility, even though they are coarser, [Crowther, Mohamed and Mintz, 1987p1929] because they are formed only at the boundaries, Fig. 40. Vanadium and Al-containing steels generally have better hot ductilities than Nb microalloyed steels because, in the former two steels, prior precipitation when present is coarser and, in the case of V, more random[Crowther and Mintz, 1986p1099].

By contrast, dynamic precipitation has been shown to be more effective in reducing the hot ductility in Nb-containing steels [Wilcox et al, 1987] and [Mintz and Stewart, 1987].

This is partly because dynamic precipitation is much more extensive in Nb-containing steels, (cf Figs. 2-40 and 2-41).

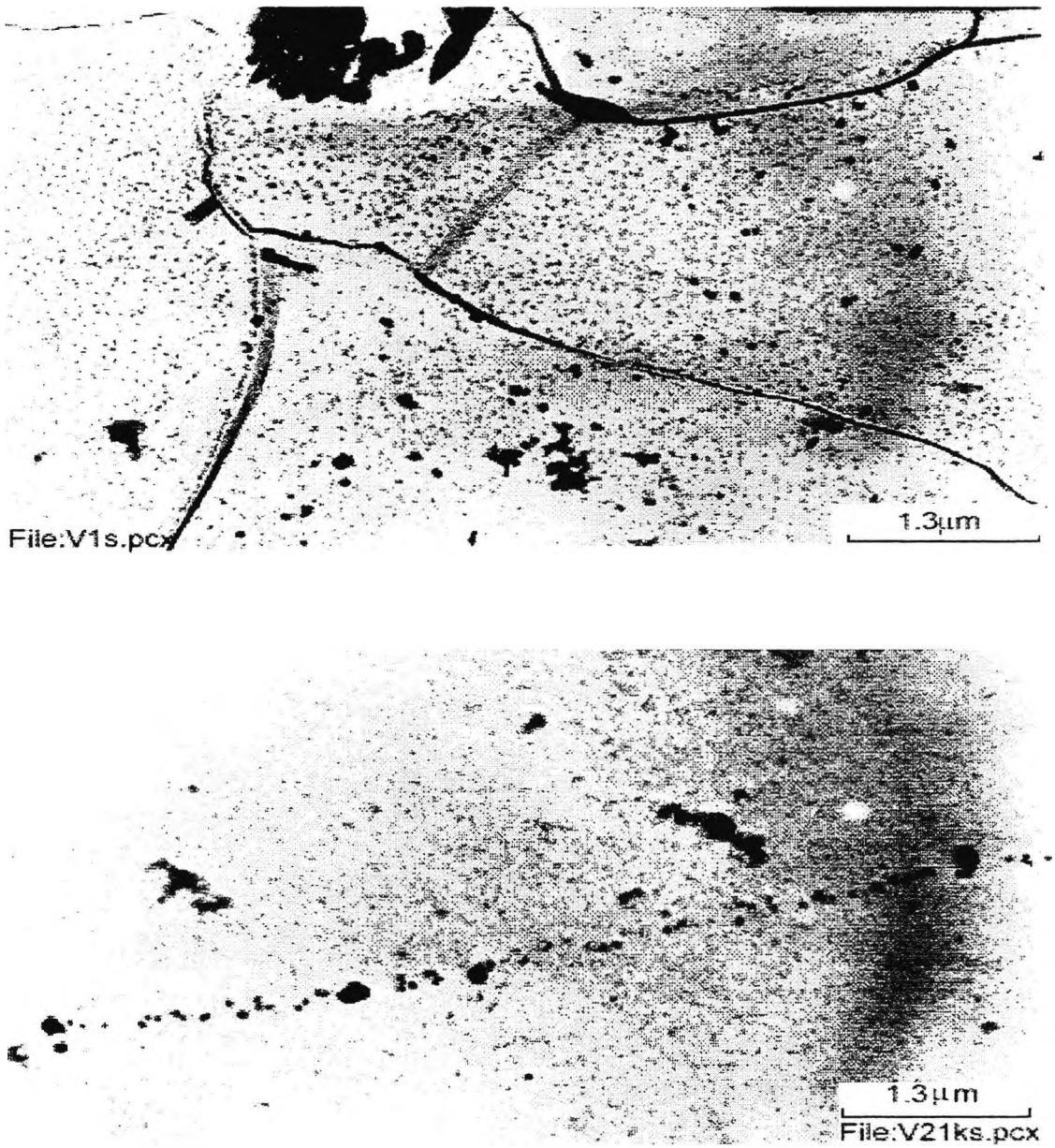


Figure 2–40: ***- Microstructures and corresponding precipitates size distributions in C-Mn-V-Al steel, after holding for a, 1s (average size 15nm) and b) 21000s (average size 50nm before testing at 850°C[Crowther, Mohamed and Mintz , 1987p1929];***

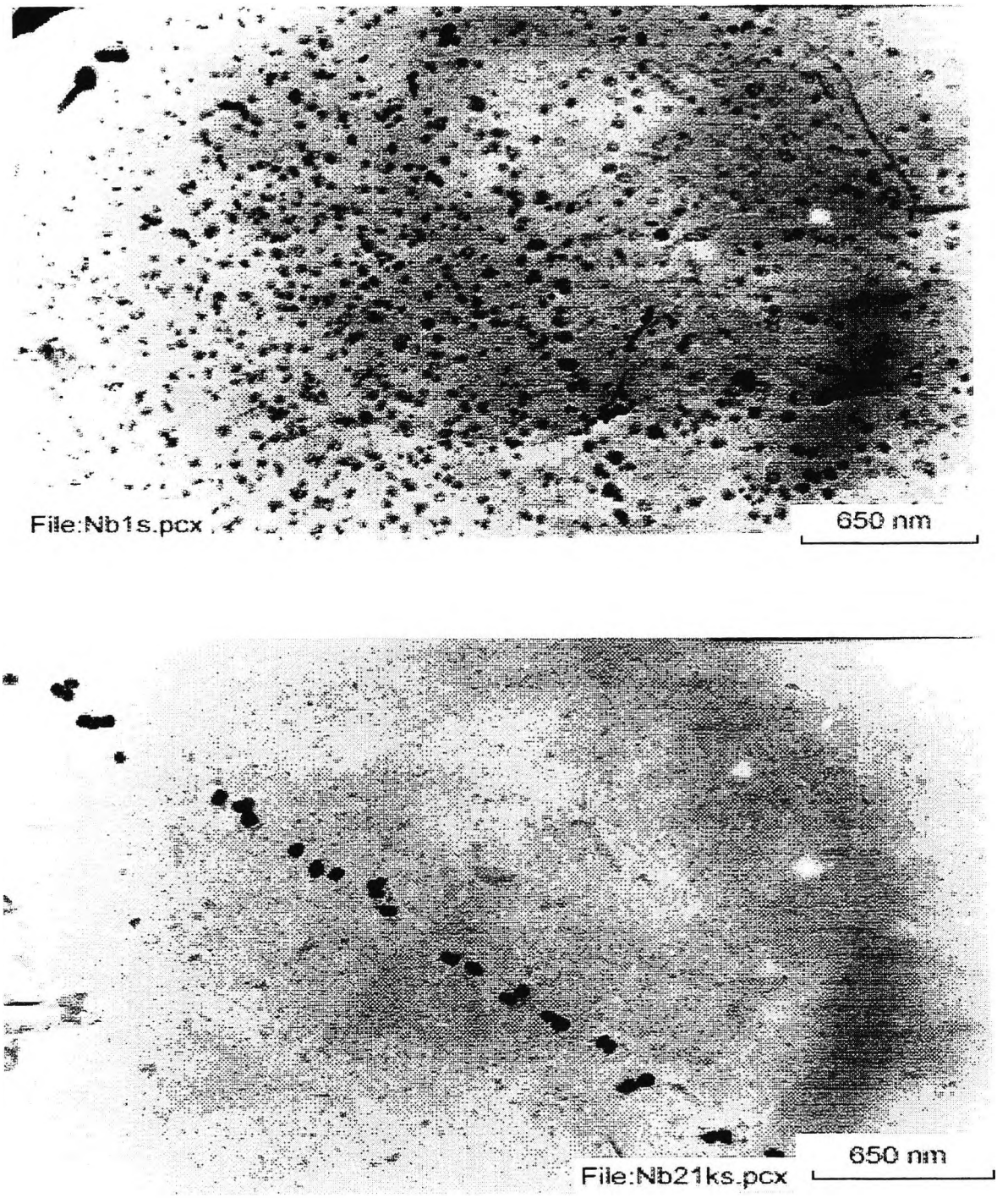


Figure 2–41: ***- Microstructures and corresponding precipitates size distributions in C-Mn-Nb-Al steel, after solution treated at 1330°C, cooled at 950°C and held for a, 1s (average size 15nm)and b, 21000s (average size 55nm) before testing at 850°C[Crowther, Mohamed and Mintz, 1987p1929];***

It also occurs in a finer form, [Crowther et al, 1987] and [Weiss et al, 1980] both at the austenite boundaries and within the matrix, as long as the Nb(C,N) is taken into solution before deformation, Fig. 2-41. The highest ductilities are displayed by these steels when the precipitates are present before deformation in a coarse form and randomly precipitated throughout the structure[Crowther and Mintz, 1986p1099]. This occurs in Nb-containing steels when they are reheated to temperatures somewhat below the Nb(C,N) solution temperature (typically about 1100°C), which coarsens the precipitates without taking any significant volume fraction back into solution.

Finally, the effect of Nb(C,N) on the hot ductility can also depend on the chemical composition of the precipitate[Ouchi et al, 1982]. At a constant Nb level (0.015%), it has been found that an increase in the N concentration from 0.002 to 0.006% markedly reduces the plasticity. Low N levels promote the formation of $NbC_{0.85}$ particles, whereas high nitrogen concentrations lead to the precipitation of $NbC_{0.6}N_{0.25}$. The higher ductilities associated with the former precipitate have been ascribed to its lower rate of precipitation in austenite.

Aluminium Nitrides precipitates

The precise effect of AlN precipitates on hot ductility depends on the grade of steel. In this regard, steels are divided into two categories: (a) C-Mn-Al and (b) C-Mn-Nb-Al.

C-Mn-Al steels

As noted above, when plain C-Mn steels are solution treated and cooled to the test temperature, the presence of a coarse grain size and a thin film of ferrite at the austenite grain boundaries leads to a marked ductility trough. Under these conditions, dissolved Al can extend the trough to higher temperatures, i.e. into the single phase austenite region, by combining with N to form AlN precipitates at the austenite grain boundaries. This leads to pinning of the boundaries and therefore to the encouragement of void formation by grain boundary sliding.

Most research studies [Bernard et al, 1978]; [Hasebe, 1963]; [Chamont et al, 1988]; [Hannerz, 1985]; [Vodopivec, 1974] and [Michel et al, 1981] have concentrated on the influence of very high Al and N on hot ductility. There is some doubt as to whether the precipitation of AlN can occur in austenite with conventional Al levels at the relatively high cooling rates associated with continuous casting [Wilson, 1988]. When current commercial levels for Al and N are employed (0.02-0.04%Al, 0,005%N), Al has been found to have no influence on the hot ductility for samples solution treated and cooled to the test temperature, [Mintz and Wilcox, 1980] Fig. 2-42.

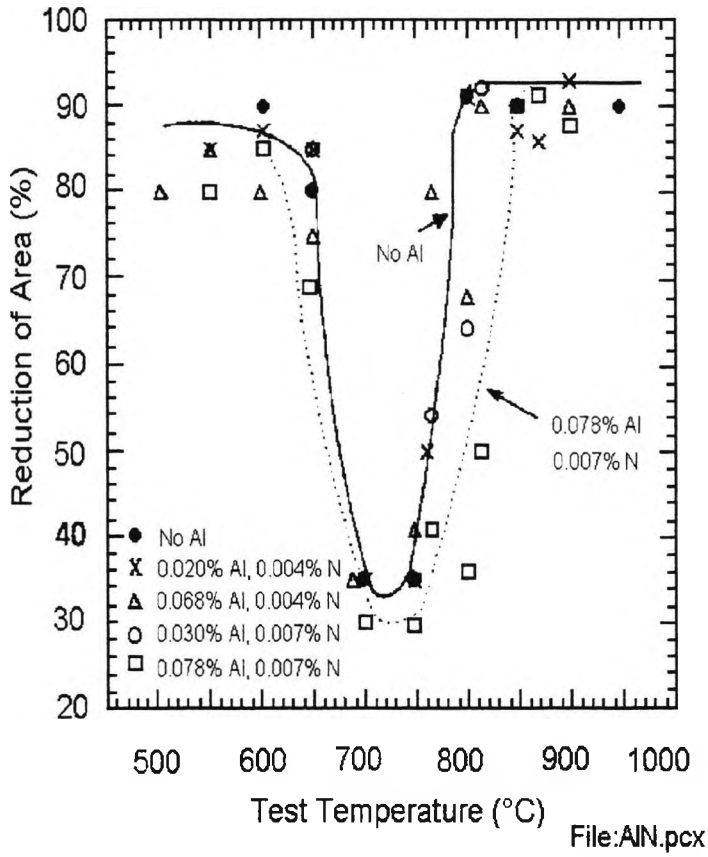


Figure 2-42: ***Influence of soluble Al and N on hot ductility of C-Mn-steels: Steels were solution treated at 1300°C, cooled to test temperature, and strained at strain rate of $3x10^{-3}s^{-1}$ [Mintz and Wilcox, 1980].***

The Al levels have to be very high (≥0.07%) in order for AlN to be precipitated out and to have an influence on hot ductility. Although it can be very difficult to extract AlN particles (because they often form very thin films at the austenite boundaries), the important point to note is that the hot ductility behaviour of a C-Mn-Al steel with a conventional Al level is the same as that of a plain C-Mn steel of otherwise similar composition. However more recent work indicates that when tensiles are cast or given cycling the very small amounts of Al and N can lead to AlN precipitate. Turkdogan [Turkdogan, 1987] has shown that on solidification the segregation of Al to the boundaries can increase the concentration of Al by a factor of 6.

There are also many reported instances of AlN precipitation in austenite,[Vodopivec, 1973] and [Vodopivec 1974] and [Hasebe, 1963] both dynamically and statically, and it is important to establish the conditions under which precipitation occurs under commercial condition in C-Mn-Al steels. Obviously, the levels of Al and N present in the steel are important, the higher the product, the greater being the driving force for precipitation. Michel and Jonas [Michel et al, 1981] have also argued that concentration of solute elements such as Mn, which increases the solubility of carbonitrides and renders them less likely to precipitate, is also important. They point out that the marked differences in the kinetics of AlN precipitation observed in the literature may be ascribed to differences in Mn level, rapid precipitation being associated with low Mn levels[Hasebe, 1963] and [Vodopivec, 1974], Table 2-1.

N level, wt-%	Mn level, wt-%	[Al][N] × 10^{-4*}
Generally ≥0·01	0·70	1·7–6·8
Generally ≥0·014	0·80	0·8–0·91
Generally ≥0·01–0·02	0·80	0·24–2·55
0·01	1·3	3·0
0·01	1·4	0·44–2·6
0·01–0·02	1·4	1·5–2·3
Generally ≥0·02	1·55	1·2–4·2
0·005	1·4	2·7–5·3

File:PsAlN.pcx

Table 2-1 :***Solubility product for Al and N at which the presence of AlN has first been detected in a variety of steels. [Mintz et al, 1991]. *lower figure represents no significant influence in RA values, while upper figure represents first indication of AlN influencing the hot ductility.***

Although there are insufficient data in this table to establish clearly the influence of Mn, it can be seen that, for steels containing 1.4% Mn, the solubility product has to approach $3x10^{-4}$ for precipitation to occur after solution treatment and straining.

Given that commercial Al additions are now often controlled to fall between 0.02 and 0.4%, and N levels continue to be reduced (e. g. to ≤0.005%), there is considerable

experimental work which indicates that AlN does not precipitate in high Mn steels (1.40%) in operations involving high temperature deformation after solution treatment, i. e. rolling or straightening. Nevertheless, there is evidence for the presence of AlN precipitates in the opened up transverse cracks of continuously cast slabs and this can be accounted for as follows[Coleman at al, 1985]. First, although AlN has difficulty precipitating in austenite because of the problem of finding suitable nucleation sites, this is not the case when it precipitates in ferrite, and thermal cycling encourages such precipitation [Wilson at al, 1988]. The hot ductility tests described above were carried out at a constant cooling of continuously cast slabs. However, the actual thermal cycle experienced at the surface of a continuously cast slab is complex, [Nozaki at al, 1978] and a temperature oscillation is set up by the alternate impingement of water sprays and rolls, as outlined above. Depending on the secondary cooling conditions, it is possible for the temperature to fall periodically below the Ar_3, particularly at slab corners. Cycling above and below this temperature will lead to the formation of copious amounts of AlN at the ferrite/austenite interface. Furthermore, as already noted considerable segregation of Al to the boundaries will have occurred encouraging AlN precipitation there. When temperatures oscillations are introduced the Al and N concentration only needs to be i.e. 0.02% Al 0.005%N for precipitation to occur. [Cardoso and Abushosha, 1994].

C-Mn-Nb-Al steels

In contrast to its effect on C-Mn steels, there is unanimous agreement that Al, even in relatively small amounts, deepens and widens the ductility trough in Nb-containing steels, [Mintz and Arrowsmith, 1979p24]; [Wilcox et al 1984]; [Ouchi et al, 1982[; [Bernard et al, 1978] and [Nachtrab et al, 1995]. This has already been shown in Fig. 2-13b.

Commercially, there is also evidence [Mintz and Arrowsmith, 1979p24] and [Hannerz, 1985] that increasing the Al and, in particular, N contents increases the likelihood of transverse cracking in Nb-containing steels. The precipitation of AlN at the austenite gain boundaries in addition to that of Nb(C,N) is normally given as the explanation[Wilcox et al, 1984]; [Bernard et al 1978] and [Coleman et al, 1985]. However, there is evidence to suggest that the deterioration in the hot ductility is not caused by the precipitation of AlN, but by the production of finer Nb(C,N) precipitates[Mintz and Arrowsmith, 1979p24]. Indeed, in hot tensile tests in which constant cooling rates pertinent to continuous casting were used, AlN precipitation was not observed by Mintz and co-workers [Mintz and Arrowsmith, 1979p24]; [Crowther, Mohamed and Mintz, 1987p1929] in any microalloyed steel. Thus the observation of AlN precipitates in continuously cast C-Mn-Nb-Al slabs again indicates the importance of cycling through the transformation if the characteristics of AlN precipitation are to be reproduced in laboratory simulations.

Titanium precipitates

Of all the microalloying elements, as already mentioned, Ti seems to be the most effective in keeping the RA values high, and reducing or eliminating the trough when

laboratory tests are carried out on unmelted samples, [Ouchi et al, 1982]; [Funnel et al, 1978]; [Mintz and Wilcox, 1980]; [Funnel, 1979] and [Ericson, 1977] Fig. 2-43.

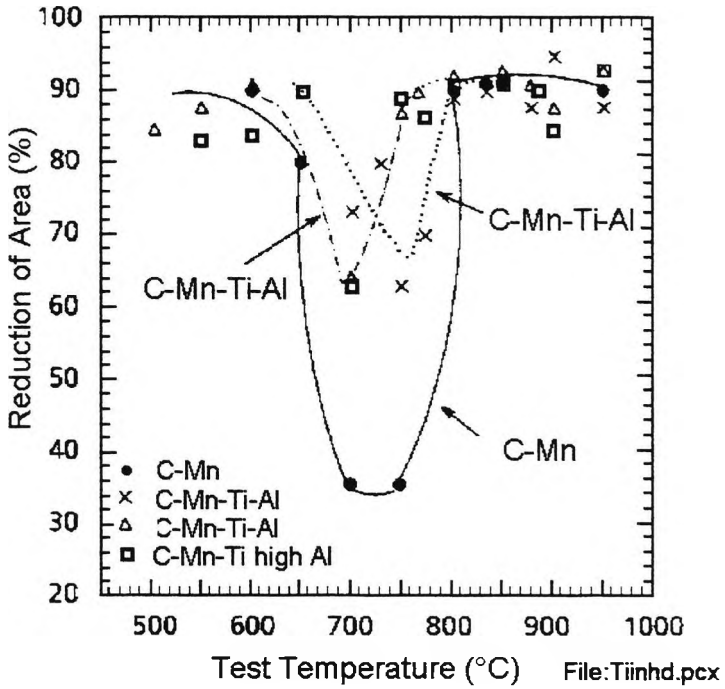


Figure 2-43: ***- Influence of small additions of Ti (0.02-0.03%) on hot ductility behaviour of C-Mn-Al steels heated to 1330°C, cooled to test temperature, and fractured at strain rate of $3x10^{-3}s^{-1}$ [Mintz and Wilcox, 1980].***

This as noted is because TiN and TiN-rich precipitates can be formed at high temperatures (close to the solidus) and so tend to be coarse and randomly distributed [Turkdogan, 1987] and [Mintz and Wilcox, 1980]. They are also sufficiently numerous and have a high enough volume fraction to restrain grain growth at high temperatures (~1350°C), while not pining the boundaries long enough for cracks to link up. TiN precipitates do not go back into solution on reheating to 1330°C. Part of the benefit of Ti addition therefore comes from the refinement of grain size, but part also arises because of its ability to combine preferentially with N, preventing the formation of the more

detrimental AlN precipitate [Ouchi et al, 1982] and reducing the amount of N available to form Nb(C,N)[Turkdogan, 1987].

However, as noted previously care must be taken in transferring these laboratory results for Ti containing steels to the continuously cast situation. Precipitate distributions in the as-cast state are unlikely to influence significantly the coarse austenite grain size obtained on solidification. The grain refinement from the TiN particles, which is obtained on reheating through the ferrite to austenite transformation, will therefore be absent. This has been confirmed in two recent laboratory examinations [Mintz and Mohamed, 1988] and [Abushosha and Vipond, 1991p613], using tensile samples directly cast and cooled to the test temperature. No grain refinement was observed and, consequently, only a limited benefit to hot ductility was observed. Some benefit from the removal of AlN might, nevertheless be expected.

Precipitates formed on casting

Precipitation is very much affected by the solidification process undergone by the as cast strand. Thus, the precipitate distributions found in the as cast state can differ from those found after solution treatment. Intense segregation of microalloying additions to the interdendritic boundaries probably occurs during solidification, and this will lead to precipitation at higher temperatures than normally encountered after a solution treatment [Turkdogan, 1987]. Mintz et al, [Mintz and Wilcox, 1986] found very coarse Nb(C,N) eutectics as well as coarse sulphides close to the interdendritic boundaries in directly cast C-Mn-Nb-Al steel which was hot tensile tested. There was less precipitation of fine Nb(C,N) (10-20 nm) at the austenite boundaries, subboundaries and within the matrix, giving improved hot ductility over material solution treated and cooled to the test

temperature. Solution treatment redissolved these coarse Nb(C,N) eutectics and took the S back into solution, both of which reprecipitated at the boundaries in a finely divided form when the samples were cooled to the test temperature. The form and distribution of Ti-containing precipitates can also be very different in the as cast condition compared with that after heating to 1350°C and cooling to the test temperature and again this will influence the hot ductility [Mintz and Mohamed, 1988].

The size distribution of precipitates is extremely important in influencing the ductility. Thus, only when tests are designed to simulate both the casting and subsequent cooling operations of the strand exactly, can the results from laboratory tests be used to predict the likelihood of transverse cracking with any degree of reliability.

INFLUENCE OF GRAIN SIZE ON HOT DUCTILITY AND TRANSVERSE CRACK;

Of all the variables that have been examined, grain size seems to have received the least attention. This is surprising considering the strong influence of grain size under creep conditions, which include the strain rate range used during straightening. Part of the reason for the lack of information regarding grain size effects has been the difficulty of isolating the influence of grain size form that of precipitation. This probably accounts for some reports which suggest that grain size refinement can be detrimental [Funnell et al, 1978]; [Wray, 1984] or have no influence on hot ductility [Ouchi et al, 1982]; [Carlsson, 1964]. However extensive creep studies have generally shown that the high temperature ductility increases as the grain size is decreased [Bywater et al, 1976]; [Evans, 1969]; [Kutumba Rao, et al, 1975] and [Reynold et al, 1980].

When the failure is intergranular, refining the grain size affects crack growth via:

1. The decrease in the crack aspect ratio, with controls the stress concentration at the crack tip; this is lower in the fine grained materials so that crack propagation is discouraged.[Kutumba Rao et al, 1975];

2. The difficulty in propagating the smaller cracks formed by sliding through triple points. [Kutumba Rao et al, 1975];

3. The increase in the specific grain boundary area (for a given volume fraction of precipitate), which reduces the precipitate density on the grain boundaries [Fu et al, 1988] and [Ouchi et al, 1982];

4. The reduction in the critical strain for dynamic recrystallisation by increasing the number of grain boundary nucleation sites, [Sellars, 1980] thereby increasing the possibility of ductility improvement via grain boundaries migration.

All these effects outweigh any detrimental influence on the hot ductility due to the slight increase in flow stress brought about by grain refinement. In others words, creep rather than recovery dominates in this strain rate range.

Where the influence of grain size on hot ductility has been examined under conditions which involve the absence of precipitation [Fu et al, 1988]; [Rizio et al, 1988]; [Crowther and Mintz, 1986p1099]; [Crowther and Mintz, 1986p951], refining the grain size leads to reductions both in the depth and width of the trough Fig. 2-44. The influence of grain size on ductility is in part related to the form and distribution of the ferrite.

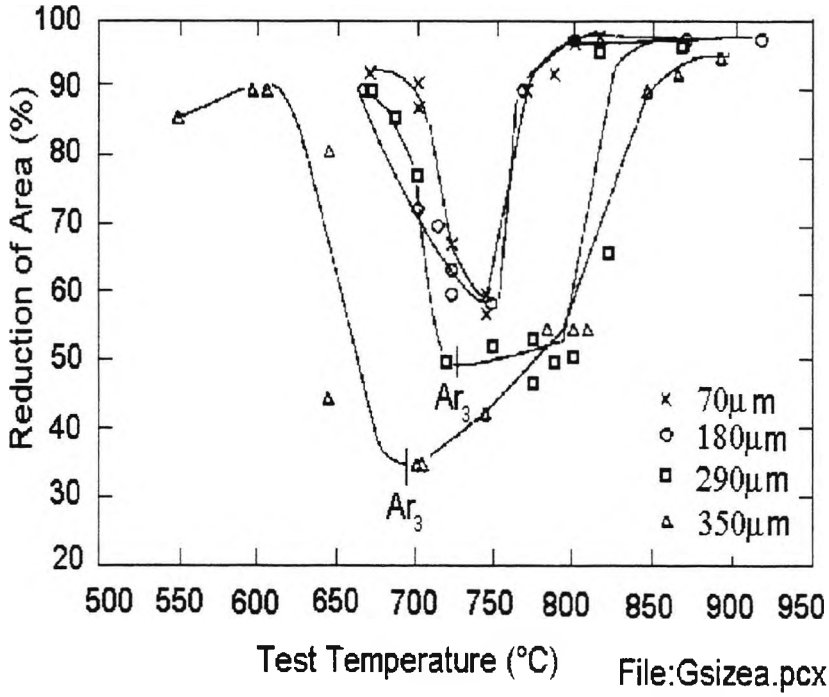


Figure 2–44: - ***Hot ductility curves for 0.19%C steel at various grain sizes[Crowther and Mintz, 1986p951]***

Generally it is found that, in coarse grained steels, undeformed ferrite forms as thin continuous films surrounding the austenite [Maki et al, 1985]; [Crowther and Mintz, 1986p951]. The volume fraction of deformation induced ferrite is always small in the coarse grained steels, and often forms over a wide temperature range from the Ae_3 to the Ar_3 (undeformed). This suggests that there is insufficient deformation away from the boundary regions to increase the volume fraction of ferrite significantly. The thin film morphology of the deformation induced ferrite thus reduces the hot ductility on the high temperature side of the trough. For fine grained steels, ferrite was observed to form, less detrimentally, as equiaxed, unconnected grains [Maki et al, 1985]; [Crowther and Mintz, 1986p951]. However, Cardoso and Yue [Cardoso, et al, 1989] has shown that, even in fine grained steels, deformation induced ferrite can form as thin, continuous films. It is possible that this had not been observed previously because of the much faster

austenite to ferrite transformation rate resulting from the fine austenite grain size. In view of this, perhaps a more relevant factor controlling ductility in a finer grained structure is the increased volume fraction of the total ferrite that is produced at a given temperature. The narrow trough in a fine grained steel is then a consequence of the rapid increase in volume fraction of the ferrite which forms when the temperature is lowered to below the Ae_3.

Alternatively, Rizio [Rizio et al, 1988] postulate that the maximum strain concentration and greatest ability to link up cracks occur when a continuous ribbon of the softer ferrite phase forms around the austenite grains. Fine grained material requires a lower temperature for this to occur, because of the higher grain boundary area. Although both of these theories account for the reduced width of the trough, they do not account for the reduction in its depth Fig. 2-44, and one or more of the explanations given in 1 to 4 above must also be included.

Microalloyed steels generally show little indication, from hot tensile tests, that grain size has a significant influence on their hot ductility, because of the overriding effect of the precipitation of AlN of Nb(C,N) at austenite boundaries, as mentioned above. Where an attempt has been made to keep the precipitate distribution constant, [Maehara et al, 1985] the changes in hot ductility with grain size were similar to those observed in plain C-Mn steels Fig. 2-45.

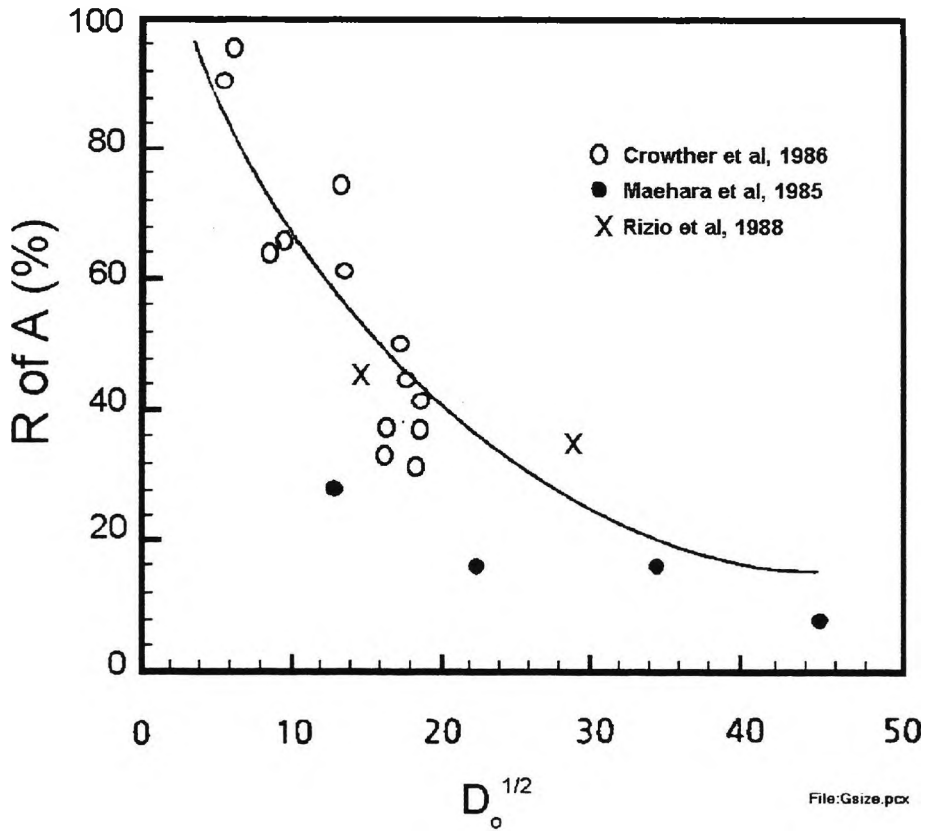


Figure 2–45: ***- Influence of D_0 (initial undeformed grain size after heat treatment) on minimum RA value. [Mintz et al, 1991] data taken from [Crowther and Mintz, 1986p1099; Maehara et al, 1985 and Rizio et al, 1988]***

When the degree of precipitation is such that the ductility trough extends into the austenite, the beneficial effects from grain refinement are, once again, readily apparent.

Finally, it should be noted that, in HSLA steels, the austenite grain size is always much coarser than the ferrite grain size. Coarser grain sizes encourage grain boundary crack propagation, so making austenite more prone to cracking than ferrite [Mintz et al, 1991].

Chapter 3 - EXPERIMENTAL TECHNIQUES

THE CASTING AND TENSILE TESTING

As already detailed, casting the samples is fundamental to simulating the continuous casting operation taking into consideration the importance of the as cast grain size and the ability to re-dissolve the microalloying precipitates. This is particularly important when the influence of Ti is being examined. In order to be able to cast the tensile samples directly, an induction equipment with an inert gas atmosphere (argon) was fitted to a conventional tensile testing machine. All of the variables were manually controlled.

Induction unit and specimen design

In the City laboratories, the samples were tested in a horizontal tensile testing machine (converted Hounsfield tensometer) to which a heating induction device had been fitted. The melting zone was approximately 22 mm in length situated at the mid-length position of the sample. The molten steel was contained in a silica tube

with an initial 0.2 mm clearance and the oxidising protection was achieved by surrounding the silica tube with a wide glass tube through which argon flowed. These details are shown in Fig. 3-1

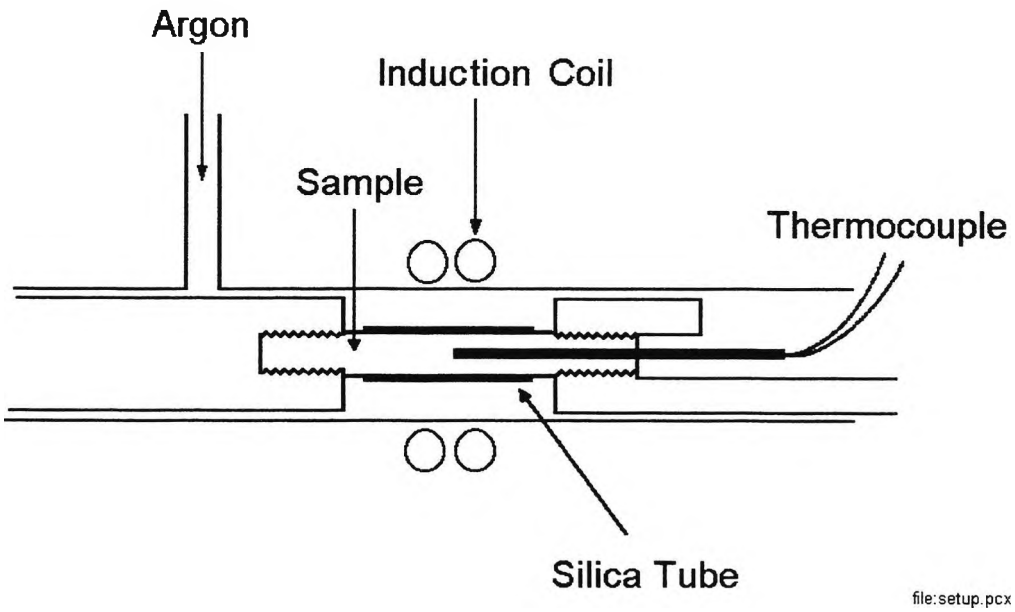


Figure 3–1: ***Schematic drawing of the test.***

The specimen design is shown in Fig. 3-2. Tensile samples were machined parallel to the rolling or forging direction. A 2mm diameter hole was drilled up to the middle of the sample so that thermocouple could be inserted.

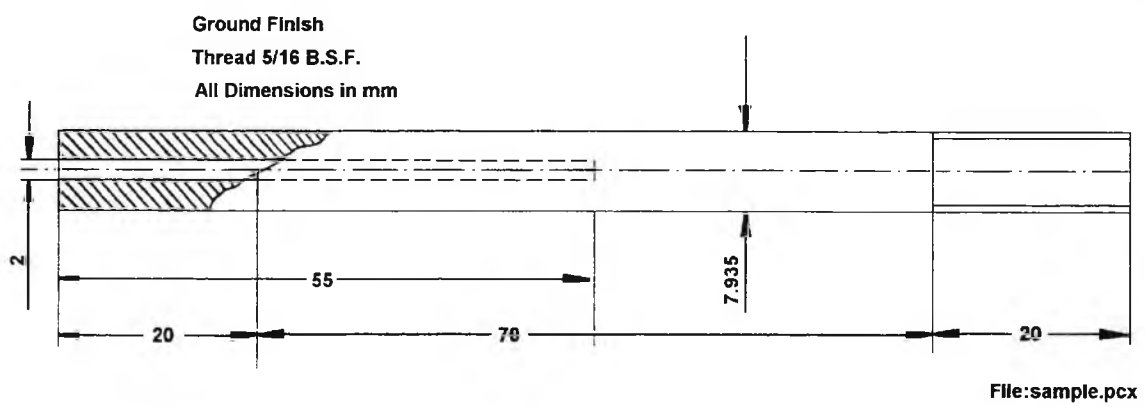


Figure 3–2: ***Schematic drawing of induction test specimen.***

Samples were melted at about 1540°C for 5 min, and cooled to the required test temperatures in the range of 800°C to 1150°C where they were kept for another 5 min before stressing to the failure using an average strain rate of $3x10^{-3}$ s^{-1} based on a gauge length of 22mm. During the hot tensile test a load/elongation graph was produced which could be used to identify the occurrence of dynamic recrystallisation.

Temperature measurements were taken using a platinum/platinum-13% rhodium thermocouple connected to a milivoltimeter. The actual measurement had to be converted into temperature by using a conversion chart, adjusting the values for room temperature (generally 25°C).

Temperature was controlled manually by adjusting the power of the induction machine according to the desired temperature. The cooling rate can be set by controlling the power/temperature and adjusting to a timer. Cooling rates were 25K and 100K/min.

The microstructure of the fractured samples were "frozen in" by increasing the argon flow immediately after the sample was broken.

Strain rate is calculated by dividing the speed of cross-head beam by the length of the melted zone (~22 mm). For this programme it was always $3x10^{-3}s^{-1}$.

Reduction of Area measurements - The shadow graph machine

Both parts of broken samples were measured in a Vickers shadow graph machine at magnification of 12.4 times. The Reduction of Area (RA) was taken from the fractured samples by the measurement of the initial (D_i) and final diameter (D_f). As the fracture surface was irregular, D_f was taken using a shadow graph, and taking the average measurement of four diameters at 90° intervals of rotation for each half of the broken tensile. D_f was therefore the average of eight measurements. The Reduction of Area (R of A) was calculated by the formula:

$$RA = \frac{D_i^2 - D_f^2}{Di^2 - 4}$$

where the number 4 in the equation arises due to the drilled 2 mm hole for inserting the thermocouple.

After the measurements of the final diameter, the samples were mounted in hot cured resin, in a mounting machine, polished to 1 micron and etched in Nital 2% or 3% for optical analyses. Carbon extraction replicas were made by deposition of C in a vacuum chamber. The fractured surfaces were used for SEM (scanning electron microscope) examinations.

Preparation for optical microscopy and carbon replica extraction

The carbon replica is a technique to copy a topography of a body to a thin film of carbon in order to study it in a transmission microscope.

Specimens were taken near to the fracture in the longitudinal direction and mounted in a mounting machine. Subsequently the sample was ground on coarse and fine sandpaper wheels and polished up to 1 micron using diamond paste as polishing abrasive. A carbon replica was taken by deposition of a thin layer of carbon after arc evaporation in a vacuum chamber. For this process the polishing had to be carried out down to 0.25 micron diamond paste. The deposited carbon layer was removed after immersing the sample in an ethanol 10% nitric acid solution until it floats on the solution.

After etching the sample in 2% Nital solution, optical microscopy was performed in order to observe the occurrence of the ferrite film and for austenite grain boundary measurements.

Scanning electron microscopy

The fracture surface of the half of the tensile was examined in a Jeol 200, scanning electron microscope in order to study the dimple size. It was also used to follow the change in fracture appearance with increase in temperature. Observations were made at magnifications from 35X to 750X. Photographs have also been taken at the same range of magnifications.

Transmission electron microscopy (Precipitate measurements)

Precipitate measurements have been carried out manually using a magnification lens fitted with a rule. It is always difficult to measure volume fraction from the replicas as this is dependent on the extraction process but size measurement presents no difficulties. Measurements were made on samples that had been tested at 950°C and 1000°C - the number of particles being measured varying from 100 to over a 1000 depending on the availability. For spherical precipitates measurements was made of their diameters while for cubic particles typical of TiN a side length was measured. The average (p_s) was calculated by taking the weighted average considering the number of precipitates counted for a range of size.

$$p_s = \frac{\sum n_i x s_i}{\sum n_i}$$

where n_i is the number of precipitates and s_i is the respective size considering range for each (i) size.

Some very large isolated precipitates were ignored. For Al and Nb Ti free steels a smaller number of precipitates were considered.

Carbon replicas were examined in Transmission Microscopy in order to obtain both the size shape and composition of precipitates. Edax analyses was carried out on the particles to help in determining the likely composition of the precipitates.

Reliability of results data

Generally the reliability of the reduction of area values in the tensile tests was good despite some curves showing considerable scatter. Scatter was greatest for the high Al steel with Ti:N ratio 1.6:1 which nevertheless showed a trend for hot ductility to improve in the temperature range 800-900°C, particularly at the slow cooling rate. The reliability of the temperature measurement was inversely proportional to the distance between the fracture surface and the tip of the thermocouple. However, the temperature gradient was small up to 5mm from the centre, as can be seen in Fig. 3-3, increasing with increase in test temperature.

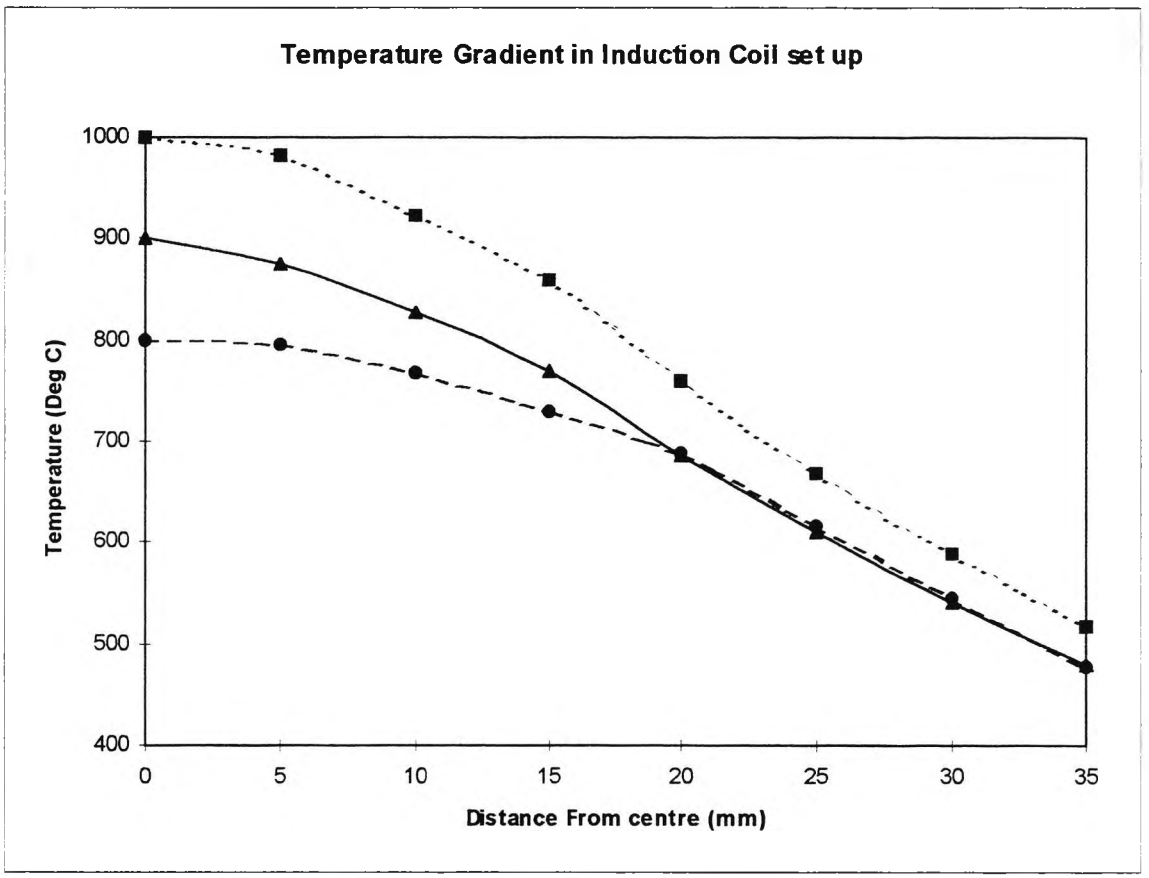


Figure 3–3 **Temperature gradient along the central axe of the induction coil**

The temperature can be seen to remain approximately constant up to 5mm from the centre but then it starts to fall quite markedly. Although the molten region is 22mm, the gauge length that should be chosen for these tests on the basis of Fig. 3-3 should be half this i.e. 11mm. Thus the average strain rate will probably be closer to $6x10^{-3}s^{-1}$, rather than the $3x10^{-3}s^{-1}$ originally suggested. Only tests in which the fracture occurred within 5-6mm from the centre were taken as being acceptable.

Fractures outside this range were repeated when the results did not fit as expected. Tests carried out at 800°C were particularly problematic. Outside of the melted zone, at this lower temperatures there is a softer region caused by the presence of thicker ferrite film. Because of this, the sample tends to break outside the melted

zone and many times either a shift in the coil had to be made at the end of the test, causing loss of reliability in test temperature or a wider glass was used to make a "pool" and decrease the diameter of the sample forcing it to break inside the melted zone. This solution could change badly the shape of the final specimen and make it difficult to interpret the final diameter, causing loss of confidence in the R of A results. When this occurred, the tests were repeated. Any unusual results not fitting the curve were repeated.

No significant changes in composition has been found during the testing. Chemical compositions were checked after testing either by British Steel or IFW of Germany. Analysis was made of the molten region on the tensile specimen and on the heads of the samples. Generally changes were small. A small loss of aluminium and manganese was noted but there was no significant change for the other elements which were analysed. Table 3-1 below shows the IFW analysis for 3 different steels taken from this work.

The British Steel analysis was only carried out for Ti but it can be seen from that melting produced no loss of Ti.

Table 3-1 ***Changes in composition after melting wt per cent.***

	Mn	Si	Al	Ti	Nb
1 unmelted	1.35	0.26	0.025	0.015	0.023
1 molten	1.09	0.27	0.018	0.014	0.027
2 unmelted	1.26	0.24	0.022	0.014	0.023
2 molten	1.20	na	0.020	0.016	0.027
3 unmelted	1.28	0.26	0.020	0.015	0.025
3 molten	1.09	na	0.016	0.011	0.024

na: not available

Precipitates size reliability was quite good due to the number of precipitates considered, especially when they were homogeneous and in large number. Nevertheless, in a few cases, the size distribution was quite scattered and their number few, bringing down the confidence. Table 3-2, shows the approximate number of precipitates considered in each case.

Table 3-2: - ***Precipitates size and number counted for temperatures of 950 and 1000°C.***

Steel	part. size (nm) and number 950°C (number)		1000°C (number)		dimple size* at 800°C (μm)	R of A (%) 950°C	1000°C	Cool. Rate (K/min)
Low Ti Ti:N 3.6;	**10.2**	**361**	**21.1**	**48**	**18**	**42**	**56**	**100**
Nb 0.042 Blue(2B)	**12.2**	**344**	**32.9**	**117**	**22**	**61**	**77**	**25**
High Ti Ti:N 8.0;	16.7	607	37.6[x]	1338	27	51	60	100
Nb 0.043 Red(1B)	57.0[xx]	7	43.5	44	24	57	65	25
Low Ti Ti:N 1.6;	**1-5**	**15/**	**20**	**60/**	**16**	**26**	**50**	**100**
no Nb Green(6B)	**10**	**30/**	**-**		**7**	**51**	**70**	**25**
High Ti Ti:N 6.2	10-15	69	26.6	72	15	46	53	100
no Nb Black(5B)	20	100/	25	15	12	55	62	25
High Al Ti:N 2.8(4)	**9.2**	**143**	**10.0**	**220**	**39**	**30**	**40**	**100**
	13.1	**168**	**14.0**	**320**	**86**	**52**	**85**	**25**
Vlow Al Ti:N 3.0(13)	8.2	181+	-		7	50	61	100
	8.2	91+	-		28	70	90	25
Ti:N 1.6 no Nb Or(7B)	**10-25**	**150/**	**-**		**10**	**45**	**63**	**100**
Ti:N 3.1 Nb Gold(4B)	15	30/	-		11	45	47	100
Ti:N 2.0 Nb Pur(3B)	**7**	**30/**	**-**		**9**	**38**	**47**	**100**
Euro 57-Al steel	77[@]	17			10	97	98	200
PS@900°C	43[@900]	7			15	97	98	25
Euro 58-Ti:N3.4	**7.5**	**575**	**9.5**	**50/**	**-**	**23**	**30**	**200**
no Nb	**7.7**	**324**	**15**	**50/**	**-**	**40**	**73**	**25**
Euro 59 - TiN3.5	8.5	208+	10.9	57+		17	30	200
Nb	10.8	1062+	14	27+		38	65	25
Euro 61 Ti:N:3.3			**11.8**	**117**		**29**	**35**	**200**
high S Nb			**20.8**	**49**		**44**	**55**	**25**
Euro 65-Ti:N 5.0	9.4	413	20		-	45	51	200
+Nb	15.9	260	44.4		-	60	79	25
V low Al(12)	**120[@800]**	**8**	**-**	**-**	**7**	**>96**	**-**	**100**
	127[@800]	**6**	**-**	**-**	**28**	**>97**	**-**	**25**
High Al(3)	73[@800]	170	-	-	5	85	96	100
	92[@800]	26	-	-	17	90	97	25
Euro 60 - Nb Steel	**13.1**	**37**				**70**	**90**	**200**
	39.7	**42**	**48.4[@975]**	**33+**		**85**	**92**	**25**

(*) measured at 800°C due SEM at higher temperatures show almost no dimples.

/ guessed; + not considered 100%; x fine precipitates gathered in clusters; xx very low number.

Grain size measurements were made by the intercept technique. Because they were very coarse, the numbers of grains in the sample was small and not many of them were considered. However, it can be seen that grain size was always very coarse and was generally in the range 1 to 3mm. There was also a trend for the grain size to be refined at the faster cooling rate but quite often differences were small, Table 3-3.

Table 3-3 - ***Austenite grain size and ferrite film measurements for samples in as cast condition at 800-850°C.***

Steel	γ grain size (mm)	α film thickness (mm)	Cooling Rate K/min
Low Ti Ti:N 3.6;	**1.45**	**.036**	**100**
Nb 0.042 Blue(2B)	**1.16**	**.022**	**25**
High Ti Ti:N 8.0;	.70	.006	100
Nb 0.043 Red(1B)	1.3	.0065	25
Low Ti Ti:N 1.6;	**1.55**	**.036**	**100**
no Nb Green(6B)	**1.48**	**.026**	**25**
High Ti Ti:N 6.2	1.10	.012	100
no Nb Black(5B)	1.62	.022	25
High Al Ti:N 2.8(4)	**1.30#**	**.022**	**100**
	1.13#	**.022**	**25**
Vlow Al Ti:N 3.0(13)	1.36	.006	100
	>2.90	.058	25
Ti:N 1.6 no Nb Or(7B)	**1.21##**	**.014##**	**100**
Ti:N 3.1 Nb Gold(4B)	1.76##	.005##	100
Ti:N 2.0 Nb Pur(3B)	**1.33##**	**.019##**	**100**
Euro 57-Al steel			200
			25
Euro 58-Ti:N3.4			**200**
no Nb			**25**
Euro 59 - TiN3.5			200
Nb			25
Euro 61 Ti:N:3.3			**200**
high S Nb			**25**
Euro 65-Ti:N 5.0			200
+Nb			25
V low Al(12)	**1.00**	**.015**	**100**
	1.58	**.051**	**25**
High Al(3)	1.14	.016	100
	3.00	.023	25
Euro 60 - Nb Steel			**200**
			25

(#)900°C and (##)950°C.

Ar_3 and Ae_3 temperatures

The Ae_3 temperatures have been determined by the Thermocalc computer programme[Sundman et al, 1985] and are given in Table 3-4.

The Ar_3 temperatures were determined by dilatometry at the British Steel laboratories and the results are shown below, in Table 3-4, for both rates of cooling. However, it should be noted that British steel are not able to melt samples and the highest temperature that they can achieve is 1330°C. At this temperature not all the TiN particles will be dissolved particularly in the higher Ti steels. Nevertheless, some useful information can be obtained. Increasing the cooling rate under these conditions can be seen to only give rise to a relatively small decrease in the Ar_3 (~5-30°C). More importantly the addition of Nb causes the Ar_3 transformation temperature to fall by ~70°C.

However, this information will be more relevant to the lower temperature end of the trough where it might be expected that Nb containing steels would require lower temperatures to restore ductility. In the present exercise only the trough itself and the higher temperature end of the trough has been explored and therefore the information in this table is only of limited use in the present exercise.

Table 3-4;: ***Ar_3 and Ae_3 temperatures of the steels analysed***

Ar_3 and Ae_3 temperatures (°C)					
Composition	**Code**	**Cooling rate (K/min)**	**Ar_3Transf. Start**	**Ar_3Transf. Finish**	**Ae_3**
.039% Ti+	**Black(5B)**	**100**	**735**	**500**	
.021%Al	**Ti:N6.2**	**25**	**710**	**520**	**-**
.011%Ti+	Green(6B)	100	745	520	
.052%Al	**Ti:N1.6**	25	765	600	-
.014%Ti+	**Blue(2B)**	**100**	**685**	**510**	
.008%Al+Nb	**Ti:N3.6**	**25**	**685**	**490**	**-**
.045%Ti+	Red(1B)	100	645	480	
.009%Al+Nb	**Ti:N8.0**	25	650	430	-
.034%Ti+	**Gold(4B)**	**100**			
.031%Al+Nb	**Ti:N3.1**	**25**			**-**
.020%Ti+	Purple(3B)	100			
.036%Al+Nb	**Ti:N2.0**	25			-
.010%Ti+	**Orange(7B)**	**100**			
.011%Al	**Ti:N1.6**	**25**			**-**
no Ti	Euro 57	200	690	510	
.013%Al	Euro 57	25	680	520	-
.024%Ti+	**Euro 58**	**200**	**725**	**560**	
.20%Al	**Ti:N3.4**	**25**	**710**	**575**	**-**
.021%Ti+	Euro 65	200			
.030%Al+Nb	**Ti:N5.0**	25			-
no Ti	**Vlow Al**	**100**	**720**	**515**	**835**
.009%Al	**Vlow Al**	**25**	**710**	**520**	**-**
no Ti	High Al	100	745	515	843
.060%Al	High Al	25	750	560	-
.019%Ti+	**VlowAl+Ti**	**100**	**720**	**550**	**836**
<.005%Al	**Ti:N3.0**	**25**	**730**	**580**	**-**
.021%Ti+	High Al+Ti	100	750	580	848
0.45%Al	**Ti:N2.8**	25	770	600	-
.024%Ti+	**Euro 59**	**200**	**700**	**490**	
.013%Al+Nb	**Ti:N3.5**	**25**	**710**	**535**	**-**

Chapter 4 - THE EFFECT OF Ti ON THE HOT DUCTILITY OF C-Mn-Al-Ti STEELS AND ITS RELEVANCE TO THE PROBLEM OF TRANSVERSE CRACKING IN CONVENTIONAL AND THIN SLAB CASTING.

BACKGROUND

The City University as part of the programme on Thin Slab Casting (European research programme P3454) is examining the hot ductility behaviour of HSLA steels under thin slab casting conditions. Thin slab casts can be predeformed prior to unbending and are exposed to faster cooling rates at the surface compared to conventional continuously cast slabs. Both these conditions need to be explored. Previous work by Abushosha et al[Abushosha et al, 1998p227], had examined the influence of cooling rate on a vacuum cast C-Mn-Nb-Al steel. Three cooling rates were examined 25, 60 and 200 K/min. It was found that increasing the cooling rate caused the hot ductility to deteriorate.

This chapter covers the research work performed by Osvaldo Guilherme Comineli in the Laboratories of the City University, London, in the period 1st Oct 1995 to May 1997. This work forms part of a three member agreement between the Univesidade Federal do Espírito Santo - (UFES), Companhia Siderúrgica de Tubarão and City University, London, which should result in UFES becoming a

nucleus of excellence in Research & Development in steel technology and which will give technical support to the Brazilian steel industry to improve their quality and productivity. The whole programme parallels a European Programme whose main target is to develop the thin slab continuous casting process route. In addition to this, the Brazilian part of the programme will develop human resources in the field of research and development for the post-graduate students at UFES which will support the Brazilian steel industry.

INTRODUCTION

Competition in the steel industry is forcing the steel companies to invest more and more in R & D as a way of improving the quality and decreasing the price. Because of the high costs of energy and equipment related to the processing of the steels, and the large volume of steel produced even small improvements can make a significant difference to the final price. The new technology of thin slab casting should, when it is perfected produce large savings in the production of steel. Considerable investment in this new development is now being made particularly in the European Community, North America and Australia [Pleschiutschnigg et al, 1993]; [Fleming et al, 1993]; [Algoma, personal information internet]

One of the worst problems found in the continuous casting of steel, today, is the transverse cracking that occurs during the unbending process which limits the application of some of the special steels, particularly the Nb containing steels, [Mintz and Arrowsmith, 1979]. Increasing the cooling rate has been found, to impair hot ductility in laboratory controlled tensile tests[Abushosha and Mintz, 1998p227].

Previous research work[Abushosha and Mintz, 1998p346] and these findings[Abushossha and Mintz, 1998p227] raise worries with regards to thin slab casting where the cooling rate will be much faster than in conventional continuous casting. In order to process these steels, conditions have to be strictly controlled to permit a safe unbending process which prevents cracks from forming. These conditions can be established in a laboratory test where the variables that affect the hot ductility of the steels are investigated; conditions being chosen to simulate the industrial process.

Of the tests available, the simple hot ductility test has been found to be the best to determine the likelihood of a steel cracking during the unbending process in the continuous casting operation, [Mintz and Abushosha, 1992]. Generally, samples are heated to 1330°C to dissolve all the microalloying additions and produce a coarse grain structure reminiscent of the as-cast grain size. The cooling rate and strain rate are chosen to simulate that undergone by the strand during cooling and bending, respectively.

The present work has concentrated on the influence of Ti on the hot ductility of steel. Small additions of Ti are added to HSLA steel to improve the impact properties of the HAZ[Abushosha et al, 1998p227]. Ti rich particles can form which restrict grain growth at the high temperatures associated with the welding operations.

There is also some indication that small Ti additions can be beneficial to ductility during the straightening operation in continuous casting;[Coleman et al, 1985];[Turkdogan, 1987];[Hater et al ,1973];[Patrick et al, 1994],[Mintz, Private

Communication 1994] [Williams, 1984]. Grain refinement however, does not occur in Ti containing continuously cast steels[Abushosha and Vipond, 1991p613]. Here the benefits of Ti are ascribed in the case of C-Mn-Al steels to the Ti combining with N replacing the AlN precipitation with TiN. It is suggested that of the two precipitates, TiN is less detrimental as it forms at higher temperatures and is coarser. For Nb containing steels, it is assumed that coarse Ti rich particles are formed at solidification and these provide the nuclei for Nb to precipitate out on, leaving less Nb in solution to form the very detrimental fine strain induced precipitation of NbC or Nb(CN)[Abushosha, Vipond and Mintz, 1991p613];[Mintz, Abushosha and Cardoso, 1995]; [Mintz and Abushosha, 1996] and [Mintz and Crowther, 1997].

Although commercially there is evidence to show that Ti additions can on occasions be advantageous[Coleman, 1985];[Turkdogan, 1987];[Hater et al, 1973][Patrick et al, 1994];[Private Communication, 1994] and [Williams, 1984], laboratory hot ductility work has suggested that improvements are likely to be relatively small and the conditions to achieve these improvements are very critical[Abushosha, Vipond and Mintz, 1991p613].

Previous hot ductility work[Abushosha, Vipond and Mintz, 1991p613] on as-cast Ti containing steels has only found improvements at a low Ti:N ratio of 2:1. In the case of Nb containing steels, even then cooling conditions had to be slow, 25 K/min to give the opportunity for the Ti rich particles to come out at higher temperatures in a coarser form. With the advent of thin slab casting in which cooling rates are much faster there is a need to re-appraise the value of a Ti addition particularly as mini-mills are working with electric arc steel of relatively high N content. Increasing the cooling rate after casting invariably leads to worse ductility[Mintz and Crowther,

1996p399]; [Abushosha et al, 1998227];[Abushosha et al, 1998 pg 346].

Furthermore, when in the previous work[Abushosha, Vipond and Mintz, 1991p613] the cooling rate was increased to 100 K/min no improvement in ductility occurred on adding Ti. Thus, in thin slab casting where cooling conditions are much faster, Ti additions may not give rise to improvements in ductility.

Indeed, in more recent work, when the Ti:N ratio was close to stoichiometry for TiN, ductility was very poor even at the slower cooling rate and the TiN particles were very fine[Mintz Abushosha and Cardoso, 1995];[Mintz and Abushosha, 1996].

The present work is a continuation of this work to investigate more fully the influence of the Ti:N ratio on the hot ductility of steels. Because Ti particles do not go back into solution at 1330°C, the simple test has been modified so that the tensiles are directly cast and cooled to the test temperature[Abushosha, Vipond and Mintz, 1991p613].

Since cooling rate has been shown to be important in this previous work[Abushosha and Vipond, 1991p613], the present work has examined two cooling rates 25, and 100 K/min.

EXPERIMENTAL

Seven steels have been tested in this exercise, steels either having different levels of Al and or Ti:N ratios. After kind permission by Dr. Rouckaya Abushosha, this work was enriched with the inclusions of two further steels having similar composition taken from the European Programme. Brazilian casts were 50 kg laboratory vacuum

melts melted in the Aerospace Research Centre Laboratories, Brazil and forged to 12 mm thick plate at the Companhia Siderúrgica Tubarão,(CST) Brazil. Casts Euro 57 and Euro 58 were 50 kg laboratory air melted casts, made by British Steel and rolled to 12 mm thick plate. The British Steel casts were made for the European programme[Abushosha, 1996] and have been included in the present chapter to increase the data base so that greater weight can be given to the conclusions. Ti, Al and N levels have been checked at the British Steel laboratories and the Brazilian analysis was confirmed except in one instance and the British steel analysis has been used for this steel. After machining, the samples were sent by CST to the City laboratories for testing.

The tensile samples of length 70mm and diameter 7.94mm were machined in the longitudinal direction of forging following the shape of the ingot. A hole of 2 mm diameter was drilled from the end of each sample to the mid-length so that a thermocouple could be inserted. The composition of the steels tested are given in the table 4-1 below. Also included are two steels, Euro 57 and 58 from the European Programme.

Table 4-1: ***Chemical composition of the steels analysed***

Comp.	Vlow Al steel 12	High Al steel 3	Vlow Al+Ti steel 13	High Al-Ti steel 4	Black steel 5B	Green steel 6B	Orange steel 7B	57 Euro	58 Euro
C	.09	.09	.09	.08	.10	.10	.09	.09	.0
Si	.32	.29	.32	.29	.32	.31	.31	.31	.33
Mn	1.50	1.33	1.48	1.31	1.40	1.40	1.48	1.40	1.41
P	.018	.017	.016	.017	.017	.017	.019	.011	.012
S	.012	.014	.013	.013	.010	.009	.010	.004	.004
Ti	-	-	.019	.021	.039	.011	.010	-	.024
Sol. Al	.009	.060	<.005	.045	.021	.052	.011	.013	.020
N	.0067	.0064	.0064	.0076	.0063	.0070	.0062	.0068	.0070
Ti:N	-	-	3.0	2.8	6.2	1.6	1.6	-	3.4
[Al][N]	6.0×10^{-5}	3.8×10^{-4}	3.2×10^{-5}	3.4×10^{-4}	1.3×10^{-4}	3.6×10^{-4}	6.8×10^{-5}	8.8×10^{-5}	1.4×10^{-4}
[Ti][N]	-	-	1.2×10^{-4}	1.6×10^{-4}	2.5×10^{-4}	7.7×10^{-5}	6.2×10^{-5}	-	1.7×10^{-4}

For the C-Mn-Al steels, Ti:N ratios less than and greater than the stoichiometric (Ti:N ratio of 3.4) were chosen.

In the City laboratories, the samples were tested in a tensile testing machine to which a heating induction device had been fitted. The melting zone was approximately 22 mm in length situated at the mid-length position of the sample. The molten steel was contained in a silica tube with an initial 0.2 mm clearance and the oxidising protection was achieved by surrounding the silica tube with a wide glass tube through which argon flowed. Full details of the experimental set up can be found in chapter 3.

Samples were melted at 1540°C for 5 min, and cooled to the required test temperatures in the range of 800°C to 1150°C where they were held for another 5 min before straining to failure using a strain rate of 3×10^{-3} s^{-1}. During the hot tensile

test a load/elongation graph was produced which could be used to identify the occurrence of dynamic recrystallisation.

Two average cooling rates to the test temperature were examined 25 and 100K/min. In the European programme the cooling rates examined were 25 and 200K/min, the latter being the equivalent cooling conditions applicable to thin slab casting, (1/10 thickness from the surface). The microstructure of the fractured samples were "frozen" by increasing the argon flow immediately after the sample was broken.

The Reduction of Area (RA) was taken from the fractured samples by the measurement of the initial (D_i) and final diameter (D_f). As the fracture surface was irregular, D_f was taken using a shadow graph, and the average measurement of four diameters at 90° intervals of rotation for each half of the broken tensile was made. D_f was therefore the average of eight measurements. The Reduction of Area (R of A) measurements and microscopic samples preparation were made as outlined in chapter 3.

Optical metallography was also carried out on longitudinal sections including the fractured region of the quenched samples.

Austenite grain sizes and ferrite film thickness were obtained for all the steels using the intercept method from outlinement of the austenite grain boundaries by the ferrite at the minimum ductility temperature of 800°C. Values are shown in Table 3-3.

The fracture surfaces of the samples were examined using a T 200 Jeol scanning

electron microscope.

Previous work[Abushosha et al, 1988p227; Abushosha et al, 1988p346 and Cardoso, Mintz and Yue, 1995] has shown that the dimple size on the fracture surface at the temperature showing the minimum ductility is for a given strain rate related to the size of the coarser particles present at the boundaries. In this case they would be expected to be the MnS inclusions and coarser AlN particles. The size of the dimples was measured taking an average of 500 measurements.

Carbon extraction replicas were taken from close to the fracture surface and the particle size measured, the average of 500 measurements being taken as the particle size. Measurements of particle size was also made on the European steels from the photographs supplied by Dr. Abushosha.

The influence of cooling rate and Ti:N ratio on hot ductility of the C-Mn-Al steels were the main objectives of the present exercise.

Influence of cooling rate

Hot ductility behaviour

Aluminium, Ti free steels

The hot ductility curves for the Ti free steels are given in Fig. 4-1 for cooling rates of 25 K/min (dashed lines) and 100 K/min (solid lines) For the European steels the cooling rates were 25K/min and 200k/min. In the text, the cooling rate of 25K/min will be referred to as "slow" cooling and the two cooling rates of 100 and 200K/min as "fast". It can be seen that as the soluble Al level increases the ductility deteriorates. In addition, it is clear that increasing the cooling rate results in worse ductility. However, increasing the cooling rate has only a small influence on ductility at the highest Al level.

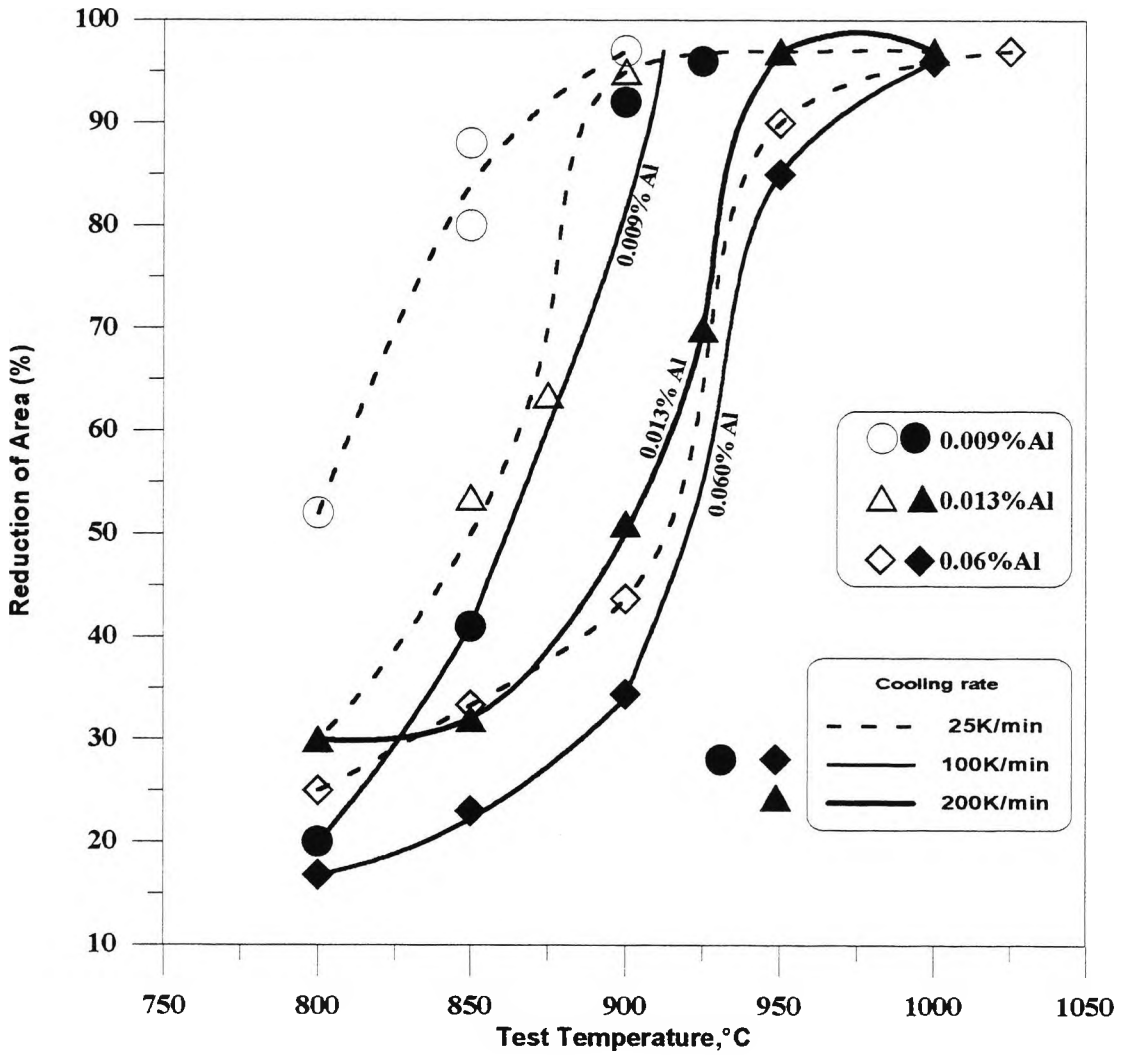
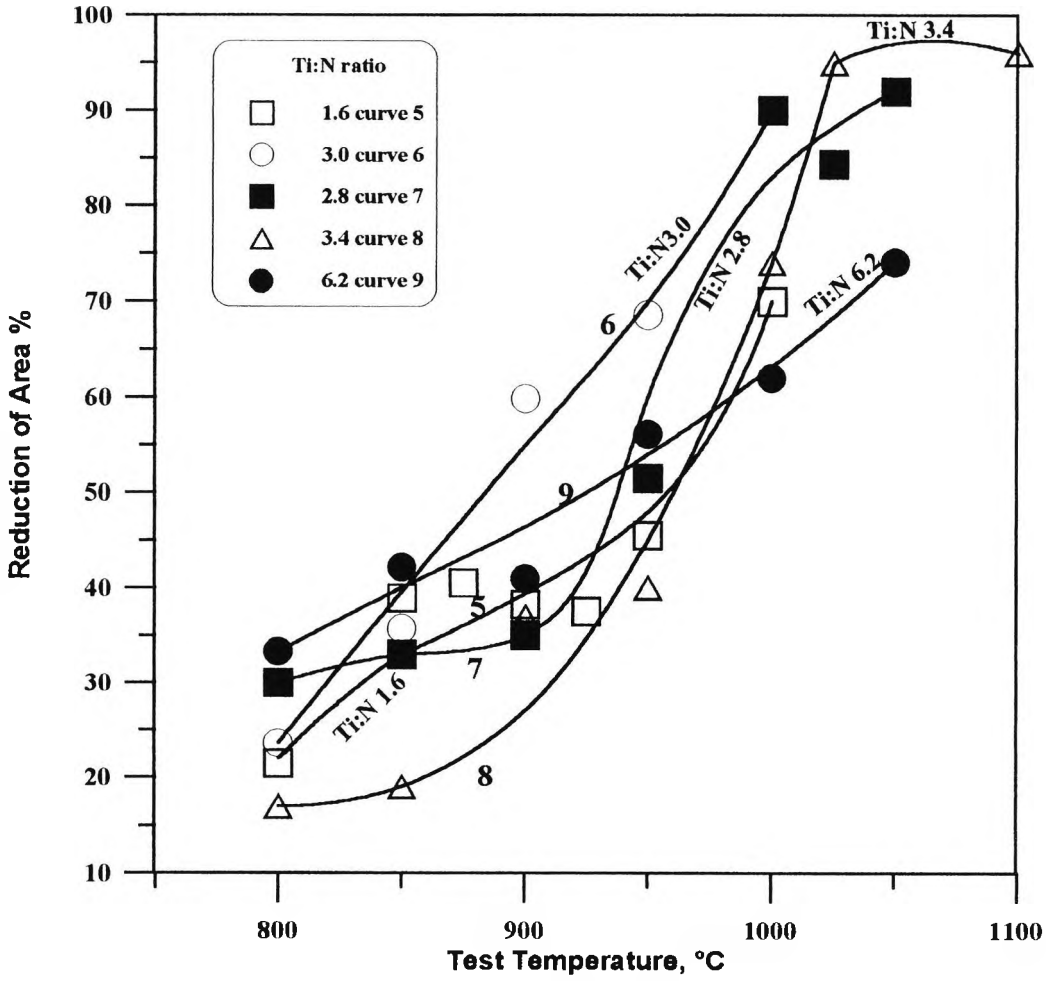


Figure 4–1: - ***Hot Ductility curves for Al containing steels tested at 25 and 100/200K/min, showing how increasing the cooling rate and the Al level impair the hot ductility. The curves for the European steel (0.013%Al), steel 57 in Table 4-I are also included.[Abushosha, 1997]***

C-Mn-Al-Ti steels with different Ti:N ratios:

The curves of R of A against test temperature for the C-Mn-Al-Ti steels having different Ti:N ratios are shown in Figs. 4-2 and 4-3, for cooling rates of 25K/min. and 100/200K/min, respectively. Again the curves for steel Euro 58 from the European

Programme have been included for comparison purposes, for the two cooling rates of 25K/min and 200K/min.



File:Ti2~.grf

Figure 4–2:***Hot ductility curves for steels with different Ti:N ratios cooled at 25K/min. Included in the figure is the curve for steel Euro 58, curve 8, taken from the European Programme[Abushosha, 1997]***

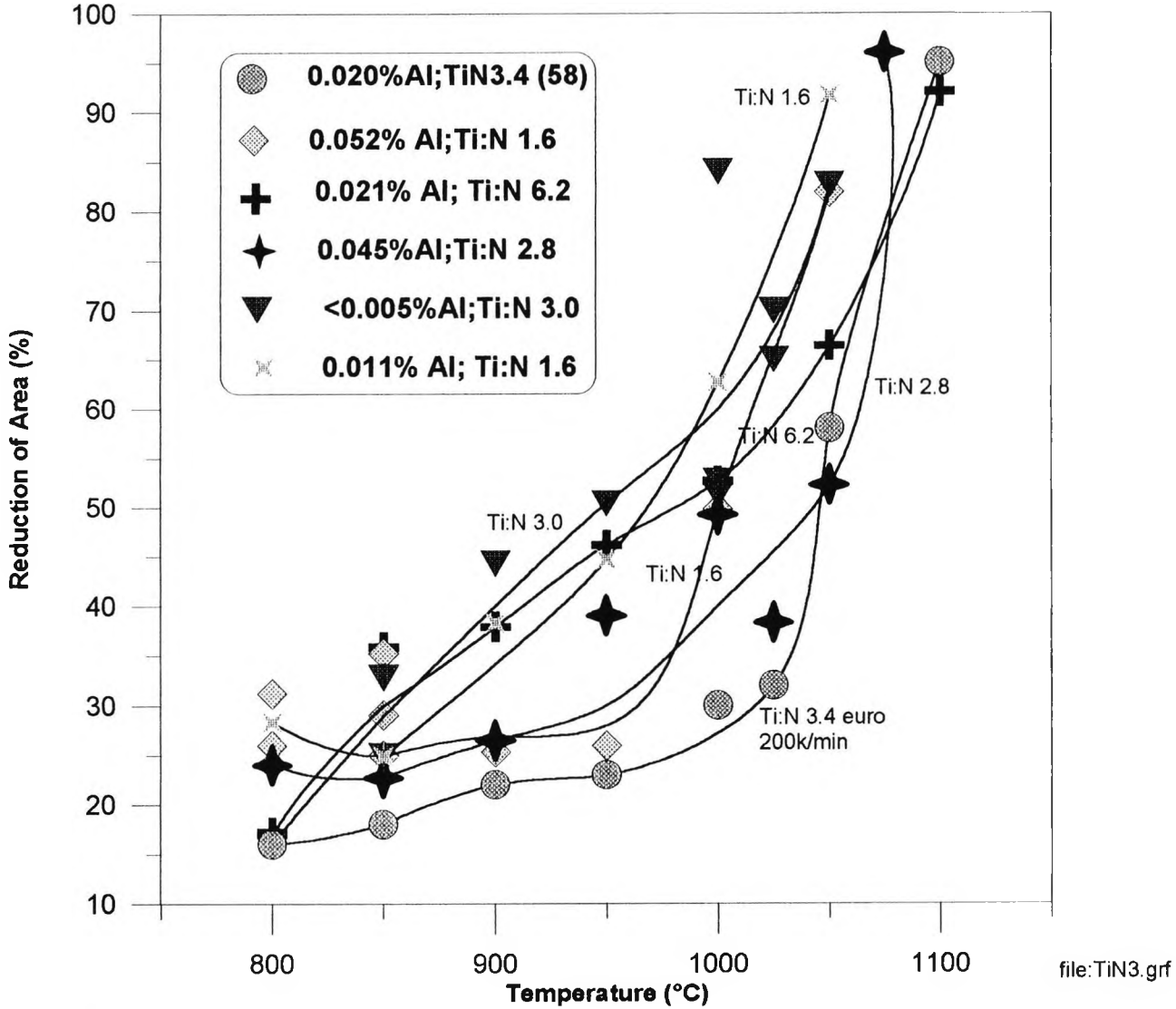


Figure 4–3: ***Hot ductility curves for steels with different Ti:N ratios cooled at 100-200 K/min. Included in the figure is the curve for the Euro 58 taken from the European Programme [Abushosha, 1997]***

Comparison of Figs. 4-2 and 4-3 indicates that again, increasing the cooling rate causes the ductility to deteriorate. The addition of Ti to the C-Mn-Al steel always results in worse ductility as shown in Fig. 4-4, for low Al steel and Fig. 4-5 for high Al steel. The general trends are for the ductility to deteriorate as the Ti:N ratio increases up to the stoichiometric composition for Ti:N, i.e. 3.4:1. At the higher Ti:N ratio of 6.2:1 ductility again improves. It is also interesting to note that at the highest Ti:N ratio there is little effect of cooling rate on hot ductility(compare steel with Ti:N ratio 6.2:1 in Figs. 4-2 and 4-3). Nevertheless, ductility at this ratio is still worse than in the Ti free steels shown in Fig. 4-1.

The hot ductility curves for the Ti containing steels are given in Figs. 4-2 and 4-3 for cooling rates of 25 and 100-200 K/min, respectively. Behaviour can be seen to be complex and comparison of the hot ductility curves for steels at the same Al level, Figs. 4-4 and 4-5, would indicate that the Ti addition generally makes the as-cast ductility worse, particularly at temperatures >900°C Figs. 4-4 and 4-5 for low and high Al containing steels, respectively. At the slow cooling rate, Fig. 4-2, increasing the Ti addition from 0.019 to 0.021% through to 0.024%, curves 6, 7 and 8 respectively, leads to ductility deteriorating. However, the steel with the very low Ti addition of 0.011%, steel 6B, Table 4-1; which might have been expected from the foregoing observations to give the best ductility gave rather poor ductility. Furthermore increasing the Ti level to 0.039%, steel 5B, a level above that for the stoichiometric composition for TiN resulted in the ductility improving again.

At the higher cooling rate Fig. 4-3, behaviour is even more complex and there are again apparently no easily determined trends. The steel with the high Ti:N ratio of 6.2:1 and highest Ti level, steel 5B, gives better ductility than some of the other

steels but the steel with the lowest Ti addition of 0.01%, steel 7B, gives one of the best hot ductility curves of the Ti containing steels. Steel 6B, which also has a low Ti addition, however, again gives poor ductility. The main difference between the steels in Figs. 4-4 and 4-5 is their soluble Al levels, it being much higher for steel in Fig. 4-5.

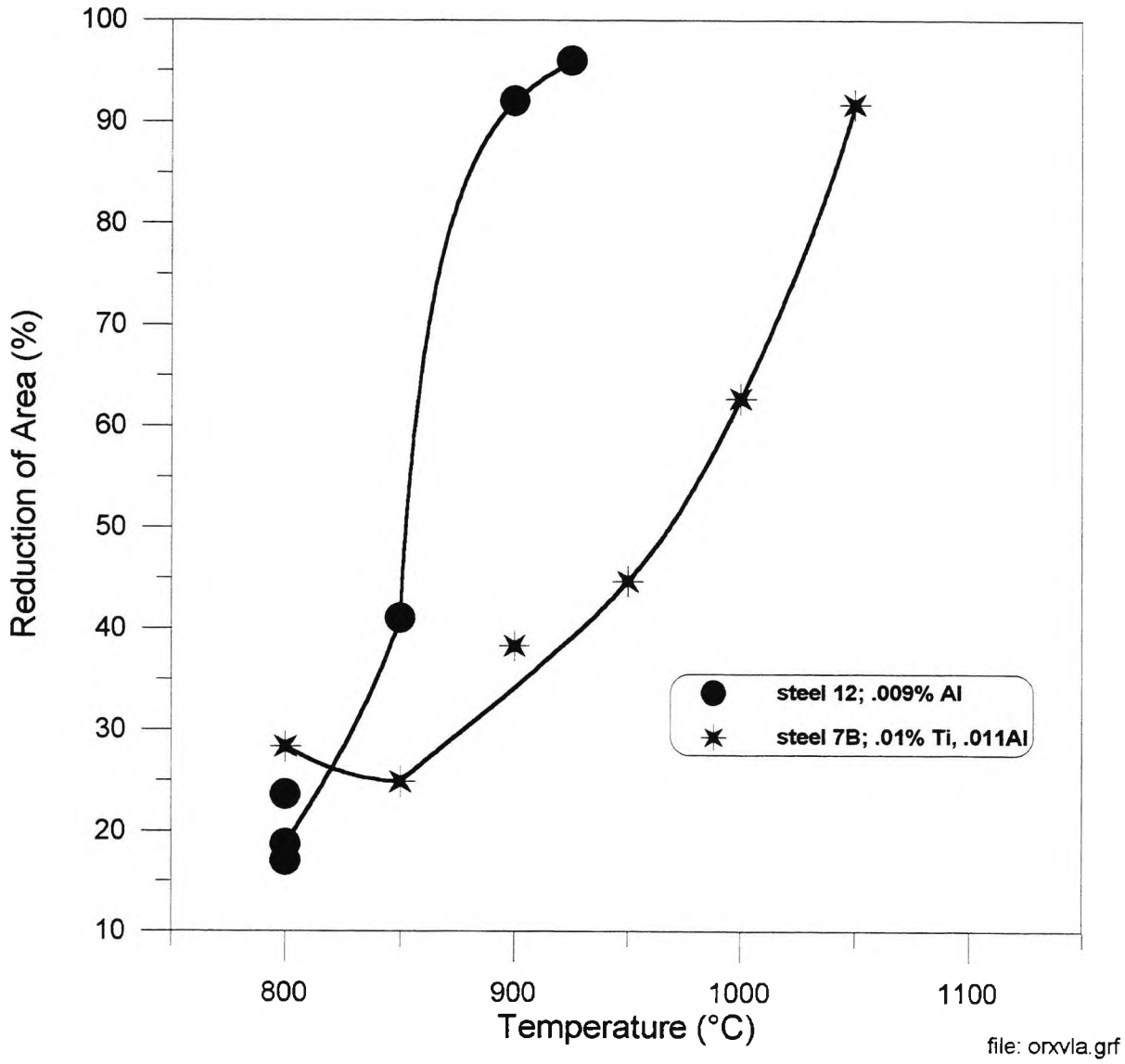


Figure 4–4: ***Effect of Ti on the ductility of as-cast, low Al steels, steels 12 and 7B cooled at 100K/min.***

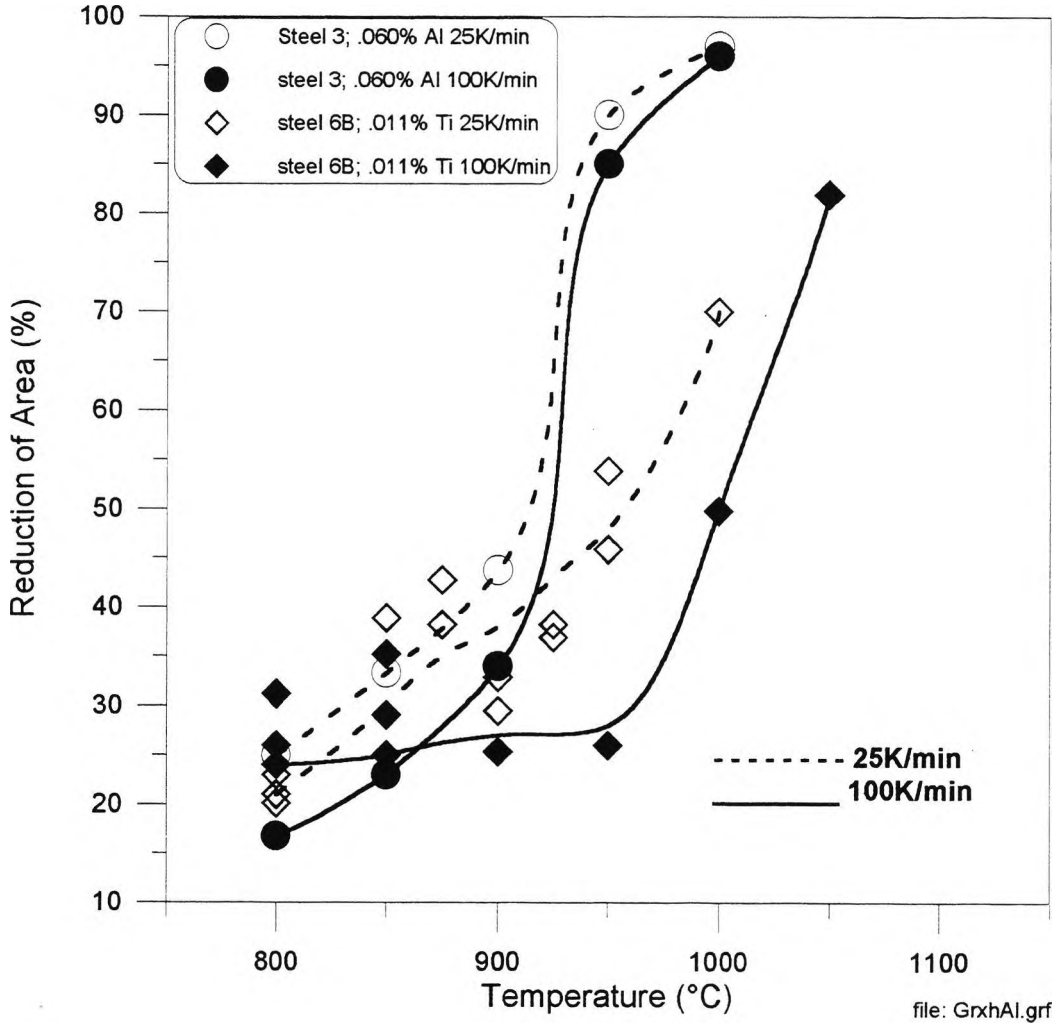


Figure 4–5 ***Effect of Ti on ductility of as-cast high Al steels, steels 3 and 6B, cooled at 25 and 100K/min:***

Behaviour on raising the cooling rate was similar to that shown by the Ti free steels, the higher cooling rate leading to worse ductility (compare Fig. 4-2 with Fig. 4-3) and the Ti additions are again detrimental to ductility.

Optical microscopy

Metallography

The austenite grain size for all the steels was very coarse being 1 to 3 mm, as shown in Table 3-3. A small refinement in grain size sometimes occurred with increase in cooling rate but from previous work, this was not regarded to be likely to have any significance on the ductility[Mintz et al, 1991]. At close to the temperature for the minimum ductility, 800°C the microstructure consisted of thin films of deformation induced ferrite outlining the prior γ grain boundaries, Fig. 4-6.

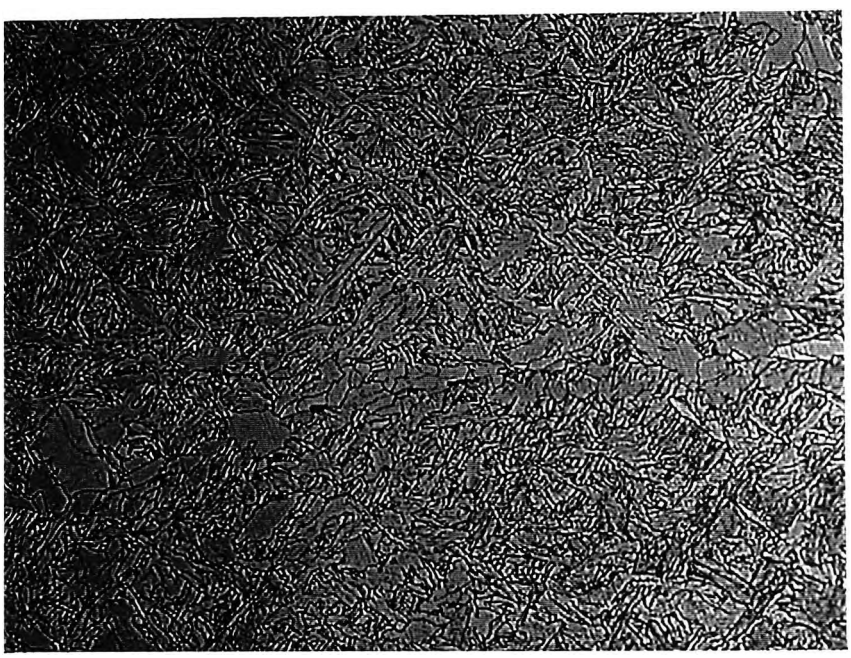


Figure 4–6: - ***Typical deformation induced ferrite film formed at 900°C in steel 4, cooled at 25K/min. (180X)***

SEM analyses of the fracture surfaces as well TEM examination using the carbon replicas were carried out on at least one sample from each curve. The SEM results will be given first.

SEM examination

Scanning electron microscope (SEM)observations

As might be expected from the observation of a thin film of ferrite surrounding the prior γ grain boundaries at the temperature giving minimum ductility, fractures were always of the micro-void coalescent type. Dimples containing particles were observed on all these fracture surfaces, Figs. 4-7 to 4-10.

It can be seen from Table 4-2 that except for two cases, at 800°C, the dimple size was generally coarser at the slower cooling rate.

Table 4-2: ***R of A, dimple size and particle size for fast and slow cooling rates.***

Steel	part. size (nm) and number				dimple size* at	R of A		Cool. Rate
	950°C	(number)	1000°C	(number)	800°C (μm)	950°C	1000°C	(K/min)
High Al Ti:N 2.8(4)	**9.2**	**143**	**10.0**	**220**	**39**	**30**	**40**	**100**
	13.1	**168**	**14.0**	**320**	**86**	**52**	**85**	**25**
Vlow Al Ti:N 3.0(13)	8.2	181+	-		7	50	61	100
	8.2	91+	-		28	70	90	25
Ti:N 1.6 Or(7B)	**10-25**	**150/**	**-**		**10**	**45**	**63**	**100**
Euro 57-Al steel	77@	17			10	97	98	200
	43@900	7			15	97	98	25
Euro 58-Ti:N 3.4	**7.5**	**575**	**9.5**	**50/**	**-**	**23**	**30**	**200**
	7.7	**324**	**15**	**50/**	**-**	**40**	**73**	**25**
V low Al(12)	**131@800**	**8**	**-**	**-**	**7**	**>96**	**-**	**100**
	122@800	**6**	**-**	**-**	**28**	**>97**	**-**	**25**
High Al(3)	73@800	170	-	-	5	85	96	100
	92@800	26	-	-	17	90	97	25
High Ti Ti:N 6.2	10-15	69	26.6	72	15	46	53	100
no Nb Black(5B)	20	100/	25	15	12	55	62	25
Low Ti Ti:N 1.6;	**1-5**	**15/**	**20**	**60/**	**16**	**26**	**50**	**100**
no Nb Green(6B)	**10**	**30/**	**-**		**7**	**51**	**70**	**25**

(*) measured at 800°C due SEM at higher temperatures show almost no dimples.

/ guessed; + not considered 100%

Typical examples of the fracture appearance at the temperature giving the minimum ductility are shown in Figs. 4-7 and 4-8, for the Ti free, low Al and high Al containing steels, respectively. The dimple size can also be seen to decrease with increase in both the Al level and cooling rate, Figs. 4-7 and 4-8. Edax analysis showed that the particles contained Mn and S, indicating the presence of MnS. A peak for Al was only found in the high Al containing steel, steel 3, indicating the likely presence of AlN. (Particles were often "triangular" in shape again suggesting AlN rather than Al_2O_3.) The size of the particles in the dimples were also found to decrease as might be expected with decreasing dimple size.

Flat facets characteristic of grain boundary sliding are found as the test temperature increases.

The larger particles in the cavities were analysed and found to be manganese sulphides. AlN particles although probably often present are likely to be an order of magnitude finer and hence difficult to detect with normal EDAX analysis.

Examination of SEM photographs of the fractured surface at 800°C indicated that in general (apart from two exceptions) the dimple size was much finer on fast cooling suggesting that for the same testing temperature, faster cooling produced a finer particle distribution. However, R of A values were often only slightly worse perhaps indicating that the volume fraction of particles was probably not significantly influenced by the cooling rate. The results from each steel will now be given in detail.

Aluminium steels:

Very low Al steel:

The low Al, Ti free steel had the best hot ductility behaviour among those analysed. At a test temperature of 800°C, the fracture surface showed an enormous difference in the size of the dimples, for samples cooled at 25K/min, compared to those cooled at 100K/min, Figs. 4-7 and 4-8 respectively. Analysis of the particles in the dimples identified them mainly as MnS. The particles in the dimples at the faster cooling rate can also be seen to be finer.

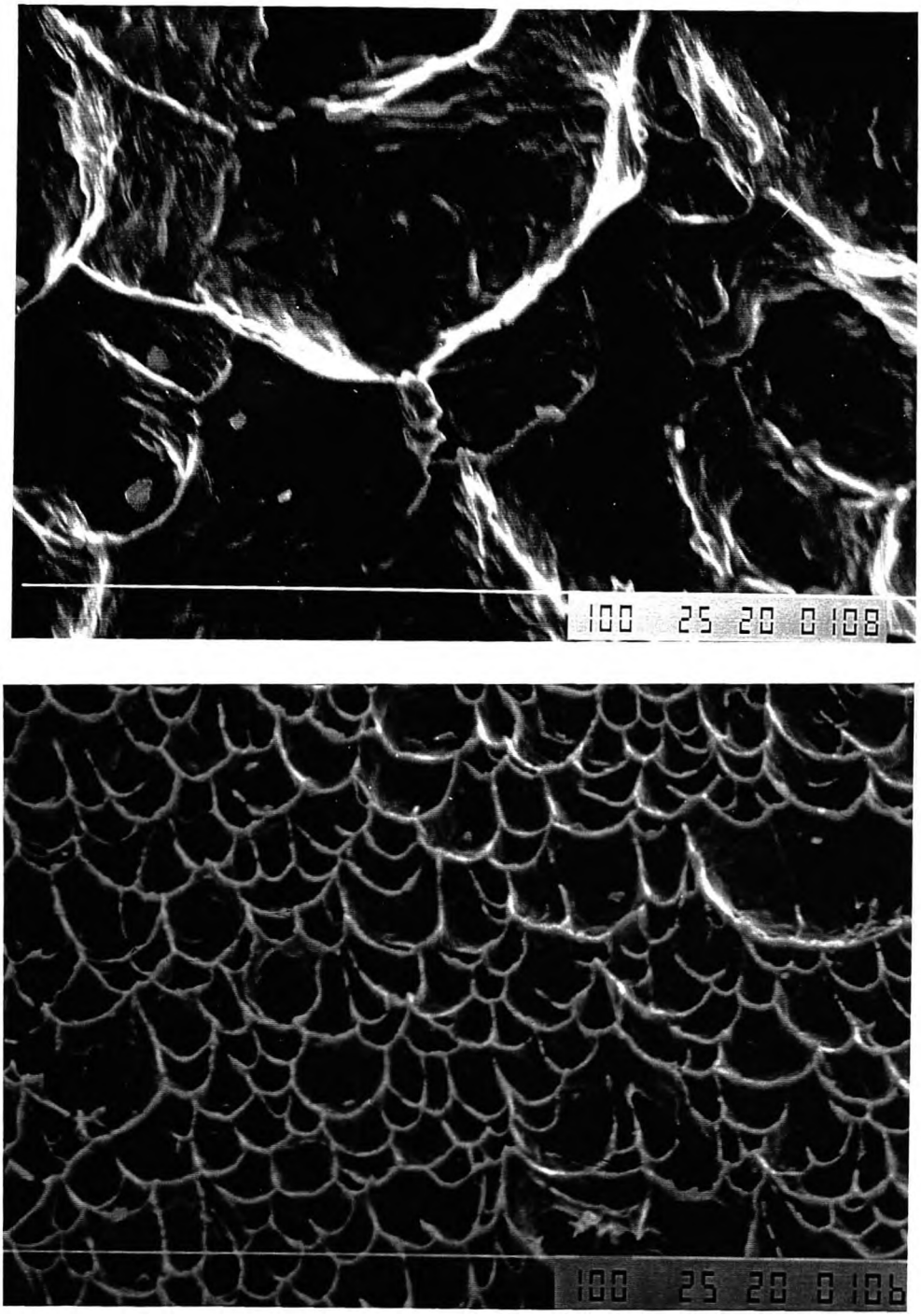


Figure 4-7: ***SEM of the fracture surfaces for low Al steel tested at 800℃, showing refinement of dimples and particles as cooling rate increases. (a) Rate of cooling: 25K/min; R of A 52%, (dimple size 28μm)and (b) 100K/min; R of A 24%(dimple size 7μm). (750X)***

Low Al steel (Euro)

Similar observations have been made by Abushosha on the low Al steel, dimple size being 15μm and 10μm for slow and faster cooling rates, respectively [Abushosha, 1996].

High Al steel:

The high Al, Ti free steel showed the smallest difference in R of A values between the two cooling rates. This difference was most marked at the temperature of 800°C (9 % difference in R of A). Again a very large difference in dimple size was noted, the faster cooling rate giving a much finer size, Figs. 4-8a and b for the slow and faster cooling rate, respectively.

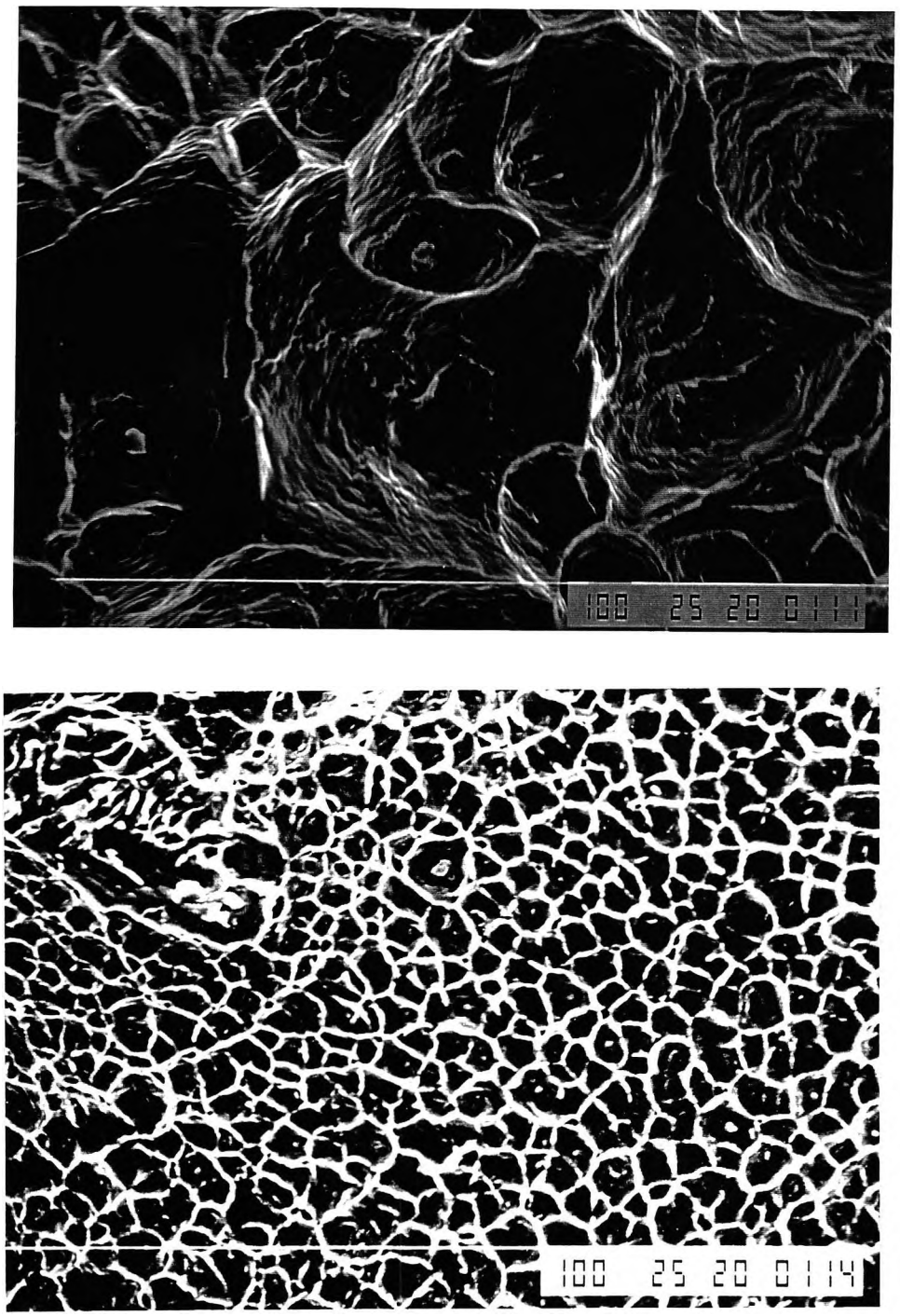


Figure 4-8: ***Comparison of the dimple sizes found in the high Al steel at the two cooling rates. R of A and average dimple size at 800°C: (a) 25%; 17μm and (b) 16%; 5μm. (750X)***

The higher Al level also led to a finer dimple size than found in the low Al steel. Compare Fig. 4-8a with Fig. 4-7a, for the slow cooling rate and Fig. 4-8b with Fig. 4-7b, for the fast.

Ti containing C-Mn-Al steels

The fracture behaviour of the Ti containing steels was less clear. Although the influence of cooling rate on the dimple size was similar, the effect of increasing the soluble Al level was to produce a coarser dimple size, Figs. 4-9 and 4-12b for low and high Al containing steels, respectively. Edax analysis of the particles in the dimples again indicated mainly MnS inclusions with occasional AlN precipitates in the high Al containing steel, steel 4.

Influence of different Ti:N ratios:

Steels having Ti:N ratio less than stoichiometric, <3.4:1

Four C-Mn-Al-Ti steels having Ti:N ratio below the stoichiometric for TiN (Ti:N ratio of 1.6:1, steels 6B and 7B; Ti:N ratio of 2.8:1, steel 4 and Ti:N ratio of 3.0:1, steel 13) were analysed. In spite of having similar composition some differences must be highlighted. For the steels with Ti:N ratios of 1.6:1 compositions were very similar, the only difference being one steel having almost five times more Al (0.052% against 0.011). The steel with a ratio of Ti:N 2.8:1, steel 4 had also high Al content

(0.045%Al) and twice the Ti content of the steels with a Ti:N ratio of 1.6:1 (0.021%Ti). The remaining steel (Ti:N ratio 3.0:1) apart from having almost no Al (<0.005% Al), had a similar composition to the steel with a Ti:N ratio of 2.8:1, steel 4. Examples of fracture appearance are shown in Figs. 4-9 and 4-10 for the steels with Ti:N ratios of 1.6:1 and 3.0:1.

In spite of all the R of A values being close and poor at 800°C the SEM, steel 13 showed considerable differences in dimples size with cooling rate, Fig. 4-10. The steel with highest Al level (Ti:N ratio 1.6:1, steel 6B) showed smaller effect of the cooling rate on the dimple size at 800°C(Fig. 4-12) reduction of area being very similar (23/24%). However, in almost all cases, eg. Figs. 4-7a and b, dimple size was refined on increasing the cooling rate. Also for the steel with Ti:N ratio 3.0:1, steel 13, the dimple size was 7μm and 28μm for the fast and slow cooling rates respectively.

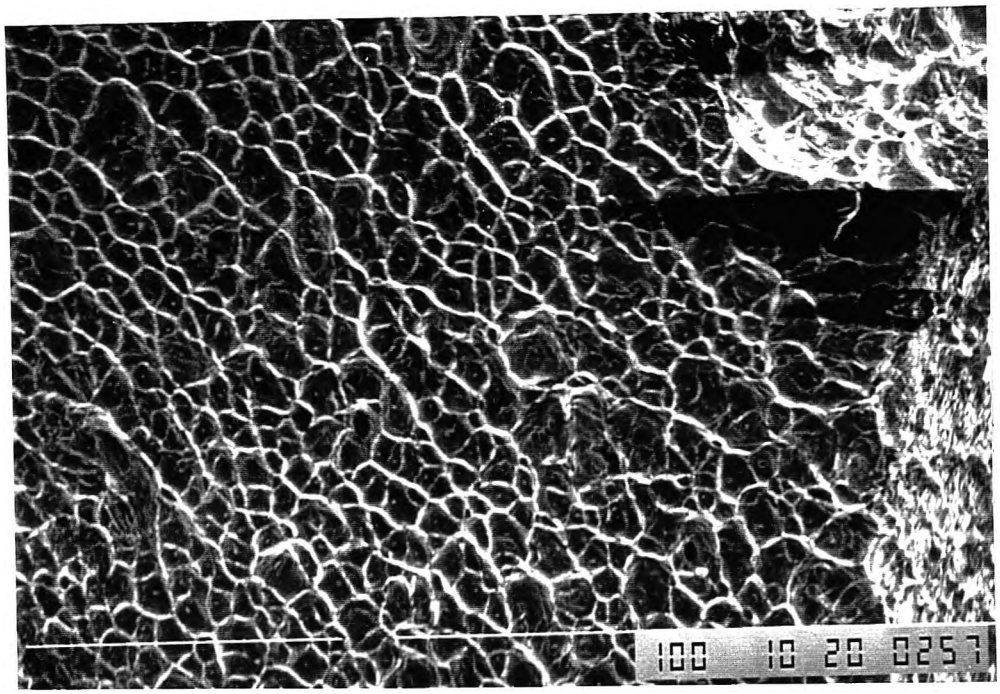


Figure 4-9: ***SEM of the fracture surfaces of low Al containing steel with Ti:N ratio of 1.6:1, tested at 800℃, using a cooling rate of 100K/min. R of A was 18% (dimple size 10μm) (350X).***

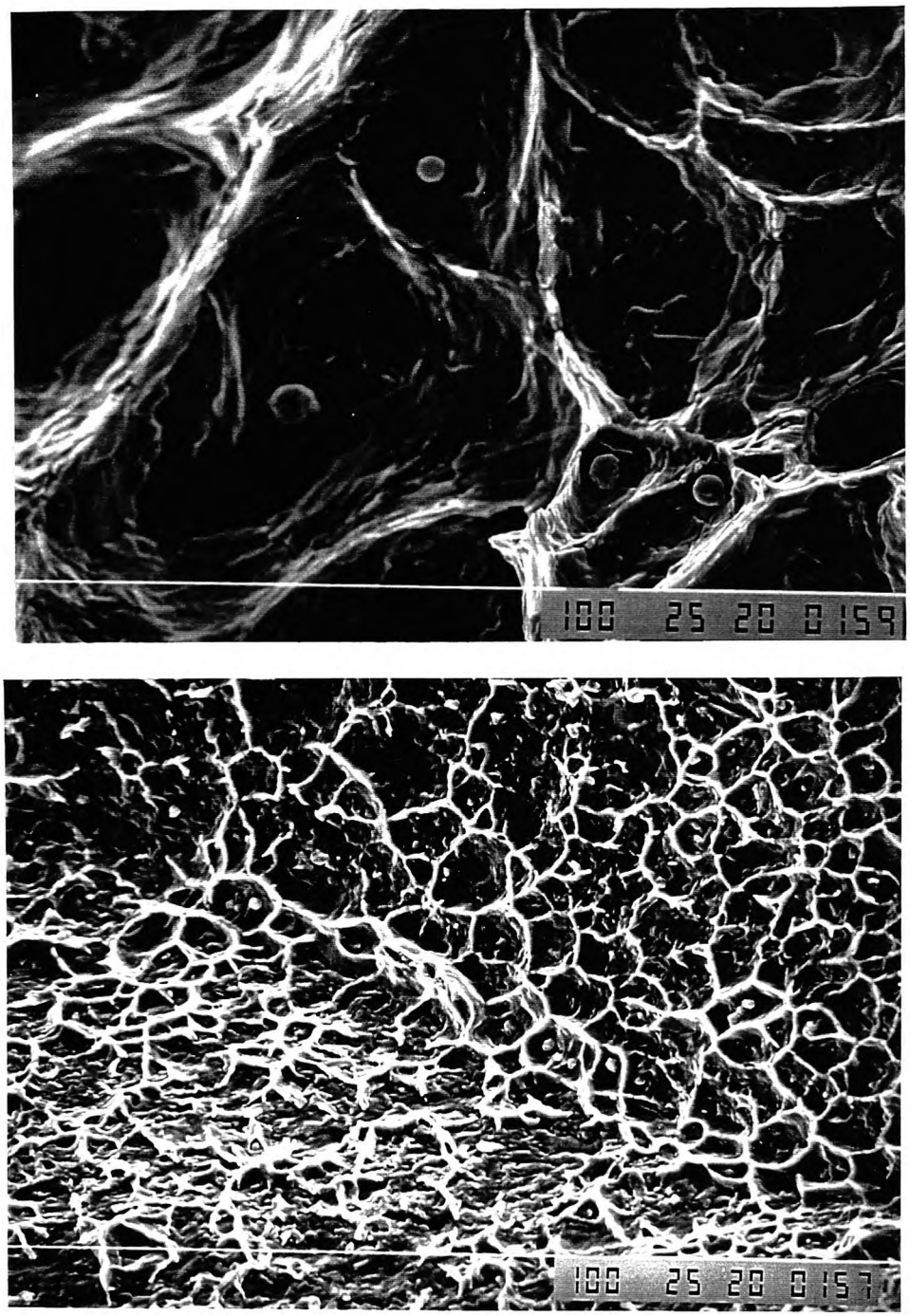


Figure 4-10: ***SEM of the fracture surfaces for steel with a Ti:N ratio of 3.0:1. Steel was tested at 800 °C, showing refinement in dimple size on increasing the cooling rate. (a) Rate of cooling: 25K/min; R of A 24%(dimple size 28μm) and (b) 100K/min; 16%(dimple size 7μm). (750X)***

Increasing the cooling rate and the temperature for the steel with higher Al within the Ti:N ratio of 1.6:1, steel 6B, caused the ductility markedly to deteriorate. At 950°C, R of A was 46% for slow cooling rate against 26% for the fast cooling rate. At this temperature, the fracture mode was essentially grain boundary sliding for the faster cooling rate. At the lower cooling rate, the fracture was again mainly grain boundary sliding but there was also areas in which microvoid coalescence was observed, Fig. 4-11.

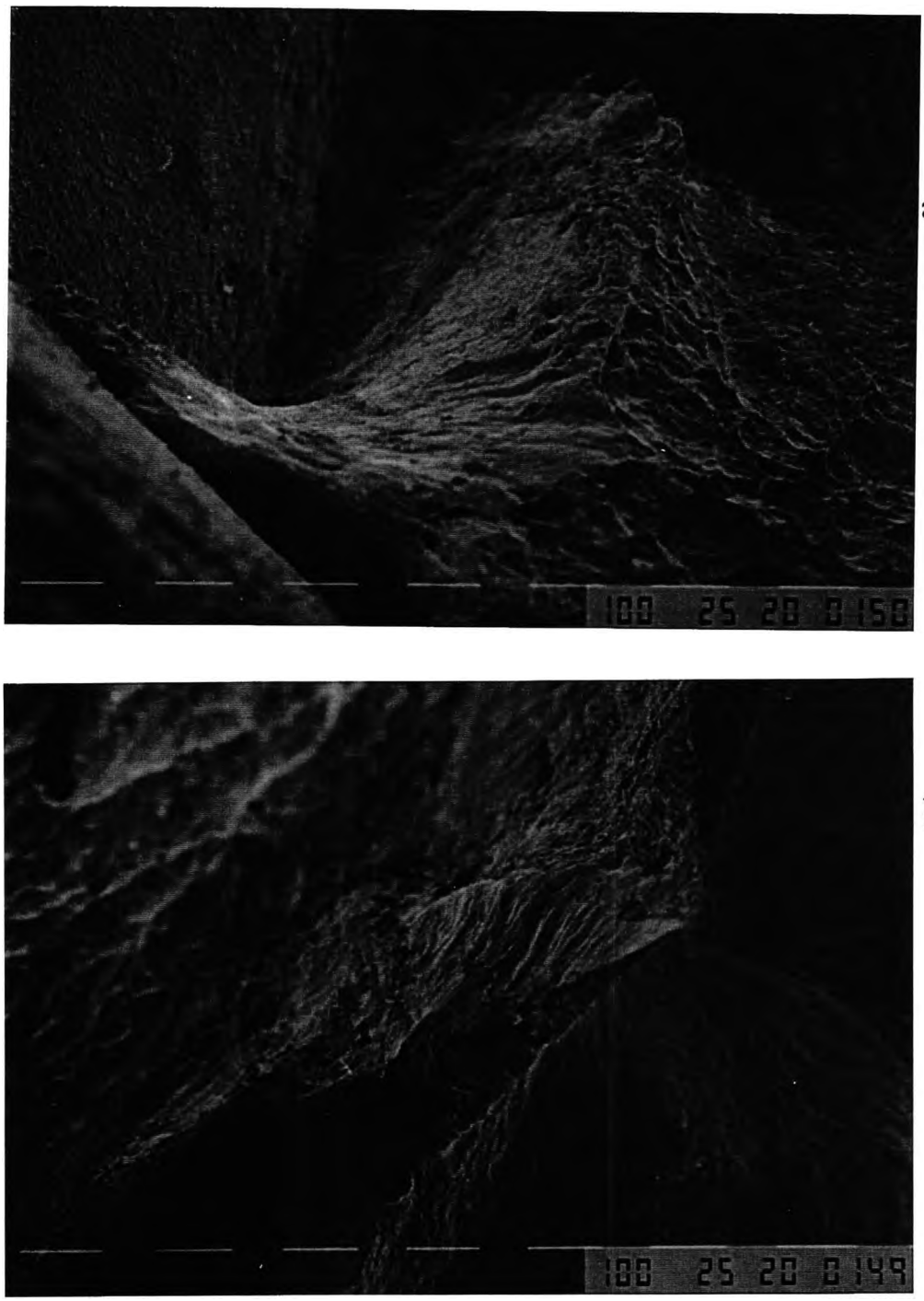


Figure 4-11: ***Low Ti (Ti:N ratio of 1.6:1) steel tested at 950°C, showing (a) mixture of grain boundary sliding and ductile fracture when cooled at 25K/min and (b) grain boundary sliding on cooling at 100K/min. R of A 46% and 26% respectively. (100X)***

At the lower temperature of 800°C, the fracture showed intergranular failure originating from microvoid coalescence. In this one case, the size of the dimples were coarser at the faster cooling rate, Fig. 4-12.

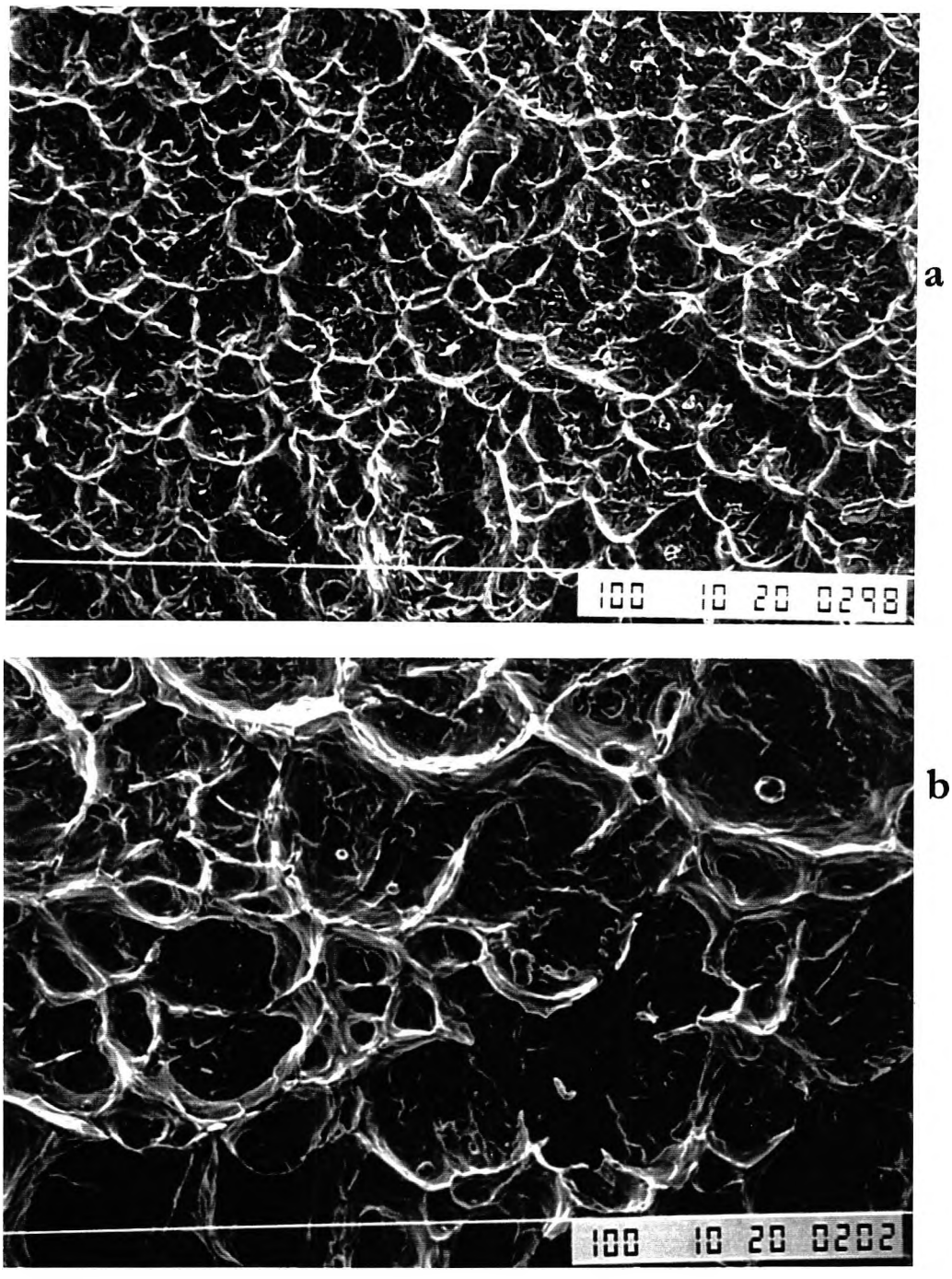


Figure 4-12: ***Same as before but tested at 800 °C, showing microvoid coalescence. Both cooling rates gave similar ductilities (23%-24% R of A) The dimple size at slower cooling rate (a) was 7μm and at the faster (b) 16μm). (750X)***

For an otherwise similar steel, increasing the Al content led ductility to deteriorate as shown below in Fig. 4-13, for the steel with Ti:N ratio of 2.8:1 and 0.045% Al.

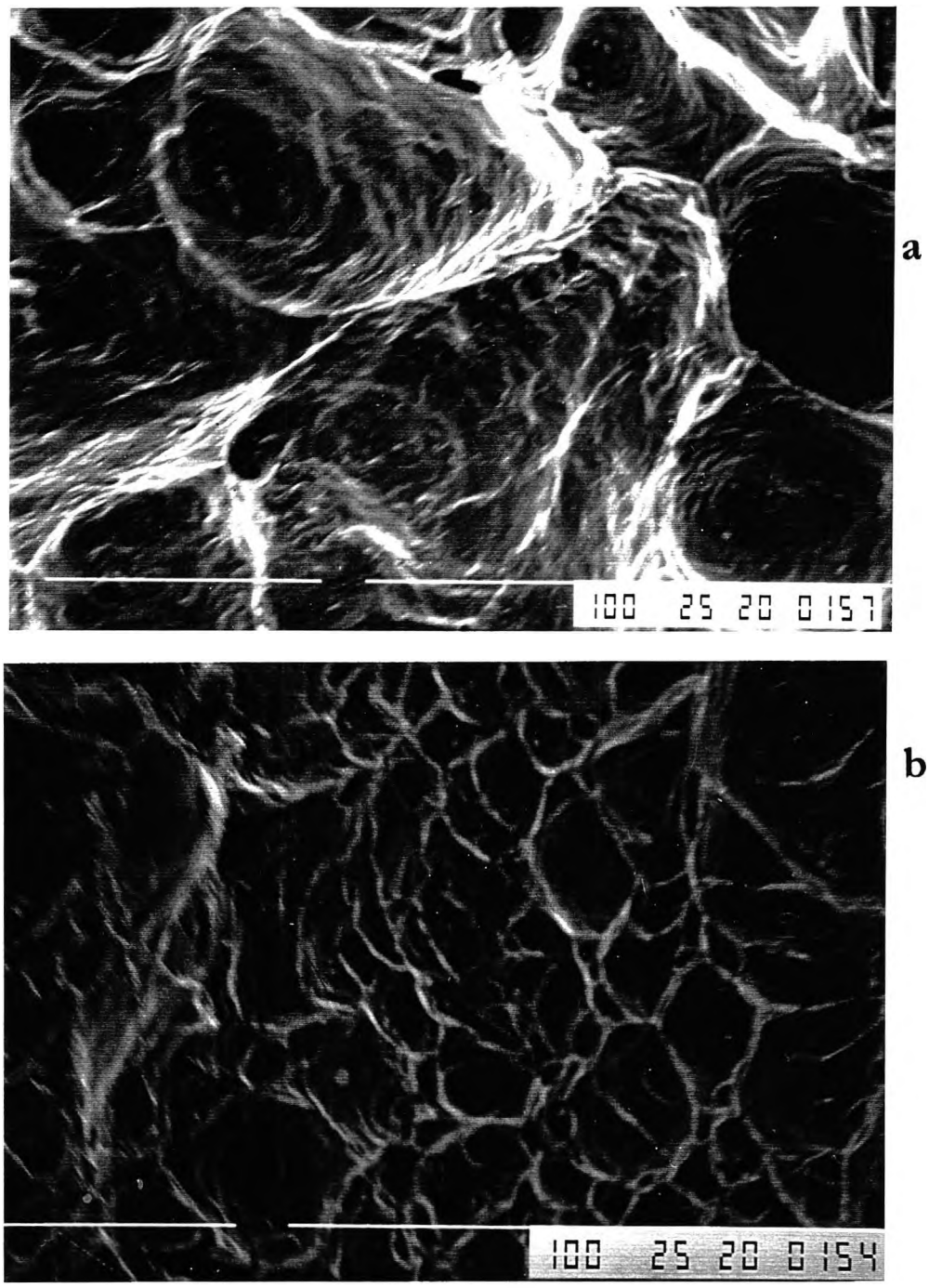
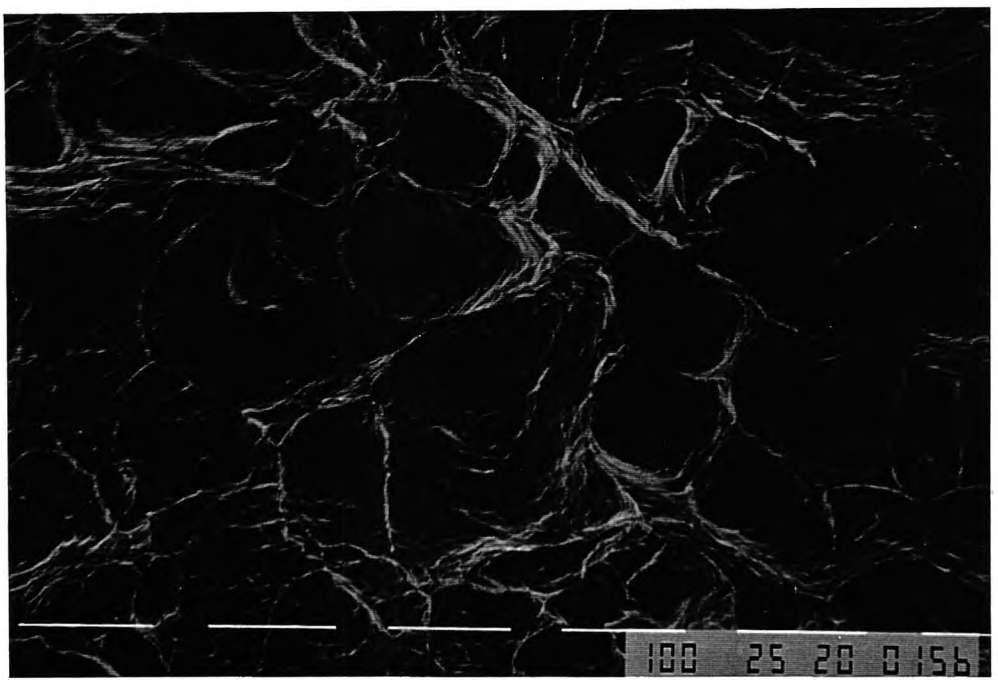
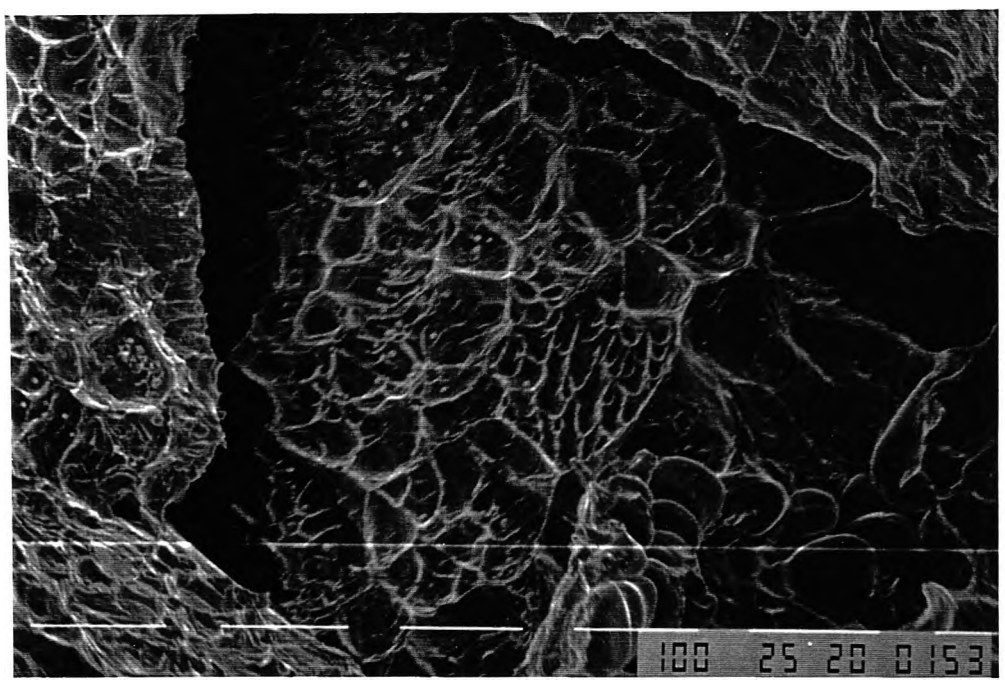


Figure 4-13: ***SEM of the fracture surfaces for high Al steel with Ti:N ratio of 2.8:1 Steel was tested at 800 ℃, showing for two magnifications, how the dimple size decreases with increase in cooling rate: compare (a)slow) and (b) fast at 350X; again, (c) slow and (d) fast at 150X. R of A 30% for fast and 24% for the slow cooling rate. Average dimple size 39μm and 86μm respectively.***



c



d

Raising the temperature to 900°C still produced intergranular fractures for the slow cooling rate, Fig. 4-14a, but at the faster cooling rate of 100K/min, this steel showed flat fracture facets typical of when grain boundary sliding is present, Fig. 4-14b.

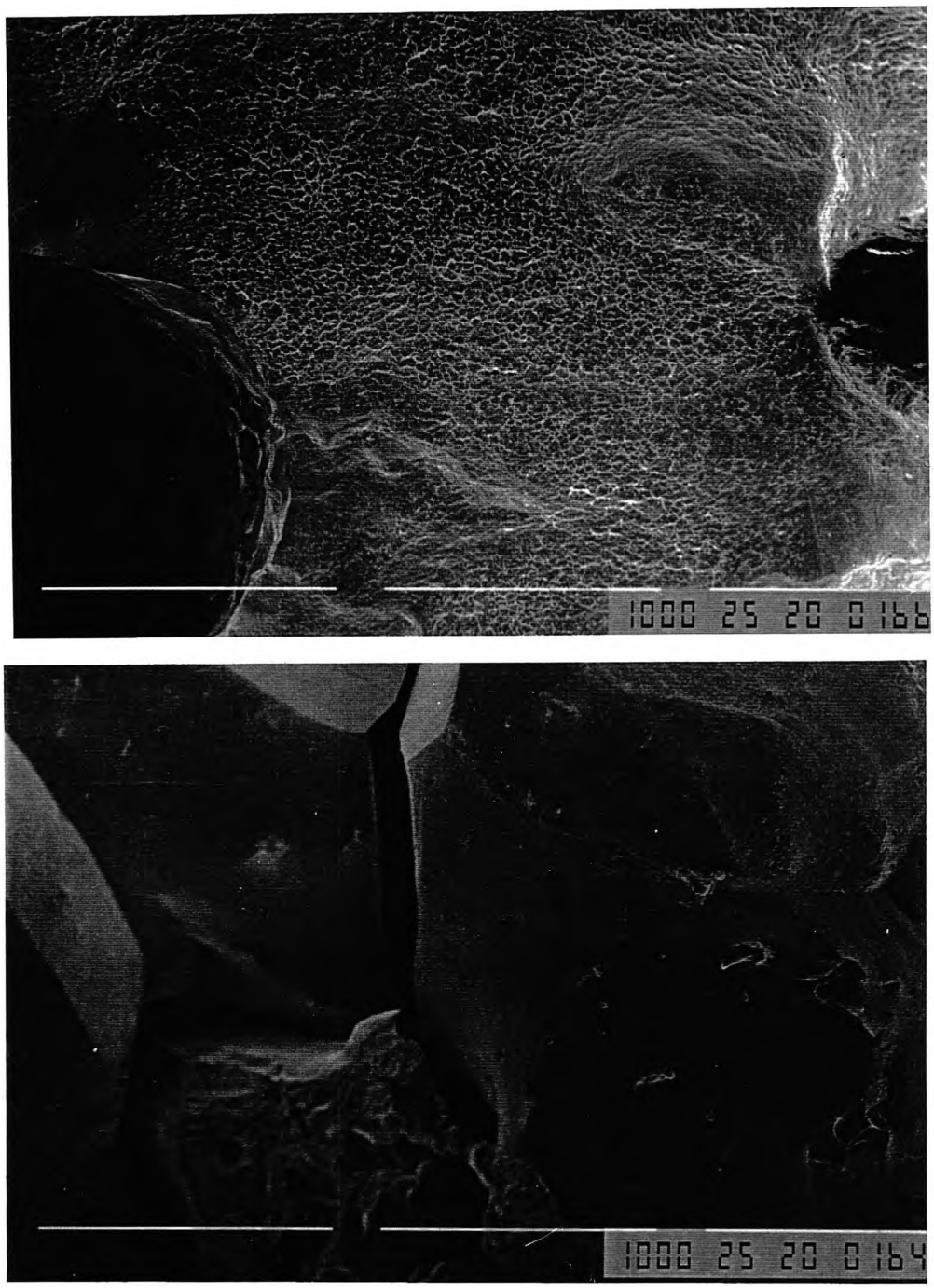


Figure 4-14: ***SEM of the fracture surfaces for the high Al steel with ratio of Ti:N ratio of 2.8:1. Steel was tested at 900°C. Ductile intergranular failure was observed at the slower cooling rate (a) (R of A 35%) and grain boundary sliding at the higher cooling rate (b) (R of A 26%). (35X)***

For this steel, Ti:N ratio of 2.8:1, steel 4, although ductility at 800°C was better than for the low Al, Ti containing steel, ductility at higher temperatures was always the worst of all the steels examined in this Ti:N range(<3.4:1), this being particularly

marked for the higher cooling rate. For samples cooled at 100K/min, even at as high a temperature as 1025°C, failure was still by grain boundary sliding and the R of A value remained low(Fig. 4-15).

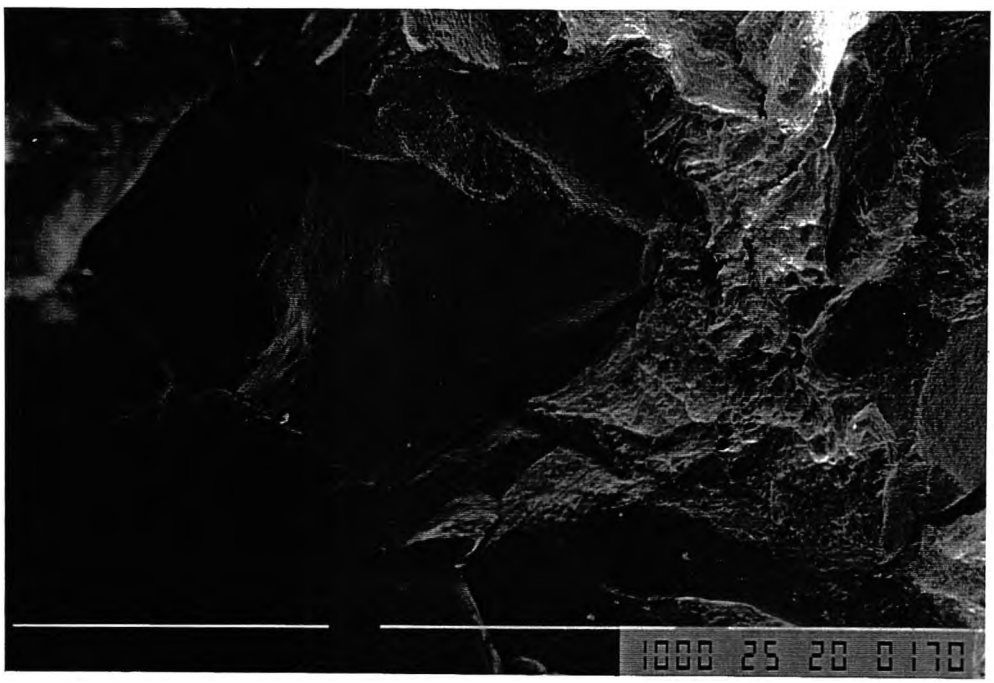


Figure 4-15: ***SEM of the fracture surfaces for High Al steel with Ti:N ratio of 2.8:1. Steel was cooled at 100K/min and tested at 1025°C showing grain boundary sliding. R of A 49%. (35X)***

This higher Al containing steel with the Ti:N ratio of 2.8:1 gave rise again to more conventional behaviour, the dimples size increasing as the cooling rate decreased. It surprisingly gave the largest dimple size of the four steels, compare Figs. 4-13a and 4-13b, 4-13c and 4-13d. It is not clear why this should be so as with all the extra precipitation, this steel might be expected to have the finest dimple size.

Stoichiometric ratio:

The worst ductility was found for the steel from European programme which was of stoichiometric composition for Ti:N ratio, steel 58, and faster cooling rate, as shown in Fig. 4-3.

Steel having Ti:N ratio greater than the stoichiometric:

Increasing the Ti:N ratio well above the stoichiometric composition to a ratio of 6.2:1, resulted in the influence of the cooling rate being very small. For this steel (Ti:N ratio of 6.2:1), the dimples size hardly changed with cooling rate but the RA values were markedly different. (Fig. 4-16)

This should be contrasted with the results for the high Al, Ti free steel with showed an enormous difference in dimple size with cooling rate at 800°C yet RA values were very close to each other.

However for the Ti containing steel the difference in the R of A and the fracture appearance were not so marked when the test temperature was increased. This was confirmed by there being little difference in the dimple size, and similar fractures (Fig. 4-17) were obtained at both cooling rates.

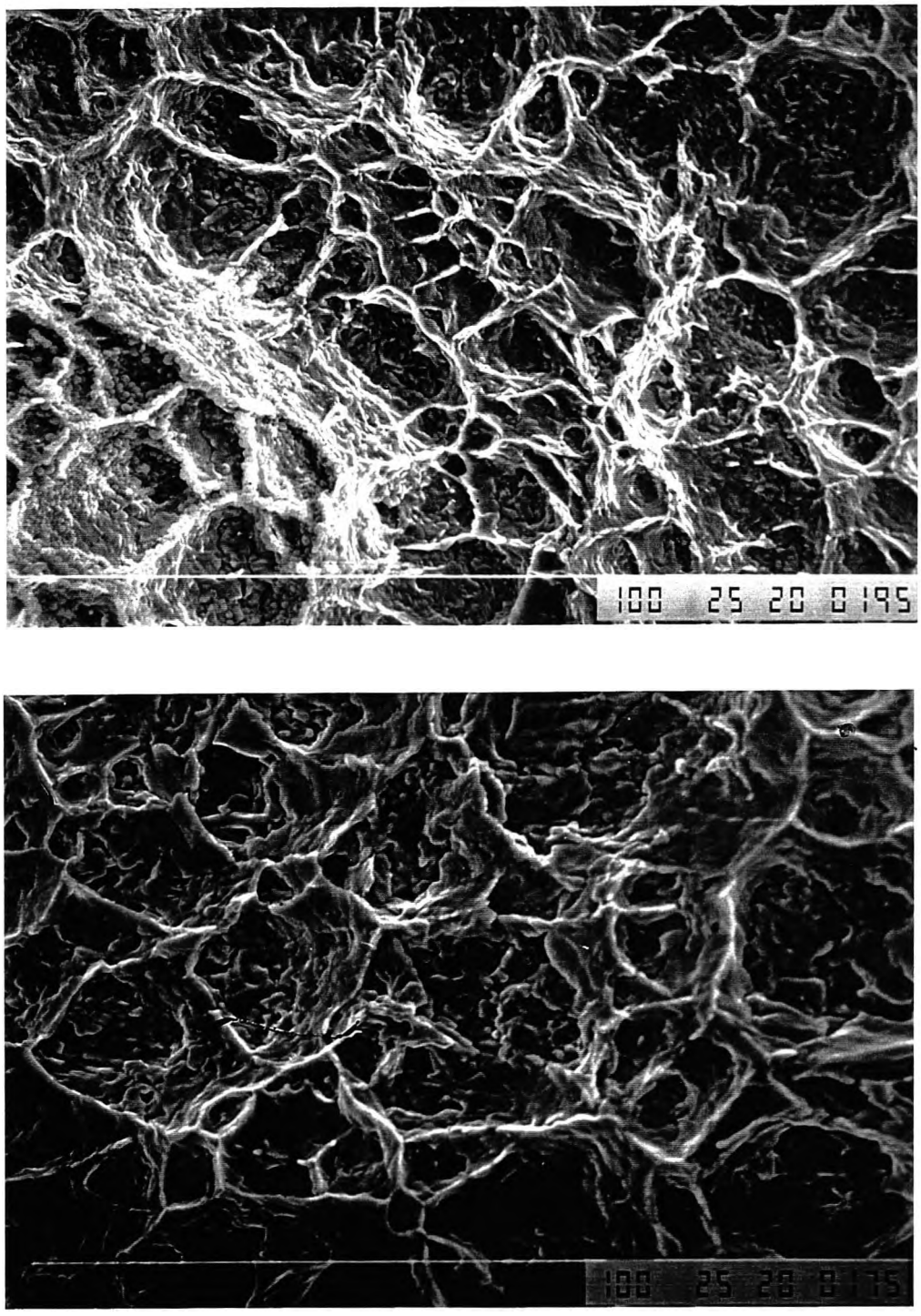


Figure 4-16: ***High Ti:N (6.2:1) steel tested at 800 °C, showing very similar dimple size at the two cooling rates: (a) 12 μm for slow (R of A 34%) and (b)15 μm for fast cooling rate(R of A 17%)(750X).***

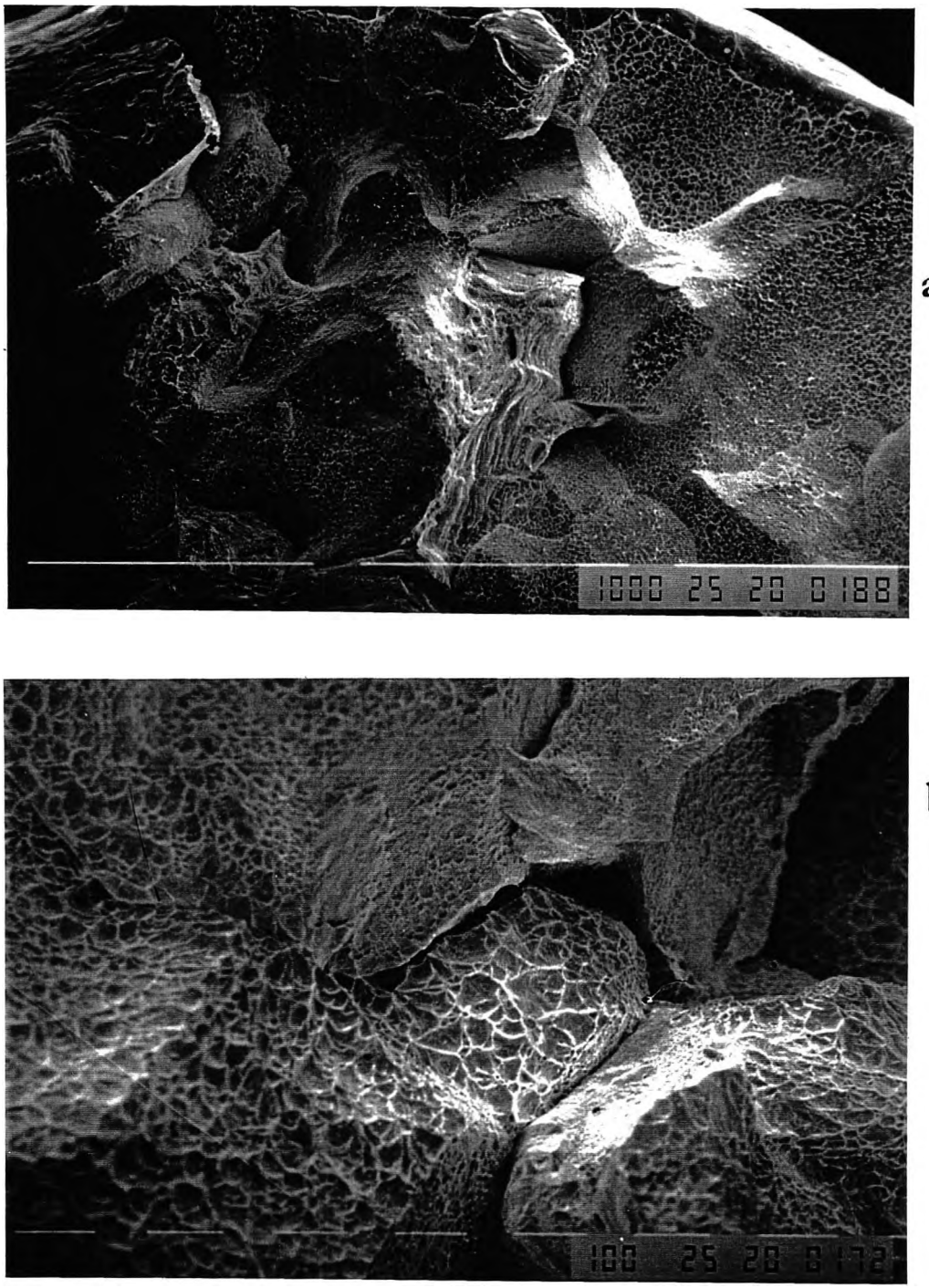


Figure 4-17: ***showing the intergranular fracture at both cooling rates for high Ti:N steel at different temperatures: (a) 850 ℃, 25K/min R of A 37% (35X) and (b) 800 ℃, 100K/min R of A 17%.(100X).***

Dimples were only observed in this steel for temperatures below 850°C.

Transmission Electron Microscopy

Transmission Electron Microscopy was carried out using carbon extraction replicas so that the size and shape of the precipitates could be determined.

Replica examinations:

Al steels:

Edax analysis of the particles in the replicas indicated the likely presence of a large volume fraction of AlN particles in the high Al, Ti free steel, steel 3, Fig. 4-19. Few AlN particles were found in the low Al, Ti free steel, steel 12. Although AlN cannot be positively identified from Edax analysis, the presence of an Al peak combined with "triangular" and hexagonal shaped particles confirms their presence.

Very low Al

Some coarse precipitates were found in this steel but they were very few making it likely that the reason for the good hot ductility is the low volume fraction of particles. Although there was a big difference in the R of A values on changing the cooling rate, the size of precipitates were quite close. Fig. 4-18.(note difference in magnification between (a) and (b).

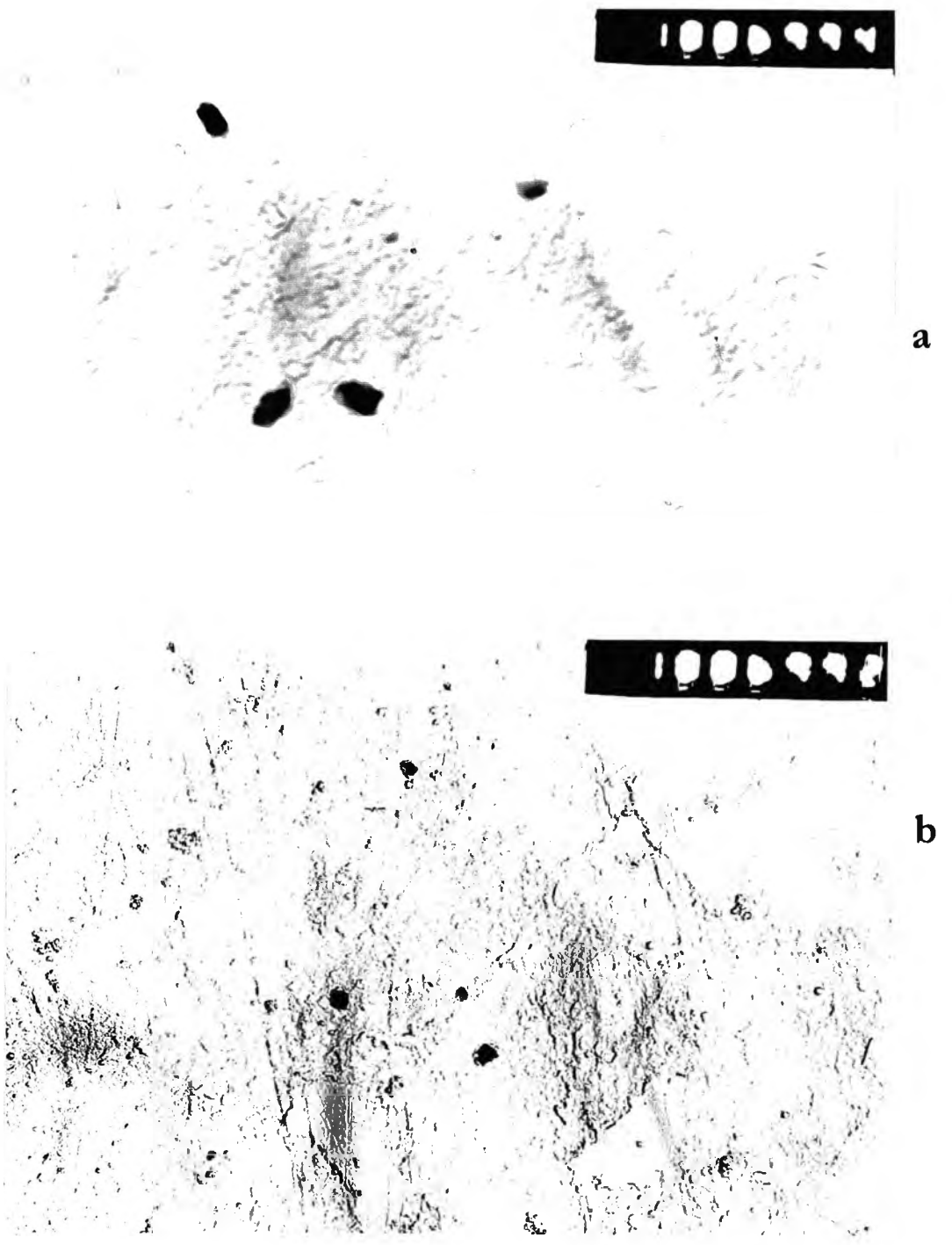


Figure 4-18: ***Coarse precipitates in Ti free, very low Al containing steels tested at 800 ℃: (a) slow cooling rate R of A 52% (150 nm) (27,000X)and (b) fast cooling rate R of A 24%.(170nm).(15,000X)***

Low Al steel from the European programme

In this case the AlN precipitates were found to be coarser at the faster cooling rate, the average particle size being 43nm at 25K/min and 77nm at 200K/min for slow and fast cooling rate, respectively. However not many particles were found (~ 10 per condition) and many unclear very fine precipitates could be observed at the faster cooling rate.

High Al containing steel

The carbon replicas showed similar sizes for the precipitates at both cooling rates. Although the precipitates were coarse they were finer than those in the very low Al containing steel. The volume fraction of AlN particles was greater in this high Al steel indicating enhanced precipitation of AlN. Fig. 4-19.

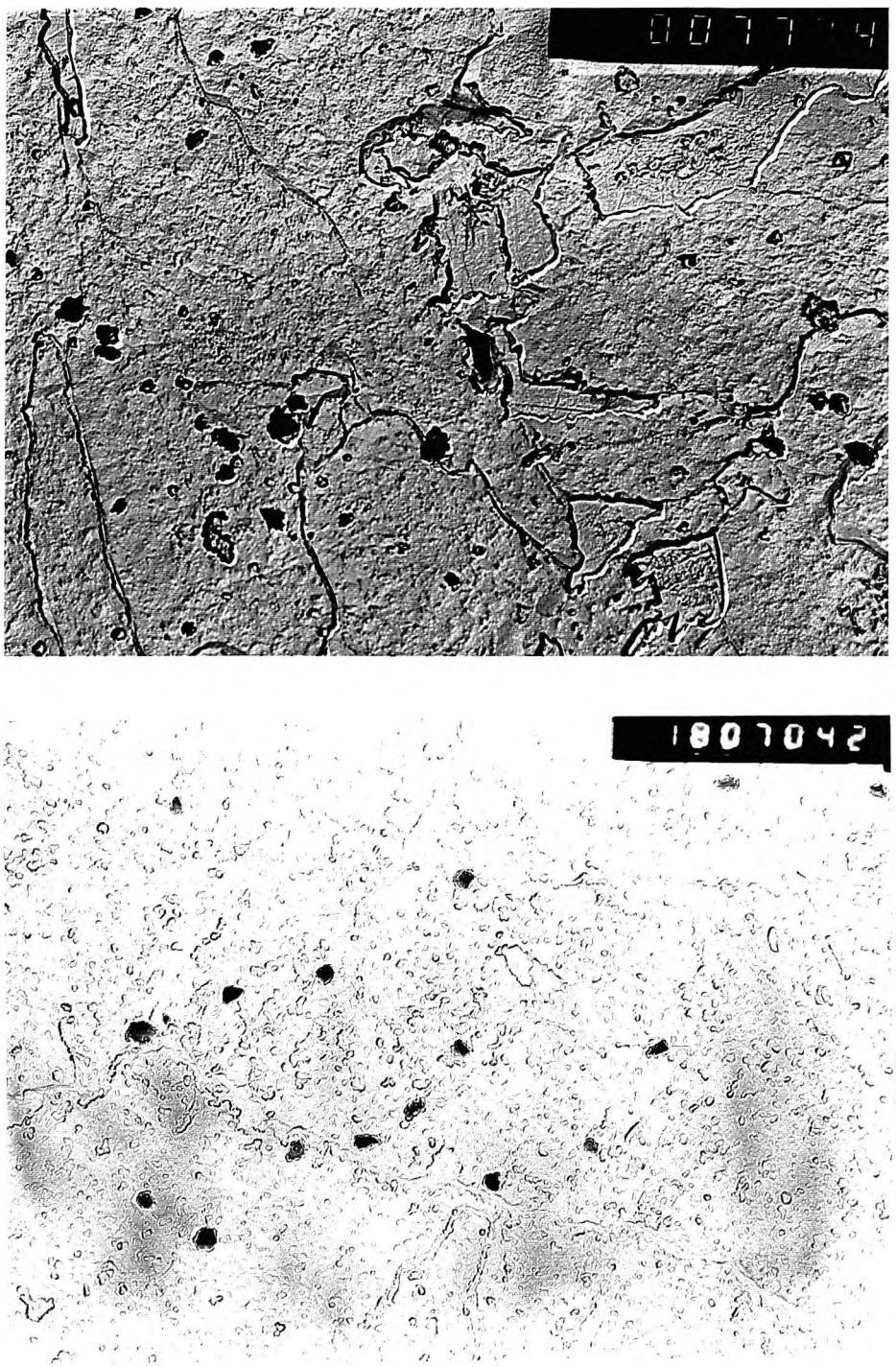


Figure 4-19: ***Similar size distribution of precipitates found in the Ti free high Al containing steel tested at 800℃: (a) slow cooling rate (92nm)and (R of A 25%)(15.000X) (b) fast cooling rate (73nm) (R of A 17%). (27,000X)***

Ti containing steels with different Ti:N ratios:

The precipitates in the Ti containing steels were coarser at slower cooling rates for both the low and the high Ti:N ratio steels. Raising the temperature also resulted in coarser precipitation. Edax analysis of these precipitates showed a Ti peak, Fig. 4-20.

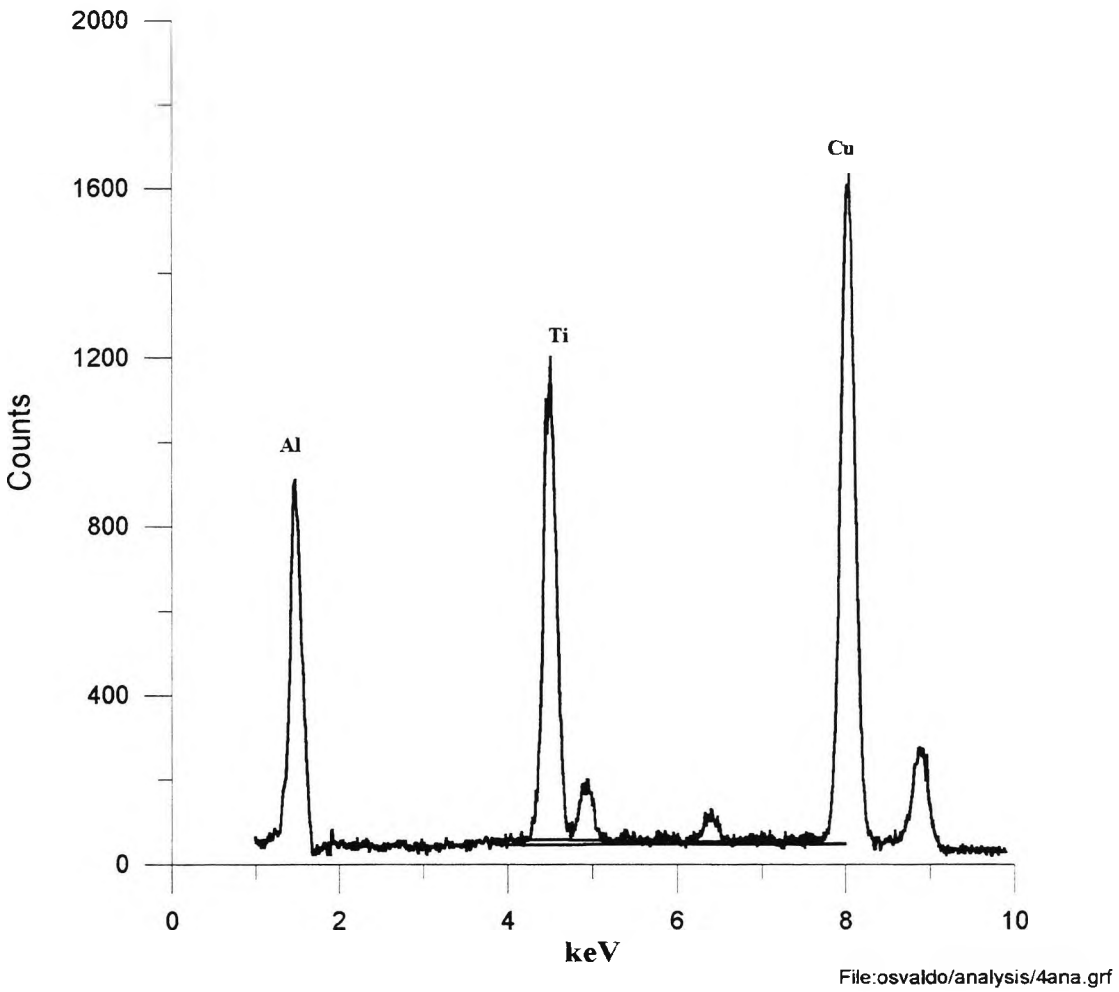


Figure 4-20: ***Edax analysis taken from precipitate of high Al Ti containing steel, steel 4 tested at 1000°C, showing presence of Al and Ti C. Cu is due to the Cu grid used to hold the carbon replica.***

Below the stoichiometric composition

The steel with a Ti:N ratio of 1.6:1, low Al, showed coarser precipitates, the size being a minimum of 10 nm at 950°C. The square shape of the particles suggests they are TiN but some AlN particles may also present Fig. 4-21.



Figure 4-21: ***Precipitates in the steel with the low Ti:N ratio of 1.6:1 at 950°C and cooled at 100K/min. The square shape is typical of TiN particles (size 25nm). (R of A 50%)(52,500X).***

For the steel with the Ti:N ratio of 3.0:1, the precipitates are again coarser at higher temperatures but precipitates were finer than those found in the other two steels at Ti:N ratios below the stoichiometric composition. The effect of the cooling rate on the precipitate size was less marked in this steel. Fig. 4-22.

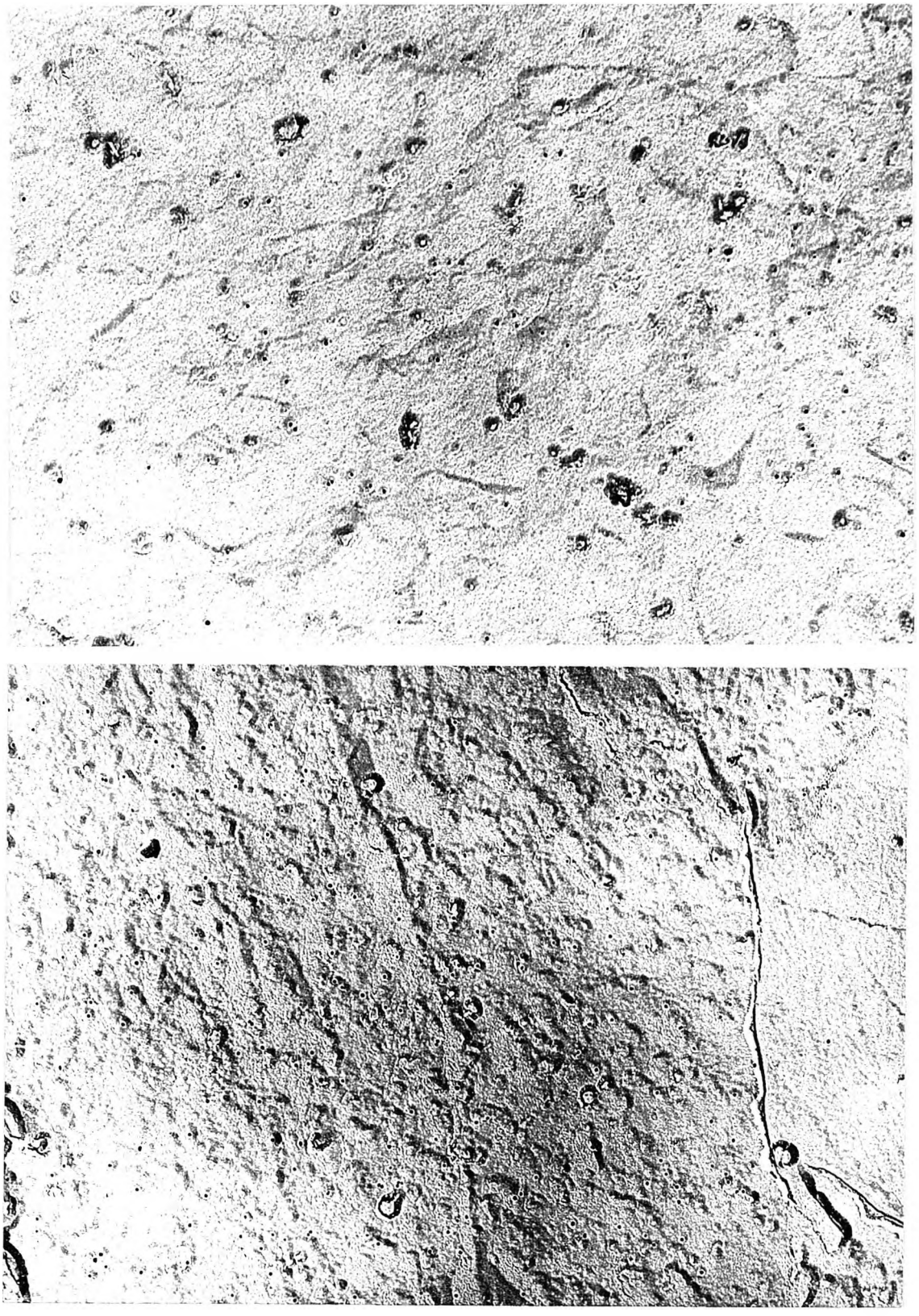


Figure 4-22: ***TEM of the carbon replicas for the low Al steel with Ti:N ratio of 3.0:1 tested at 950°C, showing fine TiN precipitation. Precipitation average is finer at the faster cooling rate. (a) Rate of cooling: 25K/min; R of A 70% (size range of 5 to 10nm); (b) 100K/min; R of A 50% (size 8 to 10nm). (76,000X)***

For the steel with the high Al level and low Ti:N ratio of 1.6:1, the precipitates were coarser due the higher test temperature (20nm), Fig. 4-23.

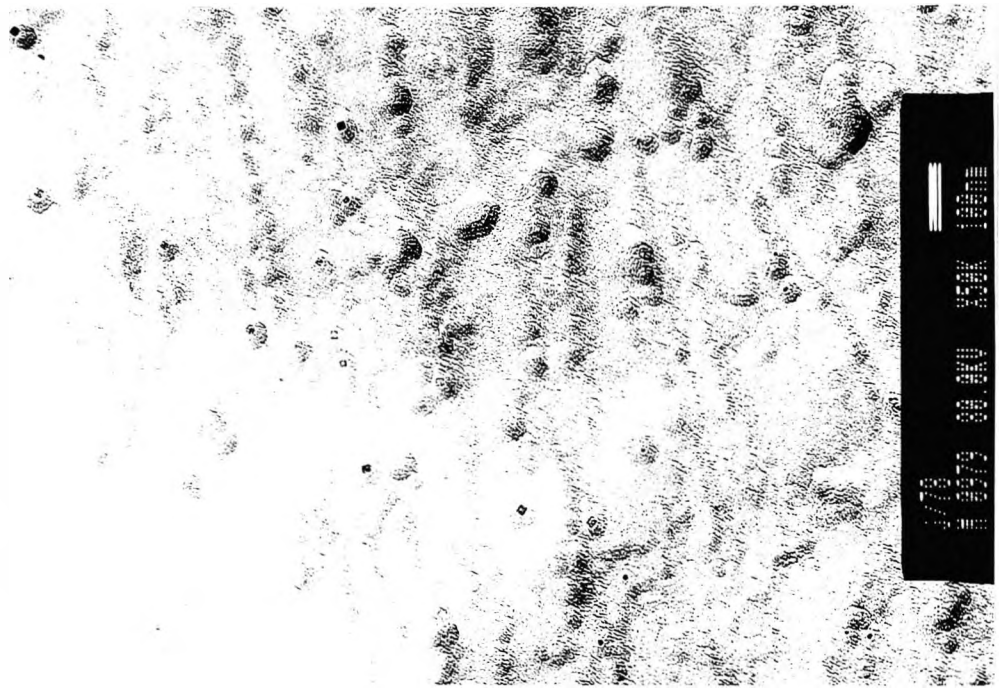


Figure 4-23: ***Precipitates in the steel with a Ti:N of 1.6:1 tested at 1000°C and cooled at 100K/min. TiN. (20nm) (R of A 50%). (52,500X)***

Surprisingly, but in accordance with the dimple sizes, this steel showed finer precipitates at 25K/min.

For the steel having Ti:N ratio of 2.8:1 steel, as usual, increasing the cooling rate gave rise to a finer particle size, Figs. 4-24a and b. Raising the test temperature to 1050°C resulted in coarser particles and the cubic shape of the particles identifies them as TiN. Fig. 4-25.

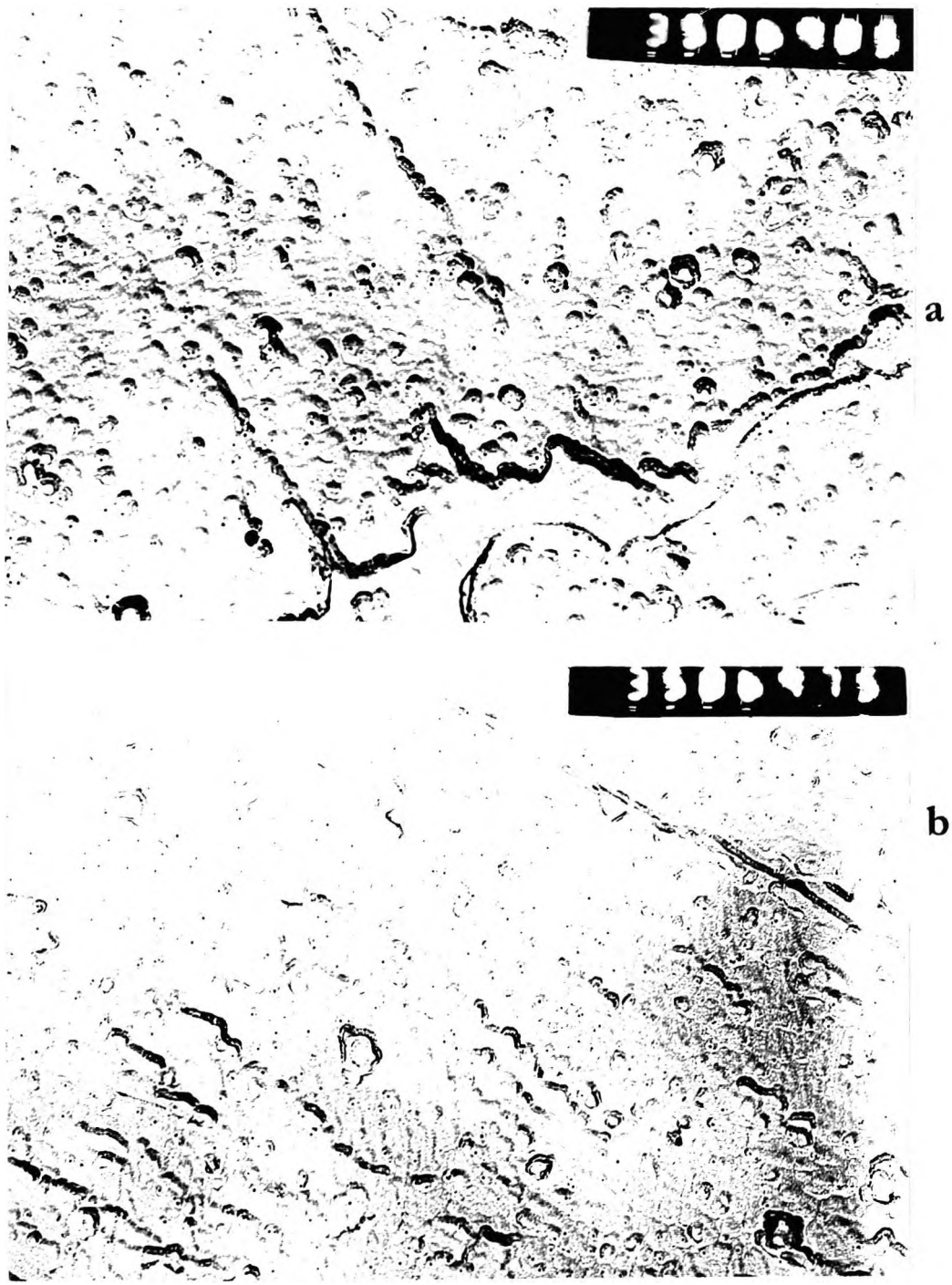


Figure 4-24: ***TEM of the carbon replicas for steel having Ti:N ratio of 2.8:1. Steel was tested at 900°C and shows finer precipitation. Precipitation is finer at the faster cooling rate. 1-3nm and 5nm for fast and slow cooling rates. (R of A 27 and 35%) respectively.(52,500X)***

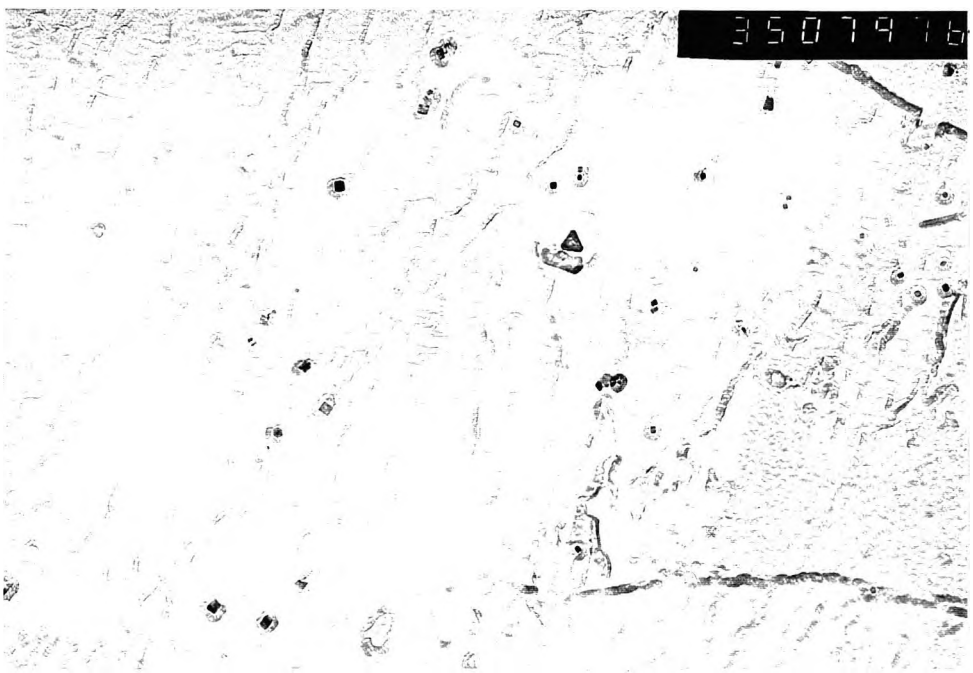


Figure 4-25: ***TEM of the carbon replica for high Al steel having Ti:N ratio of 2.8:1 tested at 1050 °C, showing coarse TiN precipitates. Rate of cooling: 100K/min; R of A 52%. (10-60nm) (52,500X)***

Stoichiometric ratio

For the European steel having a Ti:N ratio of 3.4:1 (European steel), the size of the precipitates were very fine, even for high test temperatures and slow cooling rates. The poor R of A values can be observed in the curves given in Figs. 4-2 and 4-3. This steel gave fine precipitates even for conditions in which the cooling rate was low and temperature as high 1000°C, precipitate size being 15 nm.

Increasing the Ti:N ratio to 6.2:1 resulted in coarser precipitates. Raising the test temperature also results in a coarser precipitate size. At a very high temperature of 1050°C the influence of cooling rate on the size of the precipitates is not however very marked, Figs. 4-26 a, b and c and Fig. 4-27

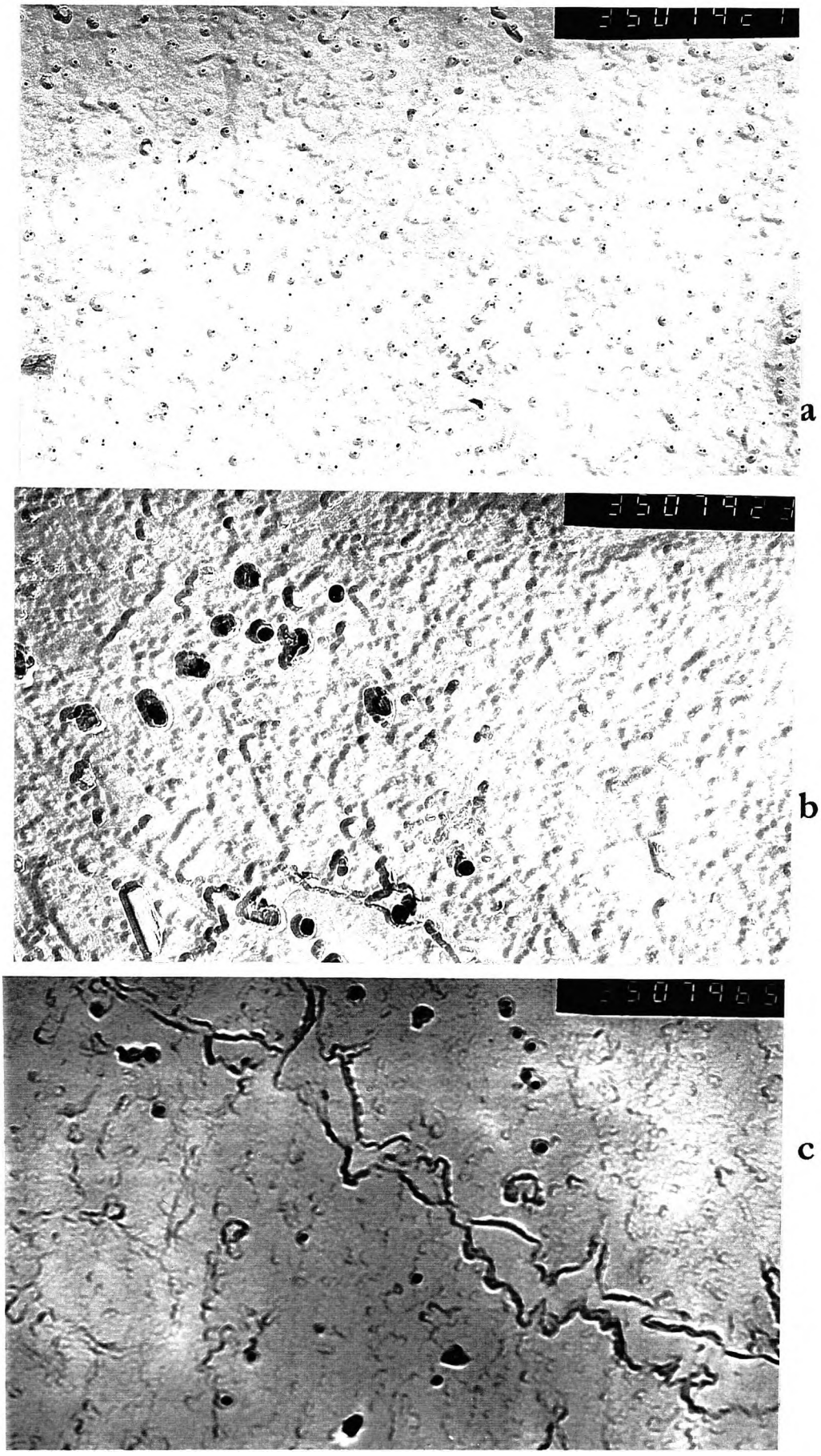


Figure 4-26: ***Steel with the Ti:N ratio of 6.2:1 showing marked coarsening of precipitates at high temperatures while the effect of the cooling rate is small: (a) tested at 900 ℃ and cooled at 100K/min,(10nm) (b) same as (a) tested at 1050 ℃ (45nm)and (c) same as (b) tested at 25K/min (30-60nm)(52,500X)***

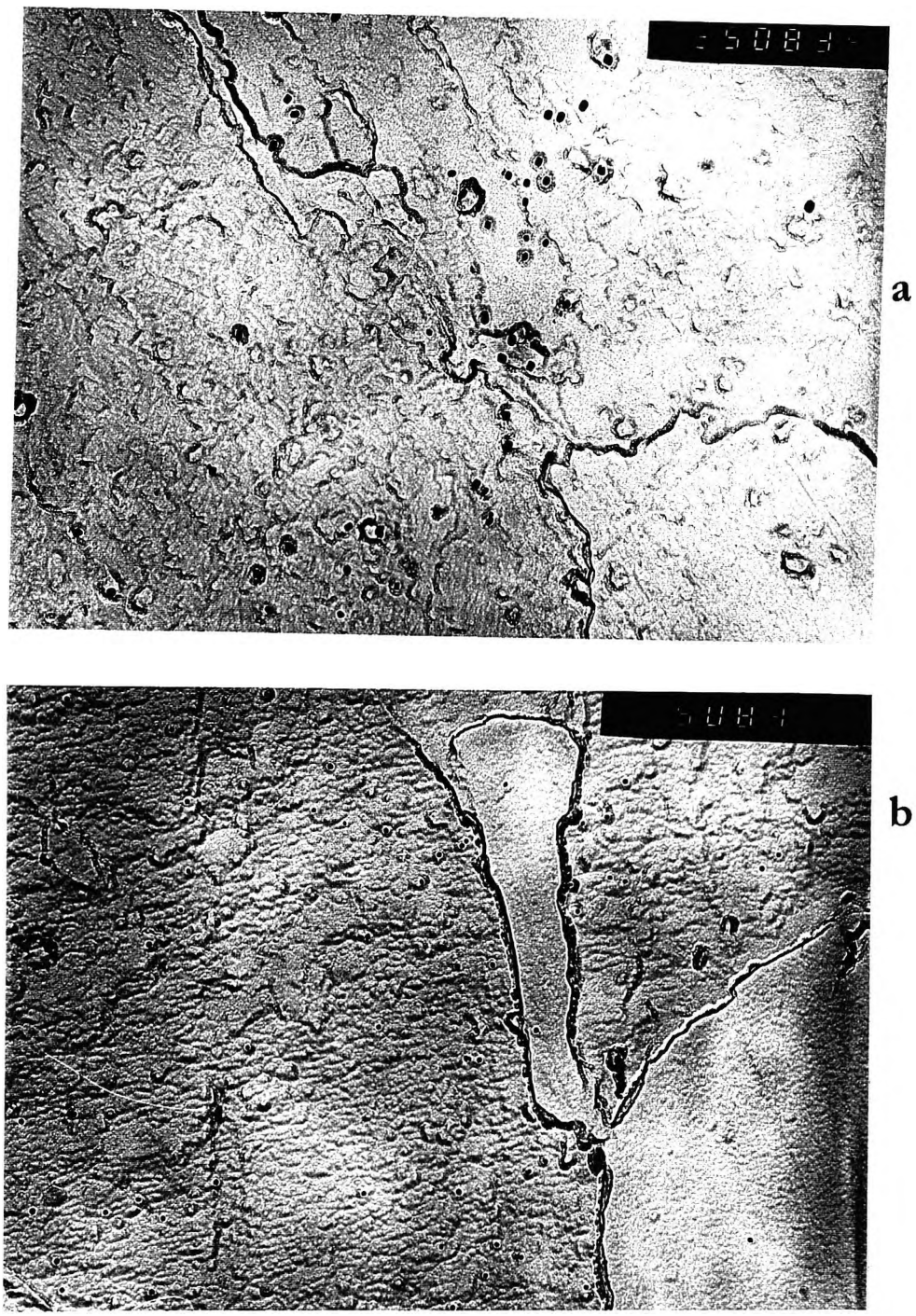


Figure 4-27: ***Steel 5B, high Ti:N ratio 6.2:1 steel, fractured at 950°C (a) cooled at 25K/min - Particle size 20 nm, R of A 55%; (b) cooled at 100K/min Particle size 12.5 nm, R of A 46%.(52,500X)***

Edax analysis of the particles in the replicas indicated in the case of the Ti containing steels, fine TiN particles were present in all the steels examined. Particle size was generally found to be finer at the faster cooling rate, Table 4-2, and a coarser particle distribution was apparent for the steel with the high Ti:N ratio, steel 5B, compare Figs. 4-22 and 4-27 for steels with low and high Ti:N ratios, steels 13 and 5B, respectively.

A full list of average particle size and average dimple size is given in Table 4-2.

The hot ductility of as cast C-Mn-Al-Ti steels

General

Previous work by Abushosha has indicated[Mintz, private communication 1998] that there is no significant difference in ductility behaviour between the air and vacuum casts used in both programmes i.e. ductility is not being affected by the casting route.

In Ti free C-Mn-Al steels, it is clear that adding Al causes a marked deterioration in ductility, Fig. 4-1. Previous work[Mintz and Abushosha, 1996];[Mintz and Crowther, 1997];[Abushosha et al, 1998 p227]; [Abushosha et al, 1998 p346] [Cardoso, Mintz and Yue, 1995] has shown that in as-cast material, AlN precipitation occurs at as low a product of soluble Al and N as $1x10^{-4}$. Thus the worsening ductility on raising the Al level is due to AlN precipitation which has been shown to occur preferentially at the γ grain boundaries. Turkdogan [Turkdogan, 1987] has calculated that segregation of Al to the grain boundaries during solidification will increase the concentration of Al at the boundaries by a factor of 6 for a steel with 0.02%Al and 0.006%N.

Adding Ti to these steels causes the ductility to deteriorate independent of the cooling rate. However, the TiN precipitation is finer than the AlN and so will be more detrimental to ductility[Mintz et al, 1991] (TiN particles were generally in the range 5

to 50nm while the AlN particles were > 50nm).

The work also suggests that ductility deteriorates further as the Ti:N ratio increases to the stoichiometric composition for TiN, 3.4:1, Fig. 4-2. Further increase causes the ductility to improve. However, it never recovers to the ductility values given by the Ti free steel. The worst ductility was given by the steel with stoichiometric composition for TiN, steel Euro 58. This can be seen clearly in Fig. 4-2 in which the same slow cooling rate was given for all the steels. This steel is also likely to give the worst ductility at the faster cooling rates, although it should be noted in Fig. 4-3 that this steel was cooled at 200K/min and not 100K/min as for all the other steels.

Because of the complex precipitation processes in these steels it is not clear as to whether raising the soluble Al level in the Ti containing steel reduces the ductility as has been found in the Ti free, Nb containing steels[Mintz and Arrowsmith, 1979p24]. However, for steels 7B and 6B which have the same Ti:N ratios, the higher Al level of steel 6B probably accounts for its worse ductility in Fig. 4-3. Furthermore, as will be seen later in the discussion, regression analysis does clearly show that AlN precipitation is detrimental.

Given a similar coarse γ grain size and samples being tested at the same strain rate then the changes in ductility are going to be related to the precipitation processes.

The most important factors influencing ductility, other things being equal will be the volume fraction and size of the precipitates present.

For the same volume fraction, the finer the precipitation the worse the ductility[Mintz et al, 1991]. This probably arises because the finer the distribution the more

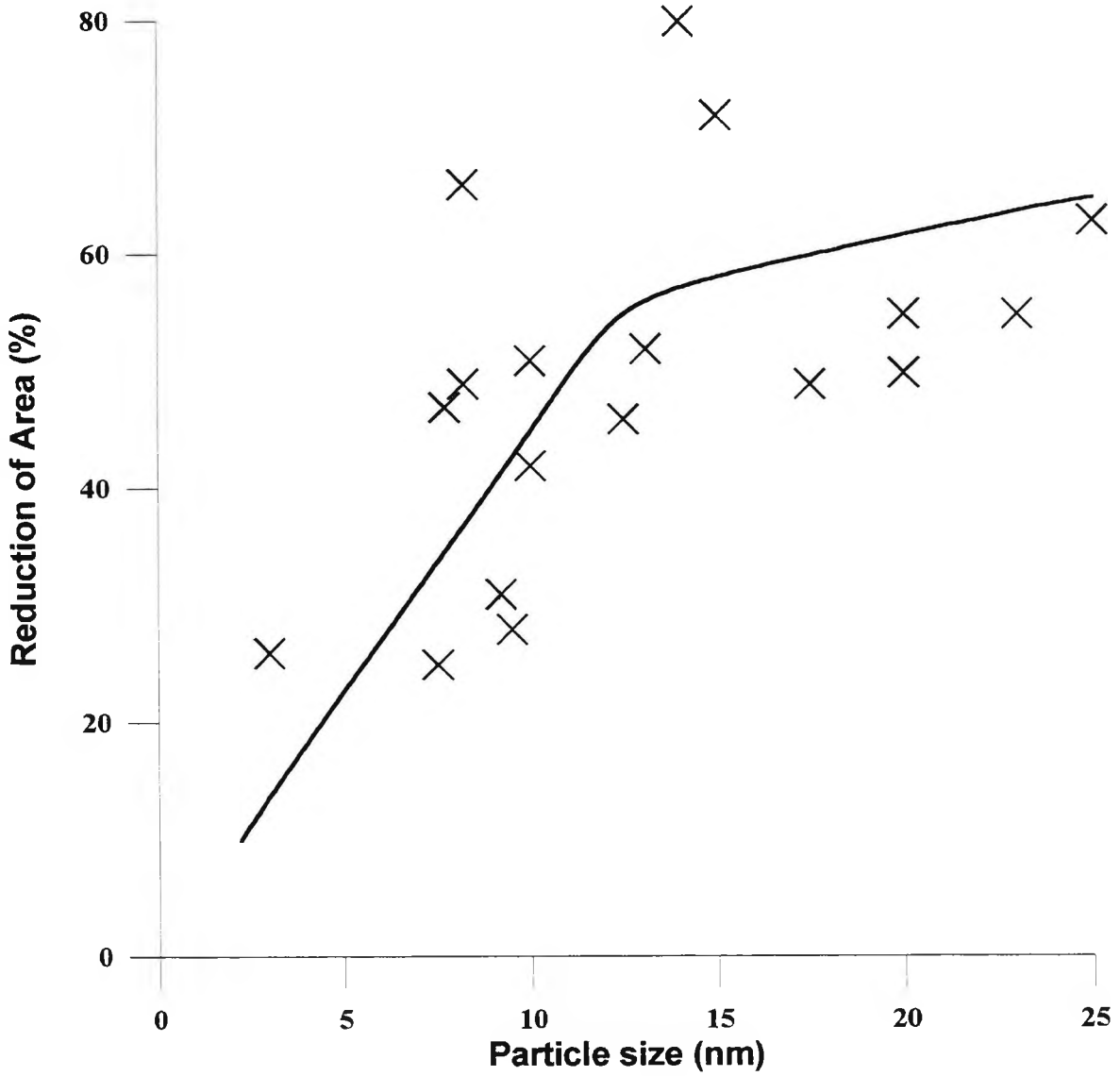
effectively are the boundaries pinned and the more readily cracks formed by grain boundary sliding are able to link up to give failure. Although there is considerable scatter there is no doubt from Fig. 4-28, that a coarser particle size leads to better ductility and the matrix particle size should be in excess of 15 nm to ensure good ductility. Although matrix particle size has been used here because of its ease of measurement, it is likely that the coarser particle size at the boundaries follows the same relationship.

There is no doubt the dimple size is controlled by both the particle size, and their volume fraction and dimples can be associated with both inclusions and particles such as AlN and or TiN. However, whereas there is a relationship between the particle size and ductility, Fig. 4-28 there is no clear relationship between the dimple size and ductility, Fig. 4-12. This indicates that the dimple size is mainly controlled by the coarser particles i.e. the inclusions whereas ductility is mainly controlled by the finer particles AlN or TiN.

There are two factors that are likely to control the ductility of as-cast steel. The first is the volume fraction of particles present, particularly those precipitated at the γ grain boundaries. The second factor is the size of particles. Very fine particles with small interparticle spacing (< 10 nm) can strengthen the matrix and increase the stress concentration in the boundary region[Mintz and Yue, 1991]. Fine particles with small interparticle spacing at the grain boundaries can encourage cracks formed by grain boundary sliding or void formation to link up[Mintz and Yue, 1991]. Generally, it is found that increasing the cooling rate results in finer sulphides and micro-alloying particles and this produces worse ductility[Abushosha et al, 1998p227; Abushosha, et al 1998p346]. In the present exercise, both the MnS

inclusions size, Figs. 4-7 to 4-10, were generally refined on faster cooling, as well as the TiN particle size Figs. 4-21 to 4-27 and Table 4-2. If it is assumed that the particle volume fraction is not much influenced by the changes in cooling rate noted here (this is probably the case for the sulphides but not necessarily so for the micro-alloying additions), then the size of the particles/inclusions will have a large effect on the ductility.

As noted already, in the present work there is a good relationship between the size of the particles (AlN particles in Ti free steel and Ti rich particles in Ti containing steels) and the R of A value, Fig. 4-28 suggesting that probably all the nitrogen has precipitated out and that growth of particles is very dependent on the amount of micro-alloying elements in solution. Increasing the Ti level above stoichiometric other things being equal would be expected to coarsen the Ti rich particles, see Table 4-2. This would arise partly because the higher product of [Ti]x[N] would encourage precipitation at higher temperature but also the more Ti there is in solution the more rapidly particles can grow. Growth of particles will be dependent on the diffusion of Ti to the particles.



File: measur.grf

Figure 4–28 ***Influence of particle size on the Reduction of Area values.***

C-Mn-Al Ti free steels

In C-Mn-Al steels that are solution treated (i.e. heated to 1330°C) it is generally very difficult to precipitate AlN either before of during deformation, its precipitation being very slow. The product of the soluble Al and N, i.e. [sol. Al]x[N], must be fairly high approaching $2x10^{-4}$, i.e. 0.04% sol Al, 0.005 N before AlN precipitates out influencing the ductility[Abushosha et al, 1988p346].

However, for as cast tensiles, as can be seen from Fig. 4-1 and 4-18, this is clearly not the case and AlN is able to precipitate out at as low a product as $6x10^{-5}$, i. e. 0.009% sol Al and 0.0067%N.

Clearly, the segregation of Al during solidification after casting to the γ grain boundaries is such as to allow precipitation to occur at much lower average levels of soluble Al. Turkdogan has calculated that the Al level at the boundaries for a steel with an initial Al level of 0.02%Al can be a factor of 6 times (0.13%Al) the total Al level at the austenite grain boundaries when solidification occurs[Turkdogan, 1987].

Increasing the Al level by increasing the volume fraction of AlN precipitated will obviously impair ductility. The effect of cooling rate is more complex. Previous work on similar C-Mn-Al steels has shown that increasing the cooling rate both refines the MnS inclusions and AlN particles situated at the γ boundaries and this leads to worse ductility[Abushosha et al, 1998p227].

Provided the volume fraction of particles is constant a finer particle distribution particularly at the boundaries will always lead to a deterioration in

ductility, as cracks formed by grain boundary sliding or micro-void coalescence can much more readily link up under these conditions[Mintz and Yue, 1991].

In the present work it is clear from the examination of the fractured surfaces, Figs. 4-7 and 4-8, that the faster cooling rate produces a finer sulphide distribution. Both finer inclusions and smaller diameter dimples are observed on the surfaces.

Although not obvious in the present examination, work by Abushosha in similar steels has also shown that the AlN particles are finer on fast cooling[Abushosha et al, 1998p227].

The AlN particles although finer are often similar in size to the MnS inclusions and therefore some indication of their influence on fracture can be made from the SEM observations.

Increasing the soluble Al level can be seen to refine the dimple size, compare Figs. 4-7 and 4-8, indicating that a greater volume fraction of the coarser particles are present i.e coarse AlN particles. This increase in volume fraction of AlN is accompanied by a decrease in the ductility, Figs. 4-4 and 4-5.

C-Mn-Ti-Al steels

The presence of Ti in a simple C-Mn-Al steel will ensure that most of the nitrogen will be combined as TiN. Thus for Ti:N ratios ≥ the stoichiometric for TiN it is likely that all the nitrogen will be combined with the Ti. For ratios less than stoichiometric some N will remain in solution and may be able to precipitate out as AlN. It can be seen from Table 5-3 (next chapter) that under equilibrium conditions the amount of N left in solution for Al to combine with is generally very small, and taking into account the slow nature of AlN precipitation, it is likely that the amount that can be precipitated is also small. Comparison between two "stoichiometric" steels 4 and 58 in Figs. 4-2 and 4-3, shows that in spite of the European steel, steel 58, having half of the Al level of presently examined steel i.e. 0.020% against 0.045%Al. However, they presented similar ductilities in the higher temperature range. Once all the N has been removed by Ti there is none available for AlN precipitation and raising the Al level will have no effect. This highlights the outstanding impairment effect of Ti compared with Al on hot ductility, suggesting that when there is enough Ti to trap the N, Al has little effect in hot ductility.

Of the two precipitates AlN and TiN, TiN is the most stable and has been shown in the present work to be the finest. Thus ductility is most likely to be controlled by the Ti addition. It can be seen that the addition of Ti produces worse ductility in all cases, compare Figs. 4-2 and 4-3 with Fig. 4-1.

This impairment of ductility is related to the fine precipitation of TiN that is produced when Ti is added.

The ductility can also be seen to bear some relationship to the Ti:N ratio, Figs. 4-2 and Fig. 4-3. Ductility first decreases as the Ti:N ratio approaches 3.4:1 i.e. stoichiometric and then improves again. The initial decrease is probably due to the volume fraction of TiN increasing, reaching a maximum at the stoichiometric ratio, Table 4-2.

Further increase then coarsens the particles, Table 4-2. As has been noted there is in general a good relationship between the size of the particles and the R of A values Fig. 4-28.

However, in contrast to the present work, previous work by Abushosha et al, 1998 [Abushosha et al, 1998p346] on a high N, (0.009%N), as cast steel with a higher product of [Ti]x[N] of $1.8x10^{-4}$, did give albeit, a very small improvement in ductility over a similar Ti free steel. These steel tensile specimens were cooled at 60K/min after casting[Abushosha and Vipond, 1991p613].

The better ductility was interpreted on the basis that AlN precipitation was more detrimental to ductility than TiN. It should be noted that because AlN precipitates preferentially at the γ grain boundaries even if it is in a coarser form it is likely to be more detrimental than TiN. The TiN particles found in this previous study were generally coarser (~50nm) than found in the present investigation[Abushosha and Vipond, 1991p613].

Clearly the very fine TiN particles in the present examination are very detrimental to ductility, Figs. 4-21 to 4-27.

The size of the TiN particles will be controlled both by the product of [Ti] x [N] and the Ti:N ratio. The higher [Ti] x [N] product in this previous work [Abushosha and Vipond, 1991p613] would have been expected to favour precipitation at higher temperatures and the TiN particles would therefore be coarser. However, only 0.006%N of the steel's total N content would be combined as TiN and 0.003% would still be available for AlN precipitation. No AlN precipitation was detected in this previous exercise so presumably segregation effects were not sufficient to allow AlN precipitation to occur. However, it is not easy to detect AlN in the replicas.

It would be therefore appear that at low Ti:N ratios there may be some benefit in having high rather than low N levels. However, the improvement was only small and certainly at this stage of the work such a recommendation could not be made.

Although working at high Ti:N ratios will ensure coarse TiN particles, the high volume fraction of TiN precipitated, may mitigate against the ductility improving over Ti free steels unless N levels are kept very low. A combination of 0.02%Ti, 0.003%N may prove to be an optimum combination to give best hot ductility.

On the basis of volume fraction, one would expect that as the product of [Ti]x[N] increases, the more TiN would be precipitated out, reaching a maximum under equilibrium conditions at the stoichiometric composition for a given N level but continuing to rise above this level for non-equilibrium conditions.

Due to the non existence data for Ti steels, it is not clear whether equilibrium conditions are obtained in the present situation but dynamic precipitation has been shown to be very rapid[Weiss et al, 1980]. In the case of Nb containing steels for example[Weiss et al, 1980], at 950°C the temperature at which precipitation occurs

most rapidly, (the nose temperature), precipitation is often complete within the time of a normal hot ductility test. Similar behaviour might be expected with TiN. Under non-equilibrium conditions, however, the volume fraction precipitated will increase with increase in the product of Ti and N concentrations.

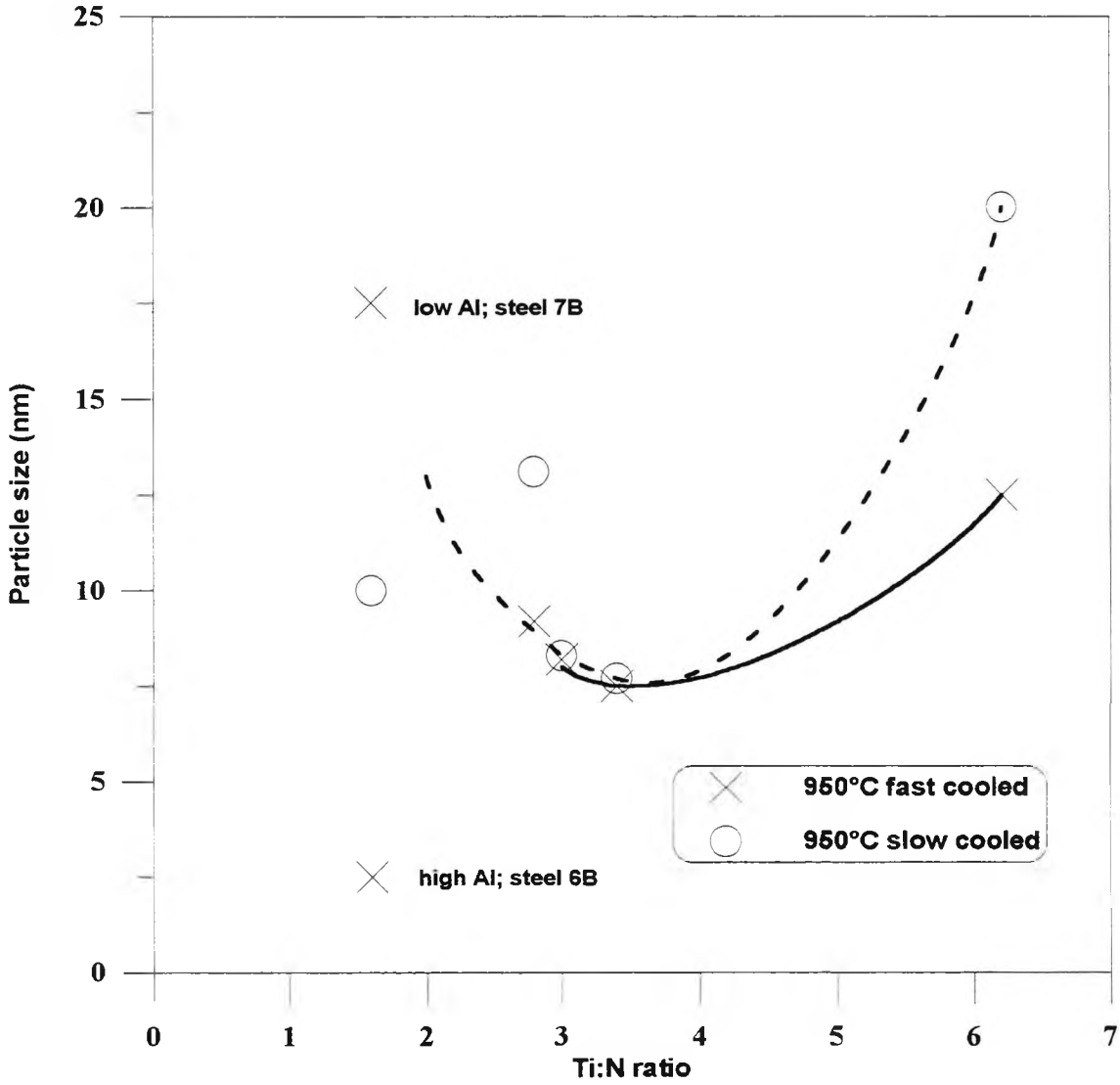
Thus, on increasing the Ti:N ratio from 3.4:1 to 6.2:1, one might expect the ductility to decrease continually for non-equilibrium conditions or remain constant for equilibrium conditions. That neither of these scenarios occur and ductility improves is probably related to the precipitate coarsening with increase in the Ti:N ratio above that required to give stoichiometry, (i.e. 3.4:1), Figs. 4-2 and 4-3 and Figs. 4-22 and 4-27.

Increasing the [Ti]x[N] as well as increasing the amount of precipitation causes the precipitation to occur at higher temperatures and hence be coarser.

Growth of the particles is dependent on the amount of Ti in solution, this being the rate controlling species for the growth of TiN particles. Thus high Ti:N ratios, (viz. 6.2:1) will ensure that there is more Ti in solution and growth of the TiN will therefore occur more rapidly.

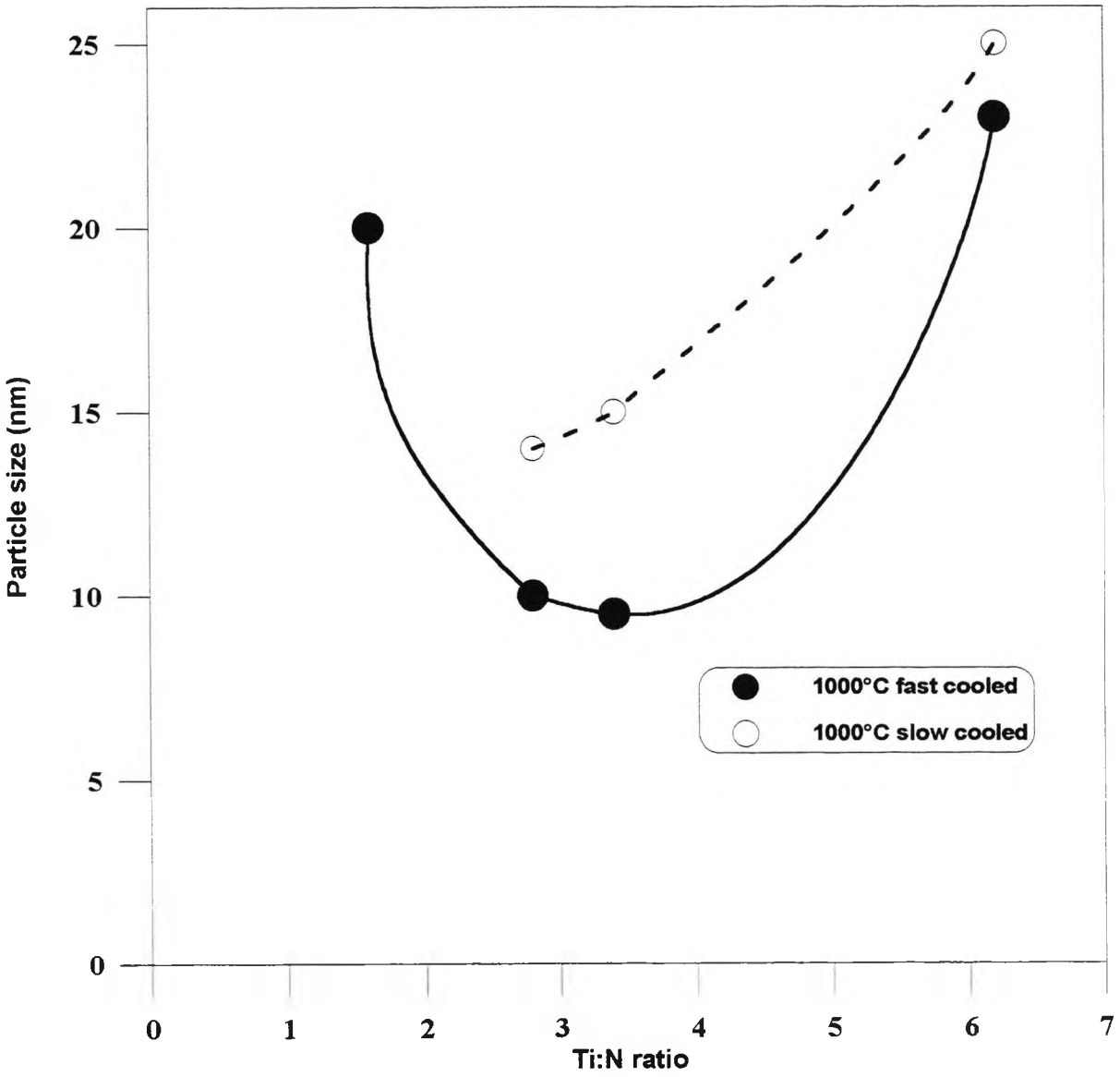
The average size of the TiN particles against Ti:N ratios are plotted in Fig. 4-29 and 4-30 for both cooling rates, at temperatures of 950°C and 1000°C, respectively generally it can be seen that coarser particles are associated with higher Ti:N ratios. At low Ti:N ratios however, the particle size seems to be very dependent on the Al level. The low Al containing steel, steel 7B which has the same Ti:N ratio of 1.6:1 as higher Al containing steel, steel 6B, has a coarser particle size and better ductility, Fig. 4-29. It should also be noted from comparison of Fig. 4-29 with 4-30, that

increasing the test temperature generally results in a coarser particle distribution leading to better ductility.



File:rat.grf

Figure 4-29 ***Average particle size against Ti:N ratio for steels tested at 950°C after cooling at 25K/min and 100-200K/min.:***



File:13b.grf

Figure 4–30 ***Average particle size against Ti:N ratio for steels tested at 1000°C after cooling at 25K/min and 100-200 K/min.***

Influence of cooling rate

As has been found with previous work on C-Mn-Al and C-Mn-Nb-Al steels[Abushosha et al, 1998 p227][Abushosha et al, 1998 p346] increasing the cooling rate always gave rise to worse ductility although changes were at times very small. The general effect of increasing the cooling rate is to produce a finer precipitate distribution, Table 4-2, and a finer sulphide distribution as can be inferred by the generally finer dimple size associated with the particles on the fracture surfaces, Figs. 4-7 to 4-17 and Table 4-2.

Thus the worse ductility on increasing the cooling rate could be related to a finer particle/inclusion distribution.

Regression analysis

The influence of both particle size and volume fraction is difficult to isolate in the present work. Because of this and the large amount of data obtained it was felt that a linear regression analysis approach may be of benefit.

The important variables controlling ductility at constant grain size and strain rate are 1) The size of the particles at the boundary and within the matrix. A smaller size in the matrix leads to higher stresses acting on the boundary and a finer closely spaced particle distribution at the boundaries makes it easier for cracks at the grain boundaries to link up. 2) The product of the [Ti]x[N] which probably controls the

volume fraction of TiN particles that are precipitated out. In the present instance as N levels are approximately constant there is small difference in the regression analysis in using either the product of [Ti]x[N] or the Ti level. However, as will be shown in the chapter on Nb containing steels, that where the N level varies better relationships are obtained by using [Ti]x[N] rather than Ti by itself in the regression analysis. 3) the inclusion size and volume fraction particularly for those inclusions situated at or near to the boundary. Although the latter effect tends to get swamped by the adverse influence of the microalloying precipitation there is no doubt that it has a large effect on precipitate free steels[Abushosha et al, 1998 p227] and there is evidence that the inclusions do have some effect even when microalloying precipitates are also present[Abushosha and Vipond, 1991p1101]. The inclusion volume fraction is likely to be controlled by the S level and their size by the cooling rate.

The likely variables that will influence the R of A values which should be included in a regression equation are therefore 1) average particle size 2) [Ti]x[N], 3) S content and 4) cooling rate.

Assuming that the Ti will always combine with the available N, then any remaining N can then combine with the soluble Al. A further variable [Al]x[N_s] has therefore been included where N_s is the remaining N after it has combined with the Ti.

The following regression equation was obtained using *Minitab* software:

$$RofA(\%) = 44.1 - 0.169CR + 16.3(\sqrt[3]{p}) - 0.935[Ti]x[N]x10^5 - 119.2(\sqrt[4]{[Al]x[N_s]}) \ldots (4-1)$$

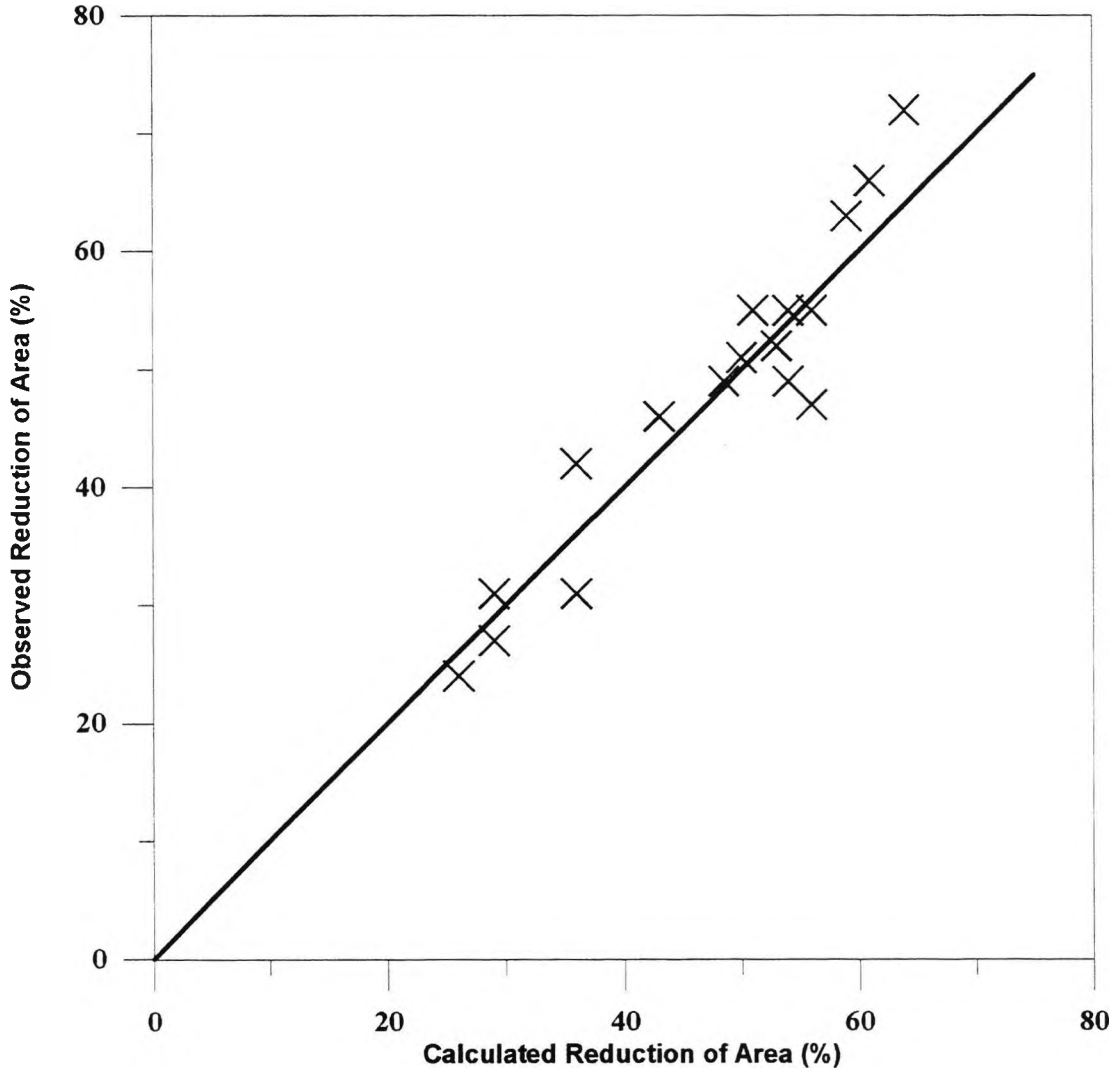
where CR is the cooling rate in K/min, p is the particle size in nm, and N_s is the

amount of N available to combine with Al assuming that there is not enough Ti present to combine with all the nitrogen.

No influence of S level was found in the regression analysis and this variable has therefore been excluded. All bar one of the steels had similar S levels so this is perhaps not too surprising. Also previous work[Mintz and Abushosha, 1996] has indicated that for as-cast steels the S level only becomes important at the higher temperature testing range when it might delay dynamic recrystallisation. The cooling rate does however, control the size of the sulphides at the austenite grain boundaries and the finer this is the worse is the ductility.

The regression equation had an index of determination of 88% and standard deviation of ±5.28. The t-ratios for the variables were all significant being -7.08, 4.05, -2.92 and -3.35 for the cooling rate, particle size, [Ti]x[N] and [Al]x[N_s], respectively. The high significance of the [Al]x[N_s] term would tend to indicate that Ti is fully effective in removing N from solution and only when there is insufficient Ti present to combine fully with all the N can AlN form.

It can be seen from Fig. 4-31 that there is excellent agreement between the observed R of A against that calculated from the regression equation 4-1.



File:calc.grf

Figure 4–31: ***Relationship between the observed Reduction of Area and that calculated from equation 4-1.***

Control of dimple size

For a given strain rate, the dimple size at the γ grain boundaries in the ferrite films will be controlled by both the size of the particles and their volume fraction. Whereas increasing the particle size will result in an increase in dimple size, an increase in volume fraction will have the opposite effect. A refinement in dimple size could therefore be due to either finer particles or a greater volume fraction. In the case of hot ductility both means of dimple refinement will lead to worse ductility. This can be seen from Table 4-2 to be the case for the simpler Ti free steels. Increasing the soluble Al level results in an increased volume fraction of AlN and this results in the average dimple size being refined; both coarser AlN and spherical MnS inclusions being present. Similar results have been obtained by Cardoso [Cardoso and Abushosha, 1995].

However, the situation is more complex for the Ti containing steels because the coarser AlN particles responsible for many of the dimples are no longer present. Ti will preferentially combine with the N and the TiN particles are generally much finer than the AlN precipitates, and because of this may be too fine to influence the dimple size.

A problem was also noted with one of the Ti containing steels with a low Ti addition, steel 13, that it had not been deoxidised well enough with Al and coarse silicates as well as spherical MnS particles were present producing a much finer dimple size than might have been expected.

Commercial Implications

The present work indicates that the faster surface cooling rate present in thin slab casting is likely to be detrimental to ductility. Although the strain rate used in thin slab casting is about 5 times that in conventional casting, the better ductility from this source is unlikely to fully compensate for the reduction in ductility from faster cooling rates. Furthermore, because surface inspection is not possible the surface quality in thin slab casting needs to be better than in conventional continuous casting.

Adding Ti to steels causes the hot ductility to be impaired in the as-cast condition. However, it should be noted that the laboratory conditions are different to those applied during continuous casting. The laboratory cooling conditions have been chosen to represent average cooling rates and do not take into account the complex cooling pattern undergone by the strand.

Commercially, cooling just below the surface is very rapid at first, reaches a minimum temperature and then rises again. The subsurface temperature prior to straightening then cycles; the temperature falling as the sprays impinge on the strand and then rises as the strand enters the guide rolls. Where attempts have been made to partially simulate this complex cooling pattern little effect on ductility was noted in Ti containing steels but a large detrimental effect was observed in Ti free steels[Mintz, Abushosha and Cardoso, 1995].

Thus, it is possible that Ti containing steels may behave better than Ti free steels

under conditions more akin to commercial cooling.

Nevertheless the best ductility from Ti containing steels are going to be achieved at

1) low N levels since this will reduce the amount of precipitation that can take place.

2) working at high Ti:N ratios, as this will ensure that there is a large amount of Ti in solution favouring the growth of the particles, and will also favour a higher [Ti]x[N] product encouraging precipitation at higher temperatures.

3) working at higher temperatures as this favours coarser precipitate distribution.

CONCLUSIONS

1)Increasing the soluble Al level in as-cast steels causes the ductility to deteriorate. Even at as low a level as 0.009% sol Al and 0.0067%N, ductility is reduced suggesting there is a considerable segregation of Al to the boundaries encouraging AlN precipitation.

2)Increasing the cooling rate from solidification to the test temperature in Ti containing C-Mn-Al steels causes the ductility to deteriorate. This can be related to the presence of a finer dispersion of the Ti containing precipitates at the faster cooling rate and a finer sulphide distribution.

The deterioration in these steels is primarily due to a finer sulphide distribution making it easier for the cavities formed by micro void coalescence to link up to give intergranular failure. Although the AlN particles might also be expected to be finer on faster cooling this was not found to be the case in the present work.

3)Adding Ti to a C-Mn-Al steel causes the ductility to fall. Ductility was worse at the stoichiometric composition for TiN, 3.4:1 but was found to improve above and below this ratio. For ratios < 3.4:1, this improvement is believed to be due to a reduced volume fraction of TiN particles and for ratios > 3.4:1 this improvement is due to a coarser TiN precipitation as a result of having an excess of Ti in solution and the higher product of [Ti]x[N] encouraging precipitation at higher temperatures.

4)Increasing cooling rate again caused the ductility to deteriorate in these Ti containing steels due to a finer TiN precipitation.

5)There was generally a good relationship between the average particle size (AlN and TiN) and the R of A values; R of A improving as the particle size increased.

6)The dimple size on the fracture surface was found to be related to coarser particles present, mainly inclusions but also the coarser AlN particles. The dimple size was not related to the R of A value.

7)Increasing the Ti:N ratio to 6.2:1 caused the ductility to improve due to a coarsening of the precipitation, but ductility was still worse than in Ti free C-Mn-Al steels.

8)The following regression equation has been obtained for the R of A values in Ti containing steels in the temperature range 950-1000°C;

$$RofA(\%) = 44.1 - 0.169CR + 16.3(\sqrt[3]{p}) - 0.935[Ti]x[N]x10^5 - 119.2(\sqrt[4]{[Al]x[N_s]})$$

where CR is the cooling rate in K/min, p is the particle size in nm, and N_s is the free N level after Ti has combined with the N.

All the variables were highly significant and the index of determination was 88%.

The equation shows that for good ductility, the particle size, (p) should be coarse and the cooling rate,(CR) slow. In addition nitrogen levels should be low to reduce the volume fraction of TiN and AlN particles that are precipitated out. When there is insufficient Ti to combine with all the nitrogen, aluminium levels should be kept low to avoid aluminium nitride precipitation.

9)Higher test temperatures result in a coarsening of the precipitate distribution and thus would suggest that an increase in the temperature at which the straightening operation is carried out at, will result in better ductility.

10) It is recommended for the best hot ductility to have a low N level ensuring a low volume fraction of Ti containing particles and a high Ti:N ratio ensuring that the particles are encouraged to coarsen.

Chapter 5 INFLUENCE OF Ti AND N ON THE HOT DUCTILITY OF C-Mn-Al-Nb STEELS

INTRODUCTION AND SUMMARY

Continuing the examination of the effect of microalloying addition on the hot ductility of steels, the examination was extended to investigate the influence of Ti and N on C-Mn-Al-Nb steels. The conditions used were identical to those in the previous chapter in which the influence of Ti on simple C-Mn-Al steels was examined.

Four Nb containing steels covering a wide range of Ti:N ratios were tested. Again to help in interpretation, another 5 steels that have been examined in the European Programme to develop the thin slab casting have also been included in this chapter for comparison, after kind permission by Dr. Abushosha. Although the tests on these 5 extra steels were carried out by Dr. Abushosha, sizing of the particles was carried out again by the author to ensure consistency of measurements. The composition of the steels are given in the table 5-1:

For the four steels tested by the author, two levels of N were examined; .004% and .011%. For the low N steels, steels 1B and 2B the Ti:N ratios were very much in excess of stoichiometric 8:1 and at the stoichiometric composition, respectively. For the high N steels, the Ti:N ratio were always below the stoichiometric level, being 2.0:1 and 3.1:1 for steels 3B and 4B, respectively. The European steels were all low

N and covered the Ti:N ratio range 3.3:1 to 5.0:1. The remaining two Nb, Ti free steels (Euro 60 and Euro 66) included, had different Al and N levels.

EXPERIMENTAL

The compositions of the steels examined are given in Table 5-1. Casts 1B to 4B were 50 kg laboratory vacuum melts melted in the Aerospace Research Centre Laboratories, Brazil and forged to 12 mm thick plate at the Companhia Siderúrgica Tubarão, (CST), Brazil. The rest of the steels were made by British steel, casts 59, 60 and 61 being 50 kg laboratory air melts and casts Euro 65 and Euro 66 being vacuum casts. All these casts were rolled to 12 mm thick plate.

Casts were chosen to give a wide range of N and Ti:N ratios.

The tensile samples of length 70 mm and diameter 7.94 mm were machined from the steel plates in the longitudinal direction of forging or in the case of the British Steel steels, parallel to the rolling direction. A hole of 2 mm diameter was drilled from the end of each sample to the mid-length so that a thermocouple could be inserted.

The specimens were tested in a tensile testing machine to which a heating induction unit had been fitted. The melting zone was approximately 22 mm in length situated at the mid-length position of the sample. The molten steel was contained in a silica tube with an initial 0.2mm clearance and the oxidising protection was achieved by surrounding the silica tube with a wide glass tube through which argon flowed.

Samples were melted at 1540°C for 5 min, and cooled to the required test temperatures in the range 800 to 1150°C where they were kept for another 5 min before stressing to failure using a strain rate of 3×10^{-3} s^{-1}. Two cooling rates were examined 25 and 100K/min, by the author and the cooling rates in the European programme were 25 and 200K/min. Immediately after failure the argon flow was increased to help "freeze in" the microstructure at the test temperature.

Optical metallography was also carried out on longitudinal sections including the fractured region of the quenched samples.

Austenite grain size measurements and ferrite film thickness were obtained for all the steels using the intercept method from outlinement of the austenite grain boundaries by the ferrite, as shown in Table 3-3. Due to the small size of the sample for microscopy, and the big austenite grain size, only a few intercepts (maximum of 6) were counted. The fractured surfaces of the samples were examined using a T 200 Jeol scanning electron microscope. Austenite grain size and ferrite thickness are shown in chapter 3, Table 3-3.

Carbon extraction replicas were taken close to surface and the particle size measured from the TEM photographs with the aid of a magnification glass device. The average of 500 measurements were taken for the particle size.

Table 5-1 ***Chemical composition of the steels analysed, wt per cent.***

Comp.	1B Red	2B Blue	3B Purple	4B Gold	Euro 59 air	Euro 60 air	Euro 61 Euro	Euro 65 vacuum	Euro 66 vacuum
C	.09	.09	.086	.092	.096	.094	.10	.087	.098
Si	.35	.35	.31	.31	.31	.32	.31	.31	.30
Mn	1.44	1.44	1.42	1.41	1.42	1.47	1.39	1.41	1.41
P	.017	.017	.019	.019	.011	.013	.012	.011	.012
S	.010	.011	.007	.007	.004	.004	.010	.002	.002
Nb	.043	.042	.040	.039	.033	.032	.032	.032	.031
Ti	.045	.014	.020	.034	.024	-	.021	.021	-
Sol. Al	.009	.008	.036	.031	.013	.015	.04	.030	.031
N	.0056	.0040	.010	.011	.0071	.0065	.0064	.0042	.0046
Ti:N	8.0	3.6	2.0	3.1	3.47	-	3.3	5.0	-
[Al][N]	5.0×10^{-5}	3.2×10^{-5}	3.6×10^{-4}	3.1×10^{-4}	9.2×10^{-5}	9.7×10^{-4}	2.6×10^{-4}	1.3×10^{-4}	1.4×10^{-4}
[Ti][N]	2.5×10^{-4}	5.6×10^{-5}	2.0×10^{-4}	3.7×10^{-4}	1.7×10^{-4}	-	1.3×10^{-4}	8.8×10^{-5}	-

RESULTS

The hot ductility curves for the steels examined are given in Figs. 5-1. It shows that increasing the cooling rate, as in previous work[Abushosha et al, 1998p227, 1998p346; Abushosha, Cominelli and Mintz, 1998], and the last chapter results in worse ductility.

At the slower cooling rate, the low N steel with the low Ti addition, steel 2B gave the best ductility. At the faster cooling rate (100K/min), the poorest hot ductility seems to be related to the volume fraction of particles i.e. [Ti]x[N] product being highest in the steels 3B and 4B the steels giving and worse hot ductility.

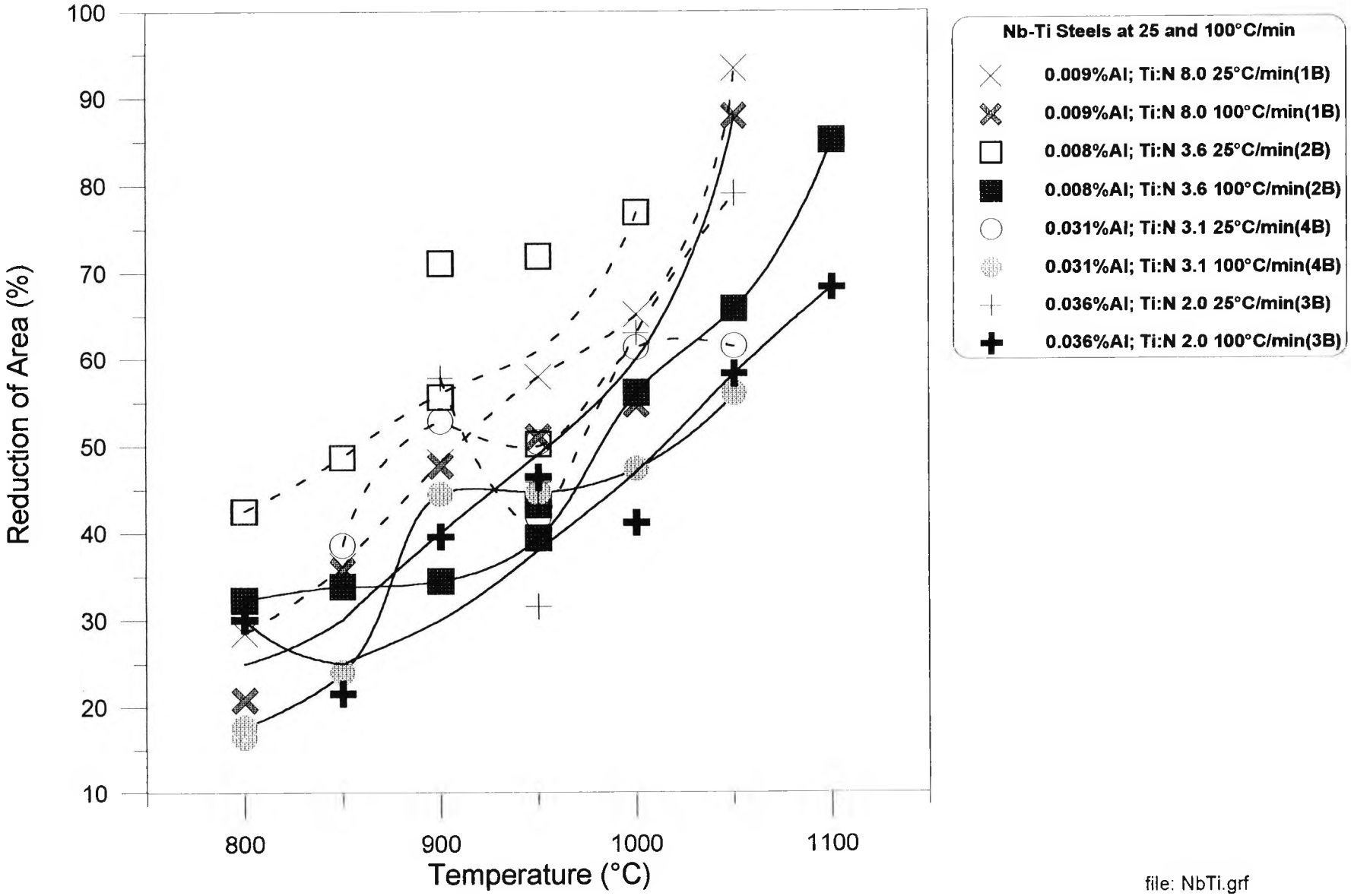


Figure 5–1 **Hot ductility curves for C-Mn-Al-Ti-Nb steels tested at 25 and 100K/min**

In order to help interpret the behaviour the hot ductility curves from the European programme have also been included, Figs. 5-2 and 5-3.

Figs 5-2 and 5-3 show the same steels including those from the European programme, for both slow and fast cooling rates, respectively. Although the European work used both air and vacuum melts no difference could be detected between the hot ductility curves for steels of similar composition cast by these different routes. The insensibility to casting route may be due to the fact that all the tensile specimens from all the casts are remelted under the same conditions. It should be noted that the steels in the European Programme were cooled at a faster cooling rate of 200K/min. Increasing the cooling rate can be seen to cause the ductility to deteriorate as noted in the previous chapter.

The code numbers in Table 5-1 are marked on the curves for ease of identification.

Hot ductility curves for Ti containing Nb steels cooled at 25K/min, Fig. 5-2

At 25K/min for the Nb containing steels the ductility deteriorated as the [Ti]x[N] product increased from 0.6 to 0.9 to $1.7x10^{-4}$, curves A(2B), C(Euro 65), and D(Euro 59) respectively in; Fig. 5-2. Increasing the [Ti]x[N] product to $2.5x10^{-4}$, curve B(1B), the steel having Ti:N ratio of 8:1, caused the ductility to improve again.

Although ductility for temperatures in excess of 900°C, was always worse for the Ti containing steels compared to the Ti free steels, Euro 60, curve E, (note that other Ti free steel, Euro 66, was tested only at 200K/min), some improvement in the lower temperature range <900°C was noted for the steel having the very high [Ti] x [N] product and the highest Ti:N ratio, steel 4B, and for the steel 2B which had a very low Ti addition and [Ti] x [N] product. Steel 2B had also a very similar composition to steel 3B but better ductility at both cooling rates. The difference is the [Al]x[N] being smaller for steels 2B. Figs 5-2 and 5-3.

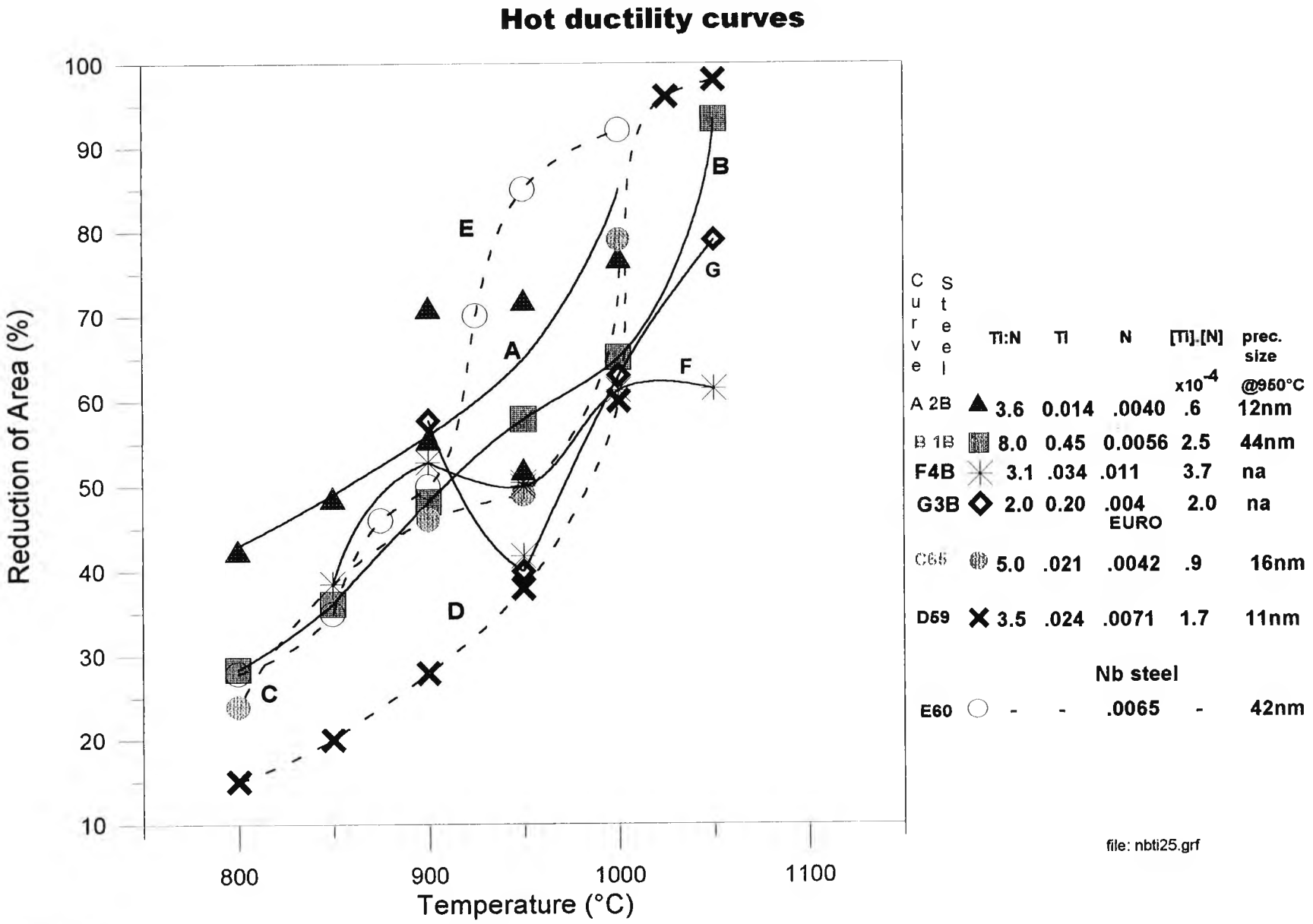


Figure 5–2 **Hot ductility curves of Nb-Ti steels tested at slower cooling rate of 25K/min. Also included are steels Euro 59, Euro 60 and Euro 65 from the European Programme**

Hot ductility curves for Ti containing Nb steels cooled at 100/200K/min., Fig. 5-3

At the higher cooling rate, behaviour was more complex. Again the steel with the highest Ti:N ratio of 8:1:1, steel 1B, curve A in Fig. 5-3, gave much better than expected hot ductility.

For the Ti containing steels, the ductility deteriorated as the [Ti] x [N] product increased from 0.6 to 0.9 to 1.7 x 10^{-4}, curves B, C_3 and D for steels 2B, Euro 65, and Euro 59 respectively, Fig. 5-3. Increasing the [Ti] x [N] product to 2.5 x 10^{-4}, steel 1B, the steel having the highest Ti:N ratio caused the ductility to improve again, curve A. Steels 3B and 4B curves C_1 and C_2, have also a high [Ti]x[N] product and gave better hot ductility than the steel having the stoichiometric composition, steel Euro 59, curve D.

There was a trend for ductility to deteriorate as the [Ti] x [N] product increased to 1.7, (curves for steels 2B, Euro 65, and Euro 59 corresponding to products of 0.6, 0.9, 1.3 and 1.7 x 10^{-4} respectively). However, the steels in the figure labelled Euro 65, 3B and 4B all had very different [Ti] x [N] products, (0.9, 2.2, and 3.7 x 10^{-4} respectively) yet all had similar hot ductility curves. At this cooling rate Nb, Ti free steels had the best hot ductility at higher temperatures, curves, E and F, for steels Euro 60 and Euro 66 respectively. Euro 60 gave the better ductility again probably due to the smaller product of [Al]x[N].

Again, ductility was always worse for the Ti containing steels compared to the Ti free steel for temperatures in excess of 900°C, compare curve E with the rest in Fig.

5-2 and Fig. 5-3. Below 900°C, only the steel with the very high Ti:N ratio of 8:1 and the steel with stoichiometric composition for TiN but with a very low [Ti] x [N] product, steel 2B, gave better ductility than the Ti free steel. Comparison between the various steels is very complex and it is clear that the volume fraction is not the only variable. Other variables will include the size of the precipitates and inclusions.

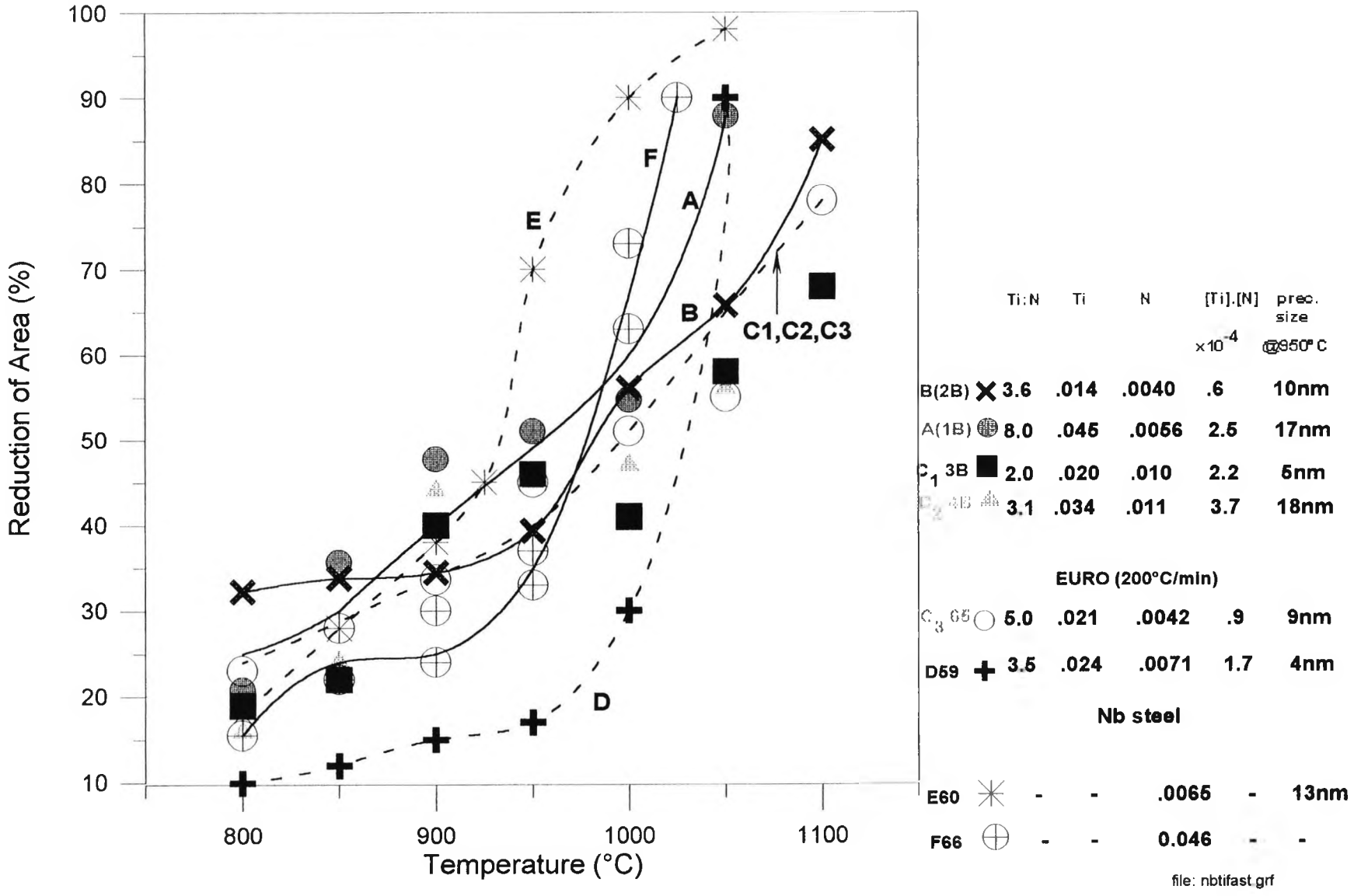


Figure 5–3 **Hot ductility curves for Nb-Ti steels tested at faster cooling rates of 100/200K/min.**

As in the previous chapter and work on Ti containing C-Mn-Al steels[Abushosha, 1998p346], at the temperature giving the minimum ductility, 800°C, thin bands of ferrite were found surrounding the prior austenite grain boundaries, Fig. 5-4.



Figure 5-4 **Crack in a thin film of ferrite surrounding coarse austenite grain(90X)**

The austenite grain size was found to be similar for all the steels as shown in chapter 3, Table 3-3, being ~1-3 mm and the grain size in the Ti containing steel was no finer than in the Ti free steels. Some refinement in grain size was found at the faster cooling rate but this was only small and from previous work[Mintz et al, 1991] was not likely to influence the hot ductility.

SEM examinations.

Fractures at the temperature giving minimum ductility were always intergranular and the fracture surfaces were covered with ductile dimples, Fig. 5-5. The fractures were therefore caused by the joining up of the cavities formed at the MnS inclusions situated in the thin ferrite films surrounding the prior γ grain boundaries. Dimple size in the Ti containing Nb steels were similar for both cooling rates for both the steels analysed, Figs. 5-3 and 5-4. The dimple size measurements are given in Table 5-2, together with the previous measurements on the Ti containing C-Mn-Al steels.

Effect of cooling rate and Ti:N ratio:

As previously reported in the previous chapter, increasing the cooling rate caused the ductility to deteriorate. However, the effect of cooling rate was much more marked for steel 2B, the steel with the Ti:N ratio close to the stoichiometric for TiN. Samples tested at 800°C, for the Nb steels, steels 3B and 4B, with the high N contents, showed intergranular failure for both cooling rates. The fracture appearance suggests one of the major causes of fracture in the trough, is voiding around the sulphide precipitates in the ferrite films surrounding the Υ grain boundaries. The similarity of dimples sizes were confirmed by an also similar reduction of area values at 800°C for both the steels 1B and 2B, Figs. 5-3 and 5-4. The dimple size measurements made on samples fractured at 800°C in the trough are given in Table 5-2.

Table 5-2 - ***Measurement of particle size at 950 and 1000°C and dimple size at 800°C. the R of A values are also given.***

Steel	part. size (nm) and number				dimple size* at 800°C (μm)	R of A (%)		Cool. Rate (K/min)
	950°C	(number)	1000°C	(number)		950°C	1000°C	
Low Ti Ti:N 3.6;	**10.2**	**361**	**21.1**	**48**	**18**	**42**	**56**	**100**
Nb 0.042 Blue(2B)	**12.2**	**344**	**32.9**	**117**	**22**	**61**	**77**	**25**
High Ti Ti:N 8.0;	16.7	607	67.4[x]	1338	27	51	60	100
Nb 0.043 Red(1B)	44.4[xx]	7	43.5	44	24	57	65	25
Ti:N 3.1 Nb Gold(4B)	**15**	**30/**	**-**		**11**	**45**	**47**	**100**
Ti:N 2.0 Nb Pur(3B)	7	30/	-		9	38	47	100
Euro 59 - TiN3.5	**8.5**	**208+**	**10.9**	**57+**		**17**	**30**	**200**
Nb	**10.8**	**1062+**	**14**	**27+**		**38**	**65**	**25**
Euro 61 Ti:N:3.3			11.8	117		29	35	200
high S Nb			20.8	49		44	55	25
Euro 65-Ti:N 5.0	**9.4**	**413**	**20**		**-**	**45**	**51**	**200**
+Nb	**15.9**	**260**	**44.4**		**-**	**60**	**79**	**25**
Euro 60 - Nb Steel	13.1	37				70	90	200
	39.7	42	48.4[@975]	33+		85	92	25

(*) measured at 800°C due SEM at higher temperatures show almost no dimples.

/ guessed; + not considered 100%; x fine precipitates gathered in clusters; very low number.

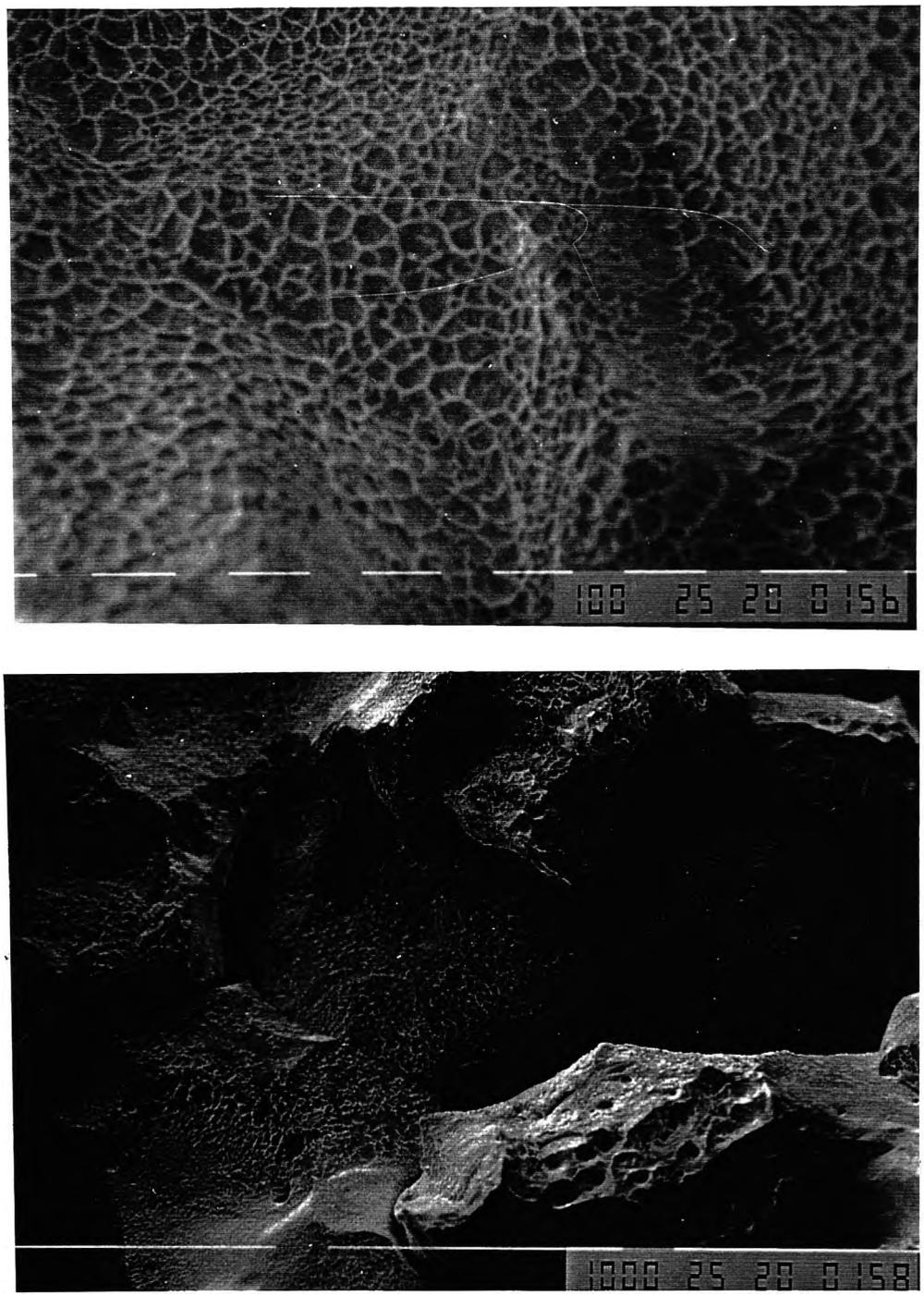


Figure 5-5 - ***SEM of the intergranular fracture surfaces for the Nb containing steel, 1B, with the high Ti (0.045%) and low N (.0056%) levels tested at 800°C, (Ti:N ratio of 8:1) showing similarity of particles as cooling rate changes. (a) Rate of cooling: 25K/min; R of A 29% (dimple size 24 μm) and (100X) (b) 100K/min; R of A 20% (dimple size 27μm). (35X)***

For the steels examined in this work, the steel with the Ti:N ratio close to stoichiometry steel 2B, curve B in Fig. 5-3 gave worse hot ductility compared to steel 1B the steel with the highest Ti:N ratio of 8:1. However, the curves A and B crossed at 850°C. The change in ductility that occurred on altering the cooling rate in steel 2B (see curve at Fig. 5-1) was the most marked for all steels examined. However for this steel, the difference was smaller at 800°C the dimple size in accordance to this, was similar for both cooling rates, Table 5-2, Fig. 5-6.

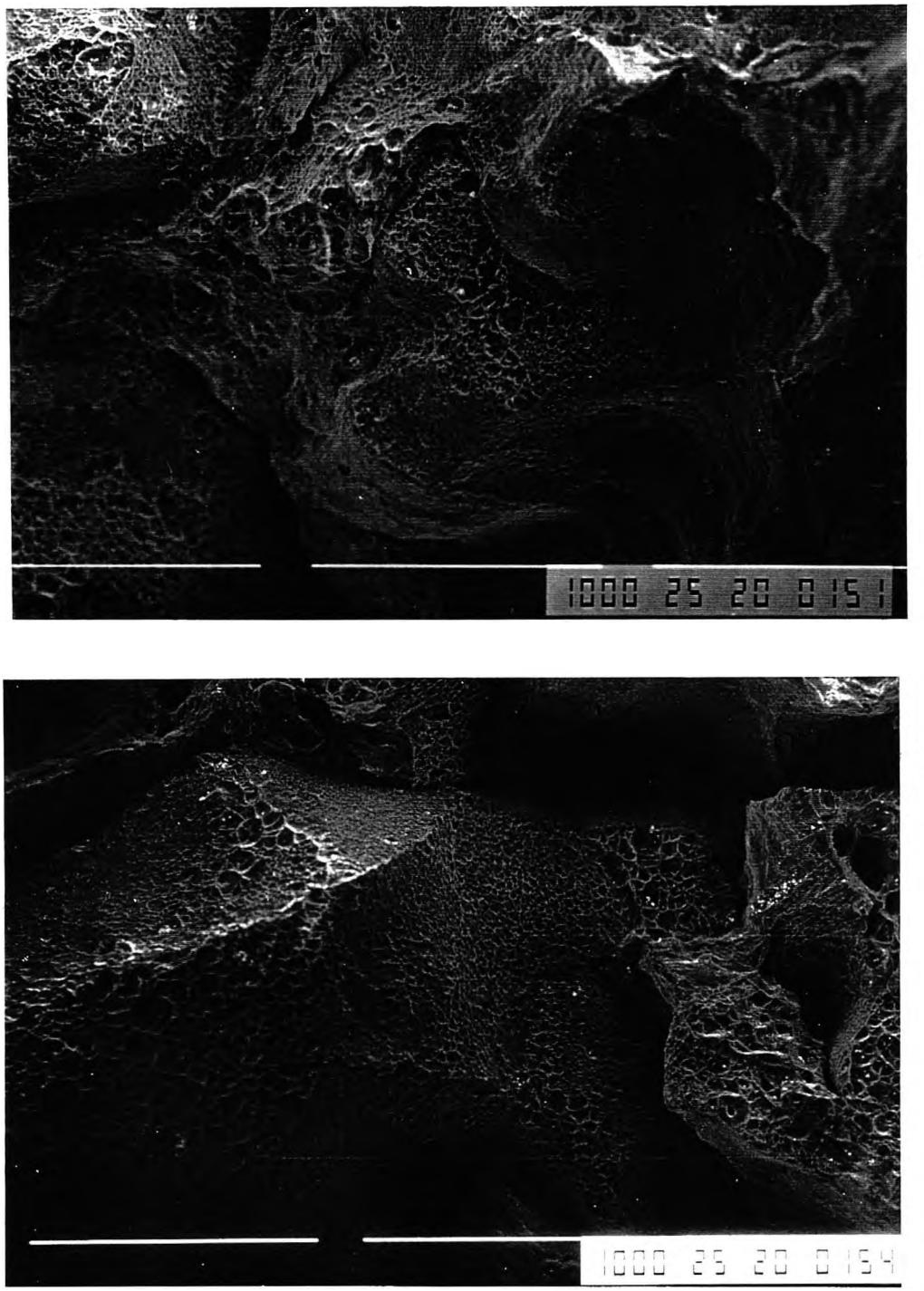


Figure 5-6 - ***Fracture surfaces of the Nb containing low N steel (Ti:N ratio 3.6:1), steel 2B, tested at 800 °C. (a)25K/min R of A 42% and (b)100K/min R of A 32% (35X). Dimple size were 22 and 18 μm respectively.***

The two other high N steels, steels 3B and 4B having low Ti:N ratios of 2 and 3.1 respectively, had very similar hot ductility curves at the faster cooling rate, (represented by only one curve in Fig. 5-3) and also similar fractures surfaces, Fig. 5-7a and b. This suggests that for these high N steels, increasing the Ti from 0.020% to 0.034% has little influence on hot ductility.

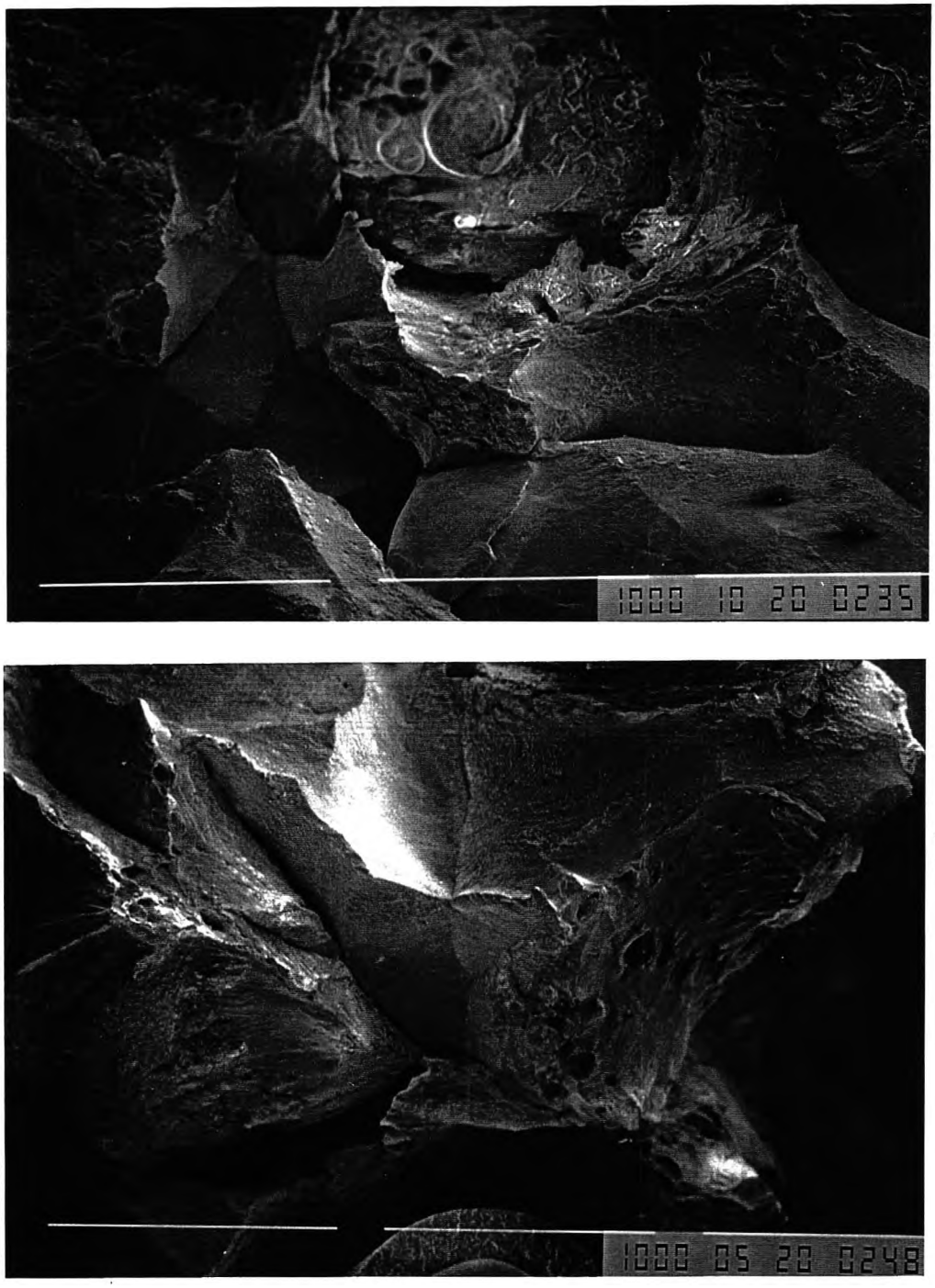


Figure 5-7 - ***Similar fracture surfaces found in a) steel 4B , 0.034% Ti, tested at 850℃ and b), steel 3B, 0.020%Ti tested at 900℃. (35X)***

The Transmission Electron Microscopy was carried out using carbon extraction replicas so that the size and shape of the precipitates could be determined.

It is important to be able to compare the precipitation in Ti containing Nb steels with that obtained in similar Ti containing, Nb free (Chapter 4) and Ti free, Nb containing steels. The Ti free Nb containing steel from the European Programme was therefore examined to give this information. Measurements were made in general at two temperatures 950 and 1000°C for each of the steels in Table 5-2.

TEM examinations:

1) Effect of cooling rate.

In the Ti free steel, marked precipitation of Nb(CN) occurred in a very fine form at 900°C, Fig. 5-8.

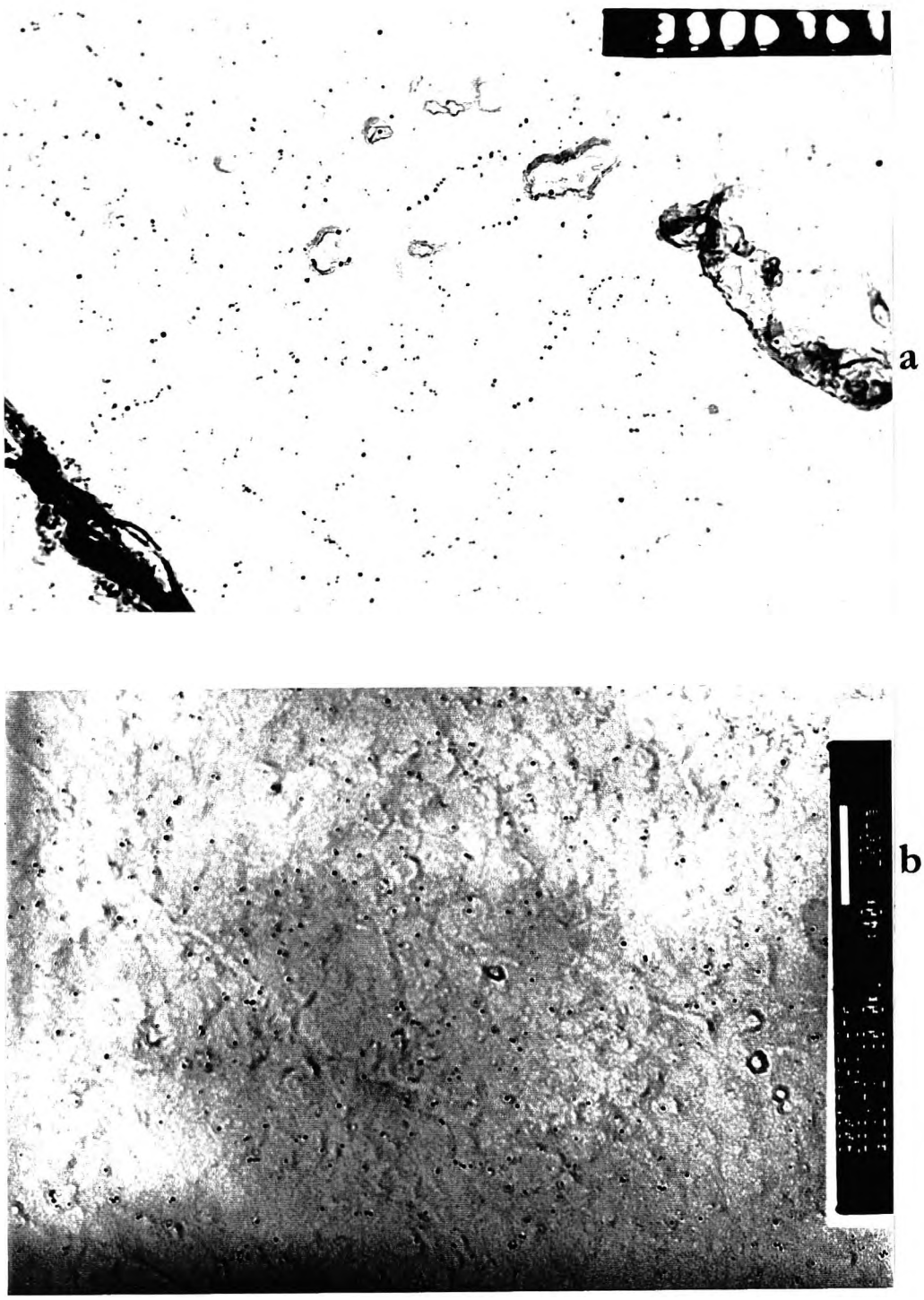


Figure 5-8 ***Finer precipitation of Nb(CN) found in higher Al vacuum melted C-Mn-Nb-Al steel tested at 900°C and cooled at 200K/min. a)air melted steel (steel, Euro 60)(10nm) (52,500X) and b) higher Al, vacuum melted(Euro 66 steel)(6nm).(75,000X)***

It is interesting to note that the precipitation in the higher Al containing Ti free steel, steel Euro 66 was finer, Fig. 5-3. This is in accord with previous work[Mintz and Arrowsmith, 1979p24] on solution treated Nb containing steels, in which it was found that increasing the Al level resulted in a finer precipitation of Nb(CN). Thus, the worse ductility of steel Euro 66, could be a combination of finer precipitation as well as a greater volume fraction of AlN. Adding Ti, resulted in again marked precipitation but the analysis of the precipitates showed both the presence of both Ti and Nb, Figs. 5-8 and 5-10. Decreasing the cooling rate, Fig. 5-9 or increasing the Ti:N ratio, Fig. 5-10, led to coarser particle distributions. The particle size measurements carried out for test temperatures of 950 and 1000°C are given in Table 5-2.

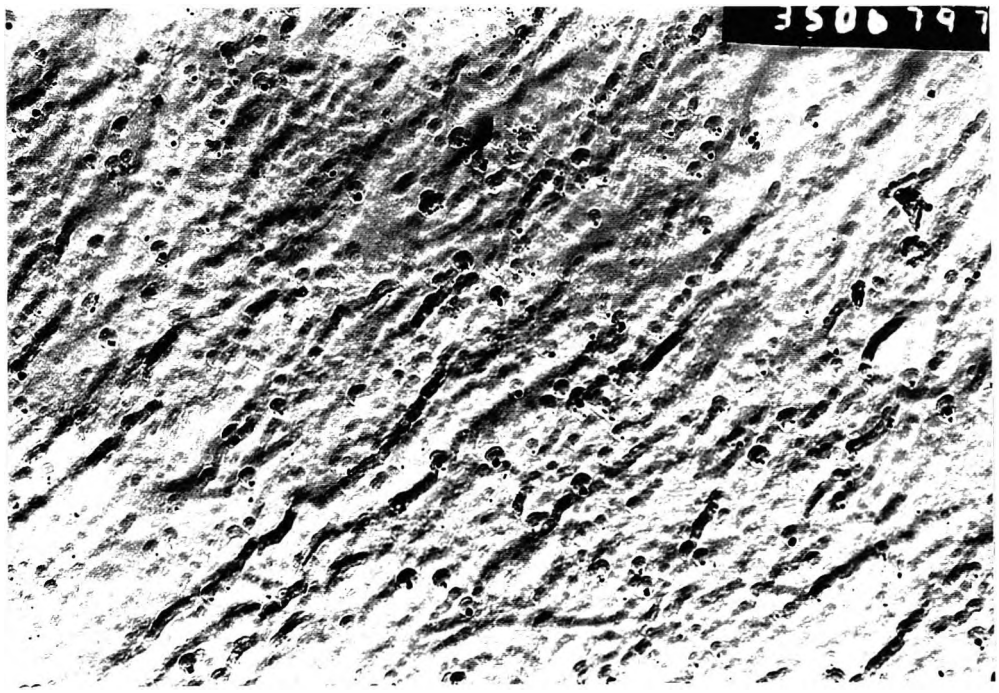


Figure 5-9 ***Fine Nb,Ti(CN) found in the low Ti:N ratio steel, tested at 950°C, and cooling rate of 25K/min. Precipitation size 10-20 nm, R of A 37%. (52,500X)[Abushosha et al. 1997].***

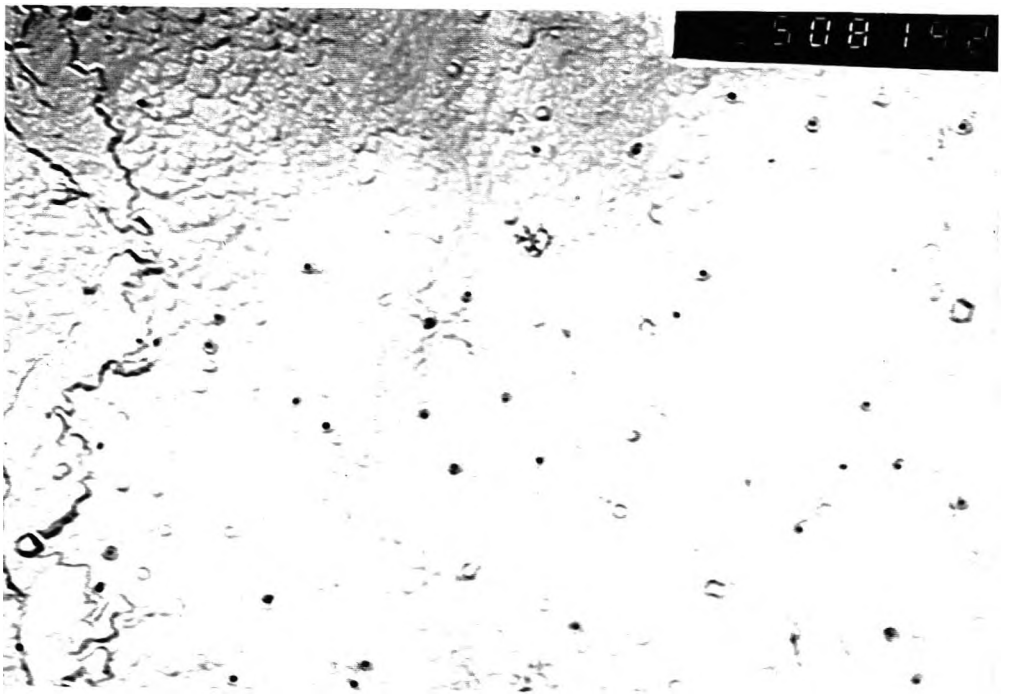


Figure 5-10 ***Fine Nb,Ti(CN) precipitation found in the high Ti:N ratio steel tested at 950°C and cooling rate of 25K/min. Precipitation size 12-30nm, R of A 49%.(52,500X)***

Generally increasing the cooling rate refined the particles as can be seen from Table 5-2 and Figs. 5-12 and 5-14.

2) Influence on Nb on particle size.

Taking into consideration the differences in composition for similar Ti:N ratios, adding Nb to these steels seems to coarsen the precipitates. For example, for steels close to stoichiometry, steels with ratios of 3.6 and 3.4, steel 2B, the Nb containing steel, and steel Euro 58, the Ti containing Nb free steel, from chapter 4, the Nb containing steel has the coarser precipitation, e.g. at 1000°C at the slower cooling rate, the average particle size was 33nm, whereas it was 19nm for the Nb free steel, see Table 5-2. Although the Ti and N levels are very different in these two steels it might be expected

that the steel with the higher [Ti]x[N] product would favour precipitation at higher temperatures, Table 5-2, the Nb free, Ti containing steel, steel Euro 58 and hence be coarser. However, this is not so and Nb can be seen to have produced a coarser precipitation. In this case the better ductility Fig. 5-11 is probably due to the Nb containing steel having both a lower volume fraction of precipitation (smaller [Ti]x[N] product) as well as a coarser particle size.

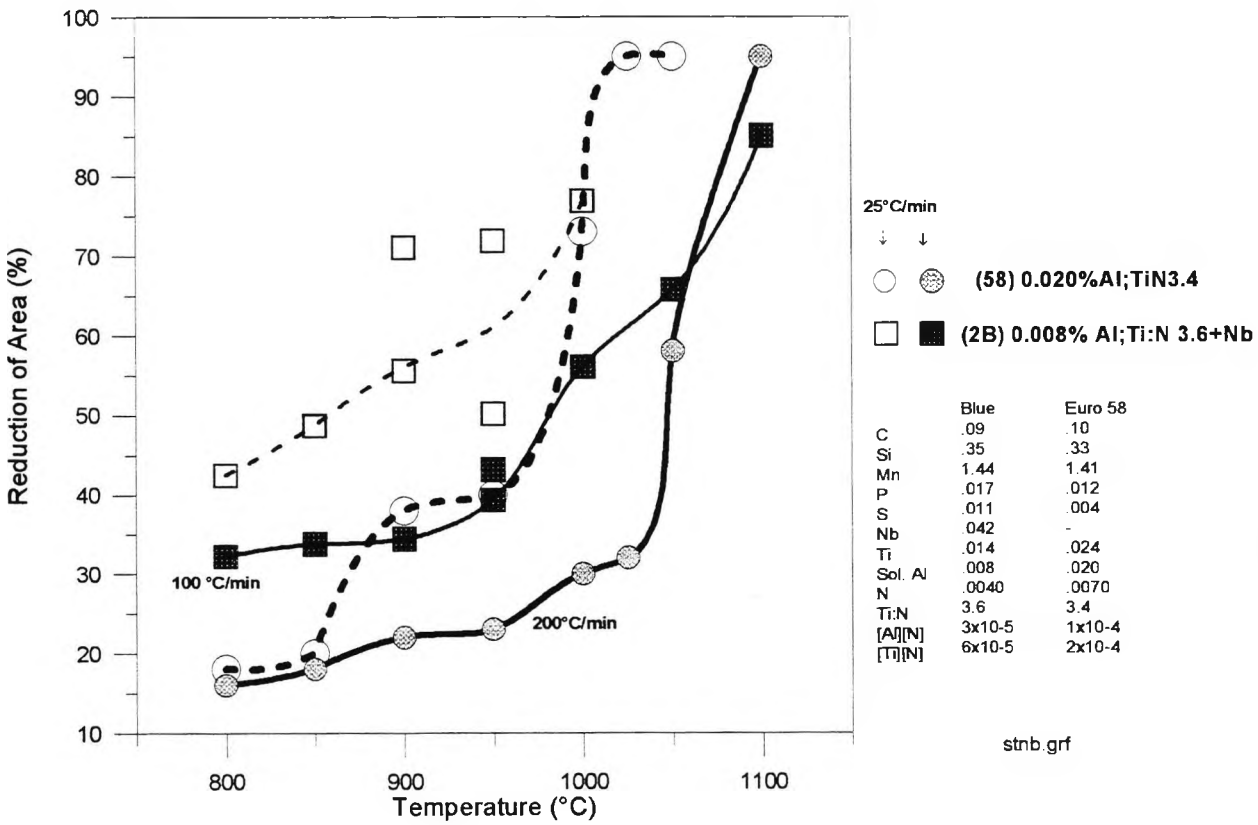


Figure 5-11 ***Reduction of area curves for Ti and Nb-Ti steels at similar Ti:N ratio close to stoichiometric.***



Figure 5-12 - ***Effect of the cooling rate on the Nb containing steel 2B, the steel with the Ti:N ratio of 3.6:1 having low Ti and low N levels tested at 1000°C precipitate size for: (a) low cooling rate(33nm) and (b) high cooling rate(21nm).(52,500X)***

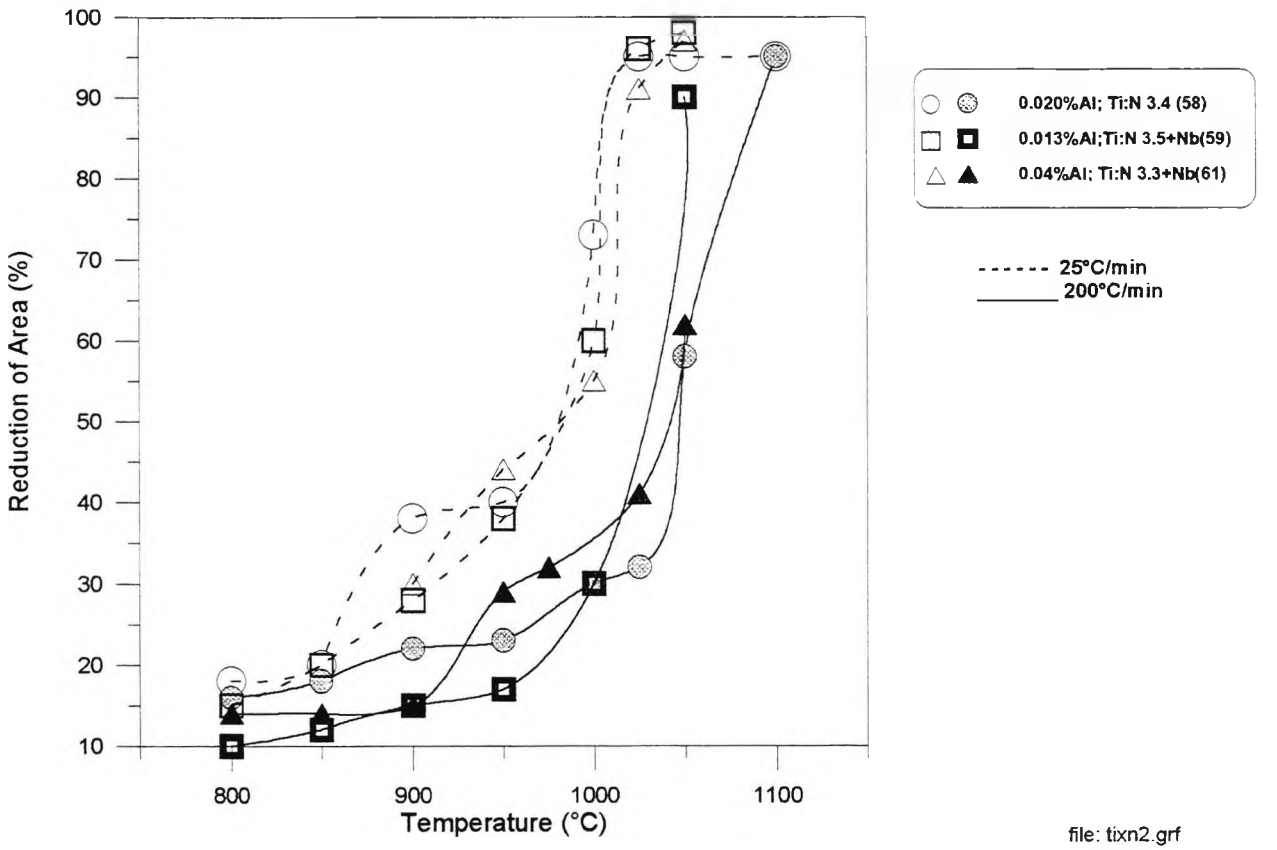


Figure 5-13 ***Hot ductility curves for steels with similar Ti and N levels (steels Euro 58, Euro 69 and Euro 61) and different Al levels cooled at 25K/min and 200K/min***

However closer examination of the hot ductility curves for steels with similar Ti and N levels, Euro 58, 59 and 61, Fig. 5-13 would suggest that for the same [Ti]x[N] product the coarsening of particles on adding Nb, leads only at most to a very small improvement in ductility. Presumably the greater volume fraction of particles due to the additional presence of Nb is offset by the coarser particle size. Despite ductilities being very poor, a small improvement was found for the Ti, Nb containing steel, steel 59, compared to the Nb free, steel 58, at higher temperatures(>1000°C) and for the higher cooling rate of 200K/min., conditions not favourable for fine precipitation due to the low "driving force". However, when the lower temperature range is reached and fine precipitates come out, the Nb addition is ineffective in sustaining the improvement and the hot ductility values get worse due to the occurrence of fine precipitates encouraged

by the their higher volume fraction. At the slower cooling rate, the increased volume fraction of precipitates in the Nb containing steel seems to offset the coarsening benefits of Nb and no improvement was found. As noted, this probably arises because adding Nb as well as coarsening the particles will also increase the volume fraction of particles that can be precipitated. Even if all the titanium can combine with all the nitrogen, the niobium can still combine with carbon to form niobium carbide. Increasing the cooling rate for steel 2B, the steel having the Ti:N ratio of 3.6:1 refined the precipitate and this was accompanied by a marked deterioration in the ductility, Fig. 5-12.

The Nb containing higher Ti, low N steel, steel 1B, (Ti:N ratio of 8.0:1) showed even coarser precipitation at 1000°C, compare Fig. 5-12 (a) and (b) with Fig. 5-14(a) and (b) and see Table 5-2. However, the effect of the cooling rate on the size of the particles was not so marked Fig. 5-14 and this was reflected in the R of A values being only slightly worse at the faster cooling rate.

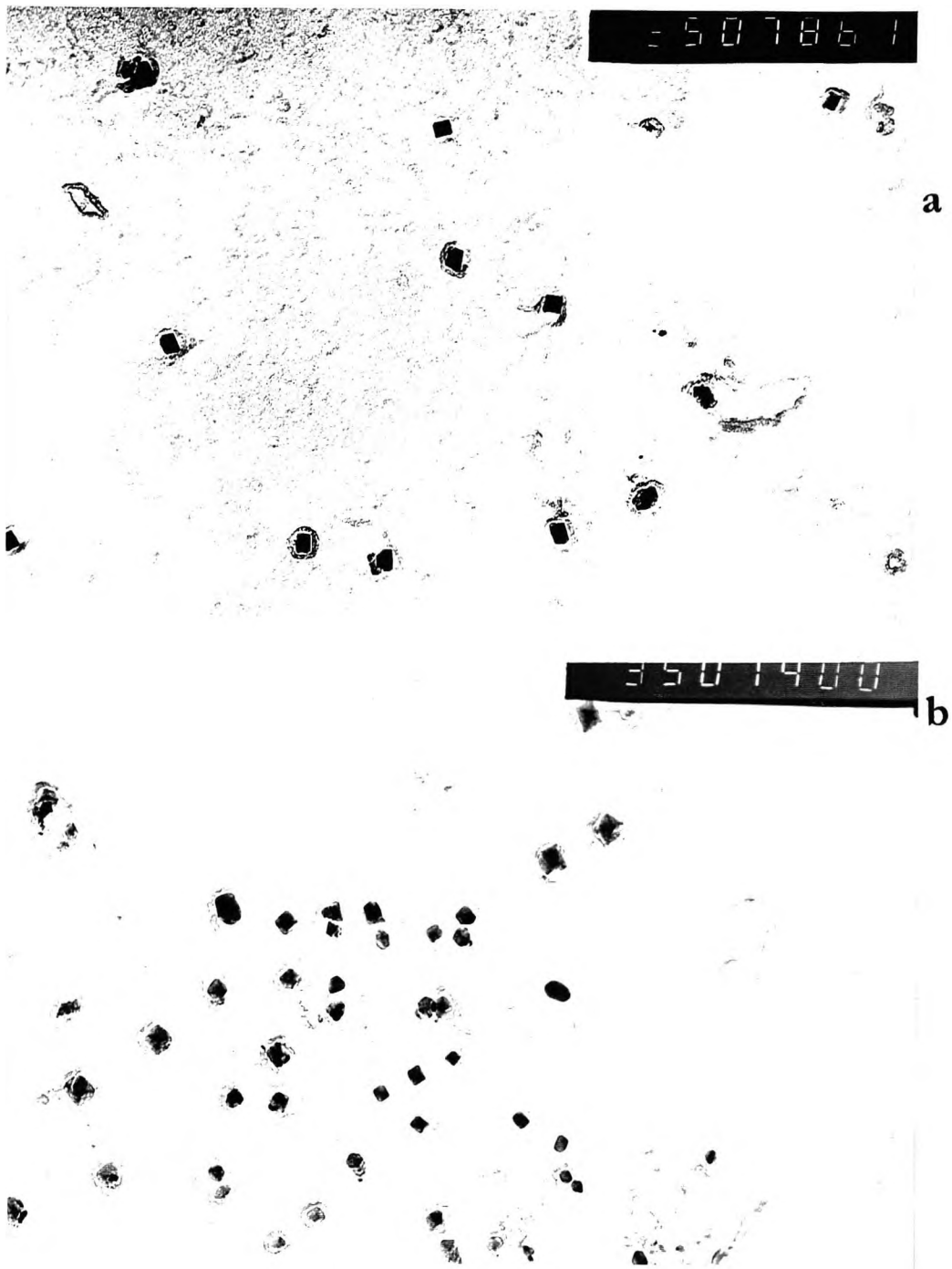


Figure 5-14 - ***Coarse Ti rich precipitates present in the Nb containing steel with high Ti:N ratio of 8.0:1, steel 1B. Steel was tested at 1000°C (a) slow cooling rate(44nm) and (b) fast cooling rate(31nm).(52,500X)***

Influence of temperature:

Increasing the test temperature invariably led to a coarser particle distribution as can seen from Table 5-2. The effect of the cooling rate on precipitate size was now smaller. Particles were now much coarser and there was considerable variation in size form one area to the next. Although in Fig. 5-15 the particles are finer on faster cooling, the actual average particle size was little affected by the cooling rate.

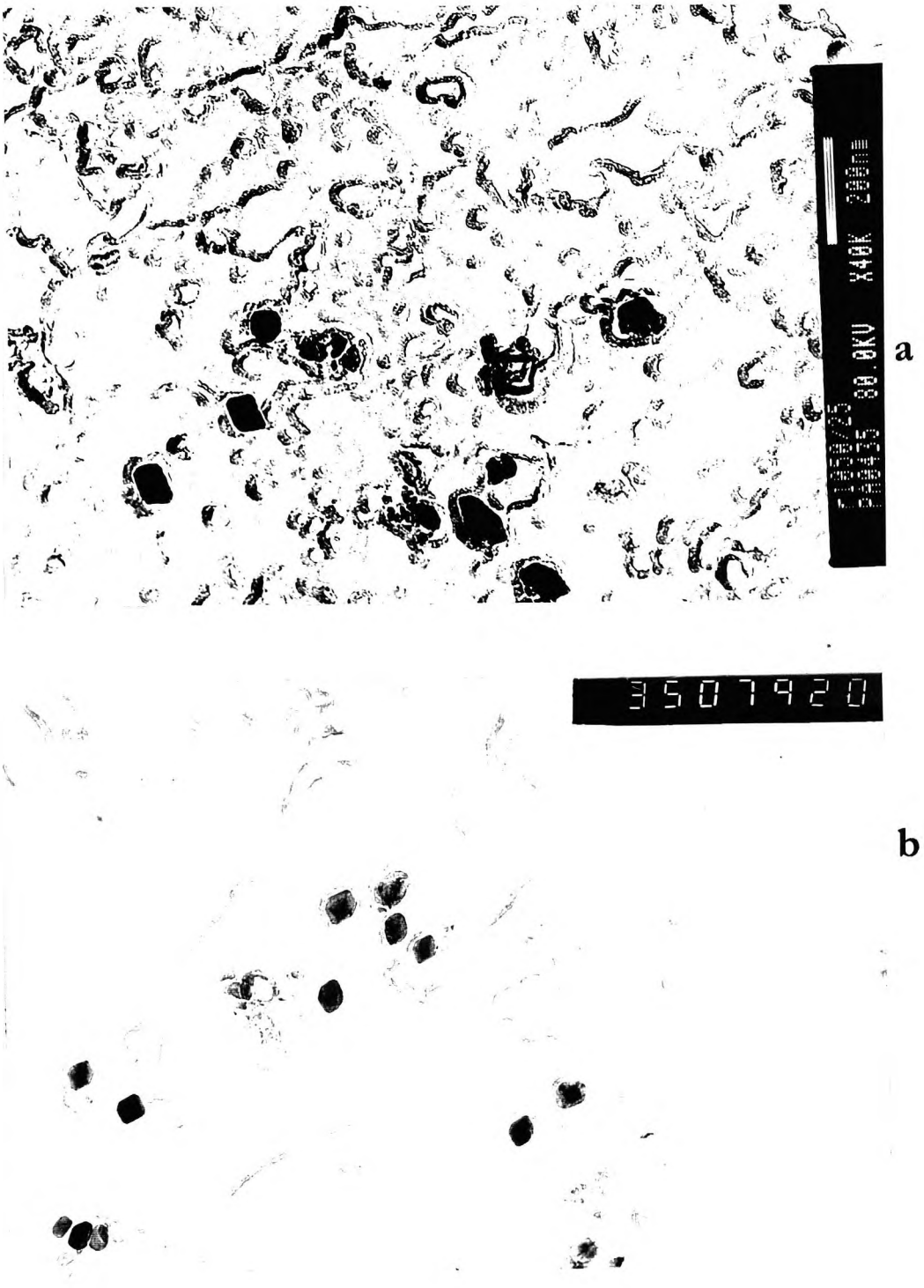


Figure 5-15: ***Nb containing steel, steel 1B, with high Ti:N ratio (8.0:1) tested at 1050 °C: (a) cooled at 25K/min (80nm)(80,000X) and (b) cooled at 100K/min, (80nm). (52,500X)***

The Nb containing steels, steels 3B and 4B (Ti:N ratio of 2.0 and 3.1 respectively) which were tested only at 100K/min had very similar hot ductility curves but the precipitate size for the higher Ti:N ratio steel (3.1) was coarser. Tests performed at higher temperatures again showed coarser precipitates in accord with the better ductility. Fig. 5-16.

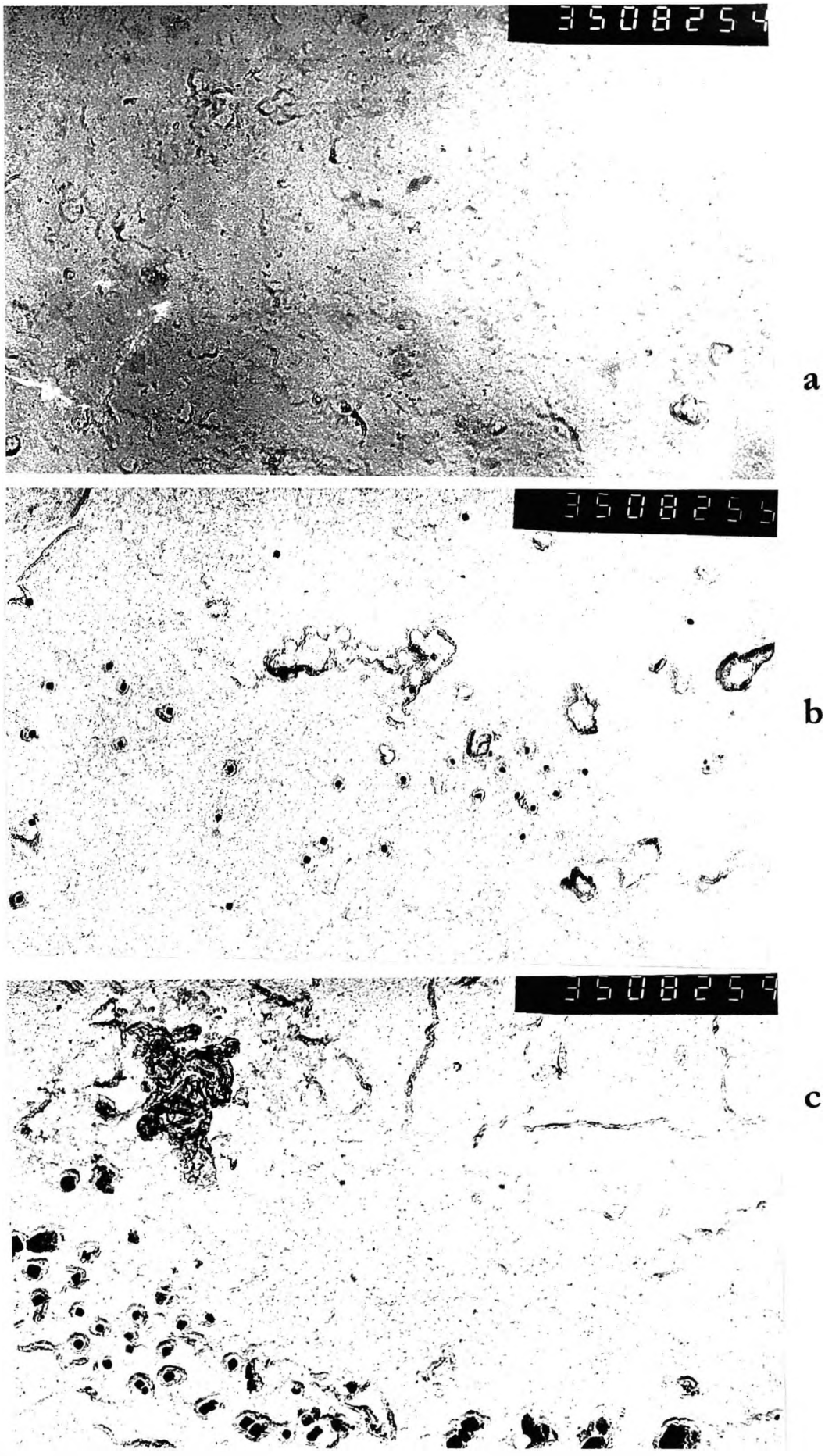


Figure 5-16: ***Nb containing steels, steels 3B and 4B with Ti:N ratios less than stoichiometric cooled at 100K/min. a) steel 3B with Ti:N ratio of 2.0:1 tested at 950℃(5nm); b) steel 4B with Ti:N ratio of 3.1:1 tested at 950℃, (18nm) and c) steel in b) tested at 1050℃, (30nm). (52,500X)***

Unfortunately, the larger particles in the cavities have not yet been analysed for Nb steels. However, from the data shown in the last chapter, they are almost certainly mainly coarse manganese sulphides. However, in the replicas analyses of the fine particles showed the presence of Al, Nb and Ti, as shown in Fig. 5-17.

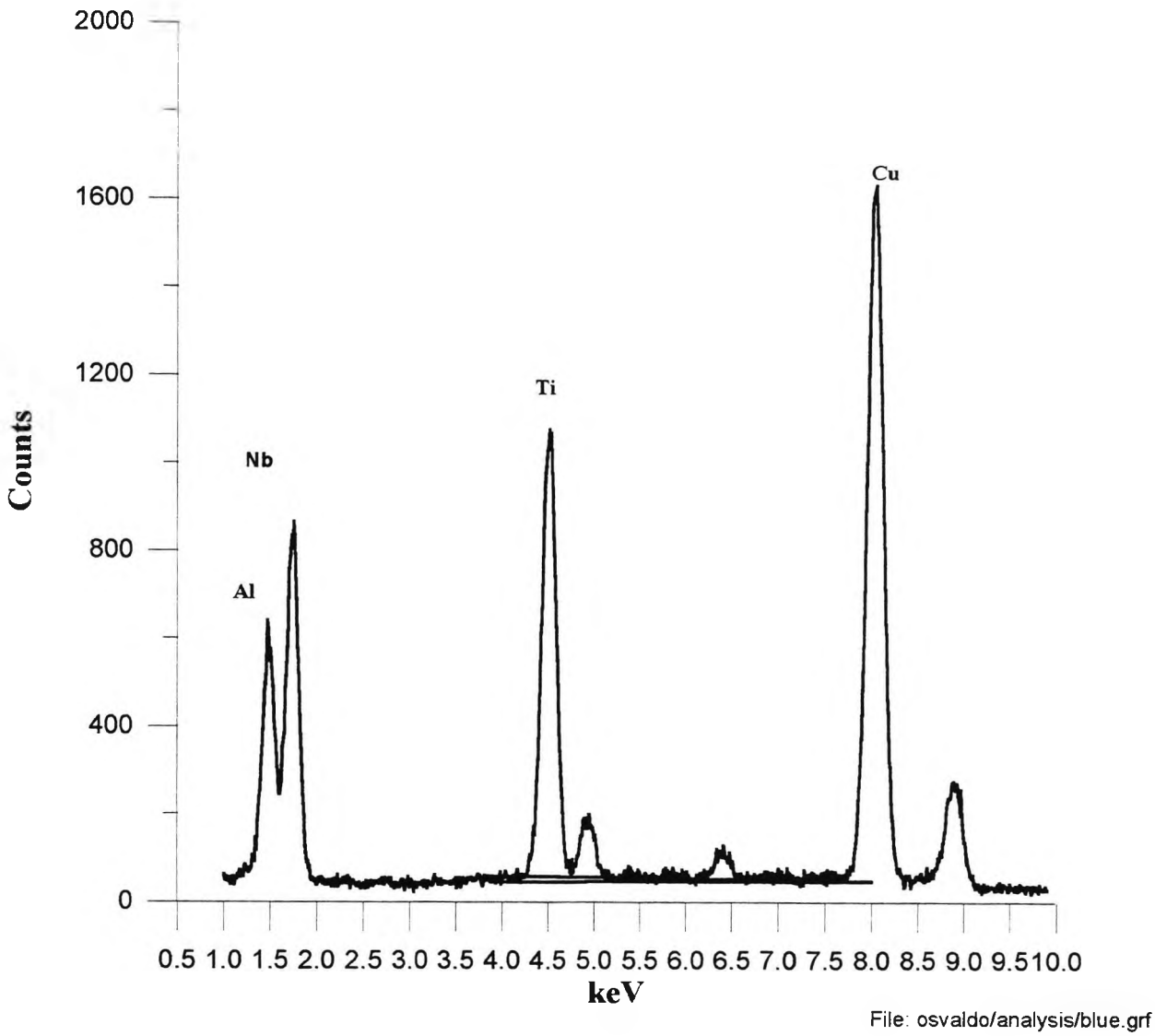


Figure 5-17 ***Edax examination of particles taken from carbon replica for C-Mn-Al-Ti-Nb steel nearly stoichiometric, steel 2B, cooled at 100K/min and tested at 950°C.***

In the previous chapter it was shown that the ductility of Ti containing Nb free steels is dependent on the cooling rate, particle size and volume fraction. Increasing the cooling rate refines the sulphides at the boundaries making it easier for cracks to join up to give intergranular failure. Fine matrix precipitation is also detrimental to ductility. A fine matrix precipitation will increase the strength of the austenite increasing the stress acting at the boundaries and the precipitates at the boundaries, (generally coarser) will help cracks to link up in the same way as do inclusions.

The effect of increasing the particle size on improving hot ductility in the temperature range 950-1000°C is shown in Fig. 5-18. This curve includes the results by the author as well as those in the European programme. The author's results are circled.

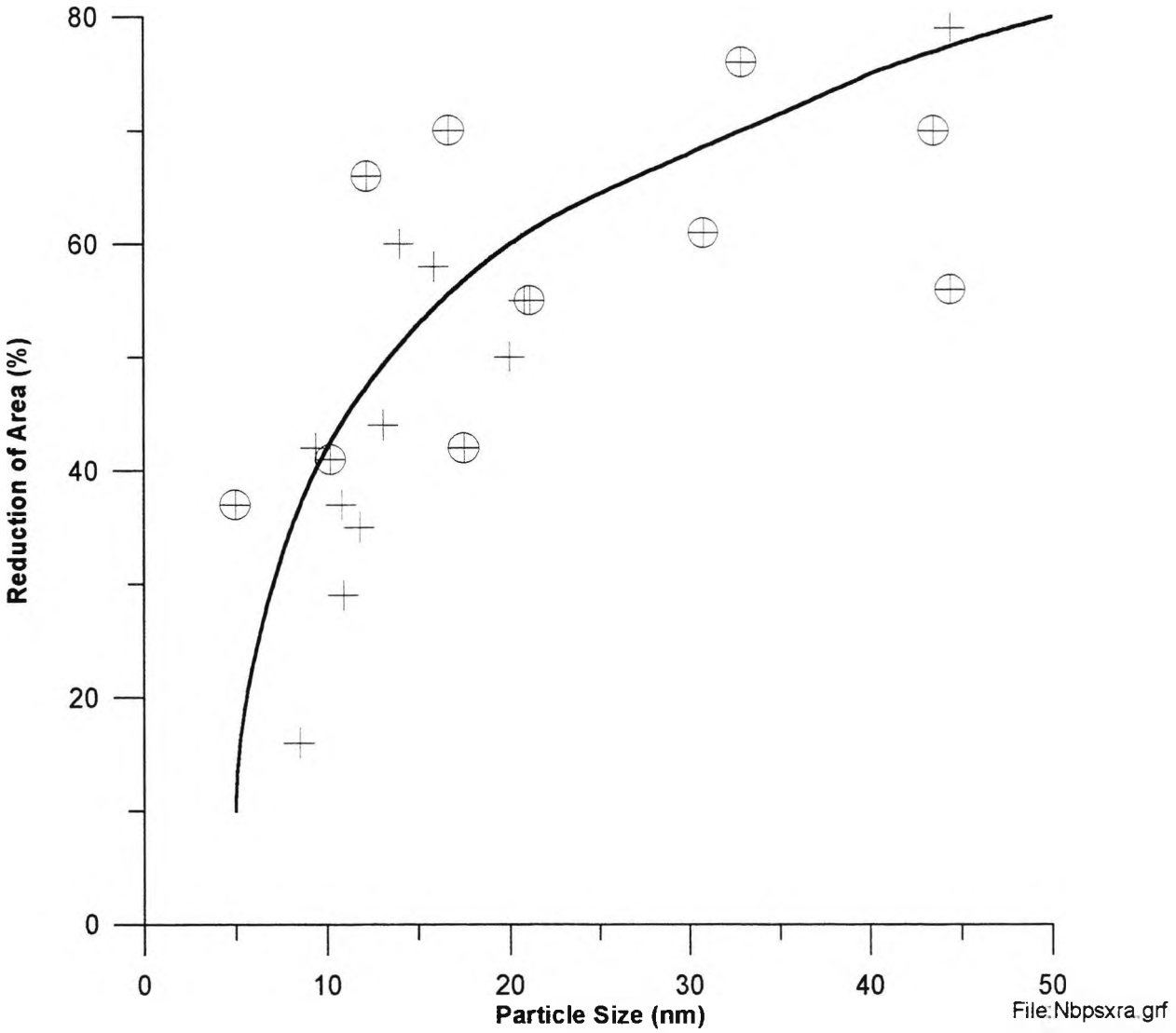


Figure 5–18. ***Influence of particle size on the Reduction of Area in the temperature range 950-1000°C***

It can be seen, although there is scatter, that to achieve >50% R of A the particle size needs to be >15 nm. This is very similar to the behaviour shown in the previous chapter.

Particle size, as well as being influenced by the cooling rate is also influenced by the Ti:N ratio, the product of the [Ti] x [N] and the test temperature.

Increasing the Ti:N ratio above that for stoichiometry coarsens the particle size as can

be seen for Figs. 5-19 and 5-20 for test temperatures of 950 and 1000°C respectively. Increasing the Ti:N ratio above that for the stoichiometric composition for TiN will increase the amount of Ti in solution and so favour the growth of the Ti containing particles. Again the author's points are circled (all at 100K/min and two at 25K/min), for both Figs. 5-19 and 5-20.

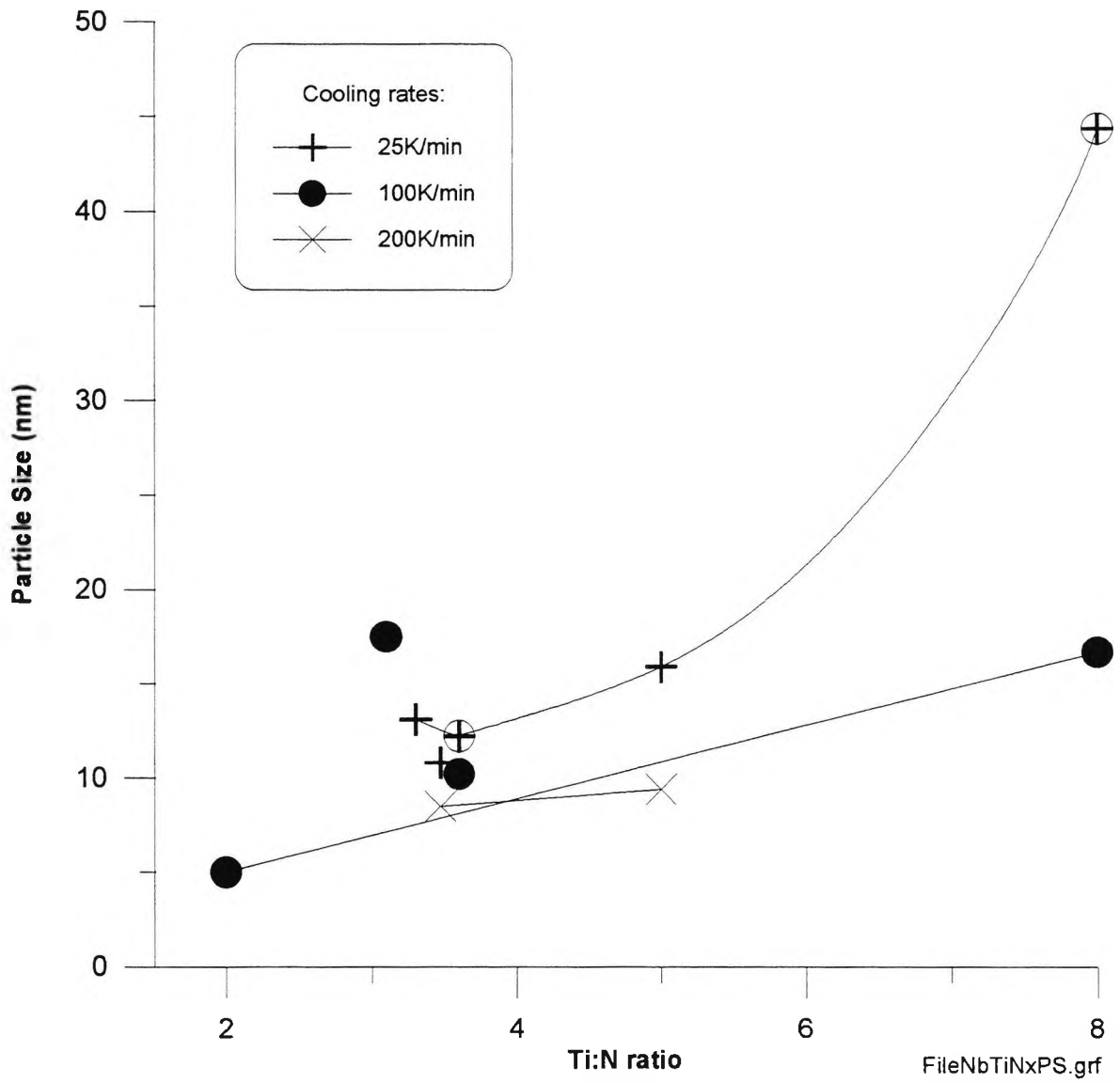


Figure 5–19: ***Influence of Ti:N ratio on particle size for samples tested at 950°C.***

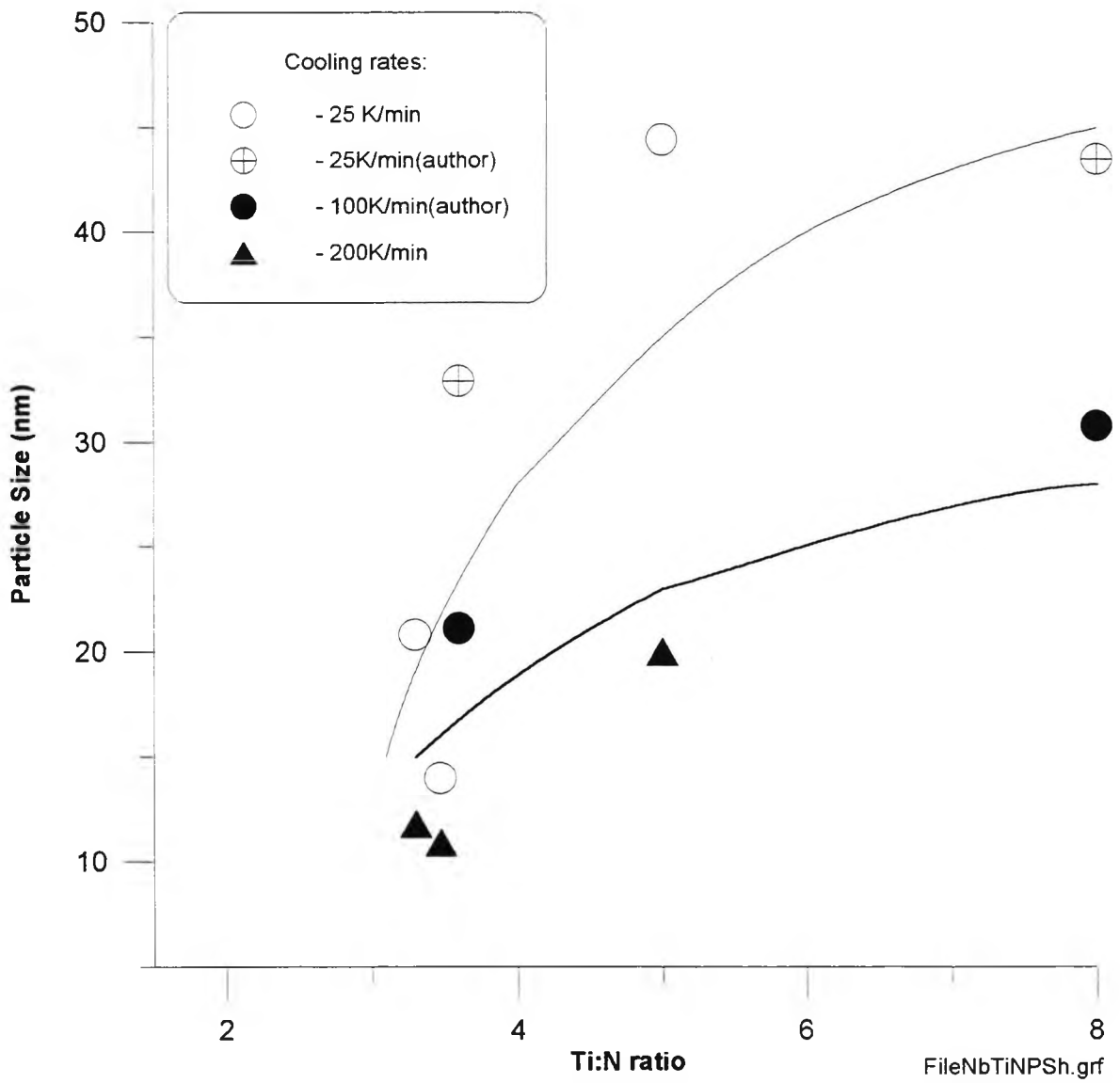


Figure 5–20 ***Influence of Ti:N ratio on particle size for samples tested at 1000°C.***

The influence of the volume fraction of Ti containing particles as measured by the product of the [Ti] x [N] is shown in Figs. 5-21 and 5-22, for the two cooling rates(author's points are circled or boxed in the legend for both graphics). The ductility can be seen to generally reduce as the product of [Ti] x[N] increases and in cases where this doesn't occur, this is due to either a high Ti:N ratio or a very high [Ti] x[N] product favouring precipitation at high temperatures.(arrowed points in the diagrams)

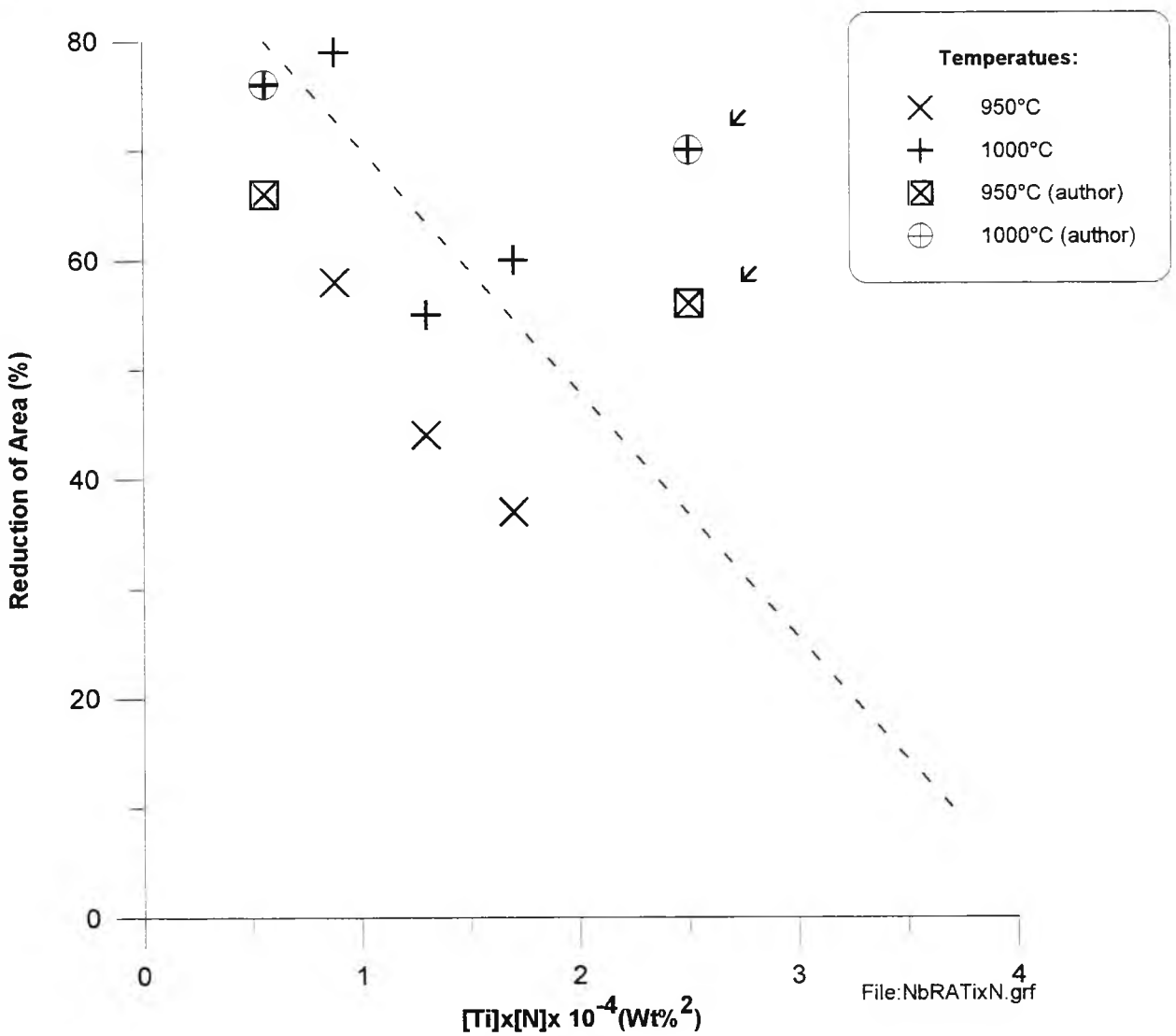


Figure 5-21: ***Influence of product of [Ti]x[N] on the R of A for a cooling rate of 25K/min.***

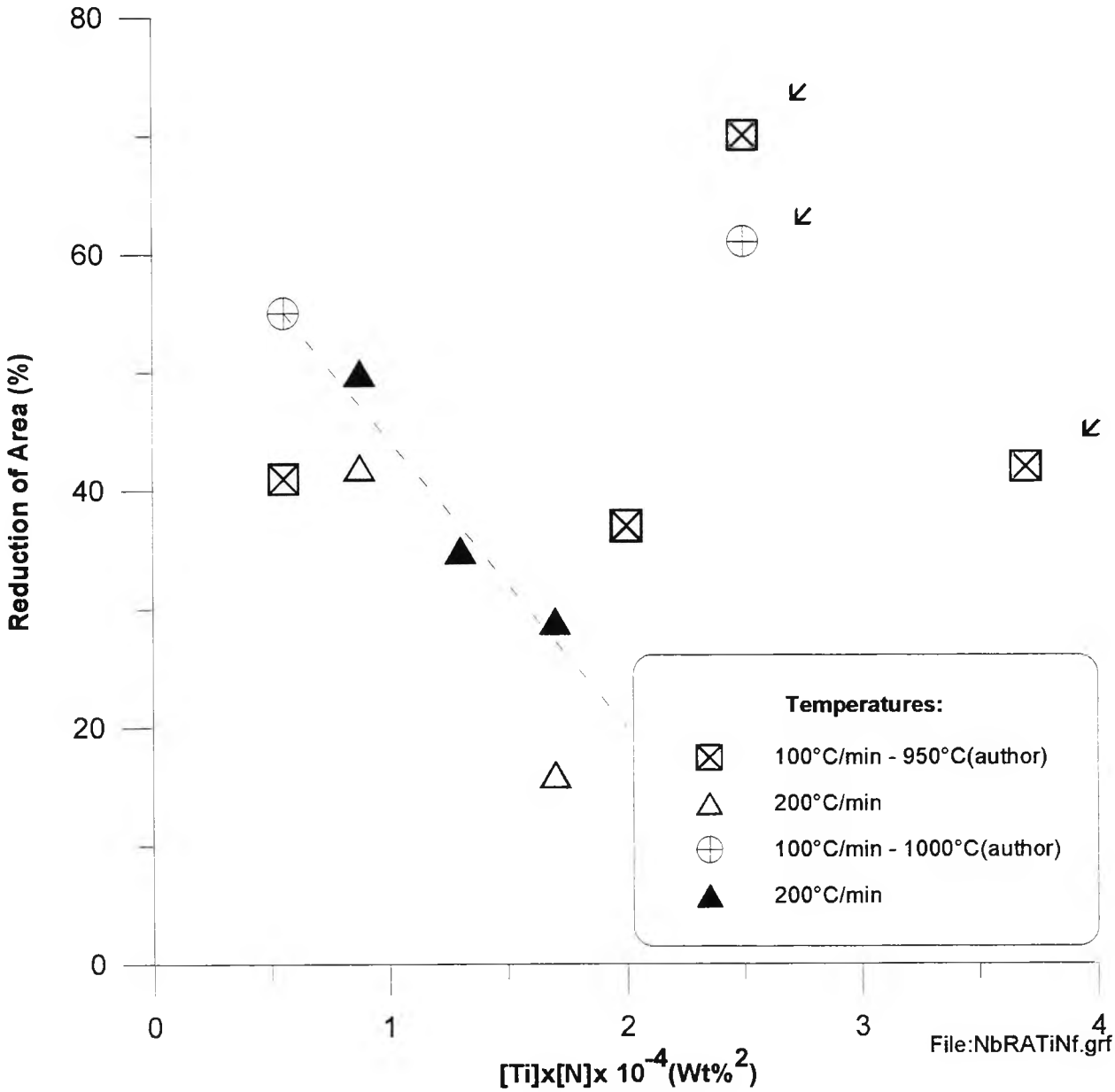


Figure 5-22: ***Influence of the product of [Ti]x[N] on the R of A for the faster cooling rates.***

Influence of composition on hot ductility of C-Mn-Nb-Al-Ti steels.

A total of seven Ti containing Nb steels have been examined and analysis of these results is complex because of the wide variation in particle size and in the [Ti] x [N] product.

Nevertheless some general comments can be made.

Steels tested at slow cooling rate - 25K/min.

It has been observed previously[Mintz et al, 1991];[Abushosha et al, 1991];[Abushosha, et al, 1998p227];[Abushosha et al, 1998p346]and [Mintz and Mohamed, 1989p2575] that in the case of Ti free, Nb containing steels, precipitation during the test is very rapid and conditions can be close to those for equilibrium. In Ti free Nb containing steels the size of the precipitate seems to play the dominant role in influencing the ductility. However in this previous work, the Nb level examined was always similar (.02%/.03%) and C levels were generally 0.1/0.2%C so that the volume fraction precipitated out would be expected to be approximately constant.

In the present instance the levels of Ti and N vary over a wide range and the hot ductility will depend on the balance between the volume fraction of microalloying precipitates (Ti,NbCN) precipitated out and the size of these particles. Increasing the volume fraction and refining the particles will cause the ductility to deteriorate. Although volume fraction can not be measured from replicas, the volume fraction precipitated

would be expected to increase as the [Ti]x[N] product increases particularly under non-equilibrium conditions.

It can be seen from Fig. 5-2 that increasing the product of [Ti]x[N] causes the ductility to deteriorate up to $1.7x10^{-4}$(curves A, C and D)(steels 2B, Euro 65 and Euro 59).

For steels 2B (A) and Euro 59 (D), the average particle size is similar(12 and 11 nm at 950°C) and the poor ductility shown in curve D will be a result of the higher volume fraction of precipitate. Steel Euro 65 (C) has a slightly coarser particle size (16nm) but has a higher volume fraction of precipitation than in the steel 2B in curve A, Fig. 5-2.

Increasing the [Ti]x[N] product further to $2.5x10^{-4}$ does not however, result in worse ductility as might be expected from the likely increase in volume fraction of Ti rich containing particles precipitated out. Instead the ductility improves and the most likely cause of this is the much coarser particle size in this steel compared to the other steels examined, (50nm compared to ~12nm). A high [Ti]x[N] product as well as increasing the volume fraction of precipitates will also encourage precipitation at high temperature and a high Ti:N ratio will increase the amount of Ti in solution so encouraging growth of the particles.

It has been observed previously that in the case of Ti free, Nb containing steels, precipitation during the tensile test is very rapid and for the low strain rate used $3x10^{-3}$ s^{-1}, conditions can be close to those for equilibrium, so that all the Nb(CN) is precipitated out[Mintz et a, 1991].

Furthermore, a high Ti:N ratio will increase the amount of Ti in solution favouring growth of the particles.

Faster cooling rate - 100/200K/min

A total of 6 steels have been included in Fig. 5-3, four from this investigation and 2 from the European Programme [Abushosha, 1996]. Analysis of these results is complex because of the wide variation in particle size and [Ti]x[N] product.

However, some general comments can be made on the basis of volume fraction and size of the precipitates.

If one takes two steels of very similar Ti:N ratio, steels 2B (curve B) and Euro 59 (curve D) in Fig. 5-3 close to the stoichiometric composition for TiN then it is interesting to note that the ductility of steel Euro 59(D) is considerably worse than 2B(B). As the particle size was similar, this arises because of the higher volume fraction of particles precipitated in the Euro 59 steel compared to steel 2B, [Ti]x[N] products of 1.7 compared to 0.6×10^{-4}, respectively. A further cause of the worse ductility given by Euro 59 steel is likely to be the faster cooling rate used in the European Programme. (200K/min compared to 100K/min to this programme) which would produce a finer sulphide distribution.

Steels shown in curves C1, C2 and C3 in Fig. 5-3 have all very similar ductilities. In terms of volume fraction precipitated one would have expected ductility to deteriorate in the order C3, C1 and C2 (product of 0.9, 2.2, and 3.7×10^{-4} respectively). However, steel 4B, shown in curve C2, because of its higher product favours precipitation at higher temperatures and hence gives rise to coarser particles than steel 3B, curve C1 (18nm compared to 5nm for C1) thus counteracting the effect of a higher volume fraction.

Again steel 3B, curve C1, might have been expected to give worse ductility than C3, steel Euro 65, ([Ti]x[N] product of $2.2x10^{-4}$ and $0.9x10^{-4}$ respectively). Examination of particle size gives a coarser particle size at the higher Ti:N (C3) ratio which again would give rise to better ductility than for the steel in curve C3. That this does not occur suggests that as noted in the previous chapter the inclusion distribution may also be influencing the hot ductility since the Euro steel was cooled at a faster cooling rate and will produce finer sulphides at γ grain boundaries.

The steel giving the best ductility steel 1B, curve A in Fig. 5-3 has the highest Ti:N ratio of 8.0:1, giving rise to a coarse particle size (17nm and 44nm for fast and slow cooling rates respectively). Thus, it is possible to qualitatively explain the results in terms of the combined influence of precipitate size and volume fraction. There is also some indication that the inclusion size and possibly volume fraction may also be important.

Ideally for good ductility, a low N level is needed in order to limit the volume fraction of particles and a high Ti level, so as to have an excess of Ti in solution to favour growth. Cooling rate should also be reduced as much as possible to ensure that the sulphides at the boundaries are coarse.

If one is working at a high N level, (electric arc furnace) then a low Ti level is likely to be preferred to limit the volume fraction of Ti containing particles that can precipitate. The high N level by giving a high product may encourage precipitation at higher temperatures resulting in coarser precipitation. This possibility needs to be examined in more detail.

Influence of cooling rate on Ti-Nb containing steels

Again, as in the previous chapter faster cooling results in a finer precipitate distribution, both the MnS inclusions and Ti containing particles having less time for growth as can be seen from the SEM photographs in Figs. 5-5 and 5-6 and the replica photography in Figs. 5-12 and 5-14 and Table 5-2. Finer particle distributions have always been found to give rise to worse ductility[Mintz et al, 1991]. The inferior ductility at faster cooling rate is hence accounted for.

It should be noted however that finer precipitation is often necessary to give the optimum mechanical properties.

At the minimum ductility temperature of 800°C, fractures were always of the microvoid coalescent type, fracture being mainly intergranular, due to joining up of the micro-voids around the inclusions and precipitates in the ferrite film surrounding the austenite grains.

Examination of SEM photographs of the fractured surface Figs. 5-5 and 5-6, at the minimum ductility temperature 800°C indicated that generally for Nb steels (Table 5-2) the ductile dimple size was similar for both fast and slow cooling also being the inclusions for the same testing temperature. R of A values were often only slightly different, suggesting that in these cases, the hot ductility was being controlled by the inclusions, similarly as already been noted in the previous chapter.

There are two factors that are likely to control the ductility of as-cast steel[Mintz et al, 1991]. The first is the volume fraction of particles present particularly those precipitated at the γ grain boundaries. The second factor is the size of particles. Very

fine particles with small interparticle spacing (<10nm) can strengthen the matrix and increase the stress concentration in the boundary region. Fine particles with small interparticle spacing at the grain boundaries also encourage cracks formed by grain boundary sliding or void formation to link up. Generally it is found that increasing the cooling rate results in finer sulphides and micro-alloying particles and this produces worse ductility[Abushosha et al, 1998p227][Abushosha et al, 1998p346]. The work in the previous chapter has shown that the dimple size is mainly controlled by the coarser particles generally sulphides but the ductility in HSLA steels is mainly controlled by the finer micro-alloying precipitates.

Influence of [Ti]x[N] product

It has been observed previously[Mintz et al 1991] that in the case of Ti free, Nb containing steels, precipitation during the test is very rapid and conditions can be close to those for equilibrium. For these Ti free, Nb containing steels, size seems to play the dominant role in influencing the ductility. However, as well as particle size being important, so is the volume fraction, and probably more so when equilibrium conditions do not exist. Unfortunately it is not possible to determine volume fraction accurately from replica examinations but the product of [Ti]x[N] should for a given cooling rate be a measure of volume fraction precipitated out.

Increasing the product of [Ti]x[N] (by allowing the Ti:N to come out at higher temperature) will not only coarsen the particles but also increase the amount of TiN particles precipitated out. These are opposing influences on hot ductility and it is not

always clear which will have the dominant effect. For this reason a regression analysis approach was favoured as for the Nb free steels in the last chapter, to sort out these opposing variables.

Regression analysis data

Although the hot ductility data can be interpreted qualitatively, sufficient data is available to make the data more quantitative using regression analysis.

As in the previous chapter the important variables likely to control ductility are as follows:

1)the product of [Ti] x[N] which probably controls the volume fraction of Ti containing particles which have precipitated out of solution.

2) the size of the particles which influences how readily cracks can link up at the grain boundary as well as the stress acting on the boundary.

3)the inclusion size and volume fraction. Although the latter effect tends to be swamped by the adverse influence of the microalloying precipitation there is no doubt that the inclusion volume fraction has a large effect on the ductility of precipitate free steels and there is also evidence that inclusions do have some effect when precipitates are present[Abushosha et al, 1998p227]. The inclusion volume fraction is likely to be controlled by the S level and their size by the cooling rate.

The variables that have been included in the regression analysis are [Ti] x [N], average particle size, S content and cooling rate, Table 5-3.

Assuming that the Ti will always combine with the available N, then any remaining N can then combine with the Al. A further variable [Al] x [N_s] was also included as in the previous chapter, where N_s is the N left over after its combination with Ti. Nb and N were also included in the analysis as it would be expected that the greater the Nb content the more Nb(CN) would be present and higher nitrogen levels would generally lead to greater precipitation.

No significant influence of the total S content, Nb level, or [Al] x [N_s] was found so these have been omitted from the analysis. Higher S levels should lead to a greater volume fraction of sulphides and worse ductility and the lack of any influence of the total S level is not understood. It is possible that the ductility is so poor in these steels due to the microalloying additions that the effect of S is being masked. Certainly, the size of the inclusions at the γ boundaries, which is related to the cooling rate, has been shown to have a pronounced influence on ductility; higher cooling rates leading to finer inclusions and worse ductility.

The regression equation obtained for these Nb and Nb Ti containing steels is as follows:

$$RofA(\%) = 15.1 + 19x\sqrt[3]{p} - 0.560[Ti]x[N]x10^5 - 0.065CR + 2326N_s \ldots (5-1)$$

where CR is the cooling rate in K/min, "p" is the particle size in nm, and N_s is the N remaining in solution after the Ti has combined with the N.

The index of determination R is 85% and the standard deviation, s=7.8.

All the variables are significant the t ratios being, 5.8,2.7, 2.8 and 2.6 for the particle size, cooling rate, [Ti] x [N], and N_s respectively. It can be seem from Fig. 5-23 there is

a good agreement between calculated and measured values.

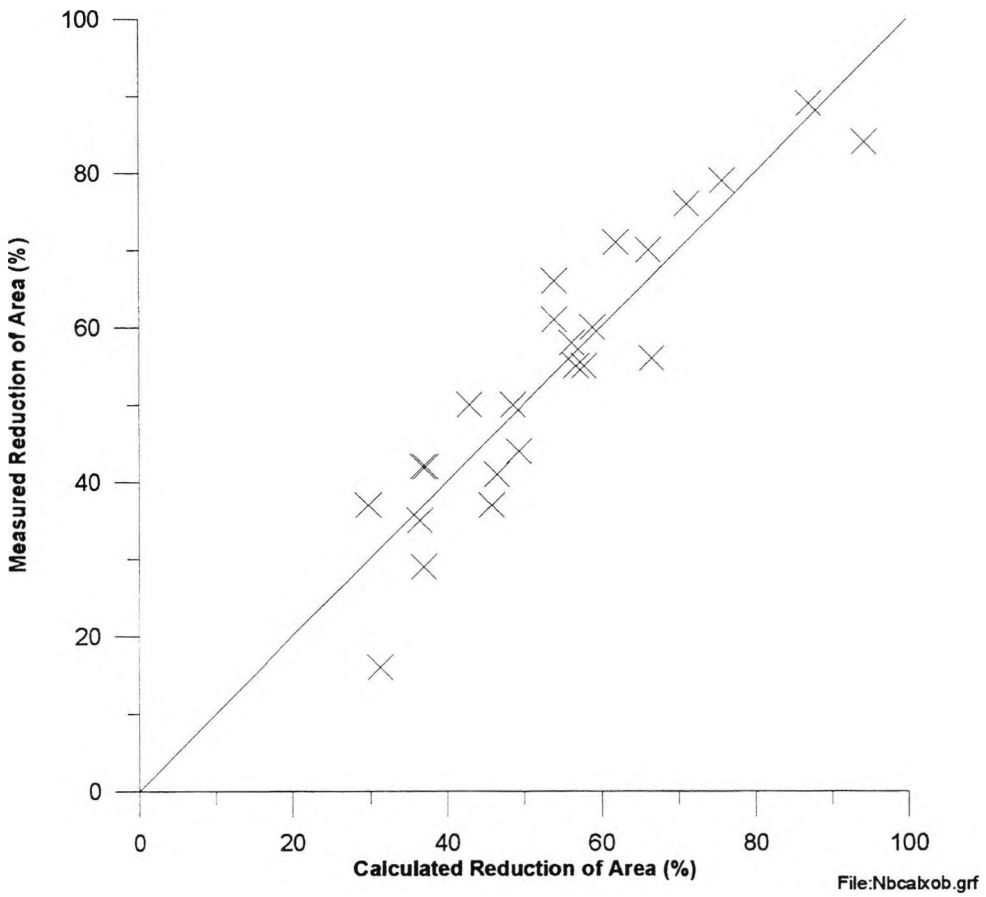


Figure 5-23: ***Comparison between R of A measured and calculated by equation 5-1.***

The regression analysis therefore confirms that increasing the [Ti]x[N] or the cooling rate will cause the ductility to decrease while coarsening the particles size will improve the ductility.

The data was obtained from a variety of steels having different residual levels and casting routes, ie vacuum and air cast and cast at British Steel or CST, Brazil. Considering that the accuracy of analysis for Ti and N were also critical and that some steels gave considerable scatter in their R of A values together with difficulties in establishing an average size for the precipitates, it can be seen from Fig. 5-24 and Table 5-2, that there is very good agreement between the observed R of A values and

those calculated from equation 5-1.

Table 5-3- ***Variables used in the regression equation.***

Steel	PS* (nm)	RofA* (%)	RofA Calc.	[Ti]x[N] x10^{-4}	Cool. Rate (K/min)	[Al]x[N] left (x10^{-4})	Sulphur %
Low Ti Ti:N 3.6;	**10.2**	**39**	**47.18**	**0.56**	**100**	**0.00**	**0.011**
Nb 0.042 Blue(2B)	**12.2**	**68**	**57.54**	**0.56**	**25**	**0.00**	**0.011**
High Ti Ti:N 8.0;	16.7	51	45.39	2.52	100	0.00	0.010
Nb 0.043 Red(1B)	44.4	59	69.29	2.52	25	0.00	0.010
Low Ti Ti:N 1.6;	**1-5**	**32**	**36.13**	**0.77**	**100**	**1.90**	**0.009**
no Nb Green(6B)	**10**	**55**	**54.45**	**0.77**	**25**	**1.90**	**0.009**
High Ti Ti:N 6.2	10-15	46	43.25	2.46	100	0.00	0.010
no Nb Black(5B)	20	55	57.47	2.46	25	0.00	0.010
High Al Ti:N 2.8	**9.2**	**35**	**44.05**	**1.60**	**100**	**0.72**	**0.013**
	13.1	**50**	**53.29**	**1.60**	**25**	**0.72**	**0.013**
Vlow Al Ti:N 3.0	8.2	49	44.49	1.22	100	0.00	0.013
	8.2	66	49.59	1.22	25	0.00	0.013
Ti:N 1.6 no NbOr(7B)	**10-25**	**49**	**55.22**	**0.62**	**100**	**0.35**	**0.010**
Ti:N 3.1 Nb Gold(4B)	10-25	42	42.48	3.74	100	0.31	0.007
Ti:N 2.0 Nb Pur(3B)	**5**	**40**	**35.41**	**2.00**	**100**	**1.44**	**0.007**
Euro 57-Al steel	7.3/77$^{@}$	97		-	200		
PS@900°C	41$^{@900}$	97		-	25		
Euro 58-Ti:N3.4	**7.5**	**23**	**23.07**	**1.68**	**200**	**0.80**	**0.004**
no Nb	**7.7**	**40**	**46.91**	**1.68**	**25**	**0.80**	**0.004**
Euro 59 - Ti:N3.5	8.5	17		1.7	200		
Nb	10.8	38		1.7	25		
Euro 61 Ti:N 3.3		**29**	**30.01**	**1.58**	**200**	**0.00**	**0.010**
high S Nb	**13.2**	**44**	**54.49**	**1.58**	**25**	**0.00**	**0.010**
Euro 65-Ti:N 5.0	9.4	45	37.01	0.88	200	0.00	0.002
+Nb	15.9	49	61.17	0.88	25	0.00	0.002
V low Al	**131$^{@800}$**	**>96**		**-**	**100**		
	122$^{@800}$	**>97**		**-**	**25**		
High Al	63$^{@800}$	85		-	100		
	94$^{@800}$	90		-	25		
Euro 60 - Nb Steel	**13.1**	**70**		**-**	**200**		
	41.6	**85**		**-**	**25**		

(*) 950°C

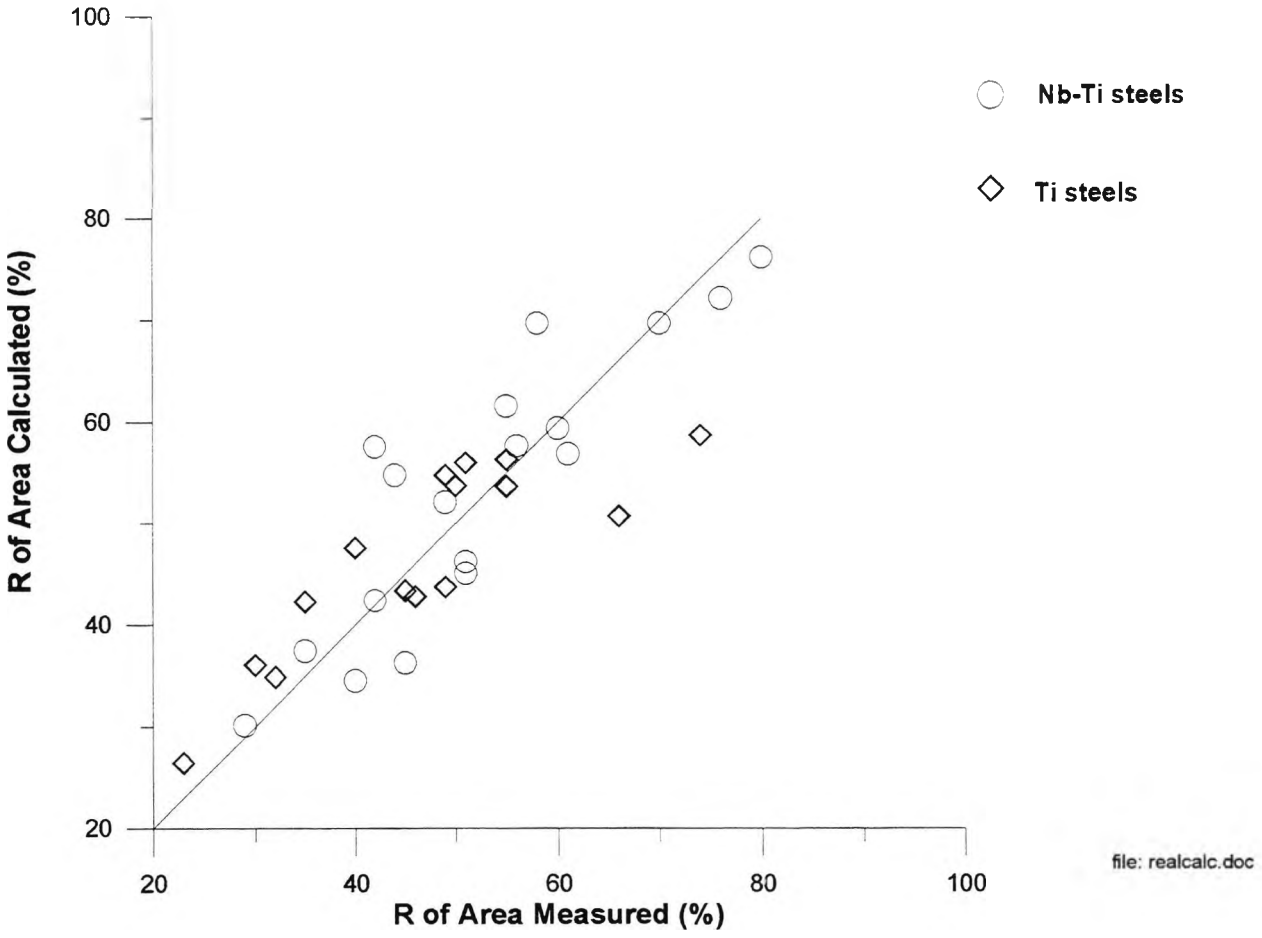


Figure 5-24 ***Reduction of area calculated against measured***

The calculated R of A values from equation 5-2 plotted against measured are given in Fig. 5-24 and agreement can be seen to be good.

It can also be seen from the Figure 5-24, that the results from Ti free and Ti containing Nb free steels fit well together. This is at first sight surprising as the addition of Nb would be expected to increase the volume fraction of precipitation and thus lead to worse ductility. However, it has been noted that adding Nb leads to a coarser precipitation and any increase in the volume fraction of precipitation is offset by this coarsening leading to similar ductilities.

If all the data is combined for both the Ti containing Nb steels of the present exercise with the previous data in the last chapter on C-Mn-Al, Ti containing steels.

The regression equation then becomes;

$RofA(\%) = 26.3 + 16.3x\sqrt[3]{p} - 0.118CR - 0.439[Ti]x[N]x10^5 \ldots (5-2)$ these being the only significant variables. The index of determination is reduced to 76% and deviation is 7.4%. The t ratios were 5.9, 5.9 and 2.6 rate and [Ti] x[N] respectively.

Commercial implications

Comparison of the hot ductility behaviour of all the steels examined.

Previous work[Mintz et al, 1991] has shown that when the tensile samples are heated to 1330°C rather than cast, increasing the Al level causes the ductility to deteriorate both for C-Mn-Al and C-Mn-Nb-Al steels. In the case of C-Mn-Al steels this was shown to be due to an increased precipitation of AlN, but this only occurred when the [Al] x [N] product was high. The more marked effect of Al found in recent work on as-cast steels compared to solution treated material, is probably due to the intense segregation of Al that is believed to occur on casting[Turkdogan, 1987]. For the Nb containing steels, the worse ductility is probably a consequence of the greater volume fraction of AlN precipitation as well as a finer precipitation of Nb(CN). Thus, for Ti free steels both Al and Nb should be restricted to the minimum required to meet the specification requirements in the final product.

The present work has shown that a Ti addition to Nb containing steels generally makes the ductility worse. This is probably related to the fine Ti particles which are stable at high temperatures causing the ductility to deteriorate. Ductility is only better with a Ti addition at the lower temperature range $\leq$ 900°C and then only in certain circumstances. The most marked improvement occurred at the slower cooling rate for the steel with the highest Ti:N ratio. This high ratio encouraged coarsening of the particles giving better ductility than obtained in the Ti free Nb containing steel at temperatures below 900°C.

At the faster cooling rate, again the steel with the highest Ti:N ratio had slightly better ductility below 900°C but the steel having the stoichiometric composition for TiN but with a very low [Ti]x[N] ratio also showed similar improved ductility.

From these findings the optimum benefit from Ti addition is to be achieved with a low N level to limit the volume fraction of nitride precipitation and a high Ti level to ensure growth. Slower cooling rates are also to be favoured.

The rather disappointing hot ductility results from the addition of Ti are likely to be due to the fine precipitation which is stable at high temperatures.

It is believed that Zr may well be a better addition to add since it is likely to produce a coarser precipitation[Baker, 1998].

1) Ti free steels

[Mintz and Arrowsmith, 1979] testing solution treated tensile specimens taken from C-Mn-Nb-Al steels have pointed out that Nb seriously impairs the hot ductility by precipitation of Nb(CN) at austenite grain boundary. Further work has shown that this

situation also occurs when the tensile specimens are as cast[Mintz and Mohamed, 1989p2575].

In accord which this behaviour, Nb steels are well known to giving rise to serious transverse cracking in continuous casting. The present work has, however, shown little effect of a Nb addition on a Ti steel with similar volume fraction. This is probably as noted due to Nb coarsening the particles (see Fig. 2-39 in chapter 2) so that even though there is an increased volume fraction of precipitate the particles are coarser.

Unfortunately it is not possible to find Nb free and Nb containing Ti steel of otherwise similar composition clearly to illustrate this conclusion. Nevertheless, it can be seen from Figs. 5-25 and 5-26 in which compositions are closest for Nb free and Nb containing steels, that there seems little difference in ductility. Similarly, when Fig. 5-24. from the regression analysis is examined, there is no indication that the Nb containing steels (circles) are any worse than the Nb free (lozenges).

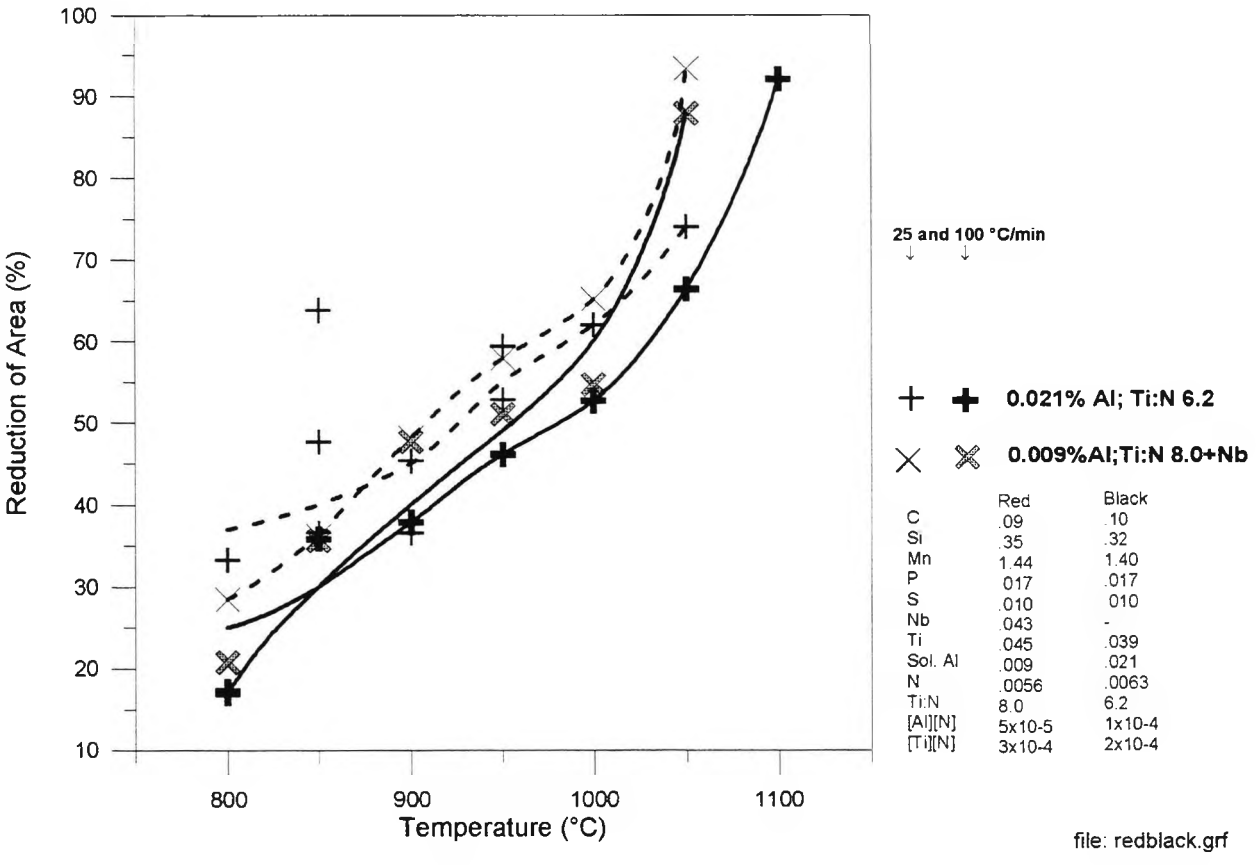


Figure 5-25 ***Reduction of area for steels with and without Nb having high Ti:N ratios cooled at 100 and 25K/min.***

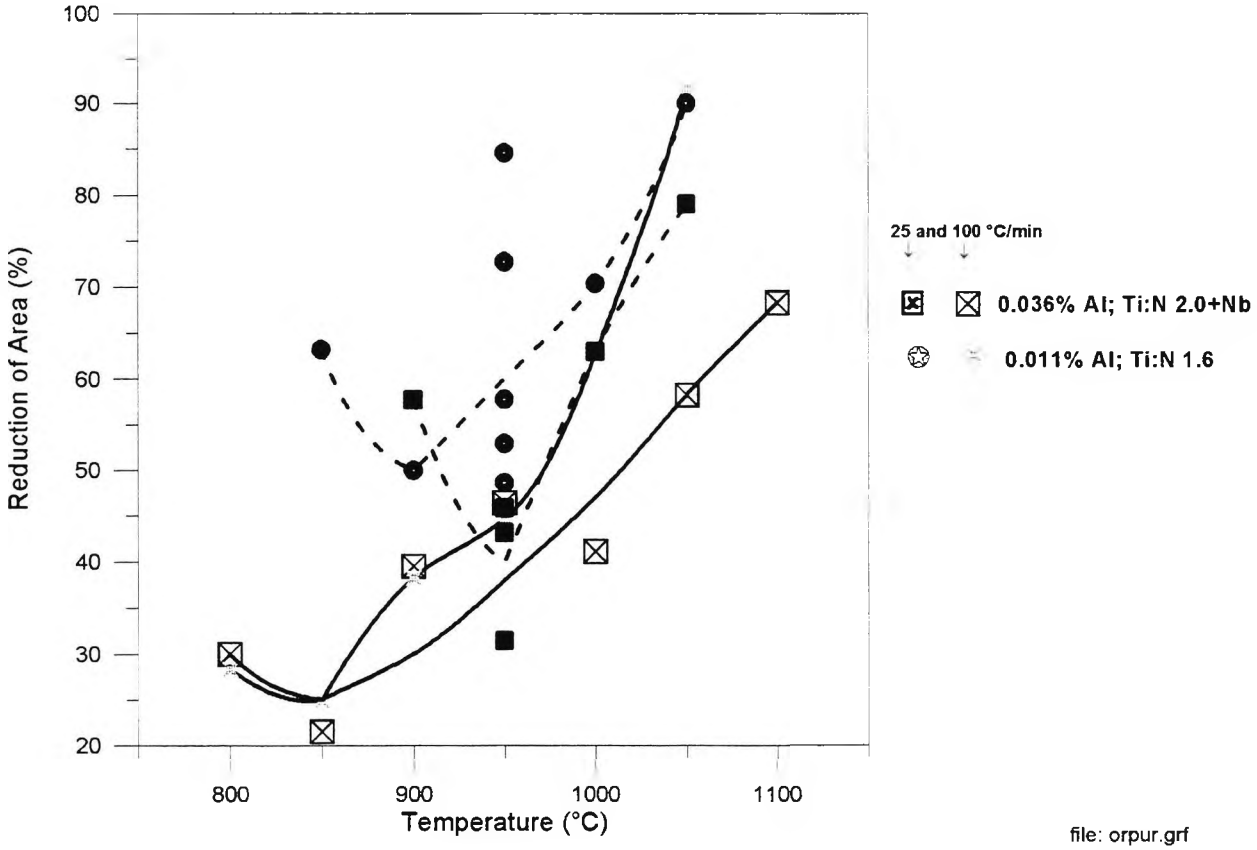


Figure 5-26 ***Reduction of area for steels with Ti:N ratio below the stoichiometric cooled at 100K/min.***

Some recent work from Finland[Karjalainen, 1998] also suggests that the addition of Nb to a Ti containing steel has little influence on hot ductility.

2) Influence of Ti on the hot ductility of Nb containing steels

It should be noted from Fig. 5-27 which gives a selection of the hot ductility curves for the same cooling rate, that adding Ti to a C-Mn-Nb-Al steel generally gives poor ductility but ductility is not made any worse with the presence of niobium. The poor ductility of Ti containing steels is due to the Ti containing precipitation being very fine and stable to high temperatures.

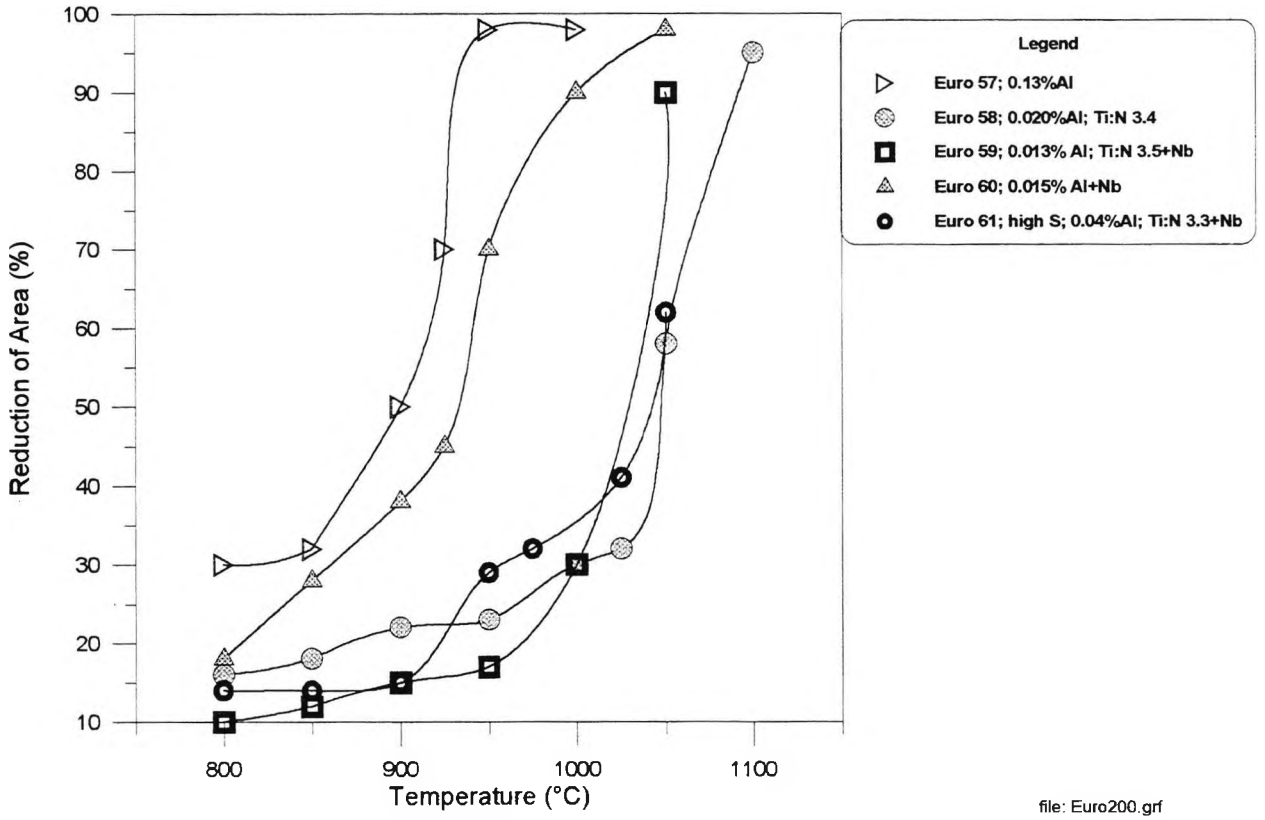


Figure 5-27: ***Hot ductility of a selection of steels examined at a cooling rate of 200K/min.***

For steels containing >0.02%Ti ductility was worse at the stoichiometric ratio of 3.4:1 and improved as the ratio increased. However, ductility of the Ti-Nb containing steels was only better than a Ti free Nb containing steel for one steel and then only at the lower temperature range <900°C. This steel had the lowest Ti level .014% Ti, and therefore lowest volume fraction of precipitates.(see Fig 5-2, curves A and E)

The most marked improvement in ductility occurred for this steel at the slower cooling rate.

At the faster cooling rate, the steel with the highest Ti:N ratio also had slightly better ductility but below 900°C the steel having the stoichiometric composition for TiN but with a very low Ti addition, steel 2B gave the best ductility.(compare curves A and B in

Fig. 5-3)

From these findings, it would appear that low Ti levels would be recommended for good ductility to limit the volume fraction of nitride precipitation.

One area which is still not clear in the present work is the influence of low Ti additions (~0.01%) on hot ductility of a high N steel. It would be expected that a low Ti level will reduce the volume fraction of precipitation and possibly with high N steels favour coarse precipitation. This possibility needs to be explored.

3)Influence of Nb on Ti containing steels

The regression analysis has shown no significant effect of a Nb addition on a Ti steel. This can be seen from examination of Fig. 5-24 which shows the ductility of Nb containing steels is no worse than the Nb free. Unfortunately, it is not possible to find hot ductility curves for Nb free and Nb containing steels of otherwise similar composition to illustrate this more clearly. However, it can be seen from Fig. 5-25 in which compositions are closest for Nb and Nb containing steels, that there is a little difference in ductility, (indeed the Nb containing steel gives slightly better ductility).

This lack of influence of Nb on hot ductility is surprising as Nb would be expected to cause additional precipitation which should impair ductility. The reason for this behaviour is that Nb coarsens the particles, so that even though there is an increased volume fraction of precipitation, this is compensated for by the coarser particle distribution. Examination of Table 5-2 which includes the full composition for the two steels in Fig. 5-24 as well as the particle size measurements for temperatures of 950 and 1000°C, clearly shows that the Nb containing steel has the coarser precipitation.

These observations are in accord with the work of Subramanian et al [Subramanian et al, 1985] who have calculated from thermodynamic data, Fig. 2-39 in chapter 2, the temperature at which Nb(CN) precipitation first occurs in a Ti containing steel. It can be seen that increasing the Nb level causes precipitation to first occur at higher temperatures. They have also examined precipitation in a continuously cast slab having a very high Nb level (0.04% Nb; 0.08%N and 0.011%Ti). The precipitate size of the Ti containing particles were from 30 to 50 nm for the cuboidal particles. From the present work the size of these particles would be expected to give good ductility. In contrast, Roberts [Roberts, 1984] found in a continuously cast slab of a V containing Nb free steel having similar high N low Ti levels very fine TiN particles, (8nm) indicating that they had precipitated out at low temperature in accord with the predicted behavicur noted in Fig. 5-24. Thus it would be expected that the particles would be coarser in the Ti, Nb containing steel than in the Nb free Ti containing steels. Hence, it would appear that the addition on Nb to a Ti containing steel will not result in worse ductility even though the volume fraction of precipitation will be increased. Recent hot ductility work by[Karjalainen et al, 1998] have also found that in Ti containing steels the addition of Nb does not influence ductility.

4) Influence of Al level

As with Nb, regression analysis indicated that raising the soluble Al level did not influence the ductility. In the present work it is difficult to select steels of exact composition to illustrate this. The closest composition are steels Euro 61 and Euro 59 which have otherwise similar compositions but steel Euro 61 has the higher Al level. The hot ductility curves are given in Fig. 5-27. Examination of Table 5-2 shows that the average particle size is coarser in the higher Al containing steel. Kirkwood [Kirkwood et

al 1987] has also found that the addition of Al results in coarser TiN particles. Loberg et al[Loberg et al, 1984] has suggested that Al associates with the N and although not producing a precipitate, this effectively increases the amount of Ti in solution encouraging growth. Certainly it has been found in previous work that Nb suppresses the precipitation of AlN[Mintz et al 1991].

5) Influence of N level

Although increasing the N level caused ductility to deteriorate as more Ti containing nitride precipitation occurred, once the N level was sufficient to combine with all the Ti present, further increase resulted in some improvement in ductility.(see regression equation). This may be related to the increase in N level favouring precipitation at higher temperatures and so giving coarser precipitates, particularly if AlN precipitation is delayed.

6) Influence of cooling rate

As in the previous chapter and all previous work[Abushosha et al, 1998p227; Abushosha et al, 1998p346], increasing the cooling rate results in a deterioration in ductility although not as marked as with the simpler C-Mn-Al-Ti steels.(multiplying factor in the regression analysis for the cooling rate is about half). Thus, the faster cooling rate pertaining to thin slab casting will cause the ductility to decrease. However, this deterioration in ductility is to some degree compensated for by the higher strain rate pertaining to thin slab casting compared to conventional, so that there may be no overall change in ductility. However, as thin slabs are directly rolled there is no opportunity for surface inspection and ductility therefore has to be better than in conventional continuous casting.

7) Influence of S

Reduction of sulphur is a very expensive commercially. However, surprisingly the present work based on limited data has not shown any marked influence of S on the hot ductility behaviour of the Nb, Ti containing steels. However, this may be related to the poor ductility shown by these steels even at the low S level. Since data is limited, no alterations to the low S practice currently used for the more expensive grades of steel would be recommended.

8) Influence of test temperature

Precipitation was always found to be coarser at the higher test temperatures in accord with better ductility, (see Table 5-2 in which the average particle size at 950°C and 1000°C can be compared). Thus, the higher the straightening temperature, the better will be the ductility and the less likely slabs will suffer from transverse cracking. For thin slab casting in which the heat is conserved to allow direct rolling, the straightening temperatures are likely to be higher than in conventional casting and this should benefit ductility.

CONCLUSIONS

1)Increasing the cooling rate leads to worse ductility independent of the steel examined. This deterioration in ductility on faster cooling could be ascribed to the formation of finer precipitation and/or a finer MnS inclusion distribution. A finer distribution of particles at the grain boundaries makes it easier for cracks to enlarge and link up to give intergranular failure. Nevertheless, this effect seems to be minimised for Nb steels at high Ti:N ratios.

2) The deterioration in ductility on fast cooling rate could be ascribed to the formation of finer MnS inclusions and or finer precipitation.

3) Ti additions of 0.02-0.045% to a Nb containing steel generally lead to worse ductility particularly at the stoichiometric ratio for TiN and at temperatures >900°C.

4) Increasing the [Ti] x [N] product which to a large degree controls the volume fraction of Ti rich particles able to precipitate out of solution, leads to worse ductility.

5) Coarser precipitation, generally leads to better ductility and this can be achieved by decreasing the cooling rate, increasing the Ti:N ratio above stoichiometry which will increase the amount of Ti in solution and favour growth, and increasing the [Ti] x [N] product which favours precipitation at higher temperatures. Whereas the first two methods are likely to improve ductility, care has to be taken with the third method as this may lead to an increased volume fraction as well.

6) It is recommended, commercially for low N steels (0.005%), that the Ti level should be low and the cooling rate as slow as possible to avoid cracking. Where electric arc steel is being used and N levels are high, the best ductility may be forthcoming again from a low Ti addition to limit the volume fraction of Ti rich particles that are formed. The high N level may by ensuring a high product of [Ti] x [N] encourage precipitation at higher temperatures and hence give coarser particles and better ductility, but further work is required to examine this possibility.

7) Precipitation can be coarsened by decreasing the cooling rate, increasing the Ti:N ratio and increasing the [Ti]x[N] which favours precipitation at higher temperatures. However, the latter method also leads to an increased volume fraction of particles.

8) A regression equation has been developed for Ti containing steels relating the R of A value to the particle size, the [Ti]x[N] and the cooling rate these being the major variables affecting the hot ductility measured by the R of A.

9) Raising the test temperature invariably results in a coarser precipitation and better ductility. For this type of steel, the straightening temperature should be as high as possible.

10) Increasing the S level in the range 0.004 to 0.019% had very little influence on the hot ductility. Further work extending the range of S levels is required to examine this more closely.

11) It is recommended commercially that the N level be kept low eg 0.003% N and the Ti:N ratio to be high $\geq$ 5:1 and cooling rate to be as low as possible.

12) Whereas the addition of both Nb and Al are detrimental to the hot ductility of Ti free steels, this is not the case for Ti containing steels. In the case of adding Nb to a Ti steel this arises because the deterioration in ductility from the higher precipitate volume fraction is balanced by Nb causing the precipitation to occur at higher temperatures and hence be coarser. The reason for the insensitivity of Al additions to the ductility of these Ti, Nb containing steels is not as yet clear.

Chapter 6 -SUGGESTIONS FOR FUTURE WORK AND ACKNOWLEDGEMENTS

FUTURE WORKS

Many important results concerning the role of microstructure and its relationship to the hot ductility behaviour have been presented in the present work, many of them are of great interest and immediate commercial application. However, as with any scientific work, many other questions have also been introduced encouraging a further and deeper scientific investigation.

Some future work is suggested and may well form part of a continued programme, to be carried out between CST, UFES and Brazil and or City University. The proposed future work is, as follows:

1- Investigation of a different range of Ti:N ratios and Al levels. So far, low N steels have been examined.

2- Further work needs to be carried out into the influence of Al and Nb on Ti containing steels. Al and Nb levels covered should be 0.02, 0.04 and 0.06% with Ti:N ratio above and below stoichiometric giving special attention to low Ti (~0.01%) and high N, in order to simulate the electric arc conditions and to improve the data bank for the regression equation.

3- A titanium addition has not generally been found to be a good addition to make to improve ductility particularly for the faster cooling conditions applicable to thin slab casting. The fine precipitation of TiN is stable up to high temperatures and keeps the ductility poor at the higher temperature end of the trough. For thin slab casting in which straightening temperatures are higher than conventional ductility is likely to be poor with a Ti addition. ZrN goes back into solution much more readily, and so a zirconium addition is likely to give better ductility than Ti. The present exercise should be repeated using Zr.

Zr has a higher atomic weight than Ti (almost twice) and so greater amounts will be needed for stoichiometry.

4- Investigation of the influence of the commercial continuous cooling pattern used by CST on the hot ductility of these Ti containing steels and comparing this with the simple cooling pattern used in the present exercise.

5- Examining the hot ductility in conditions more comparable with thin slab casting practice, i.e. higher strain rate and cooling rates. The influence of predeformation before testing should also be examined;

6- After having a good data bank, writing a first version of a computer software programme, using a variation of the proposed equation, that could predict the hot ductility by computing the casting conditions and composition of any new HSLA steel.

Some richness are in Banks, Thanks CST;

Other richness are in brains, Thank you Professor Barrie Mintz;

And other richness are in souls, Thank you very much my lovely wife Eliane.

To my parents, my father, Guilherme Comineli and my mother Maria Barlati Comineli for the love and support they have given me all my life.

The author wish to express his deepest gratitude to many people and institution. Their contributions and support were of immense value during this work.

Their names are as follows:

On the personal side

Mrs Eliane Ferreira Comineli, my wife for her hard work, understanding and encouragement;

Mr. Milton Clovis Comineli, my brother Cosi, for sponsoring the beginning of my career;

Mrs Solange Maria Comineli Beltrame and doctor Jose Basilio Beltrame, my sister and brother in law, for helping my mother kindly look after my father. This has enabled me to concentrate on my work without worry;

Mrs Vera Lucia Fiorucci, my sister Tatinha, for looking after my father and my business in Brazil, better than I would have done myself.

On the professional side

Professor A. R. David Thorley, head of department for the technical-administrative support;

Mrs Barbara Clarke, for secretarial support and for organising my wedding party;

Professor Barrie Mintz, for the high quality scientific supervision as well as for his personal advice and friendship.

Conselho Nacional de Pesquisas, CNPq for providing the grants and financial support;

Dr. David Crowther, from British Steel, for supplying the analysis and Ar_3 measurements;

Mr. Geraldo Cardoso for co-ordinating the programme or work and organising the supply of samples from Brazil;

Mrs Jenny Mintz, for the patient support in helping me which the English language;

Dr. Maria Angela Loyola de Oliveira, for the UFES and CNPq contacts;

Dr. Rouckaya Abushosha for her immense help in teaching me how to use all the scientific equipment;

Mr Roy Vipond, for his helpful teaching and advice;

Mr Tom Rose for support with the laboratory facilities;

and last but not least my office friends Andrew Cowley, Charles Spradbery, Quan Long and Seyed Hamidreza Eslimy-Isfahany for providing such a friendly working atmosphere.

To all of you, my deepest thanks.

Thank you all very much!!!

I wish also to express my regrets for any inconvenience that I have inadvertently caused to anyone.

Chapter 7 - REFERENCES AND SCIENTIFIC PRODUCTION

REFERENCES

Abken, M. G.; Weiss, I. and Jonas, J. J.: *Acta Metall.*, 1981,**29**,111;

Abushosha, R. European Contract P3454 "Thin slab casting", 1996.

Abushosha, R. European Contract "Thin Slab Casting" 2nd report.

Abushosha, R., European programme report, 1997.

Abushosha, R., Ayyad, S. and Mintz, B.: Mater. Sci. and Technol., 1998,14,227.

Abushosha, R., Ayyad, S. and Mintz, B.: Mater. Sci. and Technol. 1998, 14,346

Abushosha, R., Comineli, O. G. and Mintz, B. accepted for publ. Mater. Sci. and Technol. 1998.

Abushosha, R.; Vipond, R. and Mintz, B: *Materials Sci. Technol.*, 1991,**7**,613;

Abushosha, R., Vipond, R. and Mintz, B.: Mater. Sci. and Technol. 1991, 7,1101

Algoma steel co. Canada. Internet.

Amin, R. K. and Pickering, F. B.: in "Thermomechanical processing of microalloyed austenite", 377;1982, Warrendale, PA, Metallurgical Society of AIME;

Anelli, E., Mollo, A. and Oulhadj, A., 34th Mech. Working and Steel Processing Conf. Proc, Montreal, Canada, ISS-AIME, vol. 30, 1993,399-407;

Blake, N. W.: "Hot ductility testing of simulation castings", Rep. MRL/AMP/87/5, BHP, Melbourne, July 1987;

Baker, N, private communication, Strathclyde University

Bernard, G : Rev. Metall., 1980, 77, 307

Bernard, G.; Birat, J. P.; Conseil, B. and Humbert, C.: *Rev. Metall.*, 1978,**75**,467;

Bywater, K. A. and Gladman, T.: *Met. Technol.*, 1976,**3**,358;

Cardoso, G. I. S. L., Abushosha, R. and Mintz, B.. Proceedings of the 4th Annual Congress of the ABM, Sao Paulo, 1994, vol5 pp 295-308.

Cardoso, G. I. S. L. and Yue, S: *Proc. AIME Mech. Work. Steel Process. Conf.*, 1989,**31**,585;

Cardoso, G. I. S. L., Mintz, B. and Yue, S.: Ironmaking and Steelmaking, 1995,**22**, n5, pp. 365;

Carlsson, G.: *Jerkontorets Ann.*, 1964, **148**, 152;

Cepeda, L. E.; Rodriguez-Ibabe, J. M.; Urcola, J. J. and Fuentes, M.: *Mater. Sci. and Tech.*, 1989, **5**, 1191;

Chang, H. C., and Grant, N. J.: *Trans. AIME*, 1956,**206**, 544;

Chamont, B., Chemelle, P. and Biausser, H.: in Proc. Conf. on "Physical Simulation Techniques for Welding, Hot forming and Continuous Casting", 1988, MTL, 92-43 TR, CANMET, Ottawa, II-48

Chen, Z., Loretto, M. H., Cochrane, R. C., Mater. Sci. and Technol., 1987,3,836

Coleman, T. H. and Wilcox, J. R.: *Mater. Sci. Technol.*, 1985. **1,** 80;

Cowley, A., Abushosha, R. and Mintz, B.: Mater. Sci. and Technol., nov. 1998, vol4.

Crowther, D. N. and Mintz, B.: *Mater. Sci. and Technol.*, 1986,**2**,671;

Crowther, D. N. and Mintz, B.: *Mater. Sci. and Technol.*, 1986,**2**,951;

Crowther, D. N. and Mintz, B.: *Mater. Sci. and Technol.*, 1986,**2**,1099;

Crowther, D.N., Green, M.J.W., and Mitchell, P.S.: Conf. on "Microalloying for the 21st century" San Sebastian, Spain, Sept 1998.

Crowther, D.N. and Morrison W.B.: in "Proc. of Titanium Technology in Microalloyed steels" Univ. of Sheffield Conf. Institute of Materials, Ed. T. N. Baker, Dec. 1994,p44

Crowther, D. N.; Mohamed, Z. and Mintz, B: *Trans. Iron Steel Inst. Jpn.*, 1987,**27,**366;

Crowther, D. N. and Mintz, B.: in "Effects and control of inclusions and residuals in steels", III-83; 1986, Toronto, Canadian Institute of Mining and Metallurgy;

Crowther, D. N.; Mohamed, Z. and Mintz, B: *Metall. Trans.*, 1987,**18A,**1929;

Edwards, R. H.; Barbaro, F. J. and Gunn, K., W.: *Metal. Forum,* 1982,**5**,119;

Essadiqi, E. and Jonas, J. J.: *Metall. Trans.*, 1988,**19A,**417;

Evans, H. E.: *Met. Sci. J.*,1969,**3**,33;

Evans, H. E.: "Creep fracture"; 1984, Oxford, Pergamon Press;

Ericson, L: *Scand. J. Metall.*, 1977,**6**,116;

Fu, J.Y.; Garcia, C. I.; Pytel, S. and Ardo, A. J.: in "Processing, microstructure and properties of HSLA Steels" 27; 1988, Warrendale, PA, Metallurgical Society of AIME;

Fleming, G. Hofmann, F., Rohde, W. and Rosenthal, D.: Metallurgical Plant and Technology Int. 1993,2,pp 84-96.

Funnell, G. D.: in "Hot working and forming processes", (ed. C. M. Sellars and G. J. Davies), 104;1979, London, The Metals Society;

Funnell, G. D. and Davies, R. J.: *Met. Technol.*, 1978,**5**,150;

Gifkins, R. G.: *Int. Acta Metall.*, 1956,**4**,98;

Gittins, A.: *Int. Met. Rev.*, 1977,**22**,213;

Gittins, A. and McG. Tegart, W. J.: Met. Forum, 1981,**4**,57;

Gray, R. J., Perkins A. and Walker, B.: in "Solidification and casting of metals", 300;1979, London, The Metals Society.

Grant, N. J. and Mullendore, A. W.: "Deformation and fracture the elevated temperatures"; 1965, Cambridge, MA, MIT Press;

Guillet, A.: PhD thesis, McGill University, 1989;

Hammer, R. and Simon, R. W.: in "HSLA steels technology and applications", 359; 1984, Philadelphia, PA, American Society for Metals;

Hannerz, N. E.: *Trans. Iron Steel Inst. Jpn,* 1985,**25**,149;

Harada, S.; Tanaka, S.; Misumi, H.; Mizoguchi, S. and Horiguchi, H.: *Trans. Iron Steel Inst. Jpn.*, 1990,**30**,310;

Hasebe, S.: *Tetsu-to-Hagané(Overseas)*,1963,**3**,200;

Hater, H., Klages, R., Redenz, B. and Taffner, K. : Open Hearth Proc. AIME, 1973,202

Hubert, R. A. and Standaert, C.: in "International Conference on Thermomechanical Processing and other Materials, Thermec 97",459;1997, Wollongong Australia, ed. The Minerals and Materials Society, Warrendale PA 1997;

Irving, W. R. and Perkins. A.: Ironmaking and Stellmaking, 1977,**4**,292;

Karjalainen, L. P.; Kinnunen, H. and Porter, D.. "Hot ductility of Certain Microalloyed steels under simulated continuous casting conditions" Finland paper to be given at San Sebastian's Conference, Spain, 1998

Keene, D. N.; Sellars, C. M. and McG. Tegart, W. J.: in "Deformation under hot working conditions", 21;1968, London, The Iron and Steel Institute;

Kiessling, R: "Non-metallic inclusions in steel", Pt II; 1966, London, The Iron and Steel Institute;

Kirkwood, P. I.: in Proc. Int. Symp. on "Welding Metallurgy of Structural Steels", TMS Annual Meeting, Denvar, Co, Feb. 1987

Kutumba Rao, V.; Taplin, D. M. R. and Ramo Rao, P.: *Metall. Trans.*, 1975,**6A**,77-86;

Lankford, W.T.: *Metall. Trans.,* 1972, **3,**1331;

le Bon, A.; Rofers-Vernis, J. and Rossard, C.: *Met. Sci. J.*,1975,**9**,36;

Leslie, W. C.; Rickett, R. L.; Dotson, C. L. and Walton, C.S.: *Trans. ASM*, 1954,**46**,1470;

Linaza, M. A., Romero, J. L., Rodriguez Ibabe, J. M. and Urcola, J.J.: 36th Mech. Working and Steel Processing Conf. 1995, 483-494

Loberg, B., Nordgren, A., Strid, J. and Easterling, K. E.: Metall. Trans. 1984,15A,33

Luton, M. J. and Sellars, C. M.: *Acta Metall.*, 1969,**17**,1033;

Maehara, Y. and Ohmori: *Mater. Sci. Eng.,* 1984,**62**, 109;

Maehara, Y., Nakay, K., Yasumoto, K. and Hishima, T.: Trans. Iron and Steel Inst. Jpn. 1988,**28**,1021;

Maehara, Y.; Matsumoto, K.; Sugitani, Y. and Gunji, K.: *Trans. Iron Steel Inst. Jpn.* 1985,**25**,1045;

Maehara, Y.; Yasumoto, K.; Tomono, H.; Nagamichi, T. and Ohmori, Y.: *Mater. Sci. Technol.*, 1990,**6**,793;

Maehara, Y.; Yasumoto, K.; Tomono, H. and Ohmori, Y.: *Trans. Iron Steel Inst. Jpn,* 1987, **27**, 222;

Maehara, Y.; Tomono, H. and Yasumoto, K.: *Trans. Iron Steel Inst. Jpn,* 1987,**27**,103;

Maehara, Y.; Tomono, H. and Yasumoto, K.: *Trans. Iron Steel Inst. Jpn,* 1987, **27**,499;

Maki, T.; Nagamichi, T.; Be, N. and Tamura, I.: *Tetsu-to Hagané (J. Iron Steel Inst. Jpn.),* 1985,**71**,1367;

McQueen, H. J. and Jonas, J. J.: in "Recovery and recrystallization during high temperature deformation in plastic deformation of metals". Vol. 6,393;1975, New York, Academic Press;

Mercer, R. E. and McPherson, N. A.: *AIME Steelmaking Conf. Proc., 1979*,**62**,215;

Messmer, R. P. and Briant, C. L.: *Acta Metall.*, 1982,**30**,457;

Michel, J. P. and Jonas, J. J.: *Acta Metall.,* 1981,**29**,513;

Mills, N. T. and Joseph, R. S.: *Ironmaking Steelmaking,* 1977,**4**,181;

Mintz, B.: Private Communication, (ECSC final report on megaproject P3454" Thin slab casting," 1998).

Mintz, B.: Private communication, 1998.

Mintz, B, Private Communication, British Steel, Scunthorpe Works, 1994

Mintz. B. unpublished work

Mintz. B. unpublished work, 1994

Mintz, B.: *Mater. Sci. Technol.*, 1996,**12**,132;

Mintz, B, Abushosha, R.: *Mater. Sci. Technol.*, 1992,**8**,171;

Mintz, B. and Abushosha, R., in "Hot workability of steels and light alloy-composites". Ed. McQueen, Konopleva and Ryan, 1996, Met. Soc. of CIM, pp 399-410.

Mintz, B. and Abushosha, R. : Ironmaking and Steelmaking, 1993,20

Mintz, B, Abushosha, R., Cominelli, O. G. and Ayyad, S.: Proceedings of 7th International Symposium on Physical Simulation of Casting, Hot Rolling and Welding, Nat. Res. Inst. for Metals, Japan, ISPS, 1997, pp. 449.

Mintz, B., Abushosha, R. and Cowley, A. "A preliminary analysis of the hot ductility curve in simple C-Mn steels" accepted for publication Mat. Sci & Techn, 1997.

Mintz, B, Abushosha, R and Shaker, M.: *Mater. Sci. Technol.*, 1993,**9**,907;

Mintz, B., Abushosha, R., Ayyad, S. and Cardoso, G. I. S. L.: HSLA steel Conf. Beijing, China Oct. 1995, HSLA'95, published by China Science and Technology Press, pp. 342-345.

Mintz, B. and Arrowsmith, J. M.: Sheffield Int. Conf. on "Hot working and forming processes", Metal Soc., London, 1979, Eds. C. M. Sellars and G. J. Davies, 99

Mintz, B. and Arrowsmith, J. M.: Metals Technol. 1979,6,24-32.

Mintz, B., Cominelli, O. G., and Oliveira, M. A. L.: in "International Conference on Thermomechanical Processing and other Materials, Thermec 97",867;1997, Wollongong Australia, ed. The Minerals and Materials Society, Warrendale PA 1997;

Mintz, B. and Crowther, D. N.: in "Ti technology in microalloyed steels". Conf. Proc.. Sheffield, published by Inst. of Materials, Ed. T. N. Baker, 1997, pp. 98-114.

Mintz, B and Mohamed, Z.: in Proc. Conf. on "Physical simulation techniques for welding, hot forming and continuous casting", vol. 11 pp 26-37, MTL 92-43(TR), CANMET, Ottawa, Canada;

Mintz, B and Mohamed, Z.: *Mater. Sci. Technol.*, 1988, **4**, 895;

Mintz, B.; Mohamed, Z. and Abushosha, R.: *Mater. Sci. Technol.*, 1989,**5**,682;

Mintz, B. and Mohamed, Z. (1989). Given at 7th Int. Conf. on Fracture, Houston, Texas, March 1989, eds. Salama, Tavi-Chandoz, Taplin, Tama Rao, vol.4, pp. 2575-2583. Oxford, Pergamon The influence of carbon on the hot ductility of microalloyed steels.

Mintz, B., Yue, S. and Jonas, J. J.: Int. Mater. Rev. 1991,36,5,187

Mintz, B.; Yue, S. and Jonas, J. J.: in Proc.. Int. Conf. on "Recrystallisation in metallic materials", Wollongong, N S W, 553;1990, Warrendale, PA, Metallurgical Society of AIME;

Mintz, B., Yue, S. and Jonas, J. J.: Int. Mat. Reviews, 1991, 36, No 5, 187.

Mintz, B; Stewart, J. M. and Crowther, D. N.: *Trans. Iron Steel Inst. Jpn,* 1987,**27**,366;

Mintz, B.; Wilcox, J. R. and Arrowsmith, J. M.: in Proc. Risø Int. Conf. on "Recrystallization and grain growth of multi-phase and particle containing materials", 303;1980, Copenhagen, Risø;

Mintz, B; Wilcox, J. R. and Crowther, D. N.: *Mater. Sci. Technol.,* 1986,**2**, 589;

Nachtrab, W. T. and Chou, T. T.: *Metall. Trans.*, 1986,**17A,**1995;

Nozaki, T.; Matsuno, J.; Murata, K.; Ooi, H. and Kodama, M.: *Trans. Iron Steel Inst. Jpn.*1978,**18**,330;

Offerman, C.; Dacker, C. A. and Enstrom, C.: *Scand. J. Metall.*, 1981, **10**, 115;

Ohmori, Y. and Maehara, Y.: *Trans. Jpn. Inst. Met.*, 1984,**25**,(3),160;

Osinkolu, G.A.; Tacikowisk, M. and Kobylanky, A.: *Mater. Sci. Technol.*, 1985,**1**,520;

Ouchi, C. and Matsumoto, K.: *Trans. Iron Steel Inst. Jpn,* 1982,**22**,181;

Okazaki, T.; Tomono, H.; Ozaki, K. and Akabane, H.: *Tetsu-to-Hagané (J. Iron Steel Inst. Jpn.),* 1982, **68**,S929;

Patrick, B. and Ludlow, V.: Revue de Metallurgie, 1994,1081

Pleschiutschnigg, F. P., Hagen, I. Hoppmann, H. D. and Gosio, G.: Metallurgical Plant and Technology Int. 1993, 4 pp44-68

Razumov, S. D., Zabil'skii, V. V., Umanets, V. I., Lebedev, V. I. and Oburhov, V. A.: Steel in the USSR, 1986, May, vol. 16, pp. 225-228.

Rizio, D. P.; Oldland, R. B. and Borland, B. W.: in "Physical metallurgy of thermomechanical processing and other metals, Thermec 88",178;1988, Tokyo, The Iron and Steel Institute of Japan;

Reynold, J. H. and Gladman, T.: in "Hot working and forming processes",(ed. C. M. Sellars and G. J. Davies),171;1980, London, The Metals Society;

Roberts, W. : "Recent innovations in alloy design and the processing of microalloyed steels" in HSLA Steels Technology and Processing of Microalloyed Steels, ASM,1984,33

Saeki, T., Ooguchi, S. Misoguchi, S., Yamamoto, Y., Misumi, H. and Tsuneoka: *Tetsu-to-Hagané*(Trans. Iron Steel Inst. Jpn),1982,**68**,1773;

Sandenberg, A and Roberts, W.: in "Thermomechanical processing of microalloyed austenite", 405;1982, Warrendale, PA, Metallurgical Society of AIME;

Sakay, T. and Ohasahi, M.: "Physical metallurgy of thermomechanical processing and other metals, Thermec 88", vol. I, 162;1988, Tokyo, The Iron and Steel Institute of Japan;

Schmidt, L. and Josefsson: *Scand. J. Metall.*, 1974, **3**, 193;

Sellars, C. M.: in "Hot working and forming processes",(ed. C. M. Sellars and G. J. Davies),3;1980, London, The Metals Society;

Servi, I. and Grant, N. J.: *Trans. AIME*, 1951, **191**, 917;

Shelenberger, T. E., Ekis, A. A., Kondo, T. and Suzuki, M., in Proc. 6th Int. Iron and Steel Congress, 1990, Tokyo, The Iron and Steel Inst. Jpn, 377;

Subramanian, S. V., Shima, S., Ocampo, G., Castillo, T., Embury, J. D. and Purdy, G. R.: HSLA Steels '85, Beijing, China, 4-8th Nov. 1985, 151. Chinese Soc. of Metals

Sundman, B., Jansson, B. and Anderson, J. O. Calphat, 1985, 93, Swedish Royal Inst.

Suzuki, H. G.; Nishimura, S. and Yamaguchi, S.: *Trans. Iron Steel Inst. Jpn,* 1982, **22**,48;

Suzuki, H. G.; Nishimura, S.; Imamura, J. and Nakamura, Y.: *Trans. Iron Steel Inst. Jpn.*, 1984, **24**, 169;

Tacikowski, M.; Osinkolu, G. A. and Kobylanski, A.: *Mater. Sci. Technol.*, 1986, **2**,154;

Takeuchi, E. and Brimacombe, J. K.: *Metall. Trans.*,1985, **16B**, 605;

Thomas, B. G.; Brimacombe, J. K. and Samarasekera, I. V.: *Iron Steel Soc. Trans.,* 1986,**7**,7;

Turkdogan, E. T.: *AIME Steelmaking Conf. Proc., Pittisburg, PA* 1987,**70**,399;

Turkdogan, E. T.; Ignatowicz, S. and Pearson, J.: *J. Iron Steel Inst.*, 1955,**180**,349;

Ueda, T., Hashio, M., Kato, H. Wanatabe, T. and Matsui, K.: *Tetsu-to- Hagané*: J. Iron and Steel Inst Jpn, 1981,**67**,A37;

Umemoto, M. and Tamura, I.: Kyoto University, Japan, Personal communication to J.J. Jonas, 1985;

Ushijima, K.; Sugitami, Y.; Yamaguchi, S.; Shiode, S.; Hashio, M. and Tomono, H.: in "HLSA steels technology and applications", 403; 1984, Philadelphia, PA, American Society for Metals;

Valderes, C. A. G.,.Mundim, M. J., Barbosa, R. A. M.: Proc. Sixth Int. Iron and Steel Congress, 1990, Nagoya, ISIJ, 385

Vodopivec, F.: *J. Iron Steel Inst.*, 1973,**211**,664;

Vodopivec, F.: *Met. Technol.*, 1974,**1**,151;

Vodopivec, F.; Torkar, M.; Debelak, M.; Kmetic, M.; Haller, F. and Kaucic, F.: *Mater. Sci. Technol.*, 1988, **4**, 917;

Weinberg, F.: *Metall. Trans., 1979, **10B**,513;*

Weiss, I. and Jonas, J. J.: *Metall Trans.*, 1980,**11A**,403;

Weiss, I. and Jonas, J. J.: *Metall Trans.,* 1979,**10A**,831;

White, F. E. and Rossard, C.: in "Deformation under hot working conditions", 14; 1968, London, The Iron and Steel Institute;

Wilcox, J. R. and Honeycombe, R. W. K.: in "Hot working and forming processes". (ed. C. M. Sellars and G. J. Davies), 108; 1980, London. The Metals Society;

Wilcox, J. R. and Honeycombe, R. W. K.: *Mat. Technol.,* 1984,**11**,217;

Wilcox, J. R. and Honeycombe, R. W. K.: *Mater. Sci. Technol.*, 1987,**3,**849;

Williams, J. G.: in "HSLA steels technology and applications", 261; 1984, Philadelphia, PA, American Society for Metals;

Wilson, F. G. and Gladman, T.: *Int. Mater. Rev.*, 1988,**33**,221;

Wolf, M. and Kurz, W., Metall Trans. **12B**, 1981,85;

Wray, P. J.: *Met. Technol.* 1981,**8,**466;

Wray, P. J.: *Metall. Trans.*, 1975,**6A**,1379;

Wray, P. J.: *Metall. Trans.*, 1984,**15A**,2059;

Yasumoto, K.; Maehara, Y.; Ura, S. and Ohmori, Y.: *Mater. Sci. and Technol.*, 1985,**1**,111;

Zhang Hongtao; Guo Huawei and Wu Baorong: in "Physical metallurgy of thermomechanical processing of steels and other metals, Thermec "88", Vol. 1, 170; 1988, Tokyo, The Iron and Steel Institute of Japan;

During the PhD programme papers related to the research work were produced.

"The influence of Ti on the hot ductility of C-Mn-Al steels" co-author with Mintz and Abushosha, accepted for publication, Materials Science and Technology, 1998.

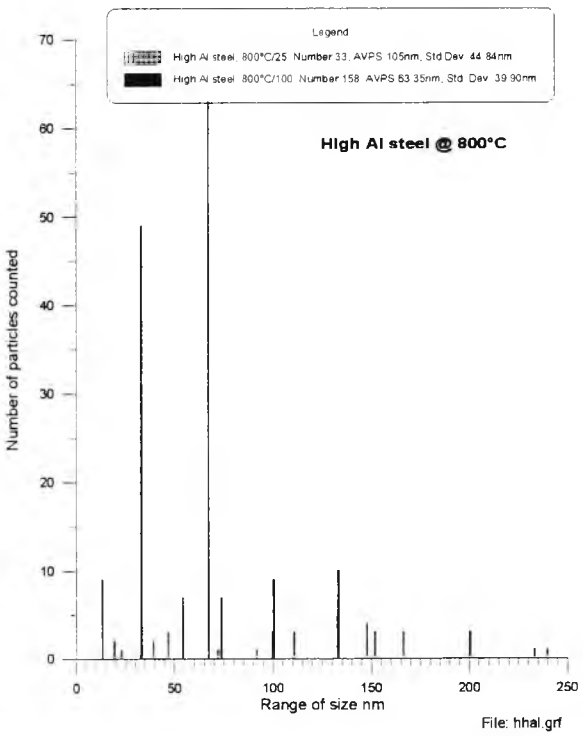
"The influence of sulphur on the hot ductility of steels" proceedings of THERMEC Conference, Wollongong, Australia, July 1997, co-author with B. Mintz, Oliveira, M. A. L. - published in the Proceedings, vol. 1, page 867.

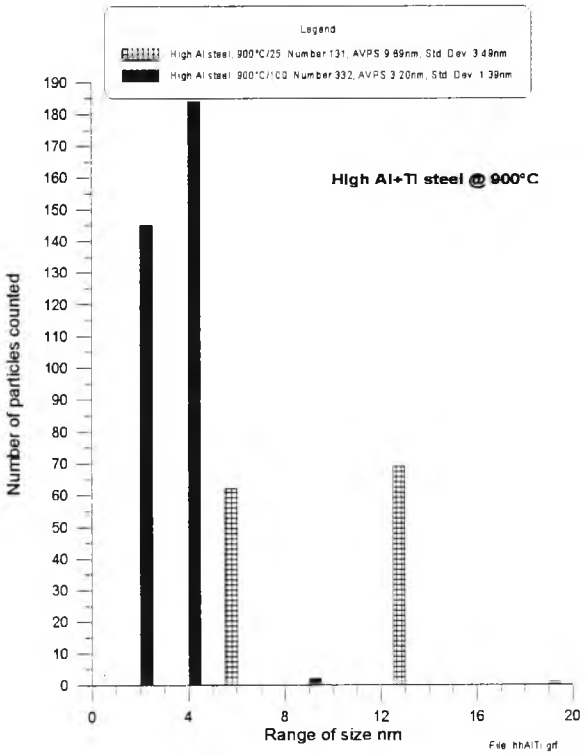
"The effect of the chemical composition and testing parameters on the hot ductility of C-Mn- steels - *Efeito da composição química e parâmetros de ensaio sobre a ductilidade a quente de acos C-Mn-Al*" presented at 51st Annual Conference of ABM (Brazilian Materials Society), 1996. co-author with Macedo, M. C. S et al;

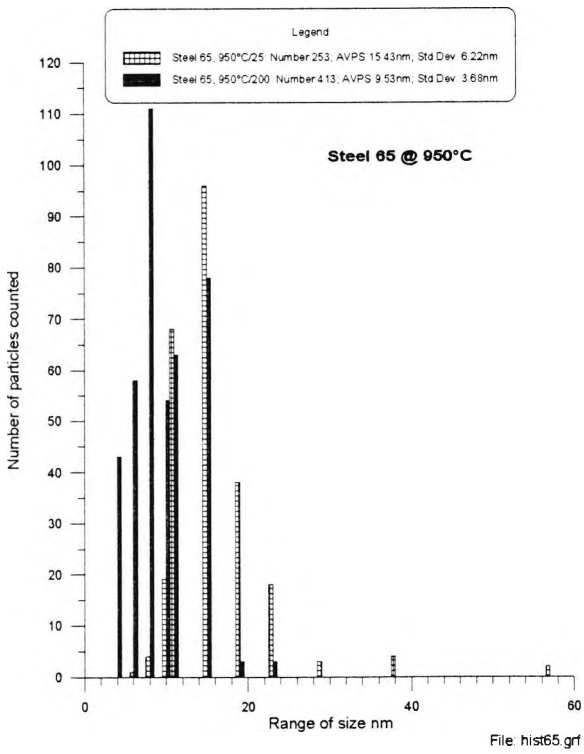
"The hot tensile test as a means of assessing the susceptibility of steel to cracking during continuous casting", Proceedings of 7th International Symposium on Physical Simulation of Casting, Hot Rolling and Welding - National Research Institute of Japan, 21-23 January 1997, p. 449-467, co-author with Mintz, B, Abushosha, R and Ayyad, S.

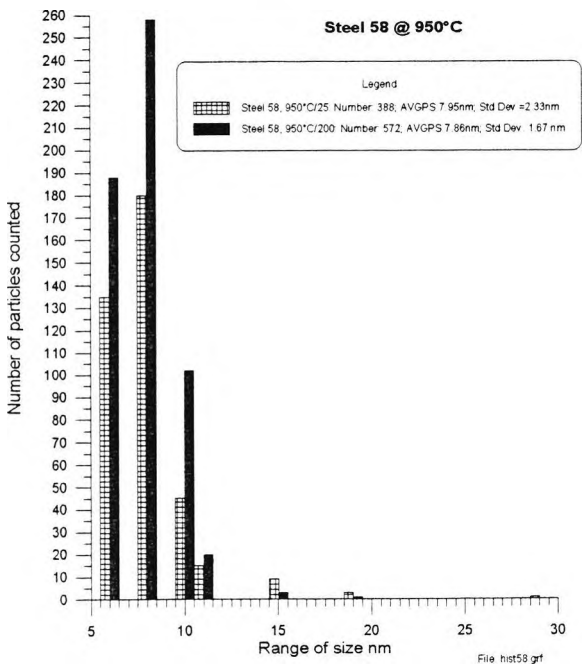
Chapter 8 : APPENDIX

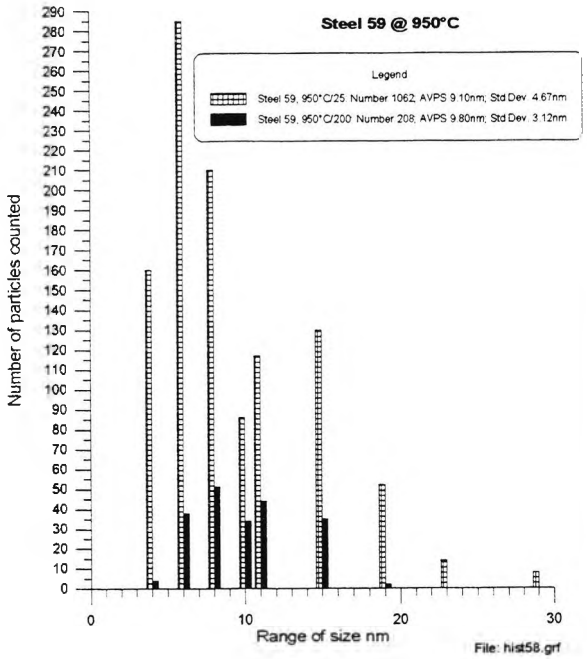
Size distributions, average particle size (AVPS) and standard deviation (Std Dev) for some of the steels

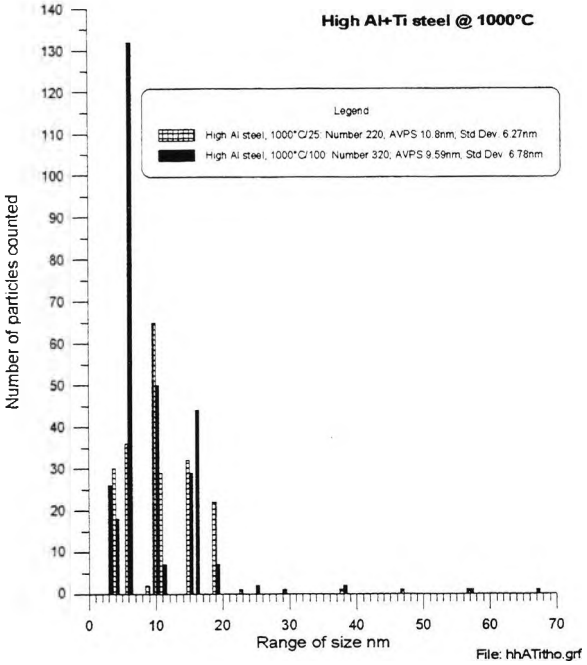


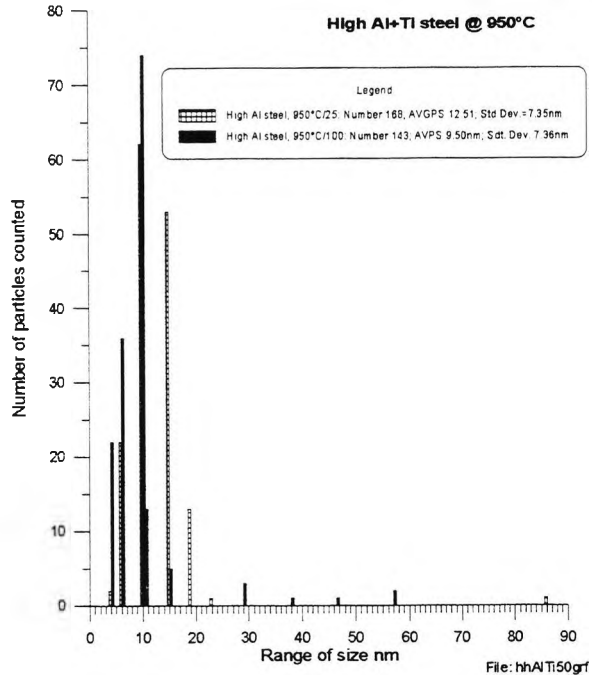


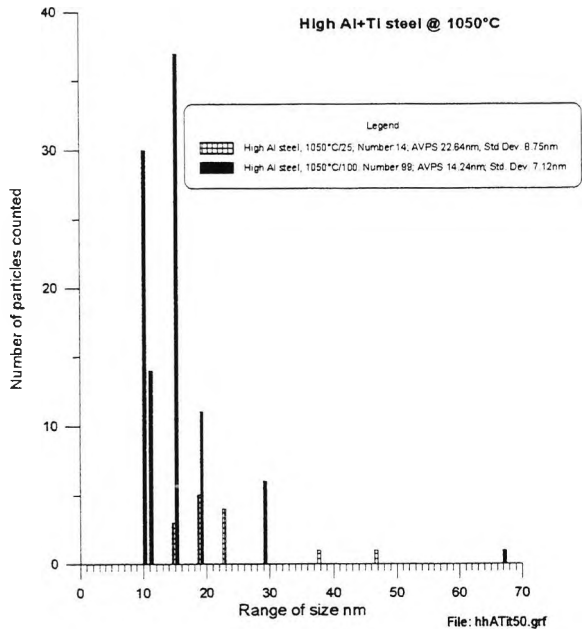


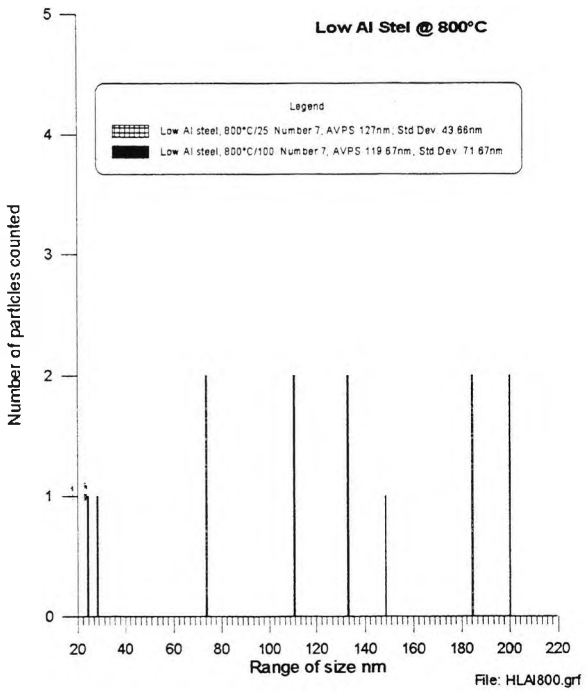


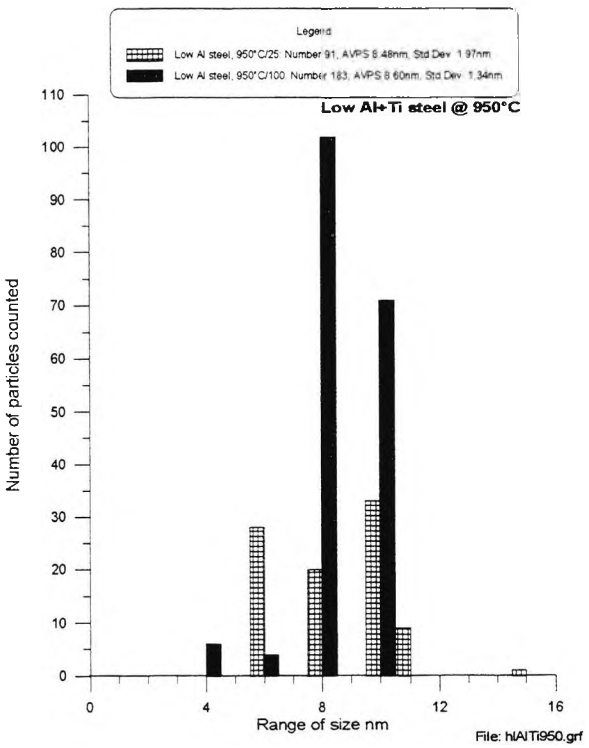

Steel 59 @ 950°C
Legend
Steel 59, 950°C/25: Number 1062; AVPS 9.10nm; Std Dev. 4.67nm
Steel 59, 950°C/200: Number 208; AVPS 9.80nm; Std Dev. 3.12nm
Number of particles counted
Range of size nm
File: hist58.grf

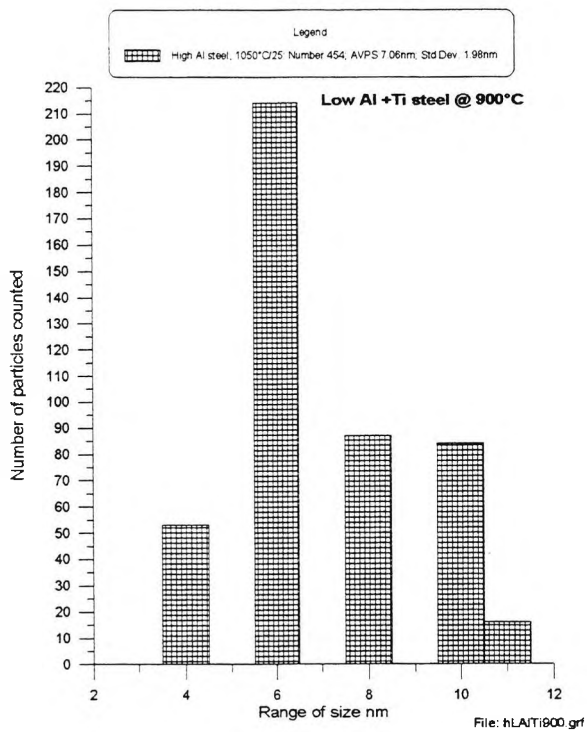

High Al+Ti steel @ 1000°C
Legend
High Al steel, 1000°C/25: Number 220; AVPS 10.8nm; Std Dev. 6.27nm
High Al steel, 1000°C/100: Number 320; AVPS 9.59nm; Std Dev. 6.78nm
Number of particles counted
Range of size nm
File: hhATitho.grf

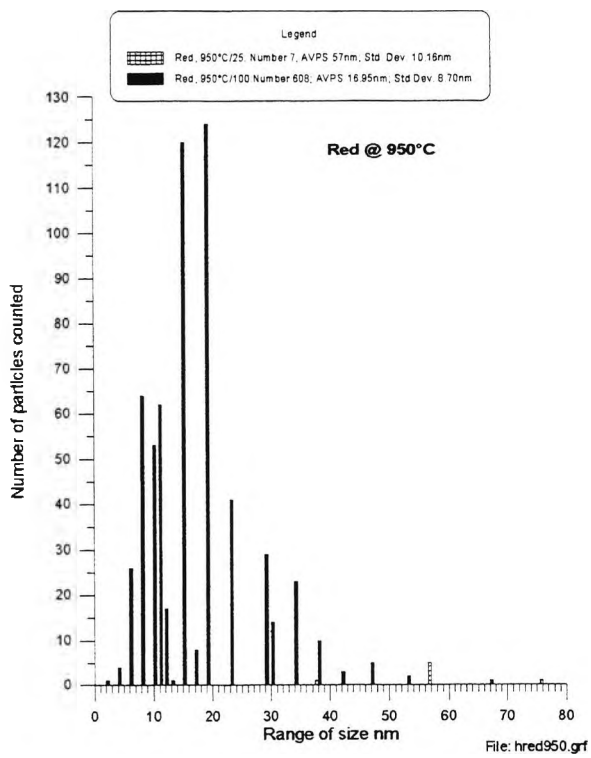

High Al+Ti steel @ 950°C
Legend
High Al steel, 950°C/25: Number 168; AVGPS 12.51; Std Dev.=7.35nm
High Al steel, 950°C/100: Number 143; AVPS 9.50nm; Sdt. Dev. 7.36nm
Number of particles counted
Range of size nm
File: hhAlTi50grf

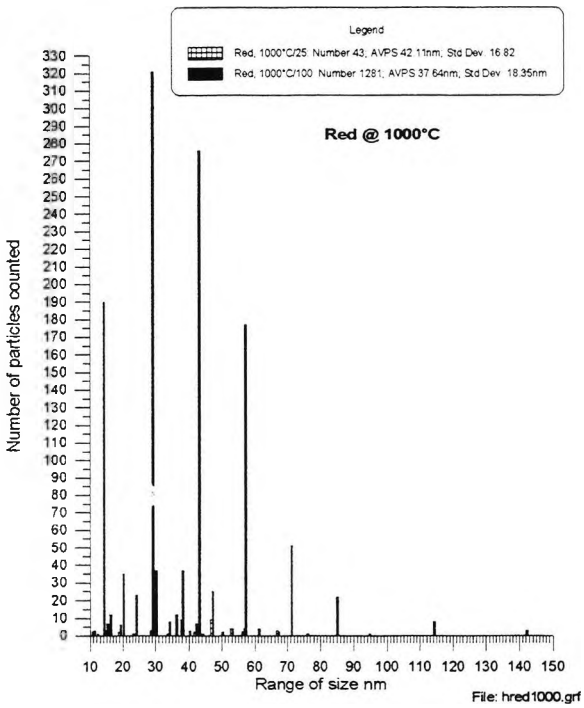

High Al+Ti steel @ 1050°C
Legend
High Al steel, 1050°C/25; Number 14; AVPS 22.64nm; Std Dev. 8.75nm
High Al steel, 1050°C/100: Number 88; AVPS 14.24nm; Std. Dev. 7.12nm
Number of particles counted
Range of size nm
File: hhATit50.grf

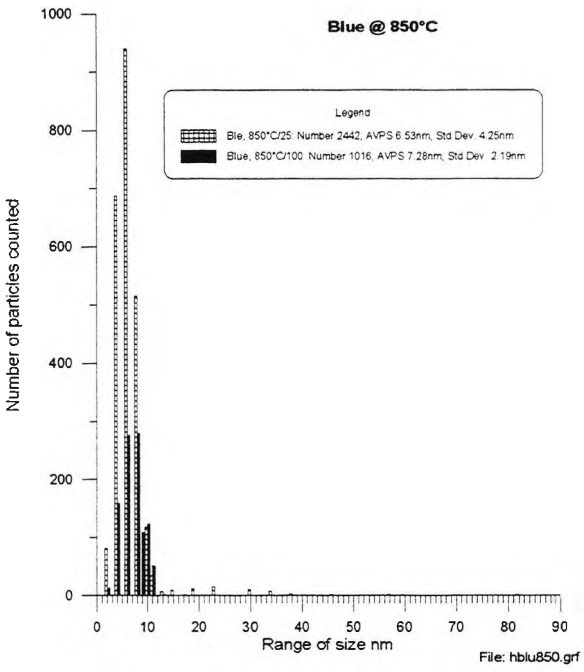

Low Al Stel @ 800°C
Legend
Low Al steel, 800°C/25 Number 7, AVPS 127nm, Std Dev 43.66nm
Low Al steel, 800°C/100 Number 7, AVPS 119.67nm, Std Dev 71.67nm
Number of particles counted
Range of size nm
File: HLAl800.grf

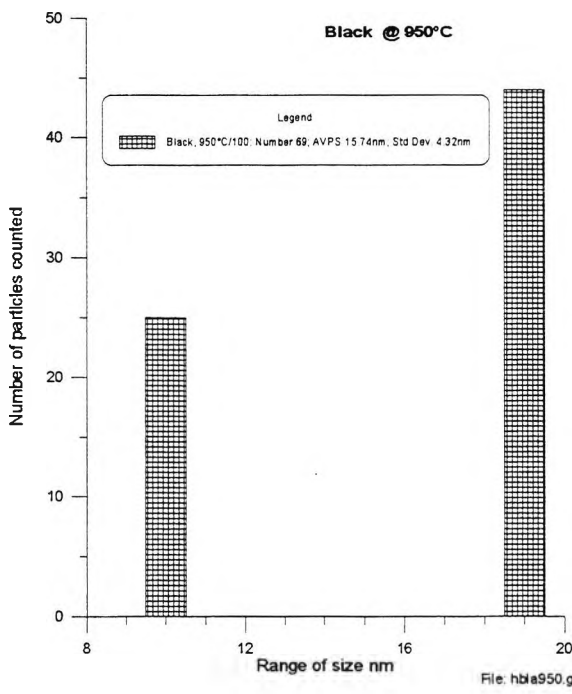

Legend
Low Al steel, 950°C/25 Number 91, AVPS 8.48nm, Std Dev 1.97nm
Low Al steel, 950°C/100 Number 183, AVPS 8.60nm, Std Dev 1.34nm
Low Al+Ti steel @ 950°C
Number of particles counted
Range of size nm
File: hlAlTi950.grf

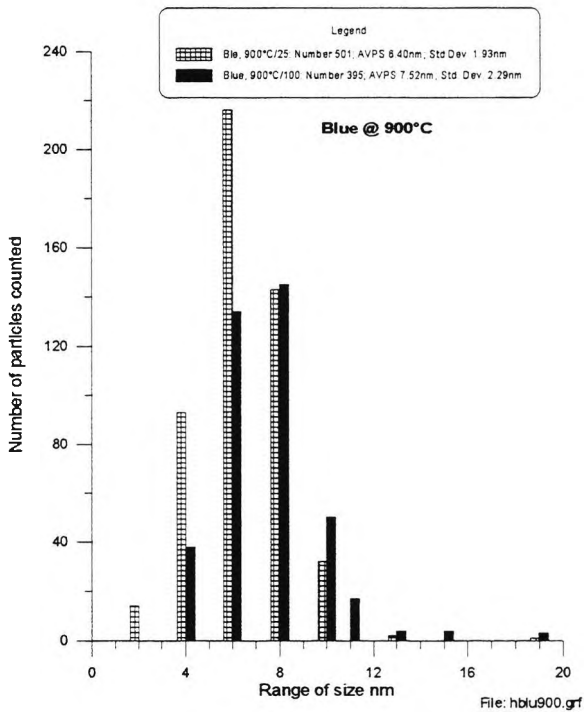

Legend
High Al steel, 1050°C/25 Number 454, AVPS 7.06nm, Std Dev 1.98nm
Low Al +Ti steel @ 900°C
Number of particles counted
Range of size nm
File: hLAlTi900.grf

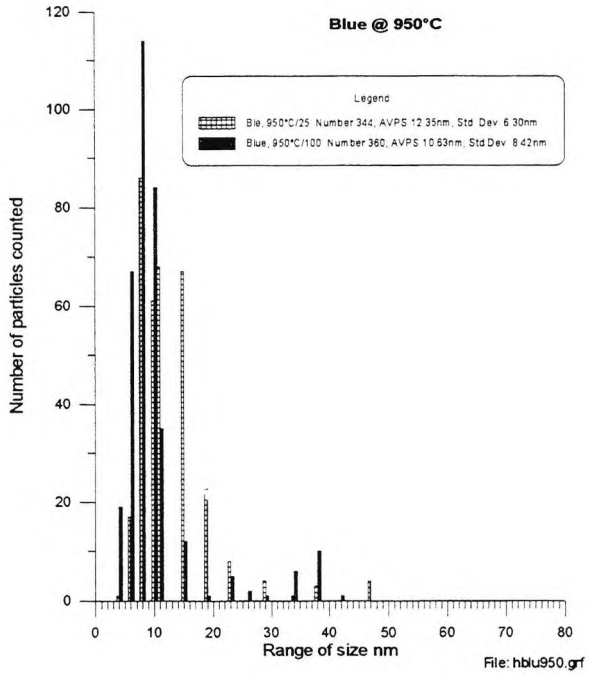

Legend
Red, 950°C/25 Number 7, AVPS 57nm, Std Dev 10.16nm
Red, 950°C/100 Number 608, AVPS 16.95nm, Std Dev 8.70nm
Red @ 950°C
Number of particles counted
Range of size nm
File: hred950.grf

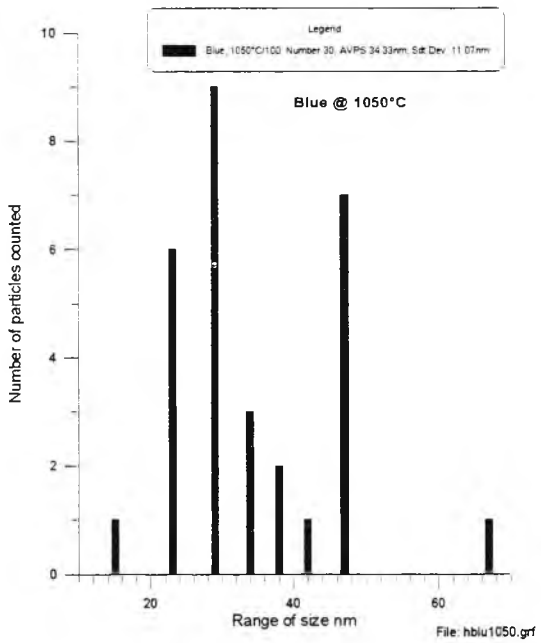

Legend
Red, 1000°C/25: Number 43; AVPS 42.11nm; Std Dev. 16.82
Red, 1000°C/100: Number 1281; AVPS 37.64nm; Std Dev. 18.35nm
Red @ 1000°C
Number of particles counted
Range of size nm
File: hred1000.grf

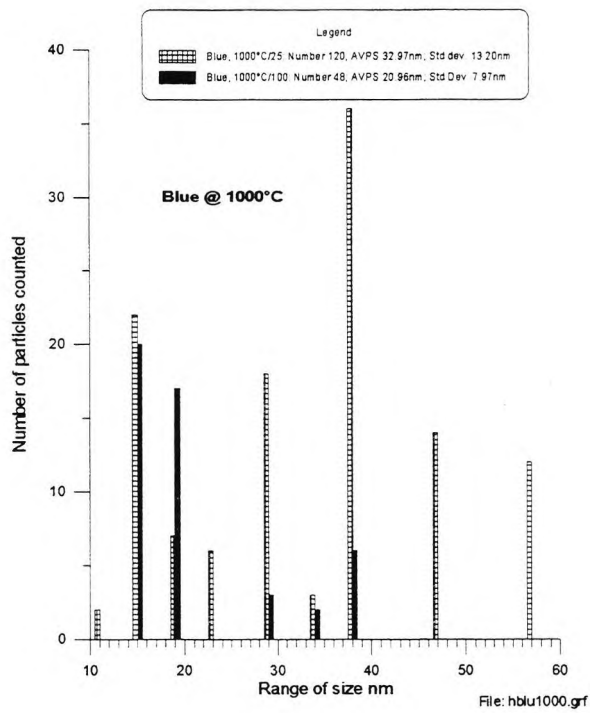

Blue @ 850°C
Legend
Ble, 850°C/25: Number 2442; AVPS 6.53nm; Std Dev. 4.25nm
Blue, 850°C/100: Number 1016; AVPS 7.28nm; Std Dev. 2.19nm
Number of particles counted
Range of size nm
File: hblu850.grf

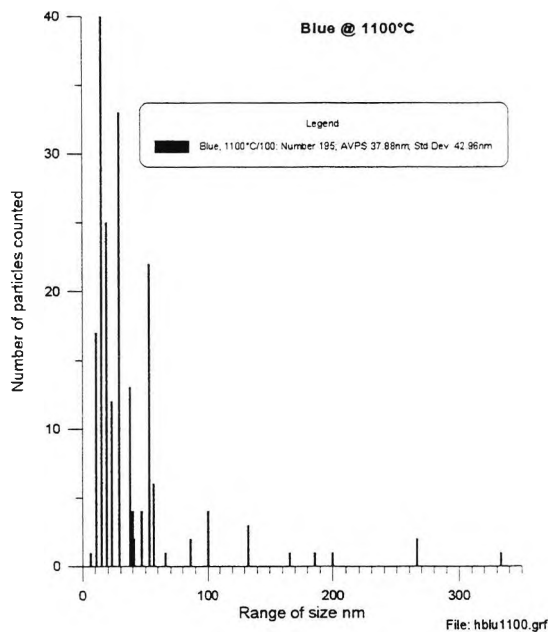

Black @ 950°C
Legend
Black, 950°C/100: Number 69; AVPS 15.74nm; Std Dev. 4.32nm
Number of particles counted
Range of size nm
File: hbla950.grf


Legend
Ble, 900°C/25: Number 501; AVPS 8.40nm; Std Dev. 1.93nm
Blue, 900°C/100: Number 395; AVPS 7.52nm; Std Dev. 2.29nm
Blue @ 900°C
Number of particles counted
Range of size nm
File: hblu900.grf









file: thesis.doc: version:15 October 199808:15